Quantifying Feedbacks between Pollution, Radiation and Dynamics in a Polluted Megacity

A thesis submitted to The University of Manchester for the degree of Doctor of Philosophy in the Faculty of Science and Engineering.

2021

Jessica Slater

School of Earth and Environmental Sciences

Contents

List of Figures

Abstract

Air pollution is a major global health concern, contributing to an estimated 7 million premature deaths per year. 91 % of the world's population live in areas with unsafe air which is a particular issue in urban areas. This is due to high levels of anthropogenic emissions from sectors such as: industry, transport, heating and biomass burning. However, natural emissions from wildfires, volcanoes, sea spray and desert dust can also contribute to poor air quality. Pollutants in the atmosphere undergo physical and chemical changes which can greatly affect their physical and chemical properties. Furthermore, they can interact with radiation to impact the climate and cause changes in meteorology, which can enhance atmospheric pollution.

Rapid urbanisation and industrialisation in countries like China and India has led to large populations living in urban environments with poor air quality. Beijing, a megacity in North Eastern China, is well known for its air quality problems. This is due to high anthropogenic emissions combined with unfavourable meteorology and topography. Despite policy interventions improving average annual air quality in Beijing, it still experiences extreme pollution episodes or haze. During haze episodes, aerosol particles accumulate in a shallow planetary boundary layer (PBL), to reduce visibility < 10 km. The interactions of aerosol particles with radiation in Beijing is believed to suppress turbulent motion, inhibit pollutant dispersion and allow for high aerosol concentrations to accumulate in a shallow PBL. This further increases the extent of aerosol-radiation interactions. The feedback between aerosols, radiation and PBL meteorology is believed to contribute significantly to the intensity and longevity of haze episodes in Beijing. However, quantifying this effect has proven difficult through observational and regional modelling studies alone. These studies struggle to fully characterise the urban PBL and directly elucidate some of the important processes and variables affecting the aerosol-PBL feedback mechanism. This work presents the development and use of a fully coupled LES-aerosol radiation model, which allows for isolation of processes and variables that impact the aerosol-PBL feedback. This has allowed for further understanding of the contribution of this process to Beijing haze episodes.

Declaration

No portion of the work referred to in the thesis has been submitted in support of an application for another degree or qualification of this or any other university or other institute of learning.

Copyright Statement

(i) The author of this thesis (including any appendices and/or schedules to this thesis) owns certain copyright or related rights in it (the "Copyright") and s/he has given The University of Manchester certain rights to use such Copyright, including for administrative purposes.

(ii) Copies of this thesis, either in full or in extracts and whether in hard or electronic copy, may be made only in accordance with the Copyright, Designs and Patents Act 1988 (as amended) and regulations issued under it or, where appropriate, in accordance with licensing agreements which the University has from time to time. This page must form part of any such copies made.

(iii) The ownership of certain Copyright, patents, designs, trademarks and other intellectual property (the "Intellectual Property") and any reproductions of copyright works in the thesis, for example graphs and tables ("Reproductions"), which may be described in this thesis, may not be owned by the author and may be owned by third parties. Such Intellectual Property and Reproductions cannot and must not be made available for use without the prior written permission of the owner(s) of the relevant Intellectual Property and/or Reproductions.

(iv) Further information on the conditions under which disclosure, publication and commercialisation of this thesis, the Copyright and any Intellectual Property and/or Reproductions described in it may take place is available in the University IP Policy (see http://documents.manchester.ac.uk/DocuInfo.aspx?DocID=24420), in any relevant Thesis restriction declarations deposited in the University Library, The University Library's regulations (see http://www.library.manchester.ac.uk/about/regulations/) and in The University's policy on Presentation of Theses.

Acknowledgements

When I first started on this PhD, I had no idea of the journey it would be. I am incredibly thankful to many people for their help, support and company throughout the past 4 years, and for the opportunities I've had. Firstly, to my wonderful family who have supported every decision I have made and always believed and encouraged me throughout my entire academic life. Particularly to my Mum, who has become my best friend and an inspiration to me always. She also instilled in me a love of running and the outdoors, which helped me stay sane during the tricky times. To my wonderful Nana who sadly passed away this year, I remember you, your strength and bravery in everything I do. To Sam for his support, love and reassurance that things would be okay, and for bringing me endless cups of tea.

I have been incredibly lucky throughout these last few years, to travel to incredible places and meet some amazing people. For that, I would like to thank my supervisors Hugh and Gordon, for encouraging me to attend conferences and meetings. Particularly encouraging me to take a trip to Beijing during the first few months of my PhD, which gave me so many opportunities. Particularly it allowed me to come close to what we call 'peng yous', Archit, Joshi, Freya, Ellie and Rob whose friendship has lasted the length of the PhD and through many an APHH meeting, I'm amazed at how far we've come and I know we'll stay close in the future. I'm proud of you all. To Archit and Joshi, we made it! Sharing a small office with you guys for 3 years I'm surprised we are still talking but maybe it's a testament to our friendship. There've been many ups and downs, laughter and shouting along the way, sharing of rooms and exploring new places - the memories are too many to name.

Chapter 1

Urban Air Pollution

1.1 Motivation

Increased urbanisation and industrialisation around the world, combined with increasing populations has led to increased emissions of aerosol particles in the atmosphere. High aerosol concentrations, particularly in urban environments, can lead to severe air pollution with negative consequences for human health Aerosols are also of interest worldwide due to their significant but uncertain climatic impact. Aerosol particles can impact climate in two ways: firstly by either scattering or absorbing radiation to directly alter the global radiation budget (aerosol-radiation interactions), and secondly through their impacts on clouds (aerosol-cloud interactions). The majority of aerosol particles exist in the planetary boundary layer (PBL). The PBL is the lowest layer of the atmosphere and is directly affected by changes in radiative flux, which can be impacted by seasonal and diurnal variations, as well as by perturbations caused by aerosol-radiation interactions (ARI). Aerosols within the PBL can interact with radiation to alter the thermal balance of the PBL and affect atmospheric stability. This can inhibit the dispersion of pollutants, leading to enhanced atmospheric stagnation and increases in surface pollutant concentrations (Kappos et al., 2004; Hertel and Goodsite, 2009; Lazaridis, 2011; Boucher, 2013; Gao et al., 2015; Kalberer, 2015; Stull, 2015; Petäjä et al., 2016).

1.2 Thesis Overview

An interdisciplinary project between UK and Chinese researchers, Air Pollution and Human Health (APHH) Beijing, aimed to further understanding of the sources, processes and health impacts of Beijing pollution episodes. The project included two field campaigns in Winter (Nov-Dec) 2016 and Summer (May-June) 2017. This research fits into the project work through providing understanding on the contribution of the aerosol-PBL feedback to pollution episodes in wintertime Beijing. This thesis is set out as follows. Chapter 1 provides an introduction to the factors influencing urban air quality, with particular focus on pollutant particulates, their health impacts, properties and interactions in the atmosphere, as well as a description of the urban environment. Chapter 2 describes the issue of air pollution in Beijing, including

a review of the current literature investigating the contribution of aerosol-PBL feedback to Beijing haze. Chapter 3 outlines the research method used, including limitations and benefits compared to other studies. Chapter 4 displays the three papers which outline the main research results and contributions performed over the PhD. Paper 1 sets out the use of a novel coupled large eddy scale (LES)-aerosol radiation model in an urban environment and its capabilities to investigate the aerosol-PBL feedback. Paper 2 highlights the importance of changing synoptic conditions on Beijing pollution episodes, and disputes the idea that aerosol-PBL feedback only occurs above a certain 'threshold' value. Paper 3 shows the impact and implications of aerosol optical properties on the aerosol PBL feedback, including the altitude and concentration of the absorbing aerosol layer. Chapter 5 highlights the importance and impact of these findings on policy and provides recommendations for future research in this area.

1.3 Atmospheric Aerosols

Aerosols, defined as suspensions of small solid or liquid particles in air, are abundant in the Earth's atmosphere. Sources of atmospheric aerosols can be both anthropogenic and natural. Aerosol particles are either directly emitted (primary aerosols) or they can form in the atmosphere from gaseous precursors (secondary aerosols). Atmospherically relevant aerosol particles typically have sizes ranging from 1 nm to 10 μm and are composed of various inorganic and organic components (Finlayson-Pitts and Pitts, 2000). Particulate matter (PM) is often used to describe mass concentrations of aerosols. Specifically, air pollution mass concentrations of $PM_{2.5}$ (particulate matter with a diameter < 2.5 μm) are often used when referring to air quality and the health effects of air pollution. The use of $PM_{2.5}$ as a metric for air quality is most commonly used for several reasons. Firstly, exposure to ambient particulate matter was found by the Global Burden of Disease study to be the fifth largest cause of all age deaths in 2015 worldwide. $PM_{2.5}$ encompasses a wide range of aerosol compositions and so takes into account both primary and secondary aerosols, which can have both natural and anthropogenic sources. Consequently, it has been found to be the air pollutant with the largest effect on human health and there is now a clear relationship between high concentrations of PM2.5 and increases in mortality and morbidity. Furthermore, reducing concentrations of $PM_{2.5}$, when all other factors remain the same, results in reduced mortality and morbidity. Finally, particulate matter (either PM_{10} or $PM_{2/5}$) is often measured and so it is a useful metric for monitoring air quality particularly in highly polluted environments (Forouzanfar et al., 2016; Yue et al., 2020).

The size and composition of an aerosol particle has an influence on its: lifetime in the atmosphere, surface reactivity and light scattering ability, and are important when considering aerosol human health and climate impacts (Lazaridis, 2011; Zheng et al., 2015). Pollutants are generally removed from the atmosphere due to meteorology, i.e transportation or dispersion through strong winds or wash out by rain. Under high humidity conditions, certain aerosol particles can also become cloud droplets (Figure 1.1). Consequently, the concentrations and properties of aerosols in urban environments are highly dependent on both pollutant sources and atmospheric conditions. There is large spatiotemporal variation in the

composition, concentration and type of aerosol particles. For example, in the Arabian gulf, countries experience severe pollution episodes due to extreme dust storms, coastal industrial and shipping emissions which contribute significantly to measured PM concentrations (Farahat, 2016). Major sources in Asian cities are typically biomass or fossil fuel burning for residential use, while some of the main sources of particulate matter (PM) in Western Europe and Northern America are from vehicles and industry (Derwent and Hjellbrekke, 2013; Marlier et al., 2016). The different sources of PM have a strong impact on particle properties. Some particles are emitted directly into the atmosphere, however, a major component of measured PM globally are secondary aerosols and are formed in the atmosphere (Figure 1.1). The formation and characteristics of secondary aerosols are strongly dependent on gaseous sources, existing particulate concentrations and atmospheric conditions (Seinfeld and Pandis, 2006a; Chan and Yao, 2008; Fiore et al., 2012; Kalberer, 2015; Fuzzi et al., 2016). This section outlines sources and removal of atmospheric aerosols as well as their physiochemical properties, with a particular focus on aerosols in urban environments.

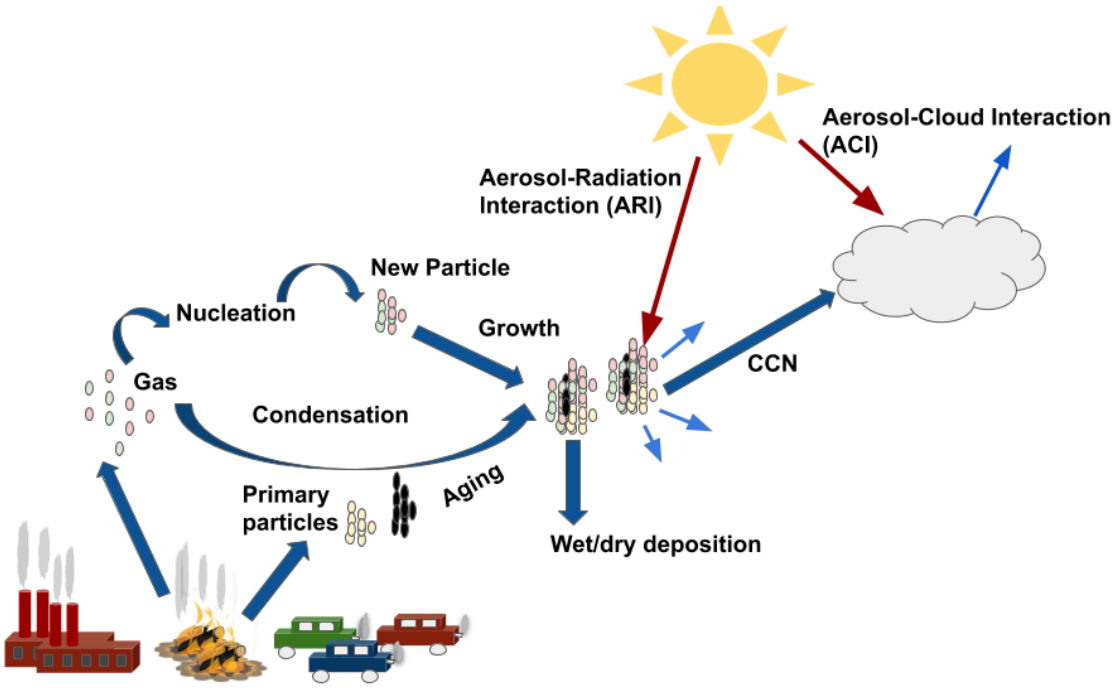

Figure 1.1: Schematic showing the process of aerosol formation, growth and removal in the atmosphere and interactions with solar radiation

1.3.1 Primary Emissions

An aerosol's physical and chemical properties impact the processes and interactions that it will undergo in the atmosphere. Aerosol particles in the atmosphere can be emitted directly from anthropogenic sources, such as combustion or mechanical processes as well as naturally from volcanic eruptions or desert dust storms. Primary aerosols in the atmosphere include: carbonaceous compounds (black and organic carbon), mineral dust, sea salt and some biological organic species such as exudate from decaying marine biota, fungal spores and algae. Primary sources of air pollution in the atmosphere vary both by region and season. The main sources of primary aerosols in urban environments are thought to be traffic, biomass

burning for residential heating and cooking, and industrial coal combustion, with open waste burning being a source in some areas. Desert dust, volcanic ash and sea spray are all forms of natural aerosol particles which can also contribute to air pollution events in urban environments. Main sources of pollutants and thus composition of typical $PM_{2.5}$ mass shows large spatial heterogeneity, with a regional variation due to differences in: local climate, meteorology and topography. Furthermore, differences in anthropogenic and industrial activity, and typical energy sources and fuel type can also lead to variation in observed pollutants (Finlayson-Pitts and Pitts, 2000; Hopke et al., 2008; Lazaridis, 2011; Quan et al., 2014; Gulia et al., 2015; Meng et al., 2016).

1.3.2 Secondary Formation

Secondary aerosols are formed in the atmosphere through gas to particle conversion. Examples of common secondary aerosols are: nitrate, sulphate and oxidation products of volatile organic matter, which can be both natural or anthropogenic. A species is considered to be volatile if it easily evaporates at room temperature, while semi-volatile species will often partition between the liquid and gas phase. A significant proportion of $PM_{2.5}$ globally is formed in the atmosphere as secondary aerosols. Major secondary aerosols in the atmosphere are inorganic salts such as: sulfate, nitrate, and ammonium as well as a variety of organic compounds. These compounds are formed from precursor gases such as ammonia (NH_3), nitrogen dioxide (NO_2), sulphur dioxide (SO_2) and volatile organic compounds (VOCs). The gases undergo reactions in the atmosphere to form oxidised low volatility products which under favourable conditions rapidly condense onto existing particle surfaces (heterogeneous nucleation) or coagulate to form new particles (homogeneous nucleation). Homogeneous nucleation typically only occurs under low temperatures and when particle concentrations are sufficiently low. However, studies in urban environments show a high formation rate of new particles when gases released from combustion, such as traffic, cool rapidly due to exposure to ambient air. This formation of new particles ambiently can be observed by high concentrations of ultrafine particles (PM $<$ 100 nm). Formation rates of secondary aerosols are dependent on gaseous precursor concentration, particle size, availability of solar radiation and meteorological variables, specifically humidity. The conversion of sulphur dioxide (SO_2), nitrous oxides (NO_x) and ammonia (NH_3) into secondary inorganic aerosols such as sulphate (SO_4^{2-}), nitrate (NO_3^-) and ammonium (NH_4^+) is reasonably well understood, however the large number and variety of VOC's abundant in the atmosphere means formation mechanisms of secondary organic aerosols is less well characterised (Finlayson-Pitts and Pitts, 2000; McMurry, 2002; Molina and Molina, 2004; Seinfeld and Pandis, 2006a; Quan et al., 2014; Aksoyoglu et al., 2017).

Emissions of gases such as NOx, SO_2 and VOC's from traffic, industry and residential energy sources mean that concentrations of aerosol precursors in urban environments can be extremely high. This leads to high rates of secondary aerosol formation. Secondary aerosol formation is believed to be one of the most important factors explaining rapid increases in $PM_{2.5}$ concentrations during severe air pollution episodes. Huang et al. (2014) found that during haze episodes in four Chinese megacities, secondary aerosols contributed 30 - 77 % of average $PM_{2.5}$ and secondary organic aerosol (SOA) contributed 44-71

% of total organic aerosol. Furthermore, relative humidity (RH) is often enhanced during heavy pollution episodes which is proposed to further increases the rate of secondary aerosol formation. This can lead to rapidly increasing $PM_{2.5}$ concentrations under certain conditions (Molina and Molina, 2004; Huang et al., 2014; Zhong et al., 2018).

1.3.3 Removal

The removal of aerosol particles from the atmosphere is an essential process which can improve air quality in urban environments. Wet and dry deposition are the main ways in which aerosol particles are removed from the atmosphere. Dry deposition is the direct transfer of atmospheric species, either gaseous or particulate, to a surface and is most common for larger particles which can settle on the earth's surface due to gravity (Tomasi and Lupi, 2017b). Wet deposition encompasses all processes that lead to removal through precipitation, including dissolved atmospheric gases in cloud droplets, wash out by precipitation or removal through acting as cloud condensation nuclei (CCN). Factors that influence the deposition process include: surface type and terrain, size and shape of particles, chemical composition, precipitation, and atmospheric turbulence. Wet deposition can occur through several different processes including precipitation scavenging, cloud interception and fog and snow deposition, where precipitation scavenging is the main form of wet deposition and involves the removal of species by a raining cloud (Finlayson-Pitts and Pitts, 2000; Seinfeld and Pandis, 2006a; Kalberer, 2015).

High concentrations of aerosols can exist in urban environments for several days. These periods are often referred to as pollution episodes, smog or haze. To 'clean up' these episodes normally requires either strong winds to disperse and transport the pollutants out of the city or rain to wash them out. However, aerosol particles can interact with meteorology to enhance stabilisation and reduce wind speeds and precipitation, meaning these episodes can often occur for long periods. Aerosol properties such as size, composition and hygroscopicity will affect the ability of a particle to be removed through wet scavenging to become a cloud droplet, which under certain conditions can significantly decrease number concentrations of aerosols (Ohata et al., 2016). Several studies have linked both the onset and dissipation of pollution episodes to large scale circulations or changes in synoptic scale meteorology. This is well characterised in the megacity, Beijing. In Beijing, pollution episodes are often linked to the strength and direction of wind. Pollutants are often advected from southern industrial areas, while clean up of the episodes is linked to advection of cold clean air (Wang et al., 2014a; Zheng et al., 2015; Panagi et al., 2019). For example, in their characterisation of a heavy pollution episode which occurred between 1st and 4th December 2016 in Beijing, Wang et al. (2019) found that changes in synoptic conditions were responsible for atmospheric stagnation, which allowed for rapid accumulation of pollutants. Furthermore, they found that a change in the synoptic conditions resulted in strong winds on 4th December which allowed for pollutant dispersion.

1.3.4 Regional Transport

High concentrations of air pollutants are frequently observed in megacities. However, particulates can be transported large distances (100's to 1000's of kilometers), to severely impact air quality in surrounding regions. The transport of pollutants is highly dependent on the strength and direction of the prevailing winds. Most aerosols are emitted into and exist within the planetary boundary layer, which is the lowest layer of the atmosphere, impacted by interactions with the surface. Typically, if particles exist in the free troposphere (above the planetary boundary layer) they will be transported further, dependent on large scale atmospheric circulations. However, this regional transport of pollutants can also impact air quality in megacities themselves. Combined with local emissions from sources such as traffic and heating, regional transport of pollutants from surrounding industrial areas can lead to worsened air quality within urban cities. This is normally caused by the entrainment of polluted air aloft into the planetary boundary layer as it develops during the day (Figure 1.2) (Baklanov et al., 2016; Ma et al., 2017; Ji et al., 2019).

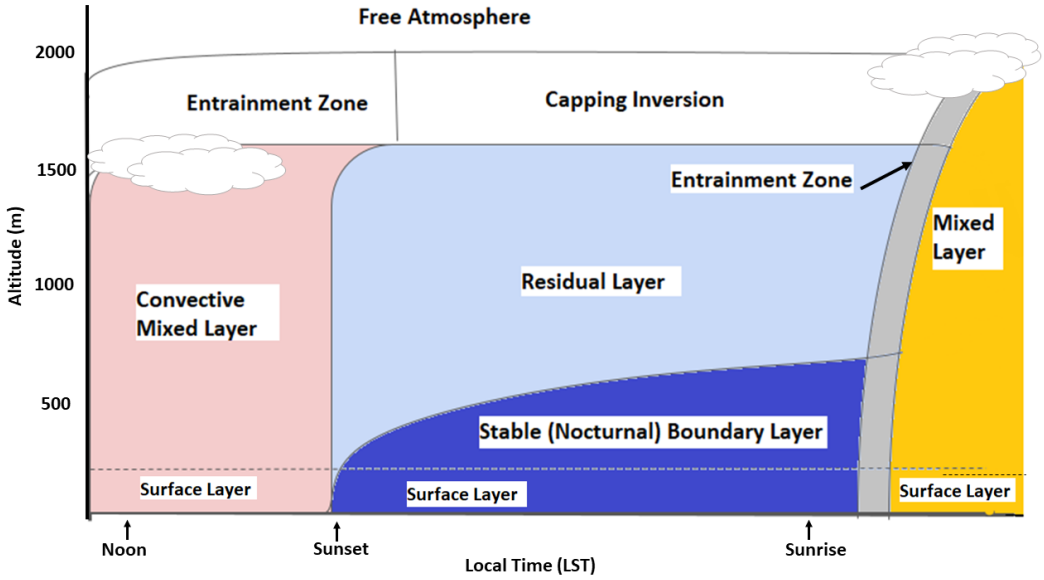

Figure 1.2: Schematic to show the diurnal cycle of the boundary layer and the structures within it. Adapted from Stull (2015)

1.3.5 Aerosol Size

The size of an aerosol particle impacts its atmospheric interactions, lifetime and surface reactivity. Atmospheric aerosols are a range of shapes and so for simplicity, size is defined according to a measured physical property. A common metric is the aerodynamic diameter, which is the spherical diameter of a particle with the same terminal velocity as the aerosol in consideration, defined as:

$$D_a = D_g \kappa \sqrt{\frac{\rho_p}{\rho_o}} \tag{1.1}$$

Where D_g is the geometric diameter, κ is the shape factor, ρ_p is the density of the particle and ρ_o is unit density (1 g/cm^3). Aerosols are often represented through size distributions. A particle size distribution presents concentration (usually mass or number) as a function of diameter or radius. From the size distributions, aerosol particles can be binned according to their diameter range to assist in categorising their behaviour in the atmosphere. The distinct size ranges are commonly described by 4 modes, which generally characterise the aerosol source, properties and reactivity in the atmosphere (Figure 1.3) (Finlayson-Pitts and Pitts, 2000; John, 2011; Kulkarni et al., 2011; Lazaridis, 2011).

Particles in the nucleation mode have diameters $<$ 10 nm and are either directly emitted or formed through nucleation in the atmosphere. These particles often have a short lifetime due to their fast coagulation rates. Typically, they will efficiently collide with and coagulate onto the surface of a larger particle. This process removes nucleation mode particles, while increasing average aerosol size. Gaseous precursors can also condense on the particle surface, causing them to grow in size. For this reason, urban aerosols in this size range are highest close to the emission source, decreasing in concentration away from the source due to atmospheric processing. Particles in the Aitken mode (10 nm $>$ 100 nm) typically form from such processing and can have significant lifetimes in the atmosphere, with most urban aerosols existing in this size range. Coagulation of these particles in the atmosphere and condensation of semi-volatile species on the particle core leads to growth to the accumulation mode (100 nm $<$ 1 μm). Furthermore, some particles in the accumulation mode can take up water to swell and grow significantly in size. Particle composition and water vapour concentrations affect an ambient aerosol particle's rate of water uptake. In cases where aerosols in the accumulation mode grow significantly, they may be removed through acting as cloud condensation nuclei (CCN) and becoming activated cloud droplets. However, under low humidity conditions, water and semi-volatile species can evaporate from the CCN to increase aerosol concentrations in the accumulation mode (Figure 1.1). Particle sources and atmospheric processing strongly impacts the size distribution of aerosol particles in the atmosphere, for example marine, arctic and urban aerosol size distributions vary greatly. The majority of urban aerosols typically have a size ranging between 20 nm $<$ 1 μm, predominantly existing in the Aitken and accumulation modes. Particles in the coarse mode ($>$ 1 μm) are present in urban environments due to mechanical processes such as road dust, construction activities and, brake and tyre wear. However, transportation of desert dust can also contribute significantly to increased levels of coarse particles. Typically, the number concentrations of larger particles is low, due to their short lifetime, however, due to their large size they can contribute large amounts to volume and mass distributions (Figure 1.3). (Seinfeld and Pandis, 2006a; Bloss, 2009; Boucher, 2013; Kalberer, 2015; Tomasi and Lupi, 2017a).

1.3.6 Chemical Composition

Aerosol composition is an important factor when understanding aerosol processes, aerosol-radiation interactions and aerosol toxicity (Lelieveld et al., 2015; Gilardoni and Fuzzi, 2017). Determining aerosol

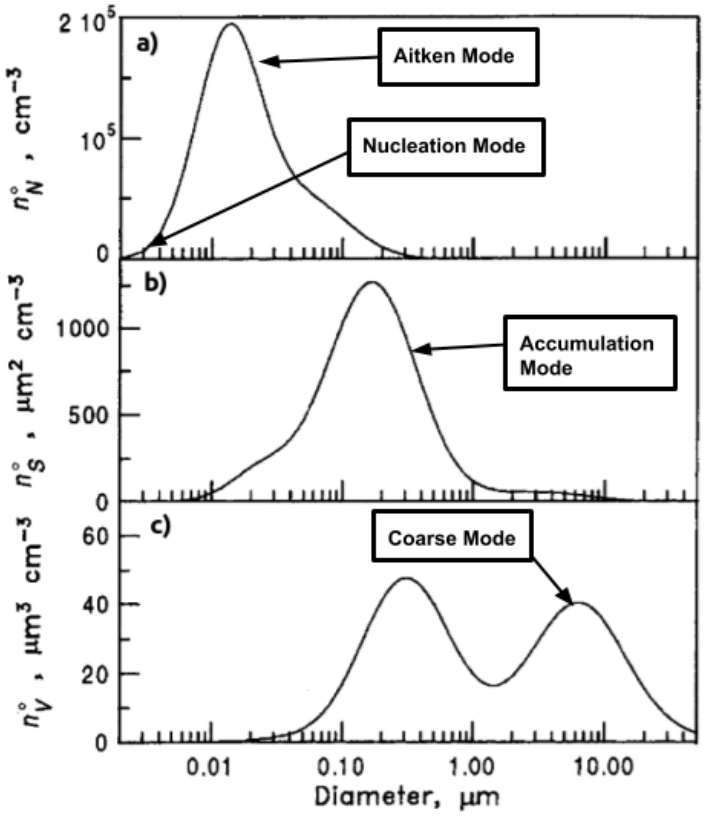

Figure 1.3: Typical urban log-normal aerosol size distribution. a) Number distribution, b) Surface distribution and c) Volume distribution. Plot taken from Seinfeld and Pandis (2006a)

composition is also useful in understanding sources of anthropogenic aerosols, particularly during heavy pollution episodes (Sun et al., 2006; Lv et al., 2016). Developments in measurement techniques have allowed for real time analysis of aerosol composition through the use of aerosol mass spectrometers (AMS) (Coe and Allan, 2006). Changes in composition over time result in high spatiotemporal variation and this can be monitored in order to better understand aerosol sources and processes. Analysis of compositional measurements can provide information on the relative contribution of primary and secondary aerosols to $PM_{2.5}$ concentrations. It can also allow for some understanding of whether pollutants have been locally emitted or regionally transported, which is useful when developing air quality policy (Finlayson-Pitts and Pitts, 2000; Pöschl, 2005; Seinfeld and Pandis, 2006a; Elser et al., 2016; Tomasi and Lupi, 2017a).

Particle mixing state, which is the distribution of chemical species within an aerosol, provides important information on surface reactivity of an aerosol particle and its optical properties. Aerosol mixing occurs primarily through particle coagulation and semi-volatile condensation. Aerosols can either be internally or externally mixed. When an aerosol is internally mixed, the different chemical species have mixed within the particle. In an ideal situation this would mean that all the aerosol particles have the same chemical composition and size distribution. If they are externally mixed, the particles have not chemically interacted with each other and each aerosol type will have a distinct chemical composition and size distribution. When there is condensation of a soluble species on an insoluble core, the particle is known to be externally mixed, with a distinct core and a surrounding coating or 'shell'. This type of mixing is common in black carbon (BC) and other insoluble particles such as dust (Jacobson, 2005; Lazaridis, 2011;

Boucher, 2013).

Black carbon (BC) is a well known primary aerosol emitted from incomplete combustion and is prevalent globally, with high concentrations found in urban environments, particularly in Indian and Chinese megacities. BC is of particular interest due to its ability to strongly absorb light in the visible spectrum, which has a positive radiative forcing effect on the atmosphere and has potential implications for global climate . BC is emitted directly into the atmosphere as a by-product of carbonaceous combustion or biomass burning. However, BC morphology, structure and size varies greatly, changing during its lifetime in the atmosphere. BC undergoes processing in the atmosphere, known as atmospheric aging. Gas phase condensation of other particles on the BC surface and coagulation with other particles can alter the mixing state of BC affecting its physical and chemical properties (Jacobson, 2001; Cappa et al., 2012; Bond et al., 2013; Wang et al., 2015; Liu et al., 2017, 2018a, 2020).

Quantification of BC radiative forcing is dependent on the magnitude and type of mixing. Liu et al. (2018a) found that the mixing state of black carbon impacts its ability to absorb radiation. Their results found that particle mixing was impacted by the source of BC and the length of time it had spent in the atmosphere. Freshly emitted particles in Beijing, from traffic, were found to be externally mixed, and aged particles, from biomass burning, were found to be internally mixed. Furthermore, their research found that black carbon particles, internally mixed with non-black carbon particles, resulted in an absorption enhancement of the BC core by the non-BC coating. The magnitude of this absorption enhancement was found to be dependent on the ratio of non-BC to BC mass in the particle and its mixing state.

1.3.7 Aerosol Hygroscopicity

The processes that urban aerosols undergo in the atmosphere are dependent on their physiochemical properties, as described above. These properties are further affected by the amount of water in the particle. The proportion of water that contributes to fine aerosols is dependent upon the relative humidity of the aerosol environment but also on the hygroscopicity of components within the aerosol (Friedlander, 2000). Aerosol hygroscopicity is size and composition dependent and describes the ability of an aerosol particle to absorb water as a function of RH. The ratio between a particle's wet diameter (diameter including condensation of water vapour) at high RH and its corresponding dry diameter describes its ability to take up water. This is known as the aerosol hygroscopic growth factor and is highly dependent on aerosol composition (Chen et al., 2019; Tang et al., 2019). The rate and extent of water uptake by an aerosol particle is also dependent on the amount of water vapour available in the atmosphere. High ambient humidity will cause soluble aerosols to grow in size, leading to decreased visibility as the mass scattering efficiency of aerosols increases. For this reason, it is important to consider aerosol hygroscopicity when examining aerosol-radiation interactions. Furthermore, aerosol liquid water content and size also strongly affect the rate of heterogeneous surface reactions and the rate of gas condensation on the aerosol surface. Consequently, aerosol hygroscopic growth can lead to higher rates of secondary aerosol formation, which

can contribute significantly to air pollution. Furthermore, if particle takes on enough water it may activate into a cloud droplet, which may impact cloud properties, with potential impacts for climate (Boucher et al., 2013; Kreidenweis and Asa-Awuku, 2013).

Inorganic salts, such as nitrates, sulphates and chlorides are extremely hygroscopic and take on water even at low RH, whereas black carbon (BC) is much less likely to take on water at all RH values. However, particle mixing state and atmospheric processing also impacts aerosol hygroscopicity. For example, in the atmosphere BC often undergoes atmospheric processing termed 'aging' where semi-volatile species condense on a BC core (Valsaraj and Kommalapati, 2009). Zhang et al. (2008) found that when sulphuric acid vapour condenses on a BC particle, the particle experiences substantial hygroscopic growth under subsaturated conditions (RH $<$ 90 %).

1.4 Air Pollution and Health

Particulate matter (PM), is a term used to describe total suspended aerosol particles, particularly in relation to their health effects. Commonly used indicators of describing air quality or levels of air pollution are mass concentrations of PM_{10}, (PM with a diameter $<$ 10 μm) and $PM_{2.5}$, (PM with a diameter $<$ 2.5 μm). $PM_{2.5}$ is of particular interest due to its ability to penetrate into airways, alveoli and the blood stream. This can cause: problems with the immune system, inflammation of the lungs, heightened allergic symptoms, and accelerated atherosclerosis. $PM_{2.5}$ is also a carrier of toxic compounds including chemical elements and heavy metals, which can cause damage to chromosomes and DNA (WHO, 2000; Lv et al., 2016). Exposure to PM is linked to cardiovascular and respiratory disease, with responses being both acute and chronic. Air pollution has thus far been linked to increased rates of chronic obstructive pulmonary disease (COPD), lung cancer, acute lower respiratory illness (ALRI) and ischaemic heart disease (IHD). Furthermore, increased risks of dementia, Parkinson's disease and multiple sclerosis have also been cited as potential health impacts (Zhang et al., 2010; Chen et al., 2017). Exposure to $PM_{2.5}$ has been linked to reduced life expectancy, representing around 7 % of total global deaths; 59 % of these in South and East Asia (Cohen et al., 2017). It is therefore clear that $PM_{2.5}$ exposure has a large human health impact, however, despite several countries and the World Health Organization (WHO) implementing air quality standards with strict $PM_{2.5}$ limits, scientific understanding on the safe level of $PM_{2.5}$ exposure is not clear (Lelieveld et al., 2015).

Research assessing the health impacts of $PM_{2.5}$ are numerous, and include extensive epidemiological and toxicological studies (WHO, 2006). Epidemiology is the study of the prevalence and cause of diseases in different population groups. These studies are essential in finding links between concentrations of ambient PM and the prevalence of cardiovascular or respiratory disease (Coggon et al., 2003). An exposure assessment from 22 European cohort studies looked at the effect of long term PM exposure on natural mortality. The results show a statistically significant association between $PM_{2.5}$

exposure and mortality of a natural cause. This was found even for $PM_{2.5}$ exposure of less than the existing WHO guidelines (annual 24-hourly average value of 25 $\mu g/m^3$), suggesting that there may be no safe level of exposure (Beelen et al., 2014). Furthermore, several studies have outlined the difference in toxicity for components of $PM_{2.5}$, with some sources of pollution known to be more damaging than others. For example, Park et al. (2018) found that particles produced from combustion are more toxic to human health compared to other sources, with particularly high toxicity found for vehicular emissions (diesel and gasoline). Understanding of particle sources in the atmosphere and their toxicity can therefore allow for better and more informed policy targeting of specific emission sources.

Air pollution is a significant issue in densely populated urban areas. Rapid economic growth and industrialisation in South and Eastern Asia particularly has led to an increase in megacities (cities with a population greater than 10 million), with air quality issues. The impact of this is two-fold: megacities tend to have high emissions, as well as having large populations, which are consequently exposed to pollutants. This leads to a high impact per pollutant concentration on human health. Health impacts of air pollution have been observed to increase rapidly with increasing city and population size Gurjar et al. (2008, 2010); Krzyzanowski et al. (2014); Marlier et al. (2016); Liu et al. (2018b). The main sources of increased air pollution in developing countries are : private vehicle use, biomass and coal burning for residential uses such as heating and cooking and nearby industrial emissions (Molina and Molina, 2004). Overall, it is estimated that 96 % of people living in the 10 largest cities are exposed to $PM_{2.5}$ concentrations higher than the WHO guidelines, with China and India having the highest premature mortality linked to outdoor air pollution in 2010 (Lelieveld et al., 2015). Furthermore, from 1960 to 2009, $PM_{2.5}$ concentrations increased by 38 % globally, while deaths attributed to air pollution increased by a minimum of 89 % over the same period. These increases were predominantly dominated by large increases in China and India, with slight decreases in Western Europe and the United States (Butt et al., 2017). Figure 1.4 shows the association with the location of megacities, concentrations of $PM_{2.5}$ and deaths attributed to air pollution. There is a clear correlation between the prevalence of megacities, annual $PM_{2.5}$ concentrations and deaths attributed to outdoor air pollution, which are high in China and India.

Epidemiological evidence clearly shows the negative health impacts associated with poor air quality, while toxicological studies show that the magnitude of the health impact is dependent on the properties of the pollutants. It can therefore be considered essential for human health to understand the composition and size of pollutants in the urban atmosphere, as well as their sources (Davidson et al., 2005; Maynard, 2009). A major limitation in tackling urban air pollution is the reliability and scope of measurements in the region. Furthermore, particles in the atmosphere undergo a variety of chemical and physical transformations and so their physicochemical properties at emission source, or at a measured point in the atmosphere, may change prior to human exposure. Therefore, even understanding the sources of PM in a region will not directly correlate to understanding exposure in that same area (Russell and Brunekreef, 2009; Fuzzi et al., 2016; Liu et al., 2016). Composition and characteristics of $PM_{2.5}$ are globally varied and tend to depend on the aerosol source and atmospheric conditions, with strong observed spatiotemporal

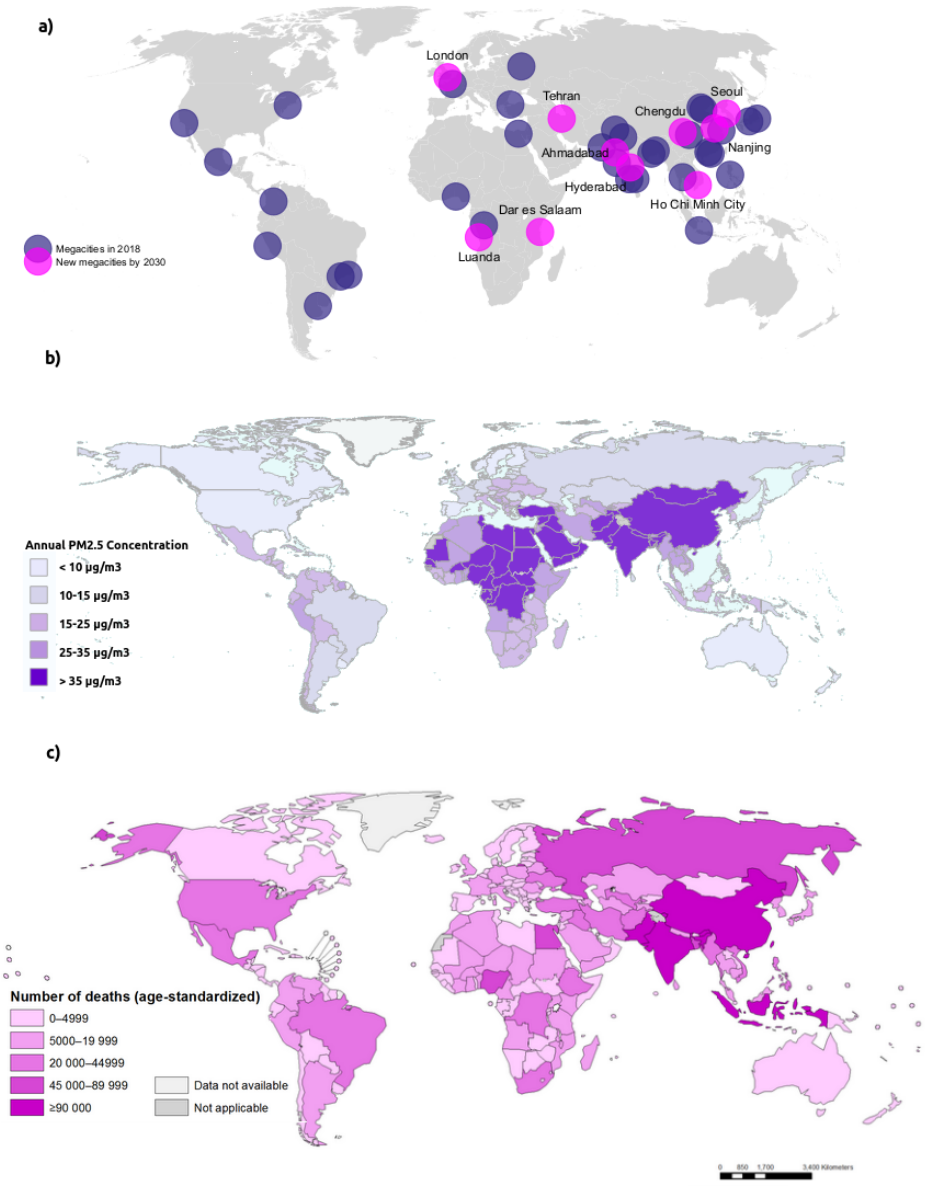

Figure 1.4: a) Distribution of megacities around the world in 2018 and projected megacities by 2030 (United Nations, 2018), b) Annual mean $PM_{2.5}$ concentrations in urban areas (2016) (World Health Organization, 2018b) and c) Deaths attributed to ambient air pollution (age standardised) for 2012 (World Health Organization, 2018a).

variations (Davidson et al., 2005). Characterisation of aerosol sources, properties and the processes which occur in the atmosphere will therefore help understand the health impacts of air pollution on human health and allow for targeted policy to improve air quality in urban environments.

1.5 Aerosols and Climate

Through directly interacting with radiation and clouds, aerosols can have a significant effect on global climate. This is particularly important in urban areas where concentrations of aerosols are high. Interactions of aerosols, can affect atmospheric temperatures, cloud cover, and both local and regional meteorology. It is essential to fully understand these interactions to better constrain and parameterise climate and air quality models.

1.5.1 Aerosol-Radiation Interactions

Aerosols are considered important due to their health impacts but also for their role in affecting the climate, both directly through radiative forcing and also through changing the properties of clouds. Aerosol radiative forcing is the perturbations caused by aerosol-radiation interactions to radiative fluxes in the atmosphere, and is one of the most uncertain components in the climate system. Overall aerosols are believed to have a global cooling effect, with a direct radiative forcing between -0.95 to + 0.05 W/m^2. Aerosol radiation interactions (ARI) describe the absorption or scattering of solar radiation by aerosol particles to alter the global radiative flux at: the surface, top of the atmosphere (TOA) and within the atmospheric column. Atmospheric aerosols can interact with both shortwave (SW) and longwave (LW) radiation. The magnitude and type of the interaction is mostly dependent on aerosol size and composition, which influence the aerosols optical properties. Aerosols such as black carbon and mineral dust can absorb SW radiation to heat the atmosphere, while inorganic aerosol particles such as sulphate, scatter solar radiation, resulting in surface cooling (Yu et al., 2006; Boucher, 2013; Boucher et al., 2014; Fu, 2015).

Factors that influence the scattering and absorption of light by a particle are: particle size, composition and wavelength (λ) of incident radiation. Types of light scattering mechanisms include: elastic scattering, when the λ of emitted radiation is the same as the incident radiation, and inelastic scattering, when the λ of emitted radiation is shifted compared to the λ of the incident beam. Elastic scattering is the main way in which aerosols interact with radiation in the atmosphere, and is described mathematically in two main ways: Rayleigh and Mie scattering. Particle size relative to the λ of the interacting radiation will impact the relative strength and type of the scattering. Rayleigh scattering describes interactions when the particle diameter is much smaller than the λ of incident radiation (normally particles with a diameter < 100 nm). Particles in this range scatter and absorb light in the shortwave (solar radiation) to a much higher extent than longwave (terrestrial) radiation. Mie scattering covers a wider range of particle sizes, particularly those whose diameter is similar to the λ of incident radiation (Seinfeld and Pandis, 2006b; Kokhanovsky, 2008; Fu, 2015).

In terms of their direct radiative effect, aerosols can be divided into those that scatter incoming radiation, thereby having a cooling effect, and those that absorb radiation creating a net warming effect.

The scattering efficiency of a particle, Q_{scat}, can be described by its scattering cross section, C_{scat} divided by the cross-sectional area of the particle ($A = \pi r^2$). Where C_{scat} is related to the intensity of incident radiation (I_0), the intensity of scattered radiation (I_{scat}) and the surface of the particle (S) (Eq. 1.2-1.3) (Seinfeld and Pandis, 2006b).

$$C_{scat} = \frac{1}{I_0} \int I_{scat} dS \tag{1.2}$$

$$Q_{scat} = \frac{C_{scat}}{A} \tag{1.3}$$

The absorption efficiency of a particle Q_{abs} is described by its absorption cross section (C_{abs}) divided by the cross sectional area, A. Where C_{abs} is related to the wavelength of radiation ($k=\frac{2\pi}{\lambda}$) the particle volume, V, the electric vector of the incident wave ($|\vec{E_0}|$), the electric vector of the scattered light ($|\vec{E}|$ and the absorption (χ) and scattering (n) parts of the refractive indices (Eq. 1.4-1.5).

$$C_{abs} = \frac{k}{|\vec{E_0}|^2} \int_V |\vec{E}|^2 (2n\chi) dV \tag{1.4}$$

$$Q_{abs} = \frac{C_{abs}}{A} \tag{1.5}$$

The refractive index of a particle characterises the way an aerosol particle will interact with various wavelengths of electromagnetic radiation. The refractive indices is composed of a scattering (real) part and absorbing (imaginary) part, which combined will provide information on the interaction of the particle with radiation. Each part of the refractive index is mainly dependent on its chemical composition and the wavelength of radiation under consideration and takes the form ($m = n + i\chi$).

The extinction of an aerosol medium, is the sum of the scattering and absorption components and overall describes the interaction of radiation as it passes through an aerosol column. The aerosol extinction coefficient (σ_{ext}) is related to the size averaged extinction cross section ($\overline{C}_{ext}$) and the number of particles in a given volume (N) (Eq. 1.6-1.7) Kokhanovsky (2008, 2016)

$$C_{ext} = C_{scat} + C_{abs} \tag{1.6}$$

$$\sigma_{ext} = N\overline{C}_{ext} \tag{1.7}$$

Direct radiative forcing by aerosol particles is not only linked to their individual properties but also the vertical distribution and total concentration of aerosols throughout the column, otherwise known

as the aerosol optical depth (AOD), which is the sum of extinction in each layer across the depth of the column (Eq. 1.8). This information tells us how much of solar incident radiation reaches the surface. Furthermore, if the incidence of radiation at TOA and at the surface under clear sky conditions is known, the AOD can provide information on the amount of attenuation caused by aerosols, which can allow for estimates of aerosol mass concentrations in the column.

$$\tau = \int_{Surf}^{TOA} \sigma^{ext}(z).dz \tag{1.8}$$

The surface albedo, describes the fraction of solar radiation which will get reflected back to space after reaching the surface. Consequently, the extent to which an absorbing or scattering aerosol layer has a net negative or positive radiative effect also depends on whether it is over a low or high albedo surface. For example, absorbing aerosols will have little effect on top of the atmosphere (TOA) short wave incoming solar radiation if the surface below is already dark and highly absorbing, as the relative increase in absorption will be low. These types of surface are common in cities. On the other hand if the underlying surface is bright, for example a cloud top or an arctic surface, then a partially absorbing aerosol layer above will lower the effective surface albedo and ability to reflect solar radiation. Thus the enhancement of absorption and consequently warming due to aerosols will be higher (Valsaraj and Kommalapati, 2009; Bond et al., 2013; Myhre et al., 2013; Fu, 2015).

An effective way to understand the impact of aerosol-radiation interactions in the atmosphere and their dependencies is through the use of a radiative transfer model. This can allow for understanding of the importance of factors such as aerosol composition, aerosol size and vertical distribution of the aerosol layer on scattering and absorption of solar radiation. Mishra et al. (2015) used a radiative transfer model to examine the impact of aerosol vertical distribution on the aerosol radiative effect. They varied the vertical aerosol profiles for four different aerosol types: dust, polluted dust, pollution and pure scattering aerosols. Overall, they found that the aerosol-radiative effect variation with height is dependent on both the type of aerosol and the wavelength of incident radiation. In a study of biomass burning aerosols, Johnson et al. (2008) showed that a low-level dust layer increased the absorption by biomass burning aerosol, due to the low level dust back-scattering solar radiation which was then absorbed by the biomass burning layer.

The sign and magnitude of aerosol's radiative forcing is dependent on bothe the aerosol properties and the albedo and properties of the underlying surface. However, aerosols can also alter the Earth's radiative budget through interacting with radiation to affect cloud properties. This is known as the semi-direct effect. The semi-direct effect can have either a positive or negative radiative forcing and is dependent on the cloud and aerosol properties. Clouds have a cooling effect on the atmosphere and so any process which reduces cloud cover will have a positive radiative forcing, while processes that enhance cloud cover will have a negative radiative forcing effect. Heating in the atmosphere by aerosols can reduce relative humidity (RH) in the planetary boundary layer (PBL), which reduces cloud formation at low altitudes. Furthermore, heating of the atmosphere can also cause evaporation of cloud droplets, further reducing cloud

cover. However, if scattering aerosols cause a cooling in the atmosphere this can have the opposite effect, increasing RH and cloudiness. Furthermore, in stratocumulus clouds, an absorbing aerosol layer above the cloud top has shown to strengthen temperature inversions, reduce entrainment of dry air, and enhance cloudiness (Ramanathan et al., 2001; Johnson, 2003; Johnson et al., 2004; Fiore et al., 2012; Tao et al., 2012; Boucher, 2013; Archer-Nicholls et al., 2016). In a recent study Herbert et al. (2020) used a Large Eddy Simulation (LES) model to examine the impact of various properties of absorbing aerosol layers on cloud and PBL dynamics. They find that an absorbing aerosol layer above cloud top increases the temperature inversion at PBL (cloud) top through warming the layer above. This reduces buoyant turbulent motion and the rate of entrainment, as more energy is required to overcome the larger temperature inversion at PBL top. Consequently, there is a reduction of entrainment of clean, warm, dry air, which suppresses PBL development, reduces cloud top height and enhances cloudiness. This produces an overall negative radiative forcing due to the clouds cooling effect on the climate.

1.5.2 Aerosol-Cloud Interactions

An aerosols ability to directly impact cloud formation through acting as cloud condensation nuclei (CCN), is known as the aerosol-indirect effect. By acting as CCN, anthropogenic aerosols modify the number concentration and size of cloud water droplets, leading to changes in cloud albedo. High aerosol concentrations can lead to increased numbers of CCN. This will mean that under the same atmospheric conditions (the same concentrations of water vapour) there will be less water vapour per CCN to condense onto the particle core. Consequently, there will be an increase in the number of cloud droplets but a reduction in the average size of each cloud droplet. This generally increases cloud coverage and lifetime through suppressing precipitation. However, aerosol impacts on precipitation are affected by cloud type, cloud depth and aerosol concentrations, further complicating the climatic impacts of aerosols (Twomey, 1977; Albrecht, 1989; Andrejczuk et al., 2010; Ekman et al., 2011; Li et al., 2011; Cheng et al., 2016a; Malavelle et al., 2017)

1.6 Urban Environments

The number of people living in urban environments is constantly increasing. As of 2018, 55.3 % of the world's population lived in urban settlements, this is expected to increase to 60 % by 2030 (United Nations, 2018). Increasing urban populations causes changes to the natural environment. Urban and rural environments have different characteristics which impact the development of the boundary layer and its structure. The urban heat island (UHI) effect describes the higher temperatures observed in urban areas compared to surrounding areas. The energetic basis for the UHI can be described through alterations to the surface energy balance equation (Eq. 1.9). Alterations include changes to the rate of heat storage (Q_s) and the inclusion of an anthropgenic heat flux (Q_f). The urban environment typically has higher sensible

heat flux, lower latent heat flux and slightly higher planetary boundary layer height than comparable suburban or rural areas. This is due to higher heat storage (Q_s) in urban environments caused by higher surface heat capacity, lower thermal conductivity and reduced water volume fraction of urban surfaces. Typical considerations when examining the urban boundary layer include surface type, surface roughness and surface heterogeneity. Surface type will impact the storage and re-release of heat. Surfaces with high heat capacity such as concrete, delay the release of heat, which consequently reduces the impact of nocturnal radiative cooling and allows for a turbulent boundary layer to exist longer through the night. Increased surface roughness can lead to stronger turbulent motion under high wind conditions, while the typical layout of a city can lead to the formation of an urban canopy which inhibits pollutant dispersion (Oke, 1973, 1982; Grimmond et al., 1991; Grimmond and Oke, 1999; Barlow, 2014a).

A heat flux caused by human activities, known as the anthropogenic heat flux (Q_f), is thought to impact urban meteorology. The anthropogenic heat flux can be split into contributions from vehicles (Q_v), buildings (Q_b) and human metabolic activity (Q_m) (Eq. 1.10). Due to its varied nature, calculations of both anthropogenic heat flux and urban heat storage are often difficult to perform. Most estimates use the surface energy balance scheme (Eq. 1.9) and measurements of net radiation (Q*), sensible (SHF) and latent heat fluxes (LHF), with Q_s and Q_f as the remaining fractions. Grimmond et al. (1991) developed an objective hysteresis model (OHM), to incorporate an equation to estimate urban heat storage (Eq 1.11) where $\frac{\Delta Q^*}{\Delta t}$ has units W/m^2h^{-1} and relates the change in radiation (ΔQ^*) over time (Δt). The coefficients a_1, a_2 and a_3 are dependent on land cover and have no units, hour and W/m^2 respectively. Values of these coefficients for roof, green space, canyon and paved environments have been calculated and can be found in Grimmond et al. (1991). Their work found that this equation worked well for calculation of daytime heat storage but was not efficient at estimating nocturnal heat storage which is assumed to be significantly lower.

$$Q^* + Q_f = SHF + LHF + dQ_s \tag{1.9}$$

$$Q_f = Q_b + Q_v + Q_m \tag{1.10}$$

$$Q_s = a_1 Q^* + a_2 (\frac{\Delta Q^*}{\Delta t}) + a_3 \tag{1.11}$$

Estimates of anthropogenic heat flux in urban environments are strongly linked to emissions. Allen et al. (2011) developed the large scale urban consumption of energy (LUCY) model to simulate the anthropogenic heat flux on the city and global scale, finding large variations within countries, cities and seasons as well as diurnally. Globally on average Q_f is higher on weekdays and in winter. Heat from metabolic activity (Q_m) generally has the lowest contributor to Q_f and is often based on population data assuming an average metabolic activity per person, however this can be outdated. Q_v can be calculated based on vehicle fleet, number and average speed, with typical peaks around rush hour due to the association with traffic emissions. Heat from buildings (Q_b) is the largest contributor to Q_f, it can be divided into sectors (industrial, commercial, residential and non-residential) with estimates normally coming from either energy consumption estimates or through grouping by building type using land use data.

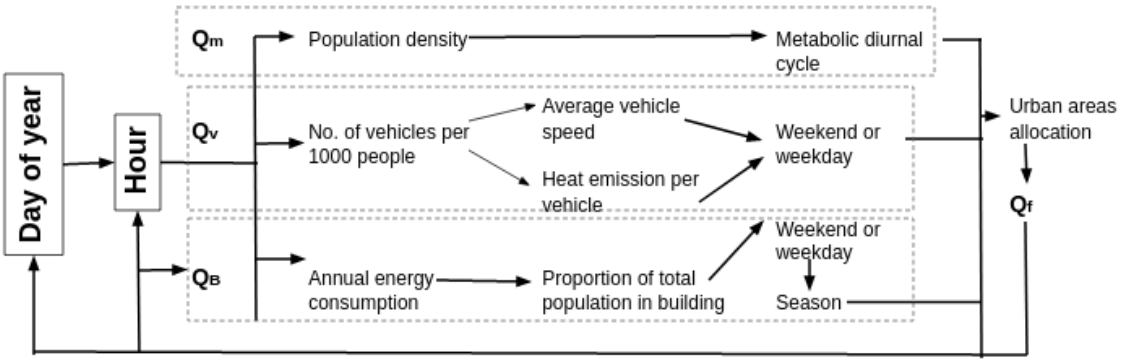

Figure 1.5: Outline of the workings of the LUCY model and overall things to consider when calculating the anthropogenic heat flux (Q_f) (Allen et al., 2011)

Dou et al. (2019) estimated the anthropogenic heat flux for Beijing summertime using the large scale urban consumption of energy (LUCY) model. Through making assumptions on vehicle fleet and vehicle speed, as well as performing footprint analyses and detailed surface properties, they found that the mean midday Q_f value was 67.2 W/m^2 while the contributions of sensible heat flux (SHF) and latent heat flux (LHF) were 94.3 and 96.4 W/m^2 respectively. This indicates that the contribution of Q_f to the urban surface energy balance scheme in certain conditions may be similar in magnitude to that of SHF and LHF.

The differences between urban and rural environments is important for understanding of pollutant dispersion. The contribution of anthropogenic heat flux (Q_f) and urban heat storage (Q_s) to the urban surface energy balance reduces nocturnal cooling and increases turbulence in the urban boundary layer. This can act to enhance the vertical mixing of pollutants. Urban areas are further impacted by the urban layout. Specifically, the height and distribution of buildings, streets and parks, varies the roughness of the surface, which can create strong mechanical turbulence. The layout of buildings and streets in cities can create an urban canopy layer, which typically decreases surface wind speeds and consequently the distribution of pollutants (Grimmond et al., 1991; Cao and Lin, 2014; Tao et al., 2016; Auvinen et al., 2020).

The urban heat island effect, which causes urban areas to be warmer than their surrounding areas, can enhance the dispersion of pollutants. As temperatures in the lower atmosphere are higher in urban environments, this causes a larger level of turbulent mixing due to buoyancy. This leads to a higher maximum PBL height, particularly through the evening and night time. This can lead to less stagnation and a higher vertical distribution, causing less pollutants to be concentrated at the surface. This is evidenced by urban areas often having higher maximum PBL height compared to rural areas (Barlow, 2014b). This effect works in contrast to the effect of aerosols in cooling the surface layer and increasing stagnation. As urban environments, such as cities, often also have higher aerosol concentrations compared to rural environments, these effects work in contrast to each other. However, the magnitude of each effect and which will have the largest impact is dependent on several factors including aerosol concentrations, composition and size,

the strength of the UHI effect in a particular area (governed by the variables outlined in the previous paragraphs) as well as the meteorology at the time. Under conditions where aerosol concentrations are very high in urban areas, the effect of aerosols on PBL height and vertical mixing is likely to be a more important process.

1.7 Aerosols and the Planetary Boundary Layer

Aerosols are emitted into and primarily exist in the planetary boundary layer (PBL), here they interact with radiation to impact boundary layer meteorology such as temperature, humidity and wind speed. They can cause large alterations to the thermal profile of the PBL which has significant impacts on turbulent motion and pollutant dispersion. This is believed to be important for heavy pollution episodes in urban environments. This section details the processes affecting the PBL and the perturbations caused by aerosols.

1.7.1 The Planetary Boundary Layer

The lower layer of the atmosphere which is directly affected by the change in radiative flux is known as the planetary boundary layer (PBL). The PBL experiences a diurnal cycle which impacts temperature, humidity, wind speed and direction, as well as causing variations in pollutant levels. Most pollutants will typically be emitted into and reside in the PBL. The height of the PBL varies regionally, seasonally and has a distinct diurnal profile. It is an important factor determining the intensity of air pollution due to its strong impact on the vertical dispersion and distribution of pollutants. The average height of the boundary layer is usually 1-2 km although this varies greatly with region and time. In polluted conditions, maximum PBL height can be < 500 m (Wang et al., 2019). PBL development is strongly dependent on turbulent motion which can be both formed through buoyancy or mechanical shear (Stull, 2015).

During the daytime, a well mixed boundary layer typically forms due to shortwave (SW) radiative heating of the surface. However, during the evening, the turbulently mixed PBL collapses due to longwave (LW) radiative cooling from the surface, to leave a static shallow boundary layer under a neutral residual layer. The residual layer contains all moisture and pollutants from the well mixed boundary layer of the previous day, but is not turbulent (Figure 1.2). The turbulence of the layer is important to consider when examining urban air quality due to its impact on PBL height and pollutant dispersion. Turbulence in the PBL is primarily caused by eddies. Eddies are rotating motions of air caused by strong wind shear and buoyancy. Heating of air by the surface causes the air to rise, forcing the air above it to sink to replace the rising air thus causing a system of circulation. Through these circulations of air, eddies transfer momentum, energy, gases and particles both vertically and horizontally. This governs the vertical mixing of pollutants in the PBL (Jacobson, 1997; Lazaridis, 2011; Stull, 2015).

The free troposphere, which exists above the PBL is not impacted by heating of the surface. In

the free troposphere, temperature decreases rapidly with height. A large temperature change between the top of the PBL and the free troposphere, known as a temperature inversion, creates an extremely stable zone which acts to trap air in the PBL. During the daytime, this zone is turbulent and is known as the entrainment zone, while at night, the turbulence in this zone stops, forming a stable layer known as a capping inversion. PBL development typically experiences a clear diurnal cycle. When the surface is heated during the day, it warms the air at the surface which rises through buoyant motion until it reaches the entrainment zone. These thermal movements result in pollutants and moisture being vertically well mixed throughout the PBL. Although the air from the mixed layer cannot escape through the entrainment zone to mix with the free atmosphere, the entrainment zone can bring in clean, dry air from the free troposphere into the mixed layer. This maximises the amount of mixing that can occur, increasing the height of the PBL, to effectively dilute pollution. However, if the residual layer contains pollution, the pollutants can be entrained into the PBL as it develops through the day, effectively increasing pollutant concentrations. At night, the lower boundary layer is cooled through interaction with the radiatively cooling surface, which forms an unmixed, stable layer. Above this, a residual turbulent layer can exist which is not affected by the cooling of the surface. As the air close to the surface is now cooler than that above it, this inhibits the buoyant movement of air parcels and so the layer has low turbulence. The capping inversion cannot bring in clean dry air like the entrainment zone and therefore PBL height remains shallow (Figure 1.6) (Jacobson, 1997; Seinfeld and Pandis, 2006b; Stull, 2015).

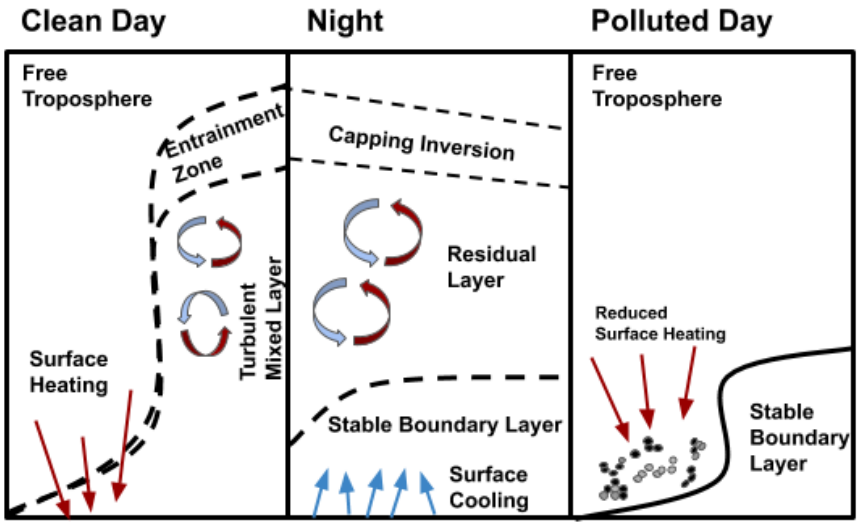

Figure 1.6: Outlines of the typical processes and interactions of the planetary boundary layer on a clean day, overnight and on a polluted day(Stull, 2015)

In addition to the diurnal cycle, the PBL structure also experiences seasonal variations. Summer time is characterised by longer days and shorter nights, amplifying the effects of warming on the surface layer and the creation of a vertically well mixed boundary layer. In the winter, this effect is usually reversed. The most important factor affecting the stability of the boundary layer is the temperature difference between the surface and the air above it. Consequently, the boundary layer structure and evolution is extremely dependent on several other factors including clouds and aerosol concentrations, and the properties of the

surface. Clouds will both reduce the amount of SW radiation reaching the surface and reflect LW radiation back to the surface, to potentially have alternative impacts on PBL development. Thus the impact of clouds on PBL structure will depend on cloud type, cover, thickness and altitude of the cloud layer. Similarly, high concentrations of aerosol particles are expected to cool the surface while warming the atmosphere; this can increase boundary layer stability and suppress PBL development. However, black carbon (BC) a strong absorber of SW radiation, will warm the atmosphere and depending on its concentration and the altitude of the aerosol layer could enhance PBL development. Consequently, the effect of aerosols on PBL development is dependent on aerosol concentrations, composition, size and the vertical profiles of the various aerosol layers (Wang et al., 2014b; Stull, 2015; Ding et al., 2016; Petäjä et al., 2016).

1.7.2 Aerosol-PBL interactions

Aerosols can impact PBL development through interacting with radiation and altering the thermal profile of the atmosphere. Urban aerosols scatter and absorb incoming solar radiation, to reduce the amount of shortwave radiation reaching the surface. This reduces the amount of SW radiation available to be absorbed and re-emitted by the surface to warm the air above the ground. This reduction results in less thermal energy at the surface and can significantly reduce buoyant turbulence. Consequently, this impacts the growth of the PBL which has been observed to be shallower on days where pollution is high. A shallow boundary layer feeds back to result in further aerosol accumulation which consequently causes more interactions between aerosols and radiation (Figure 1.7). A shallow boundary layer will also result in an increase in water vapour concentrations, causing hygroscopic aerosols to swell and grow in size and thus enhancing the aerosol-radiation interactions. Furthermore, high humidity will also enhance aqueous heterogeneous interactions, thereby increasing the rate of secondary aerosol formation through gas to particle condensation reactions (Gao et al., 2015; Ding et al., 2016; Petäjä et al., 2016; Li et al., 2017; Wu et al., 2019).

1.7.3 The Role of Absorbing Aerosols

Black carbon (BC) is a strongly absorbing aerosol, present in the atmosphere due to combustion processes. Through absorbing SW radiation, BC causes atmospheric warming, which has impacts for climate but also local meteorology. BC could either enhance or suppress the aerosol-PBL feedback effect, depending on several factors, the most important of which is believed to be the altitude of the aerosol layer. Ferrero et al. (2014) examined the impact of the altitude of BC and its effect on PBL dynamics over the Italian basin valleys. Their results found that the effect of BC was to promote atmospheric instability, weakening the temperature inversion and promoting dissipation of pollutants. This was due to the larger effect of BC surface heating compared to BC aloft. However, when examining the role of BC on aerosol-PBL interactions in 3 megacities in China, Ding et al. (2016) found the opposite effect. Their results show that BC aloft has a higher heating efficiency per unit of BC, and causes cooling below and heating above

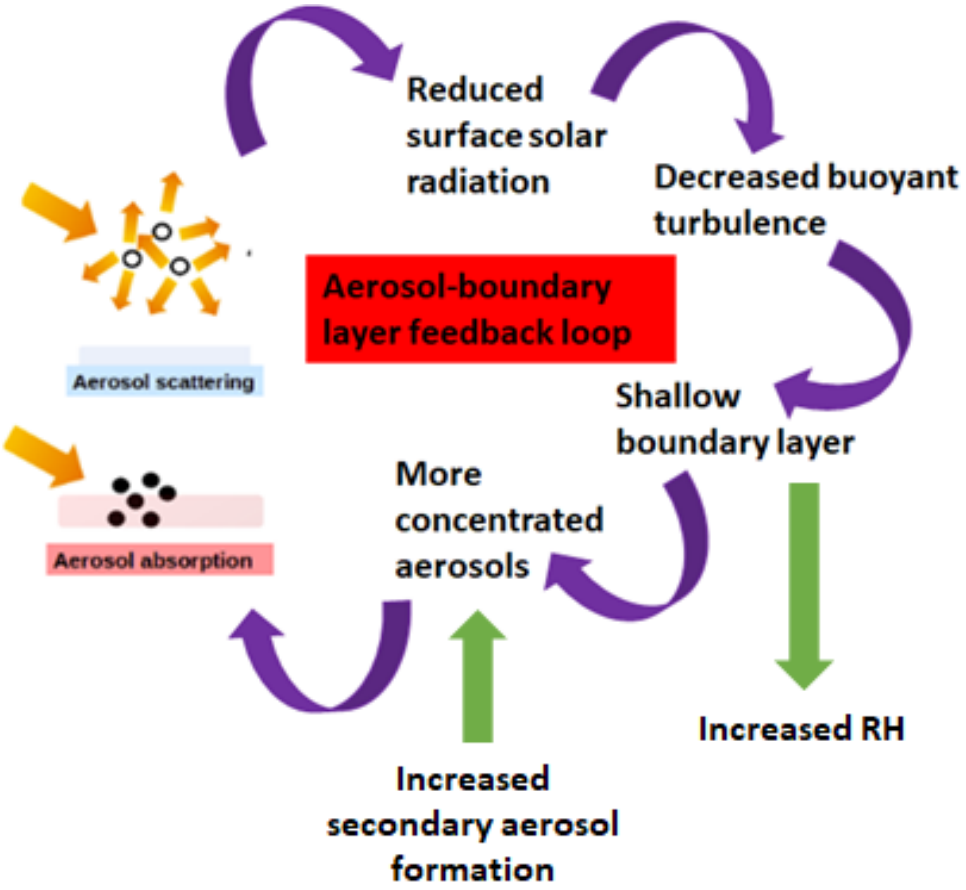

Figure 1.7: Schematic to describe the aerosol-radiation interactions and their impact on PBL dynamics which feeds back on surface aerosol concentrations, based on (Slater et al., 2020)

the PBL to enhance atmospheric stagnation, leading to worsened pollution episodes. Therefore, the exact impact of BC on the aerosol-PBL feedback and its potential impact on pollution episodes is not yet fully understood and is likely dependent on several different factors.

As well as black carbon, some other types of organic aerosol can also absorb radiation in the SW spectrum, these aerosols are termed brown carbon (BrC). Quantifying the contribution of BrC to atmospheric warming is difficult due to the varied optical properties of BrC which can be dependent on emission source and atmospheric conditions. For example, a common anthropogenic source of BrC is biomass burning but studies have found that the optical properties are not only dependent on the combustion source but also the temperature at which the combustion occurs. Furthermore, it is difficult to fully measure exact atmospheric concentrations of BrC. However, BrC has generally been found to be less absorbing than BC at visible wavelengths, but able to absorb radiation at a wider range of wavelengths, with enhanced absorption at shorter wavelengths. Furthermore, organic aerosols (OA) are often present at much higher concentrations than BC, if a significant fraction of the OA is made up of BrC then the overall warming effect of BrC could be equivalent to or higher than that of BC in some environments. BrC could therefore have significant impact as a climate forcer as well as having implications in the aerosol-PBL feedback effect(Cheng et al., 2016b, 2017; Yan et al., 2018).

1.7.4 Impact on Air Quality

This chapter has outlined some of the properties of aerosols and the processes they undergo in the atmosphere, which are important in order to understand the problem of urban air pollution. Sources of pollution and atmospheric conditions greatly influence the properties of particulate pollution and their interactions which impact both global climate and local meteorology. More people are moving to urban areas, with urbanisation and industrialisation occurring rapidly in developing countries in South America, Asia and Africa. This leads to increased emissions but also changes to the natural environment which can impact pollutant dispersion. Heavy pollution episodes, which are characterised by extreme peaks in pollution, are an issue in megacities around the world. The interactions between aerosols, radiation and PBL dynamics may enhance and elongate pollution in urban environments. The influence of aerosols on PBL dynamics is inherently complex and can be dependent on the properties and altitude of the aerosol layer, the existence of clouds and initial meteorological conditions (Gao et al., 2015; Petäjä et al., 2016).

The aerosol-PBL feedback and its implication on air pollution has been widely researched by both measurement and modelling studies in the past decade. Including aerosol-radiation interactions in regional modelling studies of polluted environments decreases surface SWR and PBL height, leading to increased surface $PM_{2.5}$ concentrations. Several factors are believed to influence the intensity of the aerosol-PBL feedback on pollution, with varied intensities observed in different cities and seasons (Zhang et al., 2019). The feedback has typically been found to be enhanced in autumn and winter due to the already limited solar radiation from shorter days and longer nights. This increases nocturnal cooling and makes temperature inversions more likely, furthermore shorter days, mean that there will be limited solar heating to break the inversion. Research of the aerosol-PBL feedback in polluted environments has focussed on Beijing due to the frequent occurence of wintertime haze episodes, commonly associated with stagnant atmospheric conditions and a shallow PBL. The next chapter will focus on air pollution in Beijing and outline current knowledge on the influence of the aerosol-PBL effect on winter haze episodes (Gao et al., 2015; Petäjä et al., 2016; Zhong et al., 2018).

References

Aksoyoglu, S., Ciarelli, G., El-Haddad, I., Baltensperger, U., and Prévôt, A. S.: Secondary inorganic aerosols in Europe: Sources and the significant influence of biogenic VOC emissions, especially on ammonium nitrate, Atmospheric Chemistry and Physics, 17, 7757–7773, https://doi.org/10.5194/acp-17-7757-2017, 2017.

Albrecht, B. a.: Fractional Cloudiness, Science, 245, 1227–1230, https://doi.org/10.1126/science.245.4923.1227, 1989.

Allen, L., Lindberg, F., and Grimmond, C. S.: Global to city scale urban anthropogenic heat flux: Model and variability, International Journal of Climatology, 31, 1990–2005, https://doi.org/10.1002/joc.2210, 2011.

Andrejczuk, M., Grabowski, W. W., Reisner, J., and Gadian, A.: Cloud-aerosol interactions for boundary

layer stratocumulus in the Lagrangian Cloud Model, Journal of Geophysical Research Atmospheres, 115, 1–13, https://doi.org/10.1029/2010JD014248, 2010.

Archer-Nicholls, S., Lowe, D., Schultz, D. M., and McFiggans, G.: Aerosol-radiation-cloud interactions in a regional coupled model: The effects of convective parameterisation and resolution, Atmospheric Chemistry and Physics, 16, 5573–5594, https://doi.org/10.5194/acp-16-5573-2016, 2016.

Auvinen, M., Boi, S., Hellsten, A., Tanhuanpää, T., and Järvi, L.: Study of realistic urban boundary layer turbulence with high-resolution large-eddy simulation, Atmosphere, 11, 1–41, https://doi.org/10.3390/atmos11020201, 2020.

Baklanov, A., Molina, L. T., and Gauss, M.: Megacities, air quality and climate, Atmospheric Environment, 126, 235–249, https://doi.org/10.1016/j.atmosenv.2015.11.059, 2016.

Barlow, J. F.: Progress in observing and modelling the urban boundary layer, Urban Climate, 10, 216–240, https://doi.org/10.1016/j.uclim.2014.03.011, 2014a.

Barlow, J. F.: Progress in observing and modelling the urban boundary layer, Urban Climate, 10, 216–240, https://doi.org/10.1016/j.uclim.2014.03.011, 2014b.

Beelen, R., Raaschou-Nielsen, O., Stafoggia, M., Andersen, Z. J., Weinmayr, G., Hoffmann, B., Wolf, K., Samoli, E., Fischer, P., Nieuwenhuijsen, M., Vineis, P., Xun, W. W., Katsouyanni, K., Dimakopoulou, K., Oudin, A., Forsberg, B., Modig, L., Havulinna, A. S., Lanki, T., Turunen, A., Oftedal, B., Nystad, W., Nafstad, P., De Faire, U., Pedersen, N. L., Ostenson, C. G., Fratiglioni, L., Penell, J., Korek, M., Pershagen, G., Eriksen, K. T., Overvad, K., Ellermann, T., Eeftens, M., Peeters, P. H., Meliefste, K., Wang, M., Bueno-De-Mesquita, B., Sugiri, D., Kramer, U., Heinrich, J., De Hoogh, K., Key, T., Peters, A., Hampel, R., Concin, H., Nagel, G., Ineichen, A., Schaffner, E., Probst-Hensch, N., Kunzli, N., Schindler, C., Schikowski, T., Adam, M., Phuleria, H., Vilier, A., Clavel-Chapelon, F., Declercq, C., Grioni, S., Krogh, V., Tsai, M. Y., Ricceri, F., Sacerdote, C., Galassi, C., Migliore, E., Ranzi, A., Cesaroni, G., Badaloni, C., Forastiere, F., Tamayo, I., Amiano, P., Dorronsoro, M., Katsoulis, M., Trichopoulou, A., Brunekreef, B., and Hoek, G.: Effects of long-term exposure to air pollution on natural-cause mortality: An analysis of 22 European cohorts within the multicentre ESCAPE project, The Lancet, 383, 785–795, https://doi.org/10.1016/S0140-6736(13)62158-3, 2014.

Bloss, W.: Atmospheric chemical processes of importance in cities, in: Air Quality in Urban Environments, vol. 28, pp. 42–64, 2009.

Bond, T. C., Doherty, S. J., Fahey, D. W., Forster, P. M., Berntsen, T., Deangelo, B. J., Flanner, M. G., Ghan, S., Kärcher, B., Koch, D., Kinne, S., Kondo, Y., Quinn, P. K., Sarofim, M. C., Schultz, M. G., Schulz, M., Venkataraman, C., Zhang, H., Zhang, S., Bellouin, N., Guttikunda, S. K., Hopke, P. K., Jacobson, M. Z., Kaiser, J. W., Klimont, Z., Lohmann, U., Schwarz, J. P., Shindell, D., Storelvmo, T., Warren, S. G., and Zender, C. S.: Bounding the role of black carbon in the climate system: A scientific assessment, Journal of Geophysical Research Atmospheres, 118, 5380–5552, https://doi.org/10.1002/jgrd.50171, 2013.

Boucher, O.: Atmospheric Aerosols. Properties and climate impacts, vol. 53, https://doi.org/10.1017/CBO9781107415324.004, 2013.

Boucher, O., Randall, D., Artaxo, P., Bretherton, C., Feingold, G., Forster, P., Kerminen, V.-M. V.-M., Kondo, Y., Liao, H., Lohmann, U., Rasch, P., Satheesh, S. K., Sherwood, S., Stevens, B., Zhang, X. Y., and Zhan, X. Y.: Clouds and Aerosols, in: Climate Change 2013: The Physical Science Basis. Contribution of Working Group I to the Fifth Assessment Report of the Intergovernmental Panel on Climate Change, pp. 571–657, https://doi.org/10.1017/CBO9781107415324.016, 2013.

Boucher, O., Granier, C., Hoose, C., and Jones, A.: IPCC Report: Clouds and Aerosols, https://doi.org/10.1017/CBO9781107415324.016, 2014.

Butt, E. W., Turnock, S. T., Rigby, R., Reddington, C. L., Yoshioka, M., Johnson, J. S., Regayre, L. A., Pringle, K. J., Mann, G. W., and Spracklen, D. V.: Global and regional trends in particulate air

pollution and attributable health burden over the past 50 years, Environmental Research Letters, 12, https://doi.org/10.1088/1748-9326/aa87be, 2017.

Cao, M. and Lin, Z.: Impact of urban surface roughness length parameterization scheme on urban atmospheric environment simulation, Journal of Applied Mathematics, 2014, https://doi.org/10.1155/2014/267683, 2014.

Cappa, C. D., Onasch, T. B., Massoli, P., Worsnop, D. R., Bates, T. S., Cross, E. S., Davidovits, P., Hakala, J., Hayden, K. L., Jobson, B. T., Kolesar, K. R., Lack, D. A., Lerner, B. M., Li, S.-M., Mellon, D., Nuaaman, I., Olfert, J. S., Petaja, T., Quinn, P. K., Song, C., Subramanian, R., Williams, E. J., and Zaveri, R. A.: Radiative Absorption Enhancements Due to the Mixing State of Atmospheric Black Carbon, Science, 337, 1078–1081, https://doi.org/10.1126/science.1223447, 2012.

Chan, C. K. and Yao, X.: Air pollution in mega cities in China, Atmospheric Environment, 42, 1–42, https://doi.org/10.1016/j.atmosenv.2007.09.003, 2008.

Chen, H., Rey, J., Kwong, C., Copes, R., Tu, K., Villeneuve, P. J., Van Donkelaar, A., Hystad, P., Martin, R. V., Murray, B. J., Jessiman, B., Wilton, A. S., Kopp, A., and Burnett, R. T.: Living near major roads and the incidence of dementia, Parkinson's disease, and multiple sclerosis: a population-based cohort study, 6736, 1–9, https://doi.org/10.1016/S0140-6736(16)32399-6, 2017.

Chen, J., Li, Z., Lv, M., Wang, Y., Wang, W., Zhang, Y., Wang, H., Yan, X., Sun, Y., and Cribb, M.: Aerosol hygroscopic growth, contributing factors, and impact on haze events in a severely polluted region in northern China, Atmospheric Chemistry and Physics, 19, 1327–1342, https://doi.org/10.5194/acp-19-1327-2019, 2019.

Cheng, F., Zhang, J., He, J., Zha, Y., Li, Q., and Li, Y.: Analysis of aerosol-cloud-precipitation interactions based on MODIS data, Advances in Space Research, https://doi.org/10.1016/j.asr.2016.08.042, 2016a.

Cheng, Y., bin He, K., yu Du, Z., Engling, G., meng Liu, J., liang Ma, Y., Zheng, M., and Weber, R. J.: The characteristics of brown carbon aerosol during winter in Beijing, Atmospheric Environment, 127, 355–364, https://doi.org/10.1016/j.atmosenv.2015.12.035, 2016b.

Cheng, Y., bin He, K., Engling, G., Weber, R., meng Liu, J., yu Du, Z., and ping Dong, S.: Brown and black carbon in Beijing aerosol: Implications for the effects of brown coating on light absorption by black carbon, Science of the Total Environment, 599-600, 1047–1055, https://doi.org/10.1016/j.scitotenv.2017.05.061, 2017.

Coe, H. and Allan, J. D.: Mass Spectrometric Methods for Aerosol Composition Measurements, in: Analytical Techniques for Atmospheric Measurement, chap. 6, pp. 265–310, 2006.

Coggon, D., Barker, D., and Rose, G.: What is Epidemiology, in: Epidemiology for the Uninitiated, 2003.

Cohen, A. J., Brauer, M., Burnett, R., Anderson, H. R., Frostad, J., Estep, K., Balakrishnan, K., Brunekreef, B., Dandona, L., Dandona, R., Feigin, V., Freedman, G., Hubbell, B., Jobling, A., Kan, H., Knibbs, L., Liu, Y., Martin, R., Morawska, L., Pope, C. A., Shin, H., Straif, K., Shaddick, G., Thomas, M., van Dingenen, R., van Donkelaar, A., Vos, T., Murray, C. J., and Forouzanfar, M. H.: Estimates and 25-year trends of the global burden of disease attributable to ambient air pollution: an analysis of data from the Global Burden of Diseases Study 2015, The Lancet, 389, 1907–1918, https://doi.org/10.1016/S0140-6736(17)30505-6, 2017.

Davidson, C. I., Phalen, R. F., and Solomon, P. A.: Airborne Particulate Matter and Human Health: A Review, Aerosol Science and Technology, 39, 737–749, https://doi.org/10.1080/02786820500191348, 2005.

Derwent, R. and Hjellbrekke, A.-G.: Urban Air Quality in Europe, https://doi.org/10.1007/978-3-642-38451-6, 2013.

Ding, A. J., Huang, X., Nie, W., Sun, J. N., Kerminen, V. M., Petäjä, T., Su, H., Cheng, Y. F., Yang, X. Q., Wang, M. H., Chi, X. G., Wang, J. P., Virkkula, A., Guo, W. D., Yuan, J., Wang, S. Y.,

Zhang, R. J., Wu, Y. F., Song, Y., Zhu, T., Zilitinkevich, S., Kulmala, M., and Fu, C. B.: Enhanced haze pollution by black carbon in megacities in China, Geophysical Research Letters, 43, 2873–2879, https://doi.org/10.1002/2016GL067745, 2016.

Dou, J., Grimmond, S., Cheng, Z., Miao, S., Feng, D., and Liao, M.: Summertime surface energy balance fluxes at two Beijing sites, International Journal of Climatology, 39, 2793–2810, https://doi.org/10.1002/joc.5989, 2019.

Ekman, A. M. L., Engström, A., and Söderberg, A.: Impact of Two-Way Aerosol–Cloud Interaction and Changes in Aerosol Size Distribution on Simulated Aerosol-Induced Deep Convective Cloud Sensitivity, Journal of the Atmospheric Sciences, 68, 685–698, https://doi.org/10.1175/2010JAS3651.1, 2011.

Elser, M., Huang, R. J., Wolf, R., Slowik, J. G., Wang, Q., Canonaco, F., Li, G., Bozzetti, C., Daellenbach, K. R., Huang, Y., Zhang, R., Li, Z., Cao, J., Baltensperger, U., El-Haddad, I., and André, P.: New insights into PM2.5 chemical composition and sources in two major cities in China during extreme haze events using aerosol mass spectrometry, Atmospheric Chemistry and Physics, 16, 3207–3225, https://doi.org/10.5194/acp-16-3207-2016, 2016.

Farahat, A.: Air pollution in the Arabian Peninsula (Saudi Arabia, the United Arab Emirates, Kuwait, Qatar, Bahrain, and Oman): causes, effects, and aerosol categorization, Arabian Journal of Geosciences, 9, https://doi.org/10.1007/s12517-015-2203-y, 2016.

Ferrero, L., Castelli, M., Ferrini, B. S., Moscatelli, M., Perrone, M. G., Sangiorgi, G., D'Angelo, L., Rovelli, G., Moroni, B., Scardazza, F., Mocnik, G., Bolzacchini, E., Petitta, M., and Cappelletti, D.: Impact of black carbon aerosol over Italian basin valleys: High-resolution measurements along vertical profiles, radiative forcing and heating rate, Atmospheric Chemistry and Physics, 14, 9641–9664, https://doi.org/10.5194/acp-14-9641-2014, 2014.

Finlayson-Pitts, B. and Pitts, J.: Chemistry of the Upper and Lower Atmosphere, 2000.

Fiore, A. M., Naik, V., Spracklen, D. V., Steiner, A., Unger, N., Prather, M., Bergmann, D., Cameron-Smith, P. J., Cionni, I., Collins, W. J., Dalsøren, S., Eyring, V., Folberth, G. A., Ginoux, P., Horowitz, L. W., Josse, B., Lamarque, J.-F., Mackenzie, I. A., Nagashima, T., O 'connor, F. M., Righi, M., Rumbold, S. T., Shindell, D. T., Skeie, R. B., Sudo, K., Szopa, S., Takemura, T., and Zeng, G.: Global air quality and climate, Chem. Soc. Rev., 41, 6663–6683, https://doi.org/10.1039/c2cs35095e, 2012.

Forouzanfar, M. H., Afshin, A., Alexander, L. T., Biryukov, S., Brauer, M., Cercy, K., Charlson, F. J., Cohen, A. J., Dandona, L., Estep, K., Ferrari, A. J., Frostad, J. J., Fullman, N., Godwin, W. W., Griswold, M., Hay, S. I., Kyu, H. H., Larson, H. J., Lim, S. S., Liu, P. Y., Lopez, A. D., Lozano, R., Marczak, L., Mokdad, A. H., Moradi-Lakeh, M., Naghavi, M., Reitsma, M. B., Roth, G. A., Sur, P. J., Vos, T., Wagner, J. A., Wang, H., Zhao, Y., Zhou, M., Barber, R. M., Bell, B., Blore, J. D., Casey, D. C., Coates, M. M., Cooperrider, K., Cornaby, L., Dicker, D., Erskine, H. E., Fleming, T., Foreman, K., Gakidou, E., Haagsma, J. A., Johnson, C. O., Kemmer, L., Ku, T., Leung, J., Masiye, F., Millear, A., Mirarefin, M., Misganaw, A., Mullany, E., Mumford, J. E., Ng, M., Olsen, H., Rao, P., Reinig, N., Roman, Y., Sandar, L., Santomauro, D. F., Slepak, E. L., Sorensen, R. J., Thomas, B. A., Vollset, S. E., Whiteford, H. A., Zipkin, B., Murray, C. J., Mock, C. N., Anderson, B. O., Futran, N. D., Anderson, H. R., Bhutta, Z. A., Nisar, M. I., Akseer, N., Krueger, H., Gotay, C. C., Kissoon, N., Kopec, J. A., Pourmalek, F., Burnett, R., Abajobir, A. A., Knibbs, L. D., Veerman, J. L., Lalloo, R., Scott, J. G., Alam, N. K., Gouda, H. N., Guo, Y., McGrath, J. J., Jeemon, P., Dandona, R., Goenka, S., Kumar, G. A., Gething, P. W., Bisanzio, D., Deribew, A., Darby, S. C., Ali, R., Bennett, D. A., Jha, V., Kinfu, Y., McKee, M., Murthy, G. V., Pearce, N., Stöckl, H., Duan, L., Jin, Y., Li, Y., Liu, S., Wang, L., Ye, P., Liang, X., Azzopardi, P., Patton, G. C., Meretoja, A., Alam, K., Borschmann, R., Colquhoun, S. M., Weintraub, R. G., Szoeke, C. E., Ademi, Z., Taylor, H. R., Wijeratne, T., Batis, C., Barquera, S., Campos-Nonato, I. R., Contreras, A. G., Cuevas-Nasu, L., De, V., Gomez-Dantes, H., Heredia-Pi, I. B., Medina, C., Mejia-Rodriguez, F., Montañez Hernandez, J. C., Razo-García, C. A., Rivera, J. A., Rodríguez-Ramírez, S., Sánchez-Pimienta, T. G., Servan-Mori, E. E., Shamah, T., Mensah, G. A., Hoff, H. J., Neal, B., Driscoll, T. R., Kemp, A. H., Leigh, J., Mekonnen, A. B., Bhatt, S., Fürst, T., Piel, F. B., Rodriguez, A., Hutchings, S. J., Majeed, A., Soljak, M., Salomon, J. A., Thorne-Lyman, A. L.,

Ajala, O. N., Bärnighausen, T., Cahill, L. E., Ding, E. L., Farvid, M. S., Khatibzadeh, S., Wagner, G. R., Shrime, M. G., Fitchett, J. R., Aasvang, G. M., Savic, M., Abate, K. H., Gebrehiwot, T. T., Gebremedhin, A. T., Abbafati, C., Abbas, K. M., Abd-Allah, F., Abdulle, A. M., Abera, S. F., Melaku, Y. A., Abyu, G. Y., Betsu, B. D., Hailu, G. B., Tekle, D. Y., Yalew, A. Z., Abraham, B., Abu-Raddad, L. J., Adebiyi, A. O., Adedeji, I. A., Adou, A. K., Adsuar, J. C., Agardh, E. E., Rehm, J., Badawi, A., Popova, S., Agarwal, A., Ahmad, A., Akinyemiju, T. F., Schwebel, D. C., Singh, J. A., Al-Aly, Z., Aldhahri, S. F., Altirkawi, K. A., Terkawi, A. S., Aldridge, R. W., Tillmann, T., Alemu, Z. A., Tegegne, T. K., Alkerwi, A., Alla, F., Guillemin, F., Allebeck, P., Rabiee, R. H., Fereshtehnejad, S. M., Kivipelto, M., Carrero, J. J., Weiderpass, E., Havmoeller, R., Sindi, S., Alsharif, U., Alvarez, E., Alvis-Guzman, N., Amare, A. T., Ciobanu, L. G., Taye, B. W., Amberbir, A., Amegah, A. K., Amini, H., Karema, C. K., Ammar, W., Harb, H. L., Amrock, S. M., Andersen, H. H., Antonio, C. A., Faraon, E. J., Anwari, P., Ärnlöv, J., Larsson, A., Artaman, A., Asayesh, H., Asghar, R. J., Assadi, R., Atique, S., Avokpaho, E. F., Awasthi, A., Ayala, B. P., Bacha, U., Bahit, M. C., Balakrishnan, K., Barac, A., Barker-Collo, S. L., del Pozo-Cruz, B., Mohammed, S., Barregard, L., Petzold, M., Barrero, L. H., Basu, S., Del, L. C., Bazargan-Hejazi, S., Beardsley, J., Bedi, N., Beghi, E., Sheth, K. N., Bell, M. L., Huang, J. J., Bello, A. K., Santos, I. S., Bensenor, I. M., Lotufo, P. A., Berhane, A., Wolfe, C. D., Bernabé, E., Roba, H. S., Beyene, A. S., Hassen, T. A., Mesfin, Y. M., Bhala, N., Bhansali, A., Biadgilign, S., Bikbov, B., Bjertness, E., Htet, A. S., Boufous, S., Degenhardt, L., Resnikoff, S., Calabria, B., Bourne, R. R., Brainin, M., Brazinova, A., Majdan, M., Shen, J., Breitborde, N. J., Brenner, H., Schöttker, B., Broday, D. M., Brugha, T. S., Brunekreef, B., Kromhout, H., Butt, Z. A., van Donkelaar, A., Martin, R. V., Cárdenas, R., Carpenter, D. O., Castañeda-Orjuela, C. A., Castillo, J., Castro, R. E., Catalá-López, F., Chang, J., Chiang, P. P., Chibalabala, M., Chimed-Ochir, O., Jiang, Y., Takahashi, K., Chisumpa, V. H., Mapoma, C. C., Chitheer, A. A., Choi, J. J., Christensen, H., Christopher, D. J., Cooper, L. T., Crump, J. A., Poulton, R. G., Damasceno, A., Dargan, P. I., das Neves, J., Davis, A. C., Newton, J. N., Steel, N., Davletov, K., de Castro, E. F., De, D., Dellavalle, R. P., Des, D. C., Dharmaratne, S. D., Dhillon, P. K., Lal, D. K., Zodpey, S., Diaz-Torné, C., Dorsey, E. R., Doyle, K. E., Dubey, M., Rahman, M. H., Ram, U., Singh, A., Yadav, A. K., Duncan, B. B., Kieling, C., Schmidt, M. I., Elyazar, I., Endries, A. Y., Ermakov, S. P., Eshrati, B., Farzadfar, F., Kasaeian, A., Parsaeian, M., Esteghamati, A., Hafezi-Nejad, N., Sheikhbahaei, S., Fahimi, S., Malekzadeh, R., Roshandel, G., Sepanlou, S. G., Hassanvand, M. S., Heydarpour, P., Rahimi-Movaghar, V., Yaseri, M., Farid, T. A., Khan, A. R., Farinha, C. S., Faro, A., Feigin, V. L., Fernandes, J. G., Fischer, F., Foigt, N., Shiue, I., Fowkes, F. G., Franklin, R. C., Garcia-Basteiro, A. L., Geleijnse, J. M., Jibat, T., Gessner, B. D., Tefera, W., Giref, A. Z., Haile, D., Manamo, W. A., Giroud, M., Gishu, M. D., Martinez-Raga, J., Gomez-Cabrera, M. C., Gona, P., Goodridge, A., Gopalani, S. V., Goto, A., Inoue, M., Gugnani, H. C., Gupta, R., Gutiérrez, R. A., Orozco, R., Halasa, Y. A., Undurraga, E. A., Hamadeh, R. R., Hamidi, S., Handal, A. J., Hankey, G. J., Hao, Y., Harikrishnan, S., Haro, J. M., Hernández-Llanes, N. F., Hoek, H. W., Tura, A. K., Horino, M., Horita, N., Hosgood, H. D., Hoy, D. G., Hsairi, M., Hu, G., Husseini, A., Huybrechts, I., Iburg, K. M., Idrisov, B. T., Kwan, G. F., Ileanu, B. V., Pana, A., Kawakami, N., Shibuya, K., Jacobs, T. A., Jacobsen, K. H., Jahanmehr, N., Jakovljevic, M. B., Jansen, H. A., Jassal, S. K., Stein, M. B., Javanbakht, M., Jayaraman, S. P., Jayatilleke, A. U., Jee, S. H., Jonas, J. B., Kabir, Z., Kalkonde, Y., Kamal, R., She, J., Kan, H., Karch, A., Karimkhani, C., Kaul, A., Kazi, D. S., Keiyoro, P. N., Parry, C. D., Kengne, A. P., Matzopoulos, R., Wiysonge, C. S., Stein, D. J., Mayosi, B. M., Keren, A., Khader, Y. S., Khan, E. A., Khan, G., Khang, Y. H., Won, S., Khera, S., Tavakkoli, M., Khoja, T. A., Khubchandani, J., Kim, C., Kim, D., Kimokoti, R. W., Kokubo, Y., Koul, P. A., Koyanagi, A., Kravchenko, M., Varakin, Y. Y., Kuate, B., Kuchenbecker, R. S., Kucuk, B., Kuipers, E. J., Lallukka, T., Shiri, R., Meretoja, T. J., Lan, Q., Latif, A. A., Lawrynowicz, A. E., Leasher, J. L., Levi, M., Li, X., Liang, J., Lloyd, B. K., Logroscino, G., Lunevicius, R., Pope, D., Mahdavi, M., Malta, D. C., Marcenes, W., Matsushita, K., Nachega, J. B., Tran, B. X., Meaney, P. A., Mehari, A., Tedla, B. A., Memish, Z. A., Mendoza, W., Mensink, G. B., Mhimbira, F. A., Miller, T. R., Mills, E. J., Mohammadi, A., Mola, G. L., Monasta, L., Morawska, L., Norman, R. E., Mori, R., Mozaff, D., Shi, P., Werdecker, A., Mueller, U. O., Paternina, A. J., Westerman, R., Seedat, S., Naheed, A., Nangia, V., Nassiri, N., Nguyen, Q. L., Nkamedjie, P. M., Norheim, O. F., Norrving, B., Nyakarahuka, L., Obermeyer, C. M., Ogbo, F. A., Oh, I., Oladimeji, O., Sartorius, B., Olusanya, B. O., Olivares, P. R., Olusanya, J. O., Opio, J. N., Oren, E., Ortiz, A., Ota, E., Mahesh, P. A., Park, E., Patel, T., Patil, S. T., Patten, S. B., Wang, J., Pereira, D. M., Cortinovis, M.,

Giussani, G., Perico, N., Remuzzi, G., Pesudovs, K., Phillips, M. R., Pillay, J. D., Plass, D., Tobollik, M., Polinder, S., Pond, C. D., Pope, C. A., Prasad, N. M., Qorbani, M., Radfar, A., Rafay, A., Rana, S. M., Rahman, M., Rahman, S. U., Rajsic, S., Rai, R. K., Raju, M., Ranganathan, K., Refaat, A. H., Rehm, C. D., Ribeiro, A. L., Rojas-Rueda, D., Roy, A., Satpathy, M., Tandon, N., Rothenbacher, D., Saleh, M. M., Sanabria, J. R., Sanchez-Riera, L., Sanchez-Niño, M. D., Sarmiento-Suarez, R., Sawhney, M., Schmidhuber, J., Schneider, I. J., Schutte, A. E., Silva, D. A., Shahraz, S., Shin, M., Shaheen, A., Shaikh, M. A., Sharma, R., Shigematsu, M., Yoon, S., Shishani, K., Sigfusdottir, I. D., Singh, P. K., Silveira, D. G., Silverberg, J. I., Yano, Y., Soneji, S., Stranges, S., Steckling, N., Sreeramareddy, C. T., Stathopoulou, V., Stroumpoulis, K., Sunguya, B. F., Swaminathan, S., Sykes, B. L., Tabarés-Seisdedos, R., Talongwa, R. T., Tanne, D., Tuzcu, E. M., Thakur, J., Shaddick, G., Thomas, M. L., Thrift, A. G., Thurston, G. D., Thomson, A. J., Topor-Madry, R., Topouzis, F., Towbin, J. A., Uthman, O. A., Tobe-Gai, R., Tsilimparis, N., Tsala, Z., Tyrovolas, S., Ukwaja, K. N., van Os, J., Vasankari, T., Venketasubramanian, N., Violante, F. S., Waller, S. G., Uneke, C. J., Wang, Y., Weichenthal, S., Woolf, A. D., Xavier, D., Xu, G., Yakob, B., Yip, P., Kesavachandran, C. N., Montico, M., Ronfani, L., Yu, C., Zaidi, Z., Yonemoto, N., Younis, M. Z., Wubshet, M., Zuhlke, L. J., Zaki, M. E., and Zhu, J.: Global, regional, and national comparative risk assessment of 79 behavioural, environmental and occupational, and metabolic risks or clusters of risks, 1990–2015: a systematic analysis for the Global Burden of Disease Study 2015, The Lancet, 388, 1659–1724, https://doi.org/10.1016/S0140-6736(16)31679-8, 2016.

Friedlander, S.: Atmospheric Aerosol Dynamics, in: Smoke, Dust, and Haze: Fundamentals of Aerosol Dynamics, pp. 359–389, 2000.

Fu, Q.: Radiation Transfer in the Atmosphere: Radiation, Solar, Encyclopedia of Atmospheric Sciences: Second Edition, 5, 1–4, https://doi.org/10.1016/B978-0-12-382225-3.00334-0, 2015.

Fuzzi, S., Gilardoni, S., Kokhanovsky, A. A., Di Nicolantonio, W., Mukai, S., Sano, I., Nakata, M., Tomasi, C., and Lanconelli, C.: Aerosol and Air Quality, in: Atmospheric Aerosols: Life Cycles and Effects on Air Quality and Climate, pp. 553–596, https://doi.org/10.1002/9783527336449.ch9, 2016.

Gao, Y., Zhang, M., Liu, Z., Wang, L., Wang, P., Xia, X., Tao, M., and Zhu, L.: Modeling the feedback between aerosol and meteorological variables in the atmospheric boundary layer during a severe fog-haze event over the North China Plain, Atmospheric Chemistry and Physics, 15, 4279–4295, https://doi.org/10.5194/acp-15-4279-2015, 2015.

Gilardoni, S. and Fuzzi, S.: Chemical Composition of Aerosols of Different Origin, in: Atmospheric Aerosols: Life Cycles and Effects on Air Quality and Climate, pp. 183–221, https://doi.org/10.1002/9783527630134.ch12, 2017.

Grimmond, C., Cleugh, H., and Oke, T.: An objective urban heat storage model and its comparison with other schemes, Atmospheric Environment. Part B. Urban Atmosphere, 25, 311–326, https://doi.org/10.1016/0957-1272(91)90003-W, 1991.

Grimmond, C. S. B. and Oke, T. R.: Heat Storage in Urban Areas: Local-Scale Observations and Evaluation of a Simple Model, Journal of Applied Meteorology, 38, 922–940, https://doi.org/10.1175/1520-0450(1999)038<0922:HSIUAL>2.0.CO;2, 1999.

Gulia, S., Shiva Nagendra, S. M., Khare, M., and Khanna, I.: Urban air quality management-A review, Atmospheric Pollution Research, 6, 286–304, https://doi.org/10.5094/APR.2015.033, 2015.

Gurjar, B. R., Butler, T. M., Lawrence, M. G., and Lelieveld, J.: Evaluation of emissions and air quality in megacities, Atmospheric Environment, 42, 1593–1606, https://doi.org/10.1016/j.atmosenv.2007.10.048, 2008.

Gurjar, B. R., Jain, A., Sharma, A., Agarwal, A., Gupta, P., Nagpure, A. S., and Lelieveld, J.: Human health risks in megacities due to air pollution, Atmospheric Environment, 44, 4606–4613, https://doi.org/10.1016/j.atmosenv.2010.08.011, 2010.

Herbert, R. J., Bellouin, N., Highwood, E. J., and Hill, A. A.: Diurnal cycle of the semi-direct effect from a persistent absorbing aerosol layer over marine stratocumulus in large-eddy simulations, Atmospheric

Chemistry and Physics, 20, 1317–1340, https://doi.org/10.5194/acp-20-1317-2020, 2020.

Hertel, O. and Goodsite, M. E.: Urban air pollution climates throughout the world, in: Air Quality in Urban Environmentsy, vol. 28, pp. 1–22, 2009.

Hopke, P. K., Cohen, D. D., Begum, B. A., Biswas, S. K., Ni, B., Pandit, G. G., Santoso, M., Chung, Y. S., Davy, P., Markwitz, A., Waheed, S., Siddique, N., Santos, F. L., Pabroa, P. C. B., Seneviratne, M. C. S., Wimolwattanapun, W., Bunprapob, S., Vuong, T. B., Duy Hien, P., and Markowicz, A.: Urban air quality in the Asian region, Science of the Total Environment, 404, 103–112, https://doi.org/10.1016/j.scitotenv.2008.05.039, 2008.

Huang, R. J., Zhang, Y., Bozzetti, C., Ho, K. F., Cao, J. J., Han, Y., Daellenbach, K. R., Slowik, J. G., Platt, S. M., Canonaco, F., Zotter, P., Wolf, R., Pieber, S. M., Bruns, E. A., Crippa, M., Ciarelli, G., Piazzalunga, A., Schwikowski, M., Abbaszade, G., Schnelle-Kreis, J., Zimmermann, R., An, Z., Szidat, S., Baltensperger, U., El Haddad, I., and Prevot, A. S.: High secondary aerosol contribution to particulate pollution during haze events in China, Nature, 514, 218–222, https://doi.org/10.1038/nature13774, 2014.

Jacobson, M.: Fundamentals of Atmospheric Modelling, 1997.

Jacobson, M. Z.: Strong radiative heating due to the mixing state of black carbon in atmospheric aerosols, Nature, 409, 695–697, https://doi.org/10.1038/35055518, 2001.

Jacobson, M. Z.: Fundamentals of Atmospheric Modelling, 2005.

Ji, D., Gao, W., Maenhaut, W., He, J., Wang, Z., Li, J., Wang, L., Sun, Y., Xin, J., Hu, B., and Wang, Y.: Impact of air pollution control measures and regional transport on China: Insights gained from long-term measurement, Atmospheric Chemistry and Physics, 19, 8569–8590, https://doi.org/10.5194/acp-19-8569-2019, 2019.

John, W.: Size Distribution Characteristics of Aerosols, in: Aerosol Measurement: Principles, Techniques, and Applications: Third Edition, pp. 41–54, https://doi.org/10.1002/9781118001684.ch4, 2011.

Johnson, B. T.: The Semi-Direct Aerosol Effect, Ph.D. thesis, 2003.

Johnson, B. T., Shine, K. P., and Forster, P. M.: The semi-direct aerosol effect: Impact of absorbing aerosols on marine stratocumulus, Quarterly Journal of the Royal Meteorological Society, 130, 1407–1422, https://doi.org/10.1256/qj.03.61, 2004.

Johnson, B. T., Heese, B., McFarlane, S. A., Chazette, P., Jones, A., and Bellouin, N.: Vertical distribution and radiative effects of mineral dust and biomass burning aerosol over West Africa during DABEX, Journal of Geophysical Research Atmospheres, 113, 1–16, https://doi.org/10.1029/2008JD009848, 2008.

Kalberer, M.: Aerosols: Aerosol Physics and Chemistry, in: Encyclopedia of Atmospheric Sciences: Second Edition, vol. 1, pp. 23–31, Elsevier, second edi edn., https://doi.org/10.1016/B978-0-12-382225-3.00049-9, 2015.

Kappos, A. D., Bruckmann, P., Eikmann, T., Englert, N., Heinrich, U., Höppe, P., Koch, E., Krause, G. H. M., Kreyling, W. G., Rauchfuss, K., Rombout, P., Schulz-Klemp, V., Thiel, W. R., and Wichmann, H. E.: Health effects of particles in ambient air., International journal of hygiene and environmental health, 207, 399–407, https://doi.org/10.1078/1438-4639-00306, 2004.

Kokhanovsky, A. A.: Aerosol Optics: Light Absorption and Scattering by Particles in the Atmosphere, vol. 53, https://doi.org/10.1017/CBO9781107415324.004, 2008.

Kokhanovsky, A. A.: Aerosol Optics, Atmospheric Aerosols, pp. 223–246, https://doi.org/10.1002/9783527336449.ch5, 2016.

Kreidenweis, S. M. and Asa-Awuku, A.: Aerosol Hygroscopicity: Particle Water Content and Its Role in Atmospheric Processes, vol. 5, Elsevier Ltd., 2 edn., https://doi.org/10.1016/B978-0-08-095975-7.00418-6, 2013.

Krzyzanowski, M., Apte, J. S., Bonjour, S. P., Brauer, M., Cohen, A. J., and Prüss-Ustun, A. M.: Air

Pollution in the Mega-cities, Current Environmental Health Reports, 1, 185–191, https://doi.org/10.1007/s40572-014-0019-7, 2014.

Kulkarni, P., Baron, P., and Willeke: Part I. Introduction to Aerosol Characterization, in: Aerosol Measurement: Principles, Techniques, and Applications, pp. 1–10, https://doi.org/10.1016/b978-0-12-800838-6.00042-4, 2011.

Lazaridis, M.: First Principles of Meteorology and Air Pollution, vol. 19, https://doi.org/10.1007/978-94-007-0162-5, 2011.

Lelieveld, J., Evans, J. S., Fnais, M., Giannadaki, D., and Pozzer, A.: The contribution of outdoor air pollution sources to premature mortality on a global scale., Nature, 525, 367–71, https://doi.org/10.1038/nature15371, 2015.

Li, Z., Niu, F., Fan, J., Liu, Y., Rosenfeld, D., and Ding, Y.: Long-term impacts of aerosols on the vertical development of clouds and precipitation, Nature Geoscience, 4, 888–894, https://doi.org/10.1038/ngeo1313, 2011.

Li, Z., Guo, J., Ding, A., Liao, H., Liu, J., Sun, Y., Wang, T., Xue, H., Zhang, H., and Zhu, B.: Aerosol and boundary-layer interactions and impact on air quality, National Science Review, 4, 810–833, https://doi.org/10.1093/nsr/nwx117, 2017.

Liu, C., Huang, J., Fedorovich, E., Hu, X.-M., Wang, Y., and Lee, X.: The Effect of Aerosol Radiative Heating on Turbulence Statistics and Spectra in the Atmospheric Convective Boundary Layer: A Large-Eddy Simulation Study, Atmosphere, 9, 347, https://doi.org/10.3390/atmos9090347, 2018a.

Liu, D., Whitehead, J., Alfarra, M. R., Reyes-Villegas, E., Spracklen, D. V., Reddington, C. L., Kong, S., Williams, P. I., Ting, Y.-C., Haslett, S., Taylor, J. W., Flynn, M. J., Morgan, W. T., McFiggans, G., Coe, H., and Allan, J. D.: Black-carbon absorption enhancement in the atmosphere determined by particle mixing state, Nature Geoscience, 10, https://doi.org/10.1038/ngeo2901, 2017.

Liu, F., Yon, J., Fuentes, A., Lobo, P., Smallwood, G. J., and Corbin, J. C.: Review of recent literature on the light absorption properties of black carbon: Refractive index, mass absorption cross section, and absorption function, Aerosol Science and Technology, 54, 33–51, https://doi.org/10.1080/02786826.2019.1676878, 2020.

Liu, Y., Wu, J., Yu, D., and Ma, Q.: The relationship between urban form and air pollution depends on seasonality and city size, Environmental Science and Pollution Research, 25, 15 554–15 567, https://doi.org/10.1007/s11356-018-1743-6, 2018b.

Liu, Z., Zhao, Y., Hu, D., and Liu, C.: A Moving Source Localization Method for Distributed Passive Sensor Using TDOA and FDOA Measurements, International Journal of Antennas and Propagation, 2016, https://doi.org/10.1155/2016/8625039, 2016.

Lv, B., Zhang, B., and Bai, Y.: A systematic analysis of PM2.5 in Beijing and its sources from 2000 to 2012, Atmospheric Environment, 124, 98–108, https://doi.org/10.1016/j.atmosenv.2015.09.031, 2016.

Ma, Q., Wu, Y., Zhang, D., Wang, X., Xia, Y., Liu, X., Tian, P., Han, Z., Xia, X., Wang, Y., and Zhang, R.: Roles of regional transport and heterogeneous reactions in the PM2.5 increase during winter haze episodes in Beijing, Science of the Total Environment, 599-600, 246–253, https://doi.org/10.1016/j.scitotenv.2017.04.193, 2017.

Malavelle, F. F., Haywood, J. M., Jones, A., Gettelman, A., Clarisse, L., Bauduin, S., Allan, R. P., Karset, I. H. H., Kristjánsson, J. E., Oreopoulos, L., Cho, N., Lee, D., Bellouin, N., Boucher, O., Grosvenor, D. P., Carslaw, K. S., Dhomse, S., Mann, G. W., Schmidt, A., Coe, H., Hartley, M. E., Dalvi, M., Hill, A. A., Johnson, B. T., Johnson, C. E., Knight, J. R., O'Connor, F. M., Stier, P., Myhre, G., Platnick, S., Stephens, G. L., Takahashi, H., and Thordarson, T.: Strong constraints on aerosol-cloud interactions from volcanic eruptions, Nature, 546, 485–491, https://doi.org/10.1038/nature22974, 2017.

Marlier, M. E., Jina, A. S., Kinney, P. L., and DeFries, R. S.: Extreme Air Pollution in Global Megacities,

Current Climate Change Reports, 2, 15–27, https://doi.org/10.1007/s40641-016-0032-z, 2016.

Maynard, R. L.: Health effects of urban pollution, in: Air Quality in Urban Environments, vol. 28, pp. 108–128, 2009.

McMurry, P. H.: A review of atmospheric aerosol measurements, Developments in Environmental Science, 1, 443–517, https://doi.org/10.1016/S1474-8177(02)80020-1, 2002.

Meng, J., Liu, J., Guo, S., Li, J., Li, Z., and Tao, S.: Trend and driving forces of Beijing's black carbon emissions from sectoral perspectives, Journal of Cleaner Production, 112, 1272–1281, https://doi.org/10.1016/j.jclepro.2015.05.027, 2016.

Mishra, A. K., Koren, I., and Rudich, Y.: Effect of aerosol vertical distribution on aerosol-radiation interaction: A theoretical prospect, Heliyon, 1, https://doi.org/10.1016/j.heliyon.2015.e00036, 2015.

Molina, M. J. and Molina, L. T.: Megacities and atmospheric pollution, Journal of the Air and Waste Management Association, 54, 644–680, https://doi.org/10.1080/10473289.2004.10470936, 2004.

Myhre, G., Myhre, C., Samset, B. H., and Storelvmo, T.: Aerosols and their Relation to Global Climate and Climate Sensitivity, Nature Education Knowlefge, 4, 2013.

Ohata, S., Moteki, N., Mori, T., Koike, M., and Kondo, Y.: A key process controlling the wet removal of aerosols: new observational evidence, Scientific Reports, 6, 34 113, https://doi.org/10.1038/srep34113, 2016.

Oke, T.: The energetic basis of the urban heat island, Quarterly Journal of the Royal Meteorological Society, 108, 1–24, 1982.

Oke, T. R.: City size and the urban heat island, Atmospheric Environment Pergamon Pres, 7, 769–779, https://doi.org/10.1016/0004-6981(73)90140-6, 1973.

Panagi, M., Fleming, Z., Monks, P., Ashfold, M., Wild, O., Hollaway, M., Zhang, Q., Squires, F., and Vande Hey, J.: Investigating the regional contributions to air pollution in Beijing: A dispersion modelling study using CO as a tracer, Atmospheric Chemistry and Physics Discussions, pp. 1–20, https://doi.org/10.5194/acp-2019-759, 2019.

Park, M., Joo, H. S., Lee, K., Jang, M., Kim, S. D., Kim, I., Borlaza, L. J. S., Lim, H., Shin, H., Chung, K. H., Choi, Y. H., Park, S. G., Bae, M. S., Lee, J., Song, H., and Park, K.: Differential toxicities of fine particulate matters from various sources, Scientific Reports, 8, 1–11, https://doi.org/10.1038/s41598-018-35398-0, 2018.

Petäjä, T., Järvi, L., Kerminen, V.-M., Ding, A. J., Sun, J. N., Nie, W., Kujansuu, J., Virkkula, A., Yang, X., Fu, C. B., Zilitinkevich, S., and Kulmala, M.: Enhanced air pollution via aerosol-boundary layer feedback in China., Scientific reports, 6, 18 998, https://doi.org/10.1038/srep18998, 2016.

Pöschl, U.: Atmospheric aerosols: Composition, transformation, climate and health effects, Angewandte Chemie - International Edition, 44, 7520–7540, https://doi.org/10.1002/anie.200501122, 2005.

Quan, J., Tie, X., Zhang, Q., Liu, Q., Li, X., Gao, Y., and Zhao, D.: Characteristics of heavy aerosol pollution during the 2012-2013 winter in Beijing, China, Atmospheric Environment, 88, 83–89, https://doi.org/10.1016/j.atmosenv.2014.01.058, 2014.

Ramanathan, V., Crutzen, P. J., Kiehl, J. T., and Rosenfeld, D.: Aerosols , Climate and the Hydrological Cycle, Science, 294, 2119–2125, 2001.

Russell, A. G. and Brunekreef, B.: A focus on particulate matter and health, Environmental Science and Technology, 43, 4620–4625, https://doi.org/10.1021/es9005459, 2009.

Seinfeld, J. and Pandis, S.: Properties of the Atmospheric Aerosol, Atmospheric Chemistry and Physics: From Air Pollution to Climate Change, pp. 408–429, 2006a.

Seinfeld, J. H. and Pandis, S. N.: Atmospheric Chemistry and Physics: From Air Pollution to Climate

Change, 2006b.

Slater, J., Tonttila, J., Mcfiggans, G., Romakkaniemi, S., Kühn, T., and Coe, H.: Using a coupled LES-aerosol radiation model to investigate urban haze : Sensitivity to aerosol loading and meteorological conditions, Atmospheric Chemistry and Physics Discussions, 5, 1–23, 2020.

Stull, R.: Atmospheric Boundary Layer, in: Practical Meteorology: An Algebra-based Survey of Atmospheric Science, pp. 453–458, https://doi.org/10.1175/BAMS-89-4-453, 2015.

Sun, Y., Zhuang, G., Tang, A., Wang, Y., and An, Z.: Chemical Characteristics of PM 2.5 and PM 10 in HazeFog Episodes in Beijing, Environmental Science Technology, 40, 3148–3155, https://doi.org/10.1021/es051533g, 2006.

Tang, M., Chan, C. K., Li, Y. J., Su, H., Ma, Q., Wu, Z., Zhang, G., Wang, Z., Ge, M., Hu, M., He, H., and Wang, X.: A review of experimental techniques for aerosol hygroscopicity studies, Atmospheric Chemistry and Physics Discussions, pp. 1–130, https://doi.org/10.5194/acp-2019-398, 2019.

Tao, M., Chen, L., Li, R., Wang, L., Wang, J., Wang, Z., Tang, G., and Tao, J.: Spatial oscillation of the particle pollution in eastern China during winter: Implications for regional air quality and climate, Atmospheric Environment, 144, 100–110, https://doi.org/10.1016/j.atmosenv.2016.08.049, 2016.

Tao, W., Chen, J., Li, Z., Wang, C., and Zhang, C.: Impact of Aerosols on boundary layer clouds and precipitation, Reviews of Geophysics, 50, https://doi.org/10.1029/2011RG000369.1.INTRODUCTION, 2012.

Tomasi, C. and Lupi, A.: Primary and Secondary Sources of Atmospheric Aerosol, in: Atmospheric Aerosols: Life Cycles and Effects on Air Quality and Climate, vol. 1005, pp. 1–86, https://doi.org/10.1021/bk-2009-1005.fw001, 2017a.

Tomasi, C. and Lupi, A.: Coagulation, Condensation, Dry and Wet Deposition, and Cloud Droplet Formation in the Atmospheric Aerosol Life Cycle, Atmospheric Aerosols, pp. 115–182, https://doi.org/10.1002/9783527336449.ch3, 2017b.

Twomey, S.: The Influence of Pollution on the Shortwave Albedo of Clouds, https://doi.org/10.1175/1520-0469(1977)034<1149:TIOPOT>2.0.CO;2, 1977.

United Nations: The World 's Cities in 2018, The World's Cities in 2018 - Data Booklet (ST/ESA/SER.A/417), p. 34, 2018.

Valsaraj, K. T. and Kommalapati, R. R.: Atmospheric aerosols, ACS Symposium Series, 1005, https://doi.org/10.1021/bk-2009-1005.fw001, 2009.

Wang, H., Xu, J., Zhang, M., Yang, Y., Shen, X., Wang, Y., Chen, D., and Guo, J.: A study of the meteorological causes of a prolonged and severe haze episode in January 2013 over central-eastern China, Atmospheric Environment, 98, 146–157, https://doi.org/10.1016/j.atmosenv.2014.08.053, 2014a.

Wang, L., Liu, J., Gao, Z., Li, Y., Huang, M., Fan, S., Zhang, X., Yang, Y., Miao, S., Zou, H., Sun, Y., Chen, Y., and Yang, T.: Vertical observations of the atmospheric boundary layer structure over Beijing urban area during air pollution episodes, Atmospheric Chemistry and Physics, 19, 6949–6967, https://doi.org/10.5194/acp-19-6949-2019, 2019.

Wang, Y. S., Yao, L., Wang, L. L., Liu, Z. R., Ji, D. S., Tang, G. Q., Zhang, J. K., Sun, Y., Hu, B., and Xin, J. Y.: Mechanism for the formation of the January 2013 heavy haze pollution episode over central and eastern China, Science China Earth Sciences, 57, 14–25, https://doi.org/10.1007/s11430-013-4773-4, 2014b.

Wang, Z. L., Zhang, H., and Zhang, X. Y.: Simultaneous reductions in emissions of black carbon and co-emitted species will weaken the aerosol net cooling effect, Atmospheric Chemistry and Physics, 15, 3671–3685, https://doi.org/10.5194/acp-15-3671-2015, 2015.

WHO: Particulate matter, Tech. Rep. 1, 2000.

WHO: Health risks of particulate matter from long-range transboundary air pollution, Pollution Atmospherique, p. 169, https://doi.org/ISBN9789289042895, 2006.

World Health Organization: Exposure to ambient air pollution from particulate matter for 2016, World Health Organization, p. 6, 2018a.

World Health Organization: Burden of disease from ambient air pollution for 2016 Description of method v5 May 2018, World Health Organization, 2017, 6, 2018b.

Wu, J., Bei, N., Hu, B., Liu, S., Zhou, M., Wang, Q., Li, X., Liu, L., Feng, T., Liu, Z., Wang, Y., Cao, J., Tie, X., Wang, J., Molina, L. T., and Li, G.: Aerosol-radiation feedback deteriorates the wintertime haze in the North China Plain, Atmospheric Chemistry and Physics, 19, 8703–8719, https://doi.org/10.5194/acp-19-8703-2019, 2019.

Yan, J., Wang, X., Gong, P., Wang, C., and Cong, Z.: Review of brown carbon aerosols: Recent progress and perspectives, Science of the Total Environment, 634, 1475–1485, https://doi.org/10.1016/j.scitotenv.2018.04.083, 2018.

Yu, H., Kaufman, Y. J., Chin, M., Feingold, G., Remer, L. A., Anderson, T. L., Balkanski, Y., Bellouin, N., Boucher, O., Christopher, S., DeCola, P., Kahn, R., Koch, D., Loeb, N., Reddy, M. S., Schulz, M., Takemura, T., and Zhou, M.: A review of measurement-based assessments of the aerosol direct radiative effect and forcing, Atmospheric Chemistry and Physics, 6, 613–666, https://doi.org/10.5194/acp-6-613-2006, 2006.

Yue, H., He, C., Huang, Q., Yin, D., and Bryan, B. A.: Stronger policy required to substantially reduce deaths from PM2.5 pollution in China, Nature Communications, 11, 1–10, https://doi.org/10.1038/s41467-020-15319-4, 2020.

Zhang, J., Mauzerall, D. L., Zhu, T., Liang, S., Ezzati, M., and Remais, J. V.: Environmental health in China: progress towards clean air and safe water, The Lancet, 375, 1110–1119, https://doi.org/10.1016/S0140-6736(10)60062-1, 2010.

Zhang, Q., Zheng, Y., Tong, D., Shao, M., Wang, S., Zhang, Y., Xu, X., Wang, J., He, H., Liu, W., Ding, Y., Lei, Y., Li, J., Wang, Z., Zhang, X., Wang, Y., Cheng, J., Liu, Y., Shi, Q., Yan, L., Geng, G., Hong, C., Li, M., Liu, F., Zheng, B., Cao, J., Ding, A., Gao, J., Fu, Q., Huo, J., Liu, B., Liu, Z., Yang, F., He, K., and Hao, J.: Drivers of improved PM2.5 air quality in China from 2013 to 2017, Proceedings of the National Academy of Sciences of the United States of America, 116, 24 463–24 469, https://doi.org/10.1073/pnas.1907956116, 2019.

Zhang, R., Khalizov, A. F., Pagels, J., Zhang, D., Xue, H., and McMurry, P. H.: Variability in morphology, hygroscopicity, and optical properties of soot aerosols during atmospheric processing, Proceedings of the National Academy of Sciences of the United States of America, 105, 10 291–10 296, https://doi.org/10.1073/pnas.0804860105, 2008.

Zheng, G. J., Duan, F. K., Su, H., Ma, Y. L., Cheng, Y., Zheng, B., Zhang, Q., Huang, T., Kimoto, T., Chang, D., Pöschl, U., Cheng, Y. F., and He, K. B.: Exploring the severe winter haze in Beijing: The impact of synoptic weather, regional transport and heterogeneous reactions, Atmospheric Chemistry and Physics, 15, 2969–2983, https://doi.org/10.5194/acp-15-2969-2015, 2015.

Zhong, J., Zhang, X., Dong, Y., Wang, Y., Liu, C., Wang, J., Zhang, Y., and Che, H.: Feedback effects of boundary-layer meteorological factors on cumulative explosive growth of PM2.5; during winter heavy pollution episodes in Beijing from 2013 to 2016, Atmospheric Chemistry and Physics, 18, 247–258, https://doi.org/10.5194/acp-18-247-2018, 2018.

Chapter 2

Air Pollution in Beijing

Beijing, a megacity situated in the North East of China, is well known for its problems with air pollution. Situated 43 m above sea level, Beijing is surrounded by high mountains to the north and west, industrial areas to the south and the Gobi desert to the north west. The surrounding mountains, although providing a source of clean air, often hinder the dispersion of pollutants (Meng et al., 2019; Zheng et al., 2015). Rapid industrialisation has transformed the Chinese economy throughout the 20th century, this combined with large populations migrating from rural to urban areas has led to air quality issues in many of the major cities (Fu and Chen, 2016; Tao et al., 2016; Zhang et al., 2016). Although annual air quality has improved in Beijing over the past decade, heavy pollution episodes termed 'haze' are still a massive issue (Chen et al., 2014; Zhang et al., 2016). Here, haze is characterised by visibility of < 10 km, caused by high concentrations of $PM_{2.5}$ (Jiang et al., 2015). Understanding of the processes affecting the haze episodes is therefore vital in order to improve air quality in Beijing and limit populatiuon exposure to high concentrations of pollutants.

Beijing, as a megacity in one of the world's most rapidly developing economies, has high anthropogenic emissions which combined with unfavourable meteorology leads to heavy pollution or 'haze' episodes. $PM_{2.5}$ concentrations during wintertime frequently exceed 100 $\mu g/m^3$, with major components being carbonaceous aerosols (organic matter and black carbon) and secondary inorganic aerosols such as nitrate, ammonium and sulphate (Sun et al., 2013, 2014; Wang et al., 2015). Beijing is impacted both by local emissions, secondary particle formation and regional transport of pollutants from surrounding provinces (Wang et al., 2017). These pollutant gases and particulates can interact in the atmosphere to potentially change their physical and chemical properties. Sources of air pollutants can be both anthropogenic and biogenic. The biggest source of natural pollutant in Beijing is dust, transported from the Gobi desert in the North; although isoprene and terpene are also significant sources in the summer. Major local sources of anthropogenic pollution in wintertime Beijing come from vehicle use (both emissions and suspended road dust), and coal combustion for residential heating and cooking (Sun et al., 2006; Zikova et al., 2016; Chang et al., 2019). Pollutants can also be transported regionally from surrounding provinces and industries (Du et al., 2019). Difficulties arise in trying to further quantify pollutant sources due to inaccurate or outdated emissions inventory, particularly from sources other than industry such as: vehicles, agriculture and cooking, which are less easily monitored. Source apportionment techniques aim to clarify

the major sources of pollutants during pollution episodes and the relative importance of regional transport vs local emissions in order to better influence policy (Pui et al., 2014; Zikova et al., 2016; Squires et al., 2020).

2.1 Pollution sources

Chang et al. (2019) examined the impact of local and regional contributions of pollutants on air pollution episodes in Beijing for January, March, July and October 2014 and found that contributions of each vary seasonally and daily. For example, they found that in Beijing, local emissions contributed 62 % of total PM in January, while in July contribution of local emissions to total PM was 33 %. Furthermore, regional transport of pollutants from surrounding provinces were found to be more important when $PM_{2.5}$ concentrations were already high, contributing 39 % of $PM_{2.5}$ in polluted days in January compared to 12 % of total $PM_{2.5}$ during clean days. Furthermore, several studies have examined the correlation between wind direction and pollutant concentrations, finding that preceding southerly winds strongly correlate with increasing $PM_{2.5}$ concentrations in Beijing. Due to policy interventions aimed at improving air quality within the city, many industries were relocated from Beijing to southern provinces, meaning that high levels of industrial emissions occur to the south of Beijing and are transported into the city, when synoptic conditions change wind flow from the north to the south (Jiang et al., 2015; Wang et al., 2019).

Zikova et al. (2016) performed a year round study examining source contributions of $PM_{2.5}$ concentrations in Beijing, using Positive Matrix Factorisation (PMF), a commonly used model for source apportionment, on collected samples. They discovered the six major sources of $PM_{2.5}$ to be: secondary sulphate (29.3%), traffic (24.7%), secondary nitrate (18.8%), biomass burning (11.7%), coal combustion (11.1%) and soil dust (4.3%). However there was significant seasonal variation, with traffic sources dominating during autumn and winter and biomass burning dominating in the summertime. Furthermore, Li et al. (2015) examined the changing contributions of individual sectors to $PM_{2.5}$ pollution in the Beijing region. Their results showed that industrial and residential sectors are the dominant contributors to average annual $PM_{2.5}$ concentrations. Separating the results by season, they found the residential sector to be the highest contributor in winter and the industrial sector in all other seasons.

Coal combustion for energy is considered to be the main industrial emission source impacting Beijing's air quality, with other important sources being iron and steel manufacturing and petroleum refining. Residential coal combustion is also believed to contribute significantly to total concentrations of PM in wintertime Beijing. In Northern China, the centralised winter heating season, which is the government subsidised central heating for homes, normally runs from mid-November to March. Many studies have found a significant contribution of residential centralised heating to pollution concentration (Zhang et al., 2015b; Lin et al., 2016; Liu et al., 2016; Li et al., 2017, 2018). Xiao et al. (2015) found that in all cities across China, air pollution worsened after the centralised heating began, but that overall the centralised heating system contributed less to PM pollution than private household heating e.g from biomass

burning and cookstoves. Li et al. (2018) used the regional model WRF-CHEM to examine the contribution of residential coal combustion to pollution episodes in the Beijing–Tianjin–Hebei (BTH) megacity cluster, finding that it contributed 23.1 % of $PM_{2.5}$ during a pollution episode in January 2014. Emissions due to transport are believed to be another major contributor to air pollution in Beijing (Sun et al., 2006). Strict emission controls on private vehicles have reduced this contribution significantly over the past decade, with the use of ultra-low sulphur fuels being implemented, reducing concentrations of sulphate aerosol (Yang et al., 2019). However, high vehicular emissions of NO_x and hydrocarbons are thought to contribute significantly to formation of both nitrate and secondary organic aerosols, which make up significant proportions of $PM_{2.5}$. Estimates of the contribution of transport to local $PM_{2.5}$ pollution in Beijing vary significantly, ranging from 7 to 25 %, while a source apportionment study by the Chinese Ministry of Environmental Protection found that vehicle emissions were the largest contributor to $PM_{2.5}$ concentrations in Beijing (Wu et al., 2017). Traffic and coal combustion are both significant sources of carbonaceous compounds (black and organic carbon) in Beijing. These compounds are of interest globally due to their ability to absorb radiation, thus having potential impacts on the climate. Black carbon (BC), otherwise known as soot, is a primary aerosol which absorbs light across the solar spectrum, and is well known for its radiative properties. Brown carbon (BrC) also absorbs SW radiation in the UV-VIS wavelength range to heat the atmosphere and cause positive radiative forcing. The magnitude of absorption by BrC is less than BC it can be present in high concentrations in urban environments, potentially contributing to global warming (Liu et al., 2020). BC and BrC may have an impact on pollution episodes through the processes outlined in section 1.7.3 and is further discussed in section 2.4.3.

2.2 Policy and Mitigation Measures

Many studies examining the success of emission controls in Beijing have focussed on the 2008 Beijing Olympics and the 2014 Asia-Pacific Economic Cooperation (APEC) Summit. Both periods were preempted by strict short term policy controls including limiting vehicles in the city, shutting or slowing down industrial output and stopping construction activities. Furthermore, both periods had so-called 'blue sky days' where air quality standards were met for the entire period (Sun et al., 2016; Wang et al., 2016). A sampling study performed by Yang et al. (2016) during winter 2013 and 2014 examined the efficiency of mitigation measures in place during APEC. Secondary aerosols were found to be the main contributor to $PM_{2.5}$ in all cases except for during the APEC period; where aerosols from biomass burning dominated. A lower average $PM_{2.5}$ mass concentration of 89.6 $\mu g/m^3$ was recorded during the APEC period compared to 117.4 $\mu g/m^3$ for the same period in 2013, this was also accompanied by a strong decrease in NO_3, SO_4 and NH_4. This indicates that the short term mitigation measures were effective in this instance, particularly in reducing the amount of secondary inorganic aerosol formed. However, the average $PM_{2.5}$ concentrations after APEC during the heating period were significant at 196.3 $\mu g\ m^3$ compared to 138.2 $\mu g/m^3$ in 2013, implying that after the controls had ended, the effects were counteracted by a strong surge in industrial activity. Furthermore, Ansari et al. (2019) found that the good air quality for the duration of the APEC summit

was more to do with favourable meteorological conditions rather than the success of emission controls, which only improved air quality by ~ 25 %.

2.3 Heavy Pollution Episodes

When locally emitted and regionally transported pollutants interact together they accumulate to cause heavy pollution episode, known as haze. These haze episodes which most commonly occur in autumn and winter, severely impact visibility (Figure 2.1). Concentrations typically build up quite rapidly during these episodes with mass concentrations of $PM_{2.5}$ peaking > 300 $\mu g/m^3$.

2.3.1 Characteristics

Typically haze episodes in Beijing, can be characterised by three stages with distinct meteorology. The clean stage occurs prior to the onset of pollution and is identified by strong northerly winds, low humidity and high surface pressure. During the clean stage, there is a strong high pressure anticyclone system to the northwest of Beijing, which allows for the advection of cold, clean air into Beijing. This stage is typically cold and dry with high surface wind speeds and a deep turbulent mixed layer. Following this, during the transport stage, a weakened high pressure to the North and a weakened high pressure system to the south west of Beijing, brings southerly winds into Beijing. This transports, warmer, humid air and typically pollutants from the surrounding industrial air from the south. The cold air mass from the north and warm polluted air mass from the south converge over Beijing, which exists in a saddle type pressure field between the two high pressure systems. This forces the cold air down and creates a temperature inversion over Beijing and is associated with high atmospheric stability and weak surface winds. In the third stage, known as the cumulative stage, regionally transported and locally emitted pollutants will rapidly accumulate in a stable and shallow planetary boundary layer. This provides conditions favourable for rapid increases in pollutant concentrations. During this stage, pollutant concentrations increase rapidly (often doubling within several hours), humidity increases, pressure decreases and a strong temperature inversion occurs (Zheng et al., 2015; Zhong et al., 2018; Chen, 2019; Wang et al., 2019; Zhong et al., 2019b). When these conditions exist, the interactions of aerosols with radiation are believed to enhance haze episodes further, through reducing surface temperatures and buoyant turbulence, increasing atmospheric stagnation. This aerosol-PBL feedback (described in section 1.7) is believed under appropriate conditions, to increase the intensity and longevity of pollution episodes in Beijing.

Changes in synoptic conditions are also primarily responsible for the dissipation of wintertime pollution episodes in Beijing. Following the build up of pollutants during the cumulative stage of the episode, there is increased atmospheric stagnation, and greatly reduced surface heating. Therefore, the dissipation of the pollution is reliant on strong advection of winds from the north west, which breaks the feedback between aerosols and atmopsheric stability. This strong wind may work to clean up the air

Figure 2.1: Beijing skyline in clear and hazy conditions

aloft, with a slight lag in the clean up of surface pollutant concentrations due to the extremely strong atmospheric stability, and high aerosol concentrations preventing PBL growth and entrainment of clean air to the surface (Wang et al., 2019).

2.3.2 Causes

Beijing and other areas in North China suffer from pollution episodes termed haze. Haze episodes in Beijing occur due to a combination of high pollutant loading combined with atmospheric processes and unfavourable meteorological conditions. In a thorough investigation of a haze episode which occured from 1st-4th December 2016, Wang et al. (2019) showed that the cause of heavy pollution episode was primarily synoptic conditional changes from the clean to transport stage as described above. These conditions lead to a temperature inversion and atmospheric stagnation, and are suggested to be the primary reason for the reduction in PBL height observed during pollution episodes. This reduction in PBL height leads to locally emitted and regionally transported pollutants being trapped in a shallow layer, which increases their concentrations at the surface. This will enhance aerosol-radiation interactions which can feedback on aerosol concentrations through affecting boundary layer dynamics. Aerosol-PBL interactions are thought to be important in enhancing haze longevity and intensity, through allowing for pollutant accumulation in a shallow boundary layer (Gao et al., 2015a; Petäjä et al., 2016).

However, although large scale atmospheric conditions preempt pollution episodes in Beijing, locally emitted and regional transported pollutants are also an essential contributor. As described in section

2.1, the sources of these pollutants are varied but are mainly caused by high sources of anthropogenic emissions, with main sources being transport, combustion for heating and residential energy use and industrial emissions from surrounding provinces. Furthermore, secondary aerosol formation is believed to contribute significantly to the high concentrations of $PM_{2.5}$ in Beijing. Understanding which sources and processes contribute most to haze episodes, will be important for effective air quality policy and improvement in Beijing.

Humidity levels also impact haze formation in several ways, for example, Yang et al. (2015) focused on the effect of relative humidity changes on heavy pollution episodes in Beijing during Autumn 2014 and found that RH levels higher than 40 % were found to accelerate secondary aerosol formation, showing a particularly strong correlation with the formation of sulphate. In humid conditions, RH $>$ 80 %, the aerosol scattering coefficients were also recorded to be twice as high compared to dry conditions, meaning that humidity directly impacts on visibility reduction during haze episodes. Furthermore, increased concentrations of water vapour in the atmosphere directly increases the size of hygroscopic aerosols, which take up water at a faster rate when RH is high. Water vapour also absorbs long wave terrestrial radiation, leading to increased heat in the atmosphere in conditions of high RH, likely to reduce vertical mixing due to the potential that the atmosphere may be warmer than the surface beneath it. Increasing temperature of the atmosphere can also accelerate chemical reactions of aerosols, further causing aerosol growth and haze persistence.

2.4 Aerosol-PBL feedback in Beijing

When the boundary layer in urban settings is deep and strongly turbulent, concentrations of pollutants at the surface are dispersed, resulting in clean or moderately polluted air. However, megacities in China experience extreme variations in boundary layer depth and dangerously high levels of air pollution. Petäjä et al. (2016) suggest that this abrupt change in boundary layer properties under polluted conditions is due to feedback between aerosol mass concentration and static stability. If the planetary boundary layer (PBL) in a city becomes heavily polluted due to increased emissions and suitable conditions for secondary formation, the magnitude of shortwave radiation (SWR) reaching the surface is reduced. This reduction in PBL height is strongly dependent on the optical depth of the layer and the aerosol optical properties. A significant portion of the incoming radiation will be absorbed by the aerosol layer, while the rest will be scattered in numerous directions. Increased temperatures at the top of the PBL compared to the surface reduces turbulence and vertical mixing, consequently reducing PBL height and increasing aerosol concentrations. The study also makes the claim for a supercritical pollution level, dependent on other conditions, whereby at a certain aerosol concentration level, SWR is decreased to a point where the PBL static stability changes from unstable to stable. During haze episodes in the North China Plain, the PBL height is around 50% lower than on non-haze days as the growth of the PBL is dependent upon surface solar radiation, which is often lower when aerosol concentrations are high. Meteorological stagnation is one

of the major factors affecting the formation and lifetime of haze. Weak surface winds suppress mixing of polluted and clean air, with typical wind speeds during haze episodes at around 1 m/s (Guo et al., 2014; Quan et al., 2014; Jia et al., 2015; Zhang et al., 2015a).

2.4.1 Observations

Research examining the feedback between aerosols, radiation and meteorology has increased over the past decade, with several studies focusing on Beijing. Multi-year observations of aerosol concentrations and PBL height have found a clear anti-correlation between the two, with PBL height decreasing as aerosol concentrations increase. Petäjä et al. (2016). suggested that under stable synoptic conditions, the polluted to non-polluted ratio of PBL height can scale to the square root of vertical turbulent fluxes. E.g – a PBL height decrease of 400 m would be equivalent to a 20 W/m^2 decrease in, for example, sensible heat flux. Zhong et al. (2019b) estimated that in the North China Plain, feedback of unfavourable meteorological conditions explained 60-70 % of the increase in $PM_{2.5}$ during the cumulative stages of haze episodes. Furthermore, through comparison of radiosonde and ECMWF reanalysis data, they estimated that when $PM_{2.5} > 400$ $\mu g/m^3$, aerosol-radiation interactions caused a 4 degree near surface cooling, which led to stratification of the lower boundary layer. This study and another by Zhong et al. (2019a) also suggests the importance of a threshold value of 100 $\mu g/m^3$, above which the aerosol-PBL feedback effect is enhanced, leading to rapid accumulation and formation of aerosol particles in a shallow PBL.

Zou et al. (2017) studied the impact of high aerosol concentrations (PM > 75 $\mu g/m^3$) on Beijing meteorology over a year-long period. Their results found that the aerosol impact on meteorology was different depending on the season, with particularly large reductions in sensible heat flux, boundary layer height and shortwave surface radiation (SWR) reported in autumn and winter .Liu et al. (2018) used the same PM threshold to estimate the impact of high aerosol concentrations on observed meteorological data over a one month period where haze episodes occurred every 4-7 days. During high aerosol periods they found that on average, SWR was 36 % lower and daily maximum boundary layer height was 0.6 km compared to 1.3 km during low aerosol periods .Bi et al. (2014) characterised aerosol optical and radiative properties during a heavy haze episode in Beijing. By using both measurements and a radiative transfer model, they found that during a heavy haze episode in Beijing, aerosol radiative forcing was negative at the surface and top of the atmosphere, but positive in the middle part of the atmosphere. This suggests cooling of the surface and warming of the air above it, potentially caused by the impact of black carbon (BC) on the aerosol-PBL feedback.

High relative humidity and reduced visibility are characteristic of Beijing haze episodes. Liu et al. (2013) suggests that aerosol hygroscopic growth links these two phenomena through causing aerosols to increase in size and increasing aerosol-radiation interactions under high ambient relative humidity (RH). Furthermore, Jia et al. (2019) suggests that the aerosol-PBL feedback varies in magnitude between haze pollution episodes (RH < 90 %) compared to polluted fog conditions (RH > 90 %). This is because

when the air is supersaturated and becomes a polluted fog, the fog can feed back on meteorology through interacting with long wave radiation. This causes long wave cooling at the fog top, which results in the upper part of the fog being cooler than the lower part. This enhances turbulence through both buoyancy and increasing LHF, particularly during the nighttime. However, during the daytime, when SW radiation is dominant the fog particles prevent SW radiation reaching the surface to a large degree, thus resulting in decreased turbulence within the PBL and enhanced stability. These conditions, although rare in Beijing, can occur overnight, towards the end of the haze period when there is strong cooling and water vapour accumulates in a shallow PBL.

Through the development of the PLAM (Parameter Linking Aerosol Pollution and Meteorological Elements), Zhong et al. (2018) attempted to isolate the impact of aerosol-PBL feedback through examining several heavy pollution episodes which occurred over a multi-year period in Beijing. By removing the impact of synoptic scale meteorology from the episodes, PLAM allows for the aerosol-PBL feedback contribution to Beijing pollution episodes to be isolated. Their work found that in 10 out of 12 heavy pollution episodes examined, high concentrations of PM were responsible for anomalous temperature inversions. These inversions were associated with reduced buoyant turbulence, as well as reduced mechanical turbulence due to weakened vertical shear of horizontal winds. Due to the reduced turbulence and increased static stability caused by the aerosol radiative cooling effect, pollutants became further concentrated in the shallow boundary layer. When these conditions occur, PLAM suggests that these stable conditions are found to explain > 70 % of explosive growth of $PM_{2.5}$ in the cumulative stages of haze episodes.

Petäjä et al. (2016), performed theoretical analysis using observations of aerosol concentrations, radiation and meteorological measurements in Nanjing, China and used this analysis to suggest the increasing importance of aerosol-PBL feedback in megacities across China. They suggest a critical value of $PM_{2.5}$ (250-300 $\mu g/m^3$) above which the aerosols cause a change in the static stability of the PBL from unstable to stable, and the aerosol-PBL feedback effect increases its impact on PBL height. So the decrease in PBL height due to PM is non-linear at these concentrations.

2.4.2 Modelling

The PLAM index is a useful tool for understanding the general contribution of aerosol-PBL feedback and synoptic meteorological changes to Beijing haze episodes. However, it cannot isolate specific factors of the aerosol-PBL feedback which may contribute to the intensity and longevity of the polluted periods. Therefore, modelling studies which can further isolate the different processes affecting the aerosol-PBL feedback are essential in furthering understanding of pollution episodes. The majority of modelling studies examining the aerosol-PBL feedback in Beijing use regional models such as the weather research and forecasting (WRF) model. For example, Wang et. al used WRF-CMAQ (WRF- Community Multi-scale Air Quality Model) to explore interactions between aerosols and meteorology during the severe Beijing haze in 2013. They performed simulations with and without aerosol-radiation interactions, in an attempt

to quantify the effect this may have on PBL dynamics. The study provides strong evidence for the importance of including aerosol-radiation interactions in models, as inclusion of these interactions led to better agreement with observed meteorological measurements and surface $PM_{2.5}$ concentrations (Wang et al., 2014).

Several studies have used WRF with an added chemistry module (WRF-CHEM) to quantify the impact of secondary aerosol formation and aerosol-radiation interactions on boundary layer meteorology. In this way, models have the ability to isolate factors which are not possible through observations alone. For example, Wu et al. (2019) used WRF-CHEM to understand how aerosol-PBL feedback impacted surface $PM_{2.5}$ concentrations in the North China Plain over a month-long period in winter 2015. Their results showed that on average, aerosol-PBL feedback accounted for a 7.8 % increase in surface $PM_{2.5}$. This effect was found to be enhanced under high aerosol concentrations (> 50 $\mu g/m^3$) which resulted in an increase of 20 % in surface $PM_{2.5}$. Gao et al. (2015b) also used WRF-CHEM to study aerosol-PBL feedback on a haze-fog episode in January 2015. Their results found that in Beijing, inclusion of aerosol-radiation interactions in the model led to a 70 % increase in maximum $PM_{2.5}$ concentrations, a surface cooling of between 0.8 - 2.8 K and a 7 - 12 % increase in surface RH. Overall, the implications of the aerosol-PBL feedback are likely to vary depending on the specific time period in question, with enhanced effects under particularly high aerosol loadings.

2.4.3 The BC effect

Ding et al. (2016) showed that black carbon (BC) can have potential negative impacts on Beijing haze episodes through absorbing shortwave radiation (SWR) above the PBL. The impact of this on boundary layer dynamics is two-fold. 1) BC above the PBL will causes warming aloft, 2) BC aloft will lower the amount of SW radiation available for absorption by the surface and by any absorbing aerosols at the surface. These two effects combined will enhance temperature inversions, leading to reduced buoyant turbulence, enhancing atmospheric stability and suppressing PBL growth. To examine the effects of changing composition, size and relative vertical distribution of aerosols while keeping other variables constant, Wang et al. (2018) varied the altitude of black carbon aerosols to examine specifically the interactions of BC and it's impact on pollution episodes. They found high sensitivity of PBL height to the altitude of aerosols, with higher level BC being more essential in suppressing PBL development. Furthermore, they found a > 15 % decrease in PBL height when BC aerosols were mixed with scattering aerosols, likely due to the absorption enhancement, which is believed to occur when BC is internally mixed (see section 1.3.6).

2.5 APHH Beijing

Due to the frequency and severity of pollution episodes in Beijing, as well as the strong motivation to explore the problem, research examining air pollution has increased over the past few years. A joint UK-China collaborative project, Air Pollution and Human Health (APHH) Beijing, took place from 2016-2019 and encompassed two major field work campaigns in Nov-Dec 2016 and May-June 2017. This project had 4 themes, each with different aims and objectives: 1) AIRPOLL which aimed to provide more understanding of the sources of air pollutants, 2) AIRPRO which aimed to provide more understanding of the processes affecting air pollution in Beijing, 3) AIRLESS which studies the exposure and health impacts of air pollution and 4)INHANCE which looked at potential policy interventions and mitigation solutions (Shi et al., 2018).

The work presented in this thesis was part of the AIRPRO strand of the APHH Beijing project and has focussed on understanding of the aerosol-PBL feedback process and its implications for Beijing haze episodes in wintertime. To understand this process this work used a coupled aerosol-radiation large eddy simulation model which can directly calculate turbulent motion and aerosol perturbations to the PBL development. This work utilised several measurements taken during the APHH Beijing winter field campaign to initialise and validate the model simulations. These include: meteorological measurements taken at 15 levels of a 320 m tower, aerosol size and composition at the surface, sensible and latent heat fluxes and PBL height from ceiliometer data. During the winter field campaign, there were 5 haze episodes, where concentrations of $PM_{2.5} > 100$ $\mu g/m^3$. These were often accompanied by temperature inversions, reduced surface wind speed, decreased surface temperature and increased surface humidity (Figure 2.2).

Figure 2.2 shows a timeseries of measurements taken through the whole APHH winter campaign period. This showcases the 5 periods, considered to be haze episodes, where PM concentrations (Figure 2.2 d) peak above 100 $\mu g/m^3$. Figure 2.2 (b) shows that these periods often also coincide with increases in humidity and decreases in temperature are shown in figure 2.2 (a). Figure 2.2 (d) showcases the changing relative composition of the aerosols over the period, which allows for understanding of the importance of secondary aerosol formation in each of the pollution episodes.

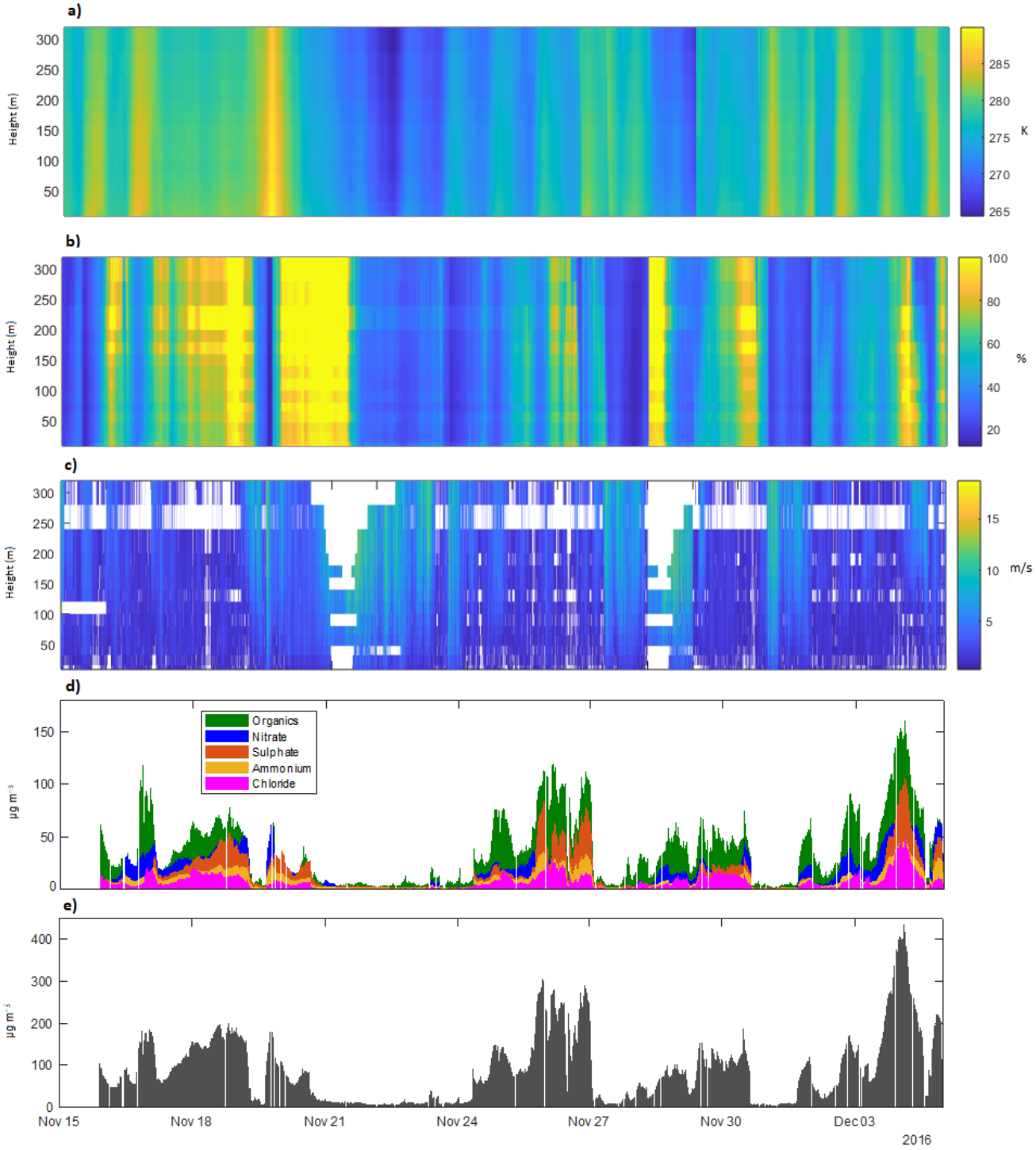

Figure 2.2: Timeseries of measurements taken during the APHH winter field campaign from Nov 15th - Dec 4th 2016. Tower meteorological measurements of a) Temperature, b) Relative Humidity, c) Wind Speed, d) Non Refractory PM_1 composition and e) Non Refractory-PM_1 concentration

References

Ansari, T. U., Wild, O., Li, J., Yang, T., Xu, W., Sun, Y., and Wang, Z.: Effectiveness of short-term air quality emission controls: a high-resolution model study of Beijing during the Asia-Pacific Economic Cooperation (APEC) summit period, Atmospheric Chemistry and Physics, 19, 8651–8668, https://doi.org/10.5194/acp-19-8651-2019, 2019.

Bi, J., Huang, J., Hu, Z., Holben, B. N., and Guo, Z.: Investigating the aerosol optical and radiative characteristics of heavy haze episodes in Beijing during January of 2013 Jianrong, Journal of Geophysical Research : Atmospheres, 119, 9884–9900, https://doi.org/10.1002/2014JD021757.Received, 2014.

Chang, X., Wang, S., Zhao, B., Xing, J., Liu, X., Wei, L., Song, Y., Wu, W., Cai, S., Zheng, H., Ding, D., and Zheng, M.: Contributions of inter-city and regional transport to PM 2.5 concentrations in the Beijing-Tianjin-Hebei region and its implications on regional joint air pollution control, Science of the Total Environment, 660, 1191–1200, https://doi.org/10.1016/j.scitotenv.2018.12.474, 2019.

Chen, A.: Analysis of meteorological factors on different stages of heavy haze pollution in Beijing, 2019, E3S Web of Conferences, 117, https://doi.org/10.1051/e3sconf/201911700018, 2019.

Chen, Y., Schleicher, N., Chen, Y., Chai, F., and Norra, S.: The influence of governmental mitigation measures on contamination characteristics of PM2.5 in Beijing, Science of the Total Environment, 490, 647–658, https://doi.org/10.1016/j.scitotenv.2014.05.049, 2014.

Ding, A. J., Huang, X., Nie, W., Sun, J. N., Kerminen, V. M., Petäjä, T., Su, H., Cheng, Y. F., Yang, X. Q., Wang, M. H., Chi, X. G., Wang, J. P., Virkkula, A., Guo, W. D., Yuan, J., Wang, S. Y., Zhang, R. J., Wu, Y. F., Song, Y., Zhu, T., Zilitinkevich, S., Kulmala, M., and Fu, C. B.: Enhanced haze pollution by black carbon in megacities in China, Geophysical Research Letters, 43, 2873–2879, https://doi.org/10.1002/2016GL067745, 2016.

Du, H., Li, J., Chen, X., Wang, Z., Sun, Y., Fu, P., Li, J., Gao, J., and Wei, Y.: Modeling of aerosol property evolution during winter haze episodes over a megacity cluster in northern China: Roles of regional transport and heterogeneous reactions, Atmospheric Chemistry and Physics, 19, 9351–9370, https://doi.org/10.5194/acp-19-9351-2019, 2019.

Fu, H. and Chen, J.: Formation, features and controlling strategies of severe haze-fog pollutions in China, Science of The Total Environment, https://doi.org/10.1016/j.scitotenv.2016.10.201, 2016.

Gao, M., Guttikunda, S. K., Carmichael, G. R., Wang, Y., Liu, Z., Stanier, C. O., Saide, P. E., and Yu, M.: Health impacts and economic losses assessment of the 2013 severe haze event in Beijing area, Science of the Total Environment, 511, 553–561, https://doi.org/10.1016/j.scitotenv.2015.01.005, 2015a.

Gao, Y., Zhang, M., Liu, Z., Wang, L., Wang, P., Xia, X., Tao, M., and Zhu, L.: Modeling the feedback between aerosol and meteorological variables in the atmospheric boundary layer during a severe fog-haze event over the North China Plain, Atmospheric Chemistry and Physics, 15, 4279–4295, https://doi.org/10.5194/acp-15-4279-2015, 2015b.

Guo, S., Hu, M., Zamora, M. L., Peng, J., Shang, D., Zheng, J., Du, Z., Wu, Z., Shao, M., Zeng, L., Molina, M. J., and Zhang, R.: Elucidating severe urban haze formation in China., Proceedings of the National Academy of Sciences of the United States of America, 111, 17 373–8, https://doi.org/10.1073/pnas.1419604111, 2014.

Jia, B., Wang, Y., Yao, Y., and Xie, Y.: A new indicator on the impact of large-scale circulation on wintertime particulate matter pollution over China, Atmospheric Chemistry and Physics, 15, 11 919–11 929, https://doi.org/10.5194/acp-15-11919-2015, 2015.

Jia, X., Quan, J., Zheng, Z., Liu, X., Liu, Q., He, H., and Liu, Y.: Impacts of Anthropogenic Aerosols on Fog in North China Plain, Journal of Geophysical Research: Atmospheres, 124, 252–265, https://doi.org/10.1029/2018JD029437, 2019.

Jiang, C., Wang, H., Zhao, T., Li, T., and Che, H.: Modeling study of PM2.5 pollutant transport across cities in China's Jing-Jin-Ji region during a severe haze episode in December 2013, Atmospheric Chemistry and Physics, 15, 5803–5814, https://doi.org/10.5194/acp-15-5803-2015, 2015.

Li, S., Feng, K., and Li, M.: Identifying the main contributors of air pollution in Beijing, Journal of Cleaner Production, 163, S359–S365, https://doi.org/10.1016/j.jclepro.2015.10.127, 2017.

Li, X., Zhang, Q., Zhang, Y., Zheng, B., Wang, K., Chen, Y., Wallington, T. J., Han, W., Shen, W., Zhang, X., and He, K.: Source contributions of urban PM2.5 in the Beijing-Tianjin-Hebei region: Changes between 2006 and 2013 and relative impacts of emissions and meteorology, Atmospheric Environment, 123, 229–239, https://doi.org/10.1016/j.atmosenv.2015.10.048, 2015.

Li, X., Wu, J., Elser, M., Feng, T., Cao, J., El-Haddad, I., Huang, R., Tie, X., Prévôt, A. S., and Li, G.: Contributions of residential coal combustion to the air quality in Beijing-Tianjin-Hebei (BTH), China: A case study, Atmospheric Chemistry and Physics, 18, 10 675–10 691, https://doi.org/10.5194/acp-18-10675-2018, 2018.

Lin, Y. C., Hsu, S. C., Chou, C. C., Zhang, R., Wu, Y., Kao, S. J., Luo, L., Huang, C. H., Lin, S. H., and Huang, Y. T.: Wintertime haze deterioration in Beijing by industrial pollution deduced from trace metal fingerprints and enhanced health risk by heavy metals, Environmental Pollution, 208, 284–293, https://doi.org/10.1016/j.envpol.2015.07.044, 2016.

Liu, F., Yon, J., Fuentes, A., Lobo, P., Smallwood, G. J., and Corbin, J. C.: Review of recent literature on the light absorption properties of black carbon: Refractive index, mass absorption cross section, and absorption function, Aerosol Science and Technology, 54, 33–51, https://doi.org/10.1080/02786826.2019.1676878, 2020.

Liu, Q., Baumgartner, J., Zhang, Y., Schauer, J. J., Xue, Y., Zhou, Z., Nie, T., Wang, K., Nie, L., Pan, T., Wu, X., Tian, H., Zhong, L., Li, J., Liu, H., Liu, S., and Shao, P.: Trends of multiple air pollutants emissions from residential coal combustion in Beijing and its implication on improving air quality for control measures, Atmospheric Environment, 126, 28–35, https://doi.org/10.1016/j.atmosenv.2015.11.031, 2016.

Liu, Q., Jia, X., Quan, J., Li, J., Li, X., Wu, Y., Chen, D., Wang, Z., and Liu, Y.: New positive feedback mechanism between boundary layer meteorology and secondary aerosol formation during severe haze events, Scientific Reports, 8, 1–8, https://doi.org/10.1038/s41598-018-24366-3, 2018.

Liu, X., Gu, J., Li, Y., Cheng, Y., Qu, Y., Han, T., Wang, J., Tian, H., Chen, J., and Zhang, Y.: Increase of aerosol scattering by hygroscopic growth: Observation, modeling, and implications on visibility, Atmospheric Research, 132-133, 91–101, https://doi.org/10.1016/j.atmosres.2013.04.007, 2013.

Meng, C., Cheng, T., Gu, X., Shi, S., Wang, W., Wu, Y., and Bao, F.: Contribution of meteorological factors to particulate pollution during winters in Beijing, Science of the Total Environment, 656, 977–985, https://doi.org/10.1016/j.scitotenv.2018.11.365, 2019.

Petäjä, T., Järvi, L., Kerminen, V.-M., Ding, A. J., Sun, J. N., Nie, W., Kujansuu, J., Virkkula, A., Yang, X., Fu, C. B., Zilitinkevich, S., and Kulmala, M.: Enhanced air pollution via aerosol-boundary layer feedback in China., Scientific reports, 6, 18 998, https://doi.org/10.1038/srep18998, 2016.

Pui, D. Y. H., Chen, S. C., and Zuo, Z.: PM2.5 in China: Measurements, sources, visibility and health effects, and mitigation, Particuology, 13, 1–26, https://doi.org/10.1016/j.partic.2013.11.001, 2014.

Quan, J., Tie, X., Zhang, Q., Liu, Q., Li, X., Gao, Y., and Zhao, D.: Characteristics of heavy aerosol pollution during the 2012-2013 winter in Beijing, China, Atmospheric Environment, 88, 83–89, https://doi.org/10.1016/j.atmosenv.2014.01.058, 2014.

Shi, Z., Vu, T., Kotthaus, S., Grimmond, S., Harrison, R. M., Yue, S., Zhu, T., Lee, J., Han, Y., Hu, M., Ji, D., Jiang, X., Jones, R., Kalberer, M., Kelly, F. J., Langford, B., Lin, C., Lewis, A. C., Li, J., Li, W., Liu, H., Lu, K., Mann, G., Mcfiggans, G., Miller, M., Mills, G., Nemitz, E., Ouyang, B., Palmer, P. I., Percival, C., Popoola, O., Reeves, C., Rickard, A. R., Shao, L., Shi, G., Spracklen, D., Stevenson,

D., Sun, Y., Sun, Z., Tao, S., Tong, S., Wang, Q., Wang, W., Wang, X., Wang, Z., Whalley, L., Wu, X., Wu, Z., Xie, P., Yang, F., Zhang, Q., Zhang, Y., Zhang, Y., Polytechnique, E., Atmospheric, W., Laboratories, C., Division, E. S., Centre, L. E., Environmental, C., and Energy, R.: Introduction to Special Issue - In-depth study of air pollution sources and processes within Beijing and its surrounding region, Atmospheric Chemistry and Physics Discussions, 2018.

Squires, F. A., Nemitz, E., Langford, B., Wild, O., Drysdale, W. S., Acton, W. J. F., Fu, P., Grimmond, C. S. B., Hamilton, J. F., Hewitt, C. N., Hollaway, M., Kotthaus, S., Lee, J., Metzger, S., Pingintha-durden, N., Shaw, M., Vaughan, A. R., Wang, X., Wu, R., Zhang, Q., and Zhang, Y.: Measurements of traffic dominated pollutant emissions in a Chinese megacity, Atmospheric Chemistry and Physics Discussions, pp. 1–33, 2020.

Sun, Y., Zhuang, G., Tang, A., Wang, Y., and An, Z.: Chemical Characteristics of PM 2.5 and PM 10 in HazeFog Episodes in Beijing, Environmental Science Technology, 40, 3148–3155, https://doi.org/10.1021/es051533g, 2006.

Sun, Y., Jiang, Q., Wang, Z., Fu, P., Li, J., Yang, T., and Yin, Y.: Investigation of the sources and evolution processes of severe haze pollution in Beijing in January 2013, Journal of Geophysical Research: Atmospheres, 119, 4380–4398, https://doi.org/10.1002/2014JD021641, 2014.

Sun, Y., Wang, Z., Wild, O., Xu, W., Chen, C., Fu, P., Du, W., Zhou, L., Zhang, Q., Han, T., Wang, Q., Pan, X., Zheng, H., Li, J., Guo, X., Liu, J., and Worsnop, D. R.: "APEC Blue": Secondary Aerosol Reductions from Emission Controls in Beijing., Scientific reports, 6, 20 668, https://doi.org/10.1038/srep20668, 2016.

Sun, Y. L., Wang, Z. F., Fu, P. Q., Yang, T., Jiang, Q., Dong, H. B., Li, J., and Jia, J. J.: Aerosol composition, sources and processes during wintertime in Beijing, China, Atmospheric Chemistry and Physics, 13, 4577–4592, https://doi.org/10.5194/acp-13-4577-2013, 2013.

Tao, M., Chen, L., Li, R., Wang, L., Wang, J., Wang, Z., Tang, G., and Tao, J.: Spatial oscillation of the particle pollution in eastern China during winter: Implications for regional air quality and climate, Atmospheric Environment, 144, 100–110, https://doi.org/10.1016/j.atmosenv.2016.08.049, 2016.

Wang, L., Liu, J., Gao, Z., Li, Y., Huang, M., Fan, S., Zhang, X., Yang, Y., Miao, S., Zou, H., Sun, Y., Chen, Y., and Yang, T.: Vertical observations of the atmospheric boundary layer structure over Beijing urban area during air pollution episodes, Atmospheric Chemistry and Physics, 19, 6949–6967, https://doi.org/10.5194/acp-19-6949-2019, 2019.

Wang, Q., Y. Sun, Q., Jiang, W., Du, C., Sun, P., Fu, P., and Wang, Z.: Chemical composition of aerosol particles and light extinction apportionment before and during the heating season in Beijing, China, Journal of Geophysical Research Atmospheres, 120, 12 708–12 722, https://doi.org/10.1002/2014JC010564.Received, 2015.

Wang, Y., Zhang, Y., Schauer, J. J., de Foy, B., Guo, B., and Zhang, Y.: Relative impact of emissions controls and meteorology on air pollution mitigation associated with the Asia-Pacific Economic Cooperation (APEC) conference in Beijing, China, Science of the Total Environment, 571, 1467–1476, https://doi.org/10.1016/j.scitotenv.2016.06.215, 2016.

Wang, Y., Bao, S., Wang, S., Hu, Y., Shi, X., Wang, J., Zhao, B., Jiang, J., Zheng, M., Wu, M., Russell, A. G., Wang, Y., and Hao, J.: Local and regional contributions to fine particulate matter in Beijing during heavy haze episodes, Science of the Total Environment, 580, 283–296, https://doi.org/10.1016/j.scitotenv.2016.12.127, 2017.

Wang, Y. S., Yao, L., Wang, L. L., Liu, Z. R., Ji, D. S., Tang, G. Q., Zhang, J. K., Sun, Y., Hu, B., and Xin, J. Y.: Mechanism for the formation of the January 2013 heavy haze pollution episode over central and eastern China, Science China Earth Sciences, 57, 14–25, https://doi.org/10.1007/s11430-013-4773-4, 2014.

Wang, Z., Huang, X., and Ding, A.: Dome effect of black carbon and its key influencing factors: A

one-dimensional modelling study, Atmospheric Chemistry and Physics, 18, 2821–2834, https://doi.org/10.5194/acp-18-2821-2018, 2018.

Wu, J., Bei, N., Hu, B., Liu, S., Zhou, M., Wang, Q., Li, X., Liu, L., Feng, T., Liu, Z., Wang, Y., Cao, J., Tie, X., Wang, J., Molina, L. T., Li, G., Chemistry, A., Physics, A., Engineering, B., City, I., and Jolla, L.: Aerosol-radiation feedback deteriorates the wintertime haze in North China Plain, Atmospheric Chemistry and Physics Discussions, pp. 1–50, 2019.

Wu, Y., Wang, X., Tao, J., Huang, R., Tian, P., Cao, J., Zhang, L., Ho, K. F., Han, Z., and Zhang, R.: Size distribution and source of black carbon aerosol in urban Beijing during winter haze episodes, Atmospheric Chemistry and Physics, 17, 7965–7975, https://doi.org/10.5194/acp-17-7965-2017, 2017.

Xiao, Q., Ma, Z., Li, S., and Liu, Y.: The impact of winter heating on air pollution in China, PLoS ONE, 10, 1–11, https://doi.org/10.1371/journal.pone.0117311, 2015.

Yang, D., Zhang, S., Niu, T., Wang, Y., Xu, H., Zhang, K. M., and Wu, Y.: High-resolution mapping of vehicle emissions of atmospheric pollutants based on large-scale, real-world traffic datasets, Atmospheric Chemistry and Physics, 19, 8831–8843, https://doi.org/10.5194/acp-19-8831-2019, 2019.

Yang, H., Chen, J., Wen, J., Tian, H., and Liu, X.: Composition and sources of PM2.5 around the heating periods of 2013 and 2014 in Beijing: Implications for efficient mitigation measures, Atmospheric Environment, 124, 378–386, https://doi.org/10.1016/j.atmosenv.2015.05.015, 2016.

Yang, Y., Liu, X., Qu, Y., Wang, J., An, J., Zhang, Y., and Zhang, F.: Formation mechanism of continuous extreme haze episodes in the megacity Beijing, China, in January 2013, Atmospheric Research, 155, 192–203, https://doi.org/10.1016/j.atmosres.2014.11.023, 2015.

Zhang, H., Wang, S., Hao, J., Wang, X., Wang, S., Chai, F., and Li, M.: Air pollution and control action in Beijing, Journal of Cleaner Production, 112, 1519–1527, https://doi.org/10.1016/j.jclepro.2015.04.092, 2016.

Zhang, Q., Quan, J., Tie, X., Li, X., Liu, Q., Gao, Y., and Zhao, D.: Effects of meteorology and secondary particle formation on visibility during heavy haze events in Beijing, China, Science of the Total Environment, 502, 578–584, https://doi.org/10.1016/j.scitotenv.2014.09.079, 2015a.

Zhang, X. Y., Wang, J. Z., Wang, Y. Q., Liu, H. L., Sun, J. Y., and Zhang, Y. M.: Changes in chemical components of aerosol particles in different haze regions in China from 2006 to 2013 and contribution of meteorological factors, Atmospheric Chemistry and Physics, 15, 12 935–12 952, https://doi.org/10.5194/acp-15-12935-2015, 2015b.

Zheng, G. J., Duan, F. K., Su, H., Ma, Y. L., Cheng, Y., Zheng, B., Zhang, Q., Huang, T., Kimoto, T., Chang, D., Pöschl, U., Cheng, Y. F., and He, K. B.: Exploring the severe winter haze in Beijing: The impact of synoptic weather, regional transport and heterogeneous reactions, Atmospheric Chemistry and Physics, 15, 2969–2983, https://doi.org/10.5194/acp-15-2969-2015, 2015.

Zhong, J., Zhang, X., Dong, Y., Wang, Y., Liu, C., Wang, J., Zhang, Y., and Che, H.: Feedback effects of boundary-layer meteorological factors on cumulative explosive growth of PM2.5; during winter heavy pollution episodes in Beijing from 2013 to 2016, Atmospheric Chemistry and Physics, 18, 247–258, https://doi.org/10.5194/acp-18-247-2018, 2018.

Zhong, J., Zhang, X., and Wang, Y.: Reflections on the threshold for PM 2.5 explosive growth in the cumulative stage of winter heavy aerosol pollution episodes (HPEs) in Beijing, Tellus, Series B: Chemical and Physical Meteorology, 71, 1–7, https://doi.org/10.1080/16000889.2018.1528134, 2019a.

Zhong, J., Zhang, X., Wang, Y., Wang, J., Shen, X., Zhang, H., Wang, T., Xie, Z., Liu, C., Zhang, H., Zhao, T., Sun, J., Fan, S., Gao, Z., Li, Y., and Wang, L.: The two-way feedback mechanism between unfavorable meteorological conditions and cumulative aerosol pollution in various haze regions of China, Atmospheric Chemistry and Physics, 19, 3287–3306, https://doi.org/10.5194/acp-19-3287-2019, 2019b.

Zikova, N., Wang, Y., Yang, F., Li, X., Tian, M., and Hopke, P. K.: On the source contribution to Beijing

PM2.5 concentrations, Atmospheric Environment, 134, 84–95, https://doi.org/10.1016/j.atmosenv.2016.03.047, 2016.

Zou, J., Sun, J., Ding, A., Wang, M., Guo, W., and Fu, C.: Observation-based estimation of aerosol-induced reduction of planetary boundary layer height, Advances in Atmospheric Sciences, 34, 1057–1068, https://doi.org/10.1007/s00376-016-6259-8, 2017.

Chapter 3

Methodology

Atmospheric models, alongside observations, are a fundamental method for understanding important atmospheric processes. These models resolve processes at different scales depending on their intended area of focus, with large differences in both domain size and timescale. Often the choice between which processes to represent in atmospheric models is a trade off between accuracy and computational efficiency. Furthermore, the domain size, resolution and timescale will all be chosen depending on the problem which is being addressed. For example, climate models often parameterise processes on the small scale but can simulate decades at a time across the entire global domain, providing important information for future projections. Regional models can span whole countries or continents and typically have resolutions in the 10's of km's. Choosing the necessary resolution and domain size will depend on the area of interest. The Weather Research and Forecasting (WRF) model is a meso-scale numerical weather forecast system used in weather forecasting and meteorological processes. The WRF model can be used with an added chemistry module (WRF-CHEM), and includes online calculation of dynamical inputs, transport, aerosol and gaseous chemical and physical processes and interactions with radiation. WRF-CHEM is frequently used to examine aerosol interactions, often for air pollution studies, including the examination of the aerosol-PBL feedback (Jacobson, 1997; Boucher, 2013; Zou et al., 2017).

Although useful in understanding processes affecting pollution events in the atmosphere, regional models such as WRF-CHEM are too coarse to capture some atmospheric dynamical processes such as turbulent motion and the energy cascade from eddies, even when performed at high resolutions. Furthermore, they are often reliant on chosen boundary layer schemes, which are heavily parameterised for computational efficiency. Consequently, boundary layer development, dynamics and processes are reliant on the chosen boundary layer schemes, which impacts model results (Cuchiara and Rappenglück, 2018). High resolution models with small domains, such as Large Eddy Simulation (LES) models, allow for direct interpretation of boundary layer meteorology and coupling of boundary layer processes. For this reason, they are useful in understanding aerosol-radiation interactions and their impacts on dynamics. In order to fully elucidate the Beijing haze problem detailed aerosol schemes, aerosol-radiation interactions and aerosol-dynamical feedbacks are essential (Hu et al., 2010; Herbert et al., 2020).

3.1 LES Models

Large eddy simulation (LES) models solve the Navier-Stokes equation which governs the motion of fluids, describes viscous flow and directly calculates the energy cascades caused by boundary layer eddies. The high resolution of LES models enables a detailed representation of boundary layer structure and dynamics, allowing for direct interpretation of turbulent motion. LES models directly calculate larger scale eddies while parameterising small eddies below the grid size for computational efficiency. The advantage of LES models is their high resolution (in the order of tens of metres) and direct calculation of turbulent fluxes. This allows for direct representation of boundary layer dynamics without the need for parameterisation. LES models are frequently used to research boundary layer interactions, with particular focus on convection, stratocumulus and cumulus clouds and in the study of radiation fogs. Furthermore, LES models have been used to examine the impact of aerosol properties on convective and marine boundary layer development, cumulus cloud dynamics and pollutant dispersion (Jiang et al., 2002; Siebesma et al., 2003; Ackerman et al., 2009; Stevens and Feingold, 2009; Ovchinnikov and Easter, 2010; Jiang and Wang, 2014; Hoffmann et al., 2015; Maalick et al., 2016; Boutle et al., 2017; Tonttila et al., 2017).

Herbert et. al (2020) used an LES model to look at the impact of biomass burning plumes on stratocumulus clouds. Through altering the properties of the absorbing aerosol layer, they could examine the semi-direct effect on the cloud properties and subsequent boundary layer development. Their results show high sensitivity to both the distance between the bottom of the aerosol layer and cloud top and the AOD of the aerosol layer, with strong feedback on both cloud and boundary layer dynamics. Using an LES model for this study allows for full coupling of boundary layer processes and can quantify the effect of different variables and the diurnal cycle. This work shows the ability and usefulness of coupling aerosol-radiation interactions within an LES model to further understanding of the development and interactions of aerosol on PBL dynamics (Herbert et al., 2020).

The use of an LES model to investigate boundary layer dynamics is common, normally they are employed in rural environments, with only a few recent studies employing an LES model in urban environments. Recently, LES models have been acknowledged as a way to better understand the problem of urban air pollution. However, the main focus of this has been the application of LES models at the local scale to examine the impact of the street/urban canyon on pollutant dispersion (Ikeda et al., 2012; Nakayama et al., 2012; Burman et al., 2019). LES models provide the perfect opportunity to capture the changing boundary layer dynamics caused by aerosol interactions, which are thought to be important in Beijing haze episodes (section 2.4). The high resolution and direct calculation of boundary layer processes by LES models and the sensitivity to dynamical perturbations will allow for quantification of the properties affecting the aerosol-PBL feedback. For the first time, in this work, a coupled dynamical aerosol model has been developed, tested and set up for the urban environments of Beijing to investigate the aerosol-PBL feedback effect on heavy pollution episodes. UCLALES-SALSA, a small scale, high resolution 3D model which includes aerosol-radiation, aerosol-meteorology and thermodynamic schemes has been developed for

urban Beijing in order to examine the sensitivity of boundary layer dynamics to changing aerosol properties.

3.2 Modelling Tools

3.2.1 UCLALES

UCLALES is an LES model designed to study convective dry boundary layers, as well as stratocumulus and cumulus clouds. Variables include the three components of wind (u,v,w), the potential temperature (θ), total water mixing ratio (qt) and a number of parameters to support microphysical and chemical processes. The model has high adaptability with the ability to calculate a range of microphysical processes as well as methods for specifying sub-grid fluxes at the lower boundary and radiation types. The LES uses a third-order Runga-Kuta scheme for time integration, fourth order centered scheme for advection of momentum and a fourth order upwind scheme for scalar advection. In the standard model a two-moment warm rain microphysical scheme is used, the vertical is spanned by a stretchable grid and a sponge layer is applied at the domain top to prevent gravity waves being released into the boundary. Boundary conditions are periodic (Stevens, 2010; Maalick et al., 2016; Tonttila et al., 2017)

3.2.2 SALSA

SALSA (Sectional Aerosol Module for Large Scale Application) is a sectional model which treats non-activated aerosol, cloud and precipitation processes separately. In the sectional approach, the particle size distribution is split into a discrete number of size bins (Figure 3.1). Sectional models are advantageous for studying aerosol interactions as they generally include more detailed microphysics than the more common modal and moment approaches. This provides a more accurate representation of the aerosol population size distribution. In the modal approach, the particle size distribution is split into modes based on the lognormal size distribution as in figure 1.1, however this approach can lead to difficulties in including relevant aerosol processes such as; formation, growth and aging. The moment approach has similar limitations as the modal approach but involves describing the size distribution through a limited number of moments, which are parameterised. The sectional approach is less computationally efficient but can describe different microphysical processes more accurately (Zhang et al., 2002; Kokkola et al., 2008). Models often make a compromise between accuracy and computational efficiency, resolution and size of domain. Therefore, different approaches are often taken to treat the aerosol population in both large and small scale models as a way to compromise between computational efficiency and detail.

SALSA is used to calculate nucleation, condensation, coagulation, cloud activation and sulphate production, however to reduce computational cost and optimise performance only relevant chemical compounds and processes are included for specific size bins. Furthermore, these processes can be switched off to allow for isolation of the importance of certain processes. Figure 3.1 describes how SALSA treats

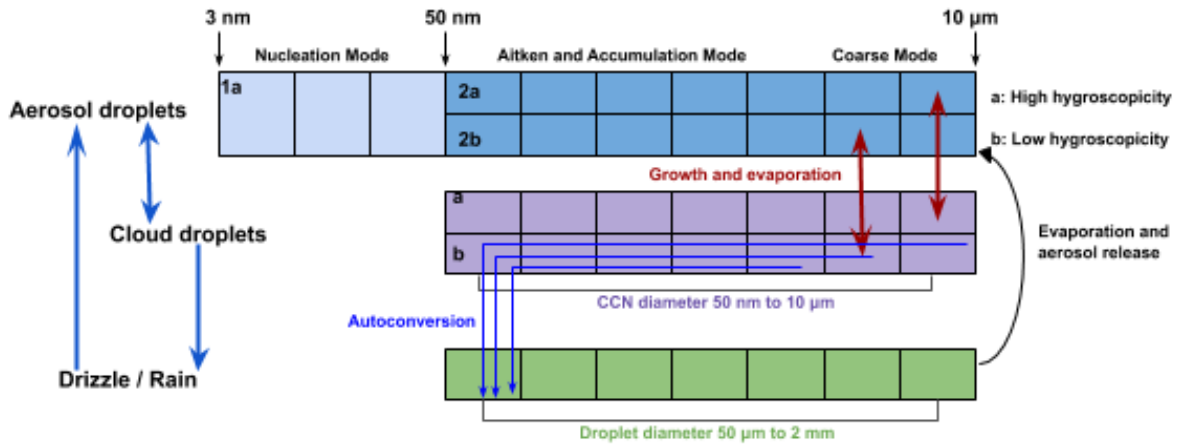

Figure 3.1: Schematic of the size bin layout for SALSA including the internal and external mixing size bins and the corresponding cloud and rain droplet bins. Taken with permission from the paper by (Slater et al., 2020) and based on the work by (Tonttila et al., 2017)

aerosols, sub-range 1 is made up of 3 size bins containing particles ranging from 3 to 50 nm in diameter and only contains organic carbon and sulphate. Aerosols in this sub-range are assumed to be internally mixed, with only condensation growth, coagulation and wet deposition as active processes. Subrange 2a includes particles larger than 50 nm and can include all chemical compositions (sulphate, organic carbon, nitrate, ammonium, black carbon, dust and sea salt). SALSA has a parallel set of bins in sub-range 2. This is to allow for externally mixed particles, with separate size distributions and fractional compositions. Although not considered in this work, particles in sub-range 2 can also take part in cloud activation. SALSA calculates all microphysical processes for each time step individually, apart from nucleation and condensation which are calculated simultaneously due to the importance of competition within these processes. After each time step there may be a redistribution of particles as they grow or shrink and move into different size bins. The SALSA module solves relevant microphysical processes for each size bin. In this thesis, the processes of nucleation, condensation of water and coagulation are considered. Wet and dry deposition and semi-volatile condensation are not considered. Nucleation is accounted for by calculating the formation rate of 3 nm particles, using a parameterised formation rate. Condensation of water vapour is based on the Analytical Predictor of Condensation scheme with a saturation vapour of zero (Kokkola et al., 2008; Tonttila et al., 2017).

SALSA has thus far been coupled to the LES models, UCLALES and PALM, as well as in the climate model ECHAM, showing its high versatility and ability to capture a variety of aerosol processes (Kokkola et al., 2008; Tonttila et al., 2017; Kokkola et al., 2018; Kurppa et al., 2019). In this work, we focus on the direct aerosol radiation interactions and the impact on PBL dynamics, this utilises both the ability of UCLALES to capture at high resolution boundary layer development and SALSA's ability to simulate aerosol processes, for different size ranges and compositions. The coupled model UCLALES-SALSA was used for all simulations in this thesis, and includes a fully coupled aerosol-radiation scheme. UCLALES-SALSA was developed at the Finnish Meteorological Institute (FMI), and the work presented here was done in collaboration and with the help of those colleagues. A comprehensive description of UCLALES-SALSA

is outlined below.

3.2.3 UCLALES-SALSA

UCLALES-SALSA, fully couples the aerosol sectional scheme with UCLALES and has thus far been used to study stratocumulus clouds, radiation fog and cloud seeding. In the paper by Tonttila et al. (2017) UCLALES-SALSA v1.0 was fully introduced and a case study compared the coupled UCLALES-SALSA with UCLALES only simulations for marine stratocumulus clouds observed during the DYCOMS II field campaign Stevens et al. (2003). Their results show the importance of including aerosol modules in modelling of cloud microphysical processes and dynamics. The model was also tested to see if it could correctly simulate a radiation fog event which occurred in Cardington, UK, finding that aerosols were essential in the interaction and formation of a well mixed radiative fog event. More recently, Tonttila et al. (2021), used UCLALES-SALSA to examine weather modification, specifically the impact of cloud seeding to enhance precipitation events in arid or semi-arid regions.

Atmospheric radiation in UCLALES is interactive and calculated through the four stream radiative transfer by Fu and Liou (1993), which takes into account atmospheric gases and is fully coupled to the aerosol properties outlined in SALSA to allow for examination of direct aerosol-radiation interactions. In this work the coupled four stream aerosol radiative transfer scheme was used for the first time. For the work presented in this thesis, UCLALES-SALSA, was set up for the first time to examine an urban environment, specifically Beijing, which required development due to the differences in urban and rural boundary layers. This is the first time to our knowledge an LES model has been used to examine the urban boundary layer in Beijing and to examine the aerosol-PBL feedback in an urban setting. Experimental setup, adaptations to the modelling framework for set up in the urban environment of Beijing for the three pieces of research in Paper 1, 2 and 3 and limitations of the modelling framework are outlined below.

3.3 Experimental Setup

UCLALES-SALSA setup as described here is the baseline set up for all simulations presented in the research papers outlined. Horizontal resolution of 30 m was applied across a domain size of 5.4 km x 5.4 km in the horizontal. The height of the domain was set to 1.8 km in the vertical with a resolution of 10 m. The horizontal domain size was chosen to be at least three times that of the vertical to allow for the movement of larger eddies. Sensitivity runs with larger domain sizes were performed (8km x 8km) but results were the same as in the smaller domain. Therefore, to save resources and time, the smaller domain size of 5.4 km x 5.4 km was used. A vertical height of 1.8 km was chosen as being higher than maximum PBL height in all cases. As with the horizontal domain test cases, sensitivity test cases were performed with vertical domain stretched to 2.5 km but this had no influence on results. A damping layer was imposed at the top of the model domain to prevent gravity waves reflecting back into the model top, which would otherwise

influence the upper boundary of the model (Maalick, 2017). Potential temperature, water vapour mixing ratio, and the u and v components of wind were used for profile initialisation which is detailed in each of the corresponding papers. Upper air soundings of ozone, temperature and water vapour were taken from ECMWF-ERA5 reanalysis data and used for radiative transfer calculations. For all results, potential temperature (θ) vertical profiles are plotted and referred to when talking about aerosol warming or cooling effects. Vertical profiles of potential temperature (θ) are plotted and referred to as the vertical variation in θ provides information on the stability of the atmosphere, whereas vertical variation in absolute temperature will be influenced by pressure changes (Stull, 2015).

3.3.1 Surface Scheme

The surface scheme used was based on the work by Ács et al. (1991). This uses soil moisture, run off and heat conductivity of the soil to calculate the surface temperatures. Concrete, the predominant surface in Beijing, has very different thermal properties than soil. Specifically compared to soil, concrete has lower porosity, higher surface heat capacity, higher thermal conductivity and lower moisture content, this leads to higher heat storage. Directly this means the absorption and release of heat into the atmosphere will be slower (Roberts et al., 2006; Russell et al., 2015; Meyn and Oke, 2009). Key equations for the surface scheme calculations include direct calculation of the sensible (Eq. 3.1) and latent (Eq. 3.2) heat flux and heat storage (Eq. 3.3) terms of the surface energy balance scheme (Eq. 3.4):

$$SHF = \rho C_p \frac{T_g - T_a}{r_a} \tag{3.1}$$

$$LHF = \frac{\rho C_p}{\lambda} \frac{f_h e_s(T_g) - e_a}{r_{surf} + r_a} \tag{3.2}$$

$$\Delta Q_s = (\frac{\omega C \lambda}{2})^{\frac{1}{2}} (T_g - \overline{T}) \tag{3.3}$$

The sensible heat flux (SHF) term is influenced by the difference between surface temperature (T_g) and air temperature (T_a). While latent heat flux (LHF) is dependent on the difference between saturation vapour pressure (e_s) at surface temperature (T_g) and water vapour mixing ratio of air (e_a). The heat storage term is shown to be influenced by volumetric heat capacity (C) and thermal conductivity (λ) of the surface and the difference between surface temperature (T_g) and average daily temperature in the 2 cm soil layer ($\overline{T}$). These terms combined with calculations of net shortwave (SW) and net longwave (LW) radiation, allow for calculation of the surface energy balance component ($F_{(T_g)}$) which is used to estimate changing surface temperature (T_g) over time (Eq. 3.5).

$$F(T_g) = S - R(T_g) - LHF(T_g) - SHF(T_g) - \Delta Q_s \tag{3.4}$$

$$T_g^{t+\Delta t} = T_g^t + F_{(T_g)}^t / (\frac{c_1}{\Delta t} - \frac{\delta F_{(T_g)}}{\delta T_g}) \tag{3.5}$$

The calculation of surface temperature at each time-step then influences the SHF, LHF and ΔQ_s terms of the surface energy balance, which in turn effect the future surface temperature calculation. Therefore, these terms are coupled and strongly influence each other. Different environments are known to have different characteristics in terms of their surface energy components, for example tropical environments typically have low Bowen ratios, calculated as the ratio of SHF to LHF ($\frac{SHF}{LHF}$), while urban environments have high Bowen ratios and high heat storage terms. As this surface scheme and UCLALES-SALSA generally have only previously been used for rural environments, the next section details adaptations made to the model framework to make it suitable for an urban environment.

Furthermore, in urban environments, as detailed in section 1.6, an additional anthropogenic heat flux (Q_f) term influences the energy balance. For the set up of the model for an urban environment this term was included in the surface energy balance scheme so that Eq. 3.5 is changed to Eq. 3.6:

$$F(T_g) = S - R(T_g) - LHF(T_g) - SHF(T_g) - \Delta Q_s + \mathbf{Q}_f \tag{3.6}$$

The inclusion of Q_f and model sensitivity to the term are outlined in the next section (3.4).

3.4 Model Adaptations

UCLALES-SALSA has been previously employed to investigate aerosol-cloud and aerosol-fog interactions in rural environments (Tonttila et al., 2017, 2021). To set up the model for the urban environment of Beijing, adaptations to the model were performed. Primarily, the alterations and testing were to the surface scheme. Adaptations and sensitivity analyses were performed against observational and reanalysis data in Beijing. Initial simulations showed a large discrepancy between observed and measured potential temperature profiles, particularly at the surface. As well as large differences in sensible and latent heat flux results (Figure 3.2). Research and discussion with colleagues outlined that this was likely due to the differences in modelling urban and rural environments. The large differences shown between modelled and measured surface heat fluxes and temperature profiles were thought to be due to differences in the physical properties of an urban environment. The surface scheme in UCLALES-SALSA is based on a coupled soil-surface model by Ács et al. (1991). As outlined in the previous section, this scheme directly calculates heat fluxes based on the temperature and water content of the soil at different depth levels as well as at the surface. Information on soil water and temperature fractions, as well as surface heat capacity was unavailable for the area in focus. Furthermore, the materials of the urban surface (e.g concrete) have different physical properties than typical rural surfaces (grassland/soil etc.) and therefore alterations and testing to the model framework were performed against measurements taken in Beijing on clean days. The use of days which had low aerosol concentrations allowed for testing of this set up without the influence of aerosols influencing either observed or measured results.

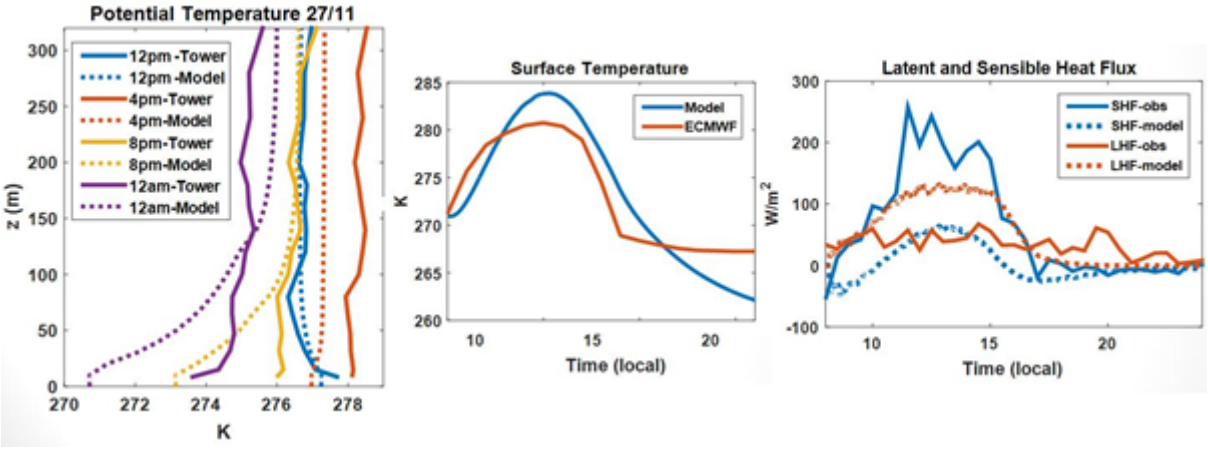

Figure 3.2: Potential Temperature, Surface Temperature, and Latent and Sensible Heat Flux for initial model simulations compared to meteorological tower measurements (Potential Temperature), ECMWF-ERA5 reanalysis data (surface temperature) and measured heat fluxes (sensible and latent heat flux)

Initial simulation comparisons of the vertical potential temperature profiles of the model results and the tower measurements show that the largest and most distinct discrepancy was in the lowest 100 m of the atmosphere. With the model simulating a distinct radiative cooling (of θ) around sunset (5pm in late November Beijing). In contrast, measured values show a less pronounced radiative cooling effect until around 11pm (Figure 3.2). The first part of the work therefore focussed on examining and tuning the surface parameters to better simulate an urban environment. These include water fraction of the surface, anthropogenic heat flux and surface heat capacity. Figure 3.2 also shows that initial simulations show a large difference in the measured and modelled sensible and latent heat flux diurnal profiles. Particularly with relation to the maximum values. The simulation underestimated sensible heat flux and overestimated latent heat flux. Due to the importance of these values as determiners for boundary layer turbulence and the surface energy balance scheme, correctly modelling these fluxes and the potential temperature profiles in the clean periods is essential in order to later examine the impact of aerosol radiation interactions on boundary layer turbulence.

3.4.1 Surface Heat Capacity (C_h)

Surface heat capacity directly impacts the rate of absorption and re-release of solar thermal energy which is responsible for radiative cooling and heating of the air above the surface. Surface heat capacity is seen as a major component governing the heat storage term (ΔQ_s) in the surface energy balance (Eq. 3.3 and 3.4). This further feeds back on the surface heat fluxes (Eq. 3.1, 3.2 and 3.5). Colleagues who developed the model at FMI, suggested that this might be the most dependent variable for adapting UCLALES-SALSA for urban environments. Therefore, the focus of the adaptation primarily focused on this value. Using the clean day of 22/11, alterations to the surface heat capacity were performed within a sensible range (Takebayashi and Moriyama, 2012). Higher surface heat capacity values resulted in less surface radiative cooling in the evening and showed a better match in this regard to modelled tower measurements. However,

increasing surface heat capacity also decreased temperatures throughout the column, particularly during the daytime (Figure 3.3).

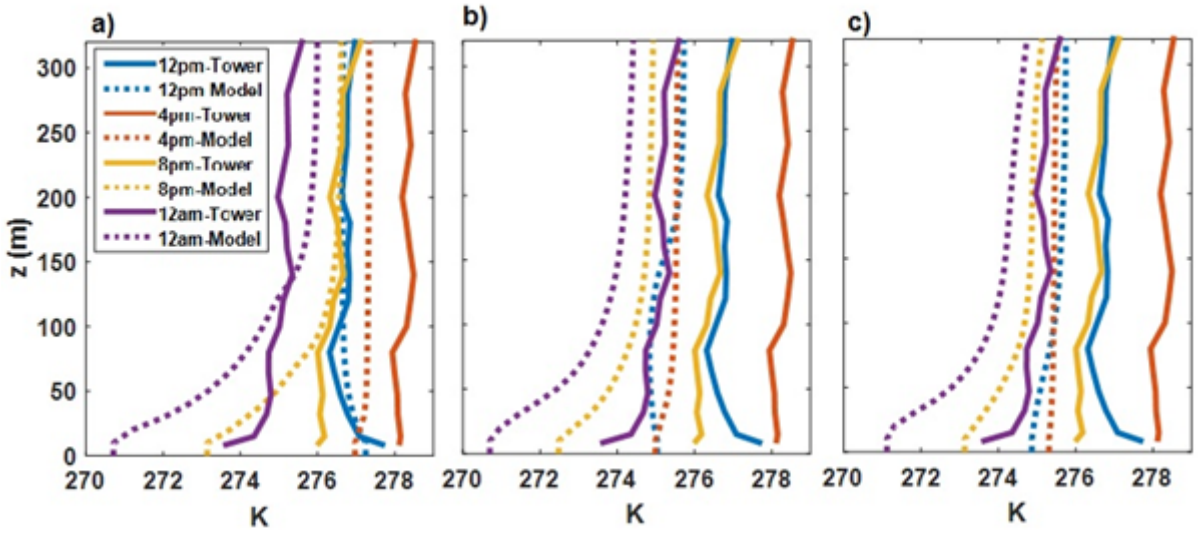

Figure 3.3: Potential temperature profile comparisons between modelled and measured values. Different surface volumetric heat capacities were used for each simulation. a)$2e^6$ b) $5e^6$ c)$7e^6$ $Jm^{-2}K^{-1}$

Furthermore, increasing surface heat capacity decreased and delayed maximum peaks in SHF and PBLH. Figure 3.4 shows that increasing surface heat capacity from $2e^6$ to $9e^6$ in these test simulations delays PBL development to 12:00 LST from 09:00 LST and delays the peak in SHF from 11:00 LST to 14:00 LST. Increasing this value also delays the collapse of the PBL in the evening. High values of C_h correspond to high heat storage, which in turn means slower absorption and re-release of heat from the surface (Eq. 3.3), consequently when this value is high, the heat absorbed by the surface is slowly released to heat the air, resulting in slightly longer but slower initial heating of the PBL throughout the day (fig. 3.3-3.4).

After several attempts of adjusting this value it became apparent that solely tuning this surface parameters could not solely account for the discrepancies in observed and modelled results, as a shift in the temperatures in the lowest 100m lowered temperatures above the surface (Figure 3.3). This resulted in a larger difference between modelled and measured results. I therefore concluded that solely altering heat capacity was not sufficient to model the urban environment of Beijing and so I explored other options.

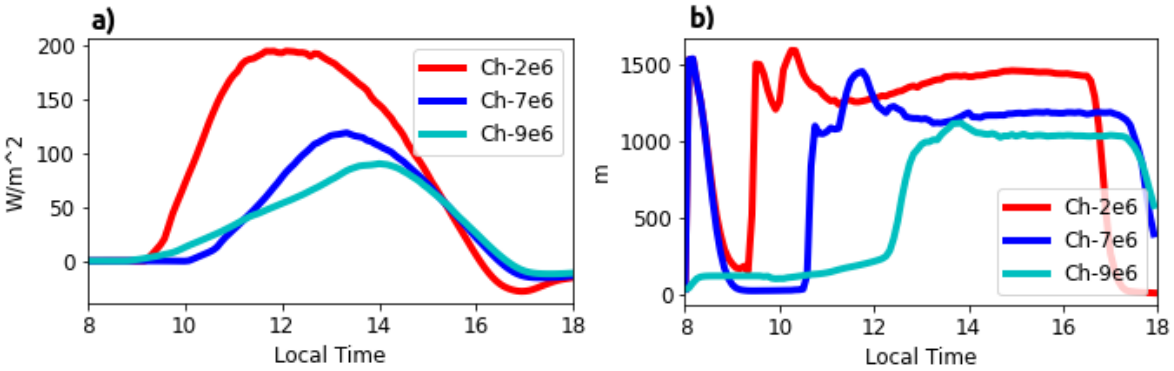

Figure 3.4: Figures showing sensitivity to varying surface heat capacity (Ch) between $2e^6$ (Red lines), $7e^6$ (Blue lines) and $9e^6$ (Turquoise lines) on a) Sensible Heat Flux and b) PBL Height

3.4.2 Anthropogenic Heat Flux (Q_f)

Through further discussion with colleagues from the APHH Beijing project, it was concluded that the higher measured surface nocturnal temperatures were likely a result of the Urban Heat Island Effect which the model wasn't accounting for. Built up cities have a delayed and lower rate of radiative cooling due to additional heat storage and release from buildings, and activities which produce heat. To account for this, the equation which calculates the surface energy balance in the model was altered to include the additional anthropogenic heat term, Q_f (Eq.3.6). Several studies have calculated the anthropogenic heat flux for different cities as described in section 1.6. Some studies calculate Q_f as the remainder after the heat storage, sensible and latent heat flux and net all wave radiation. Other studies directly calculate all individual components of Qf , using emissions from traffic and industry and building information to attribute heat to each of the components as in equation 3.7. Where Q_B is heat from buildings, Q_V the heat from vehicles and Q_M the heat from human activity (Allen et al., 2011).

$$Q_f = Q_B + Q_V + Q_M \tag{3.7}$$

Figure 3.4 shows an estimated anthropogenic heat flux from Singapore in comparison to measured latent and sensible heat fluxes on 22/11/2016 in Beijing. This shows the anthropogenic heat flux as having a similar profile to the sensible and latent heat flux, emphasising the importance in including it in urban boundary layer studies. To account for the anthropogenic heat flux in this case, different constant values were first input into the surface balance equation to examine sensitivity to the term. Typical diurnal profiles of anthropogenic heat flux is low at night, peaks at morning and evening rush hour, remaining constant throughout the day before falling off again at night.

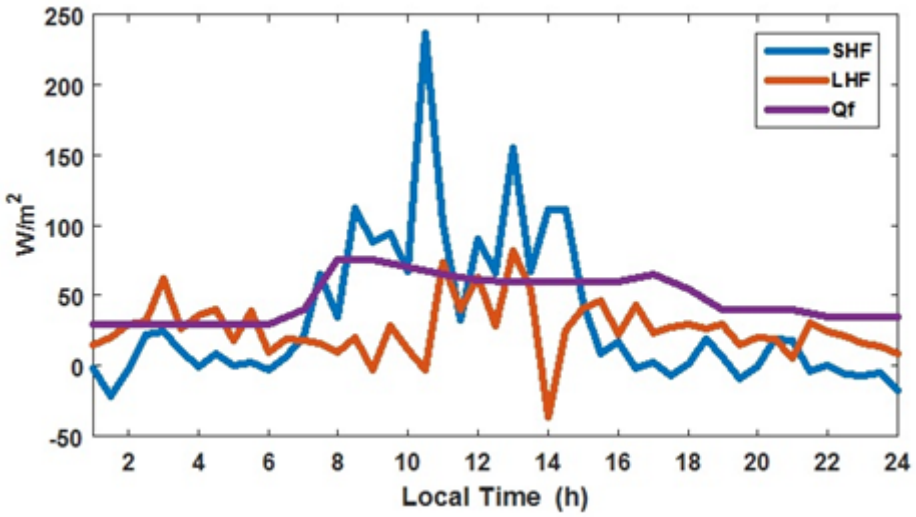

Figure 3.5: Measured sensible and latent heat flux from 22/11 and estimates of anthropogenic heat flux in Singapore(Quah and Roth, 2012)

For initial simulations, Q_f was set to the constant values of 0, 50 and 100 W/m^2. Higher values of Q_f increased temperatures across the profiles, while also reducing radiative cooling at the surface, through delaying the release of heat in the evening. A diurnal profile of Q_f was included in the surface energy balance scheme based on estimations from literature on Beijing and other cities (Quah and Roth, 2012; Lu et al., 2016). This profile was assumed to be the same for all days modelled and peaked at 70 W/m^2. Figure 3.5 shows that inclusion of the anthropogenic heat flux delayed the release of and increased modelled maximum sensible heat flux. With a particularly large effect in the evening. Potential temperature profiles show that inclusion of Q_f in simulations decreases radiative cooling and slightly increases PBL height (taken here as the height at which there is the largest gradient change in θ). This is due to the additional heat flux is being added into the model domain, which will increase temperature and promote turbulence, increasing SHF (Eq. 3.2 and 3.5). As anthropogenic heat flux is not solely released from the surface, ideally a vertical anthropogenic heat flux which would account for the release from buildings would be modelled in order to fully elucidate the impact of the anthropogenic heat on the urban boundary layer. Although this was tried, it proved too difficult and time consuming and was therefore considered to be a limitation of this work.

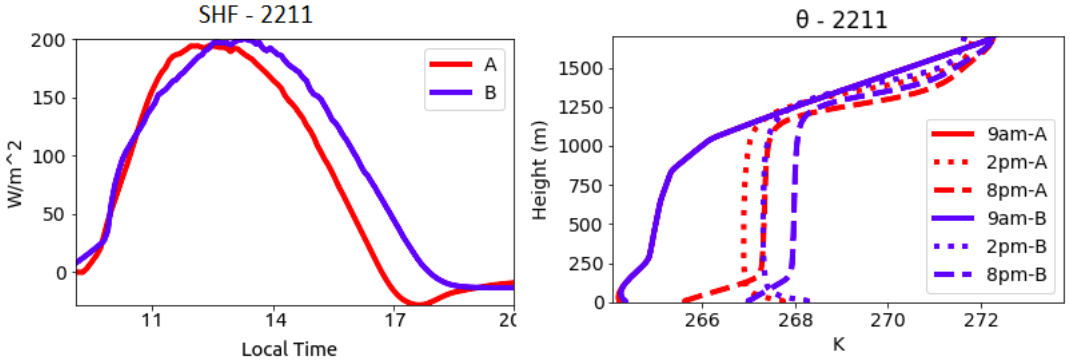

Figure 3.6: Sensible heat flux (SHF) and Potential Temperature (θ) for simulations on 22/11 with (blue lines) and without (red lines) the diurnal Q_f included

3.4.3 Water Fractions

A clear discrepancy between the initial model simulations and observations was the sensible and latent heat flux diurnal profiles. As shown in figure 3.2, LHF was much higher than observations in the original simulations, while SHF was much lower. In the initial model set up, water volume fractions were 0.9, suggesting a wet vegetative surface. However, urban areas are largely known for their irrigated surfaces and in Beijing wintertime particularly there is very little rainfall meaning the surface is typically quite dry and latent heat flux is low, while the Bowen ratio remains high (Wang et al., 2019). In the interactive coupled soil surface temperature and moisture scheme, the water volume fraction (W_1) directly impacts the calculation of LHF through the dimensionless constant (f_h) as seen in Eq. 3.2 and Eq. 3.8. Decreasing surface water volume fractions (water saturation) decreased LHF significantly, while increasing SHF to be closer to observed values. Figure 3.6 shows the variation in sensible and latent heat flux through altering the water fraction from 0.3 to 0.4.

$$f_h = W_1/0.75 \tag{3.8}$$

A higher water volume fraction meant that the contribution to the surface energy balance is higher and the Bowen ratio is lower. Reducing this term even by 0.1 increases buoyant turbulence and increases maximum PBL height (Figure 3.6(b)) in the test simulations. Values were chosen for simulations which showed results closest to measured SHF and LHF on the chosen test case. This meant that in all simulations presented in this thesis, the water fraction value was set to 0.3. Although in reality this value might change on different days, there were not reliable measurements of this value at the measurement site and so to minimise the variation between simulations, this value was kept constant.

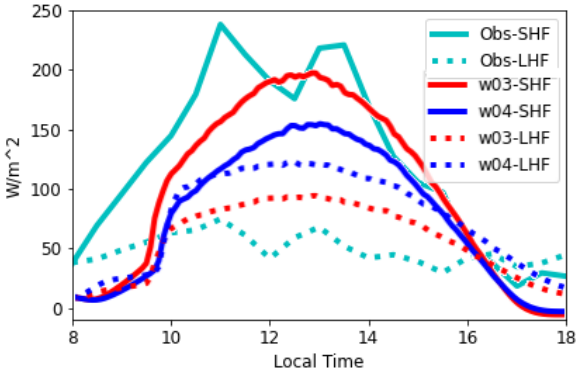

Figure 3.7: Diurnal profiles of Sensible Heat Flux (solid lines) and Latent Heat Flux (dotted lines) for simulations with water fractions set at 0.3 (red lines) and 0.4 (blue lines), compared to observations (turquoise lines)

3.4.4 Surface Temperature

Most surface variables included in the surface energy balance scheme (Eq. 3.6) had an impact on the model simulations. Initial surface temperature values were taken from ECMWF-ERA5 reanalysis data, however the resolution of this data (11 km) was larger than the model domain and it is likely that within a city there is variation of surface temperature. Figure 3.7 shows the effect of initialising the model with surface temperatures varied by 1 K. This shows that the initial surface temperature effects the diurnal profile and maximum PBL height, turbulent kinetic energy and SHF. For the higher initial surface temperature (red line), PBL height, SHF and TKE were all higher through the day. As the surface temperature varies by day, this variable is important to keep right or standardised. The main effect of surface temperature on the surface energy balance was the difference between surface and air temperature causing heat flux variations (Eq. 3.1, 3.2 and 3.3). Therefore, as all simulations began at the same time (8am) and were initialised by air temperature measurements from the same site, initial surface temperatures for all cases were taken as being 2K lower than the measured air temperature. This assumption was made to avoid variability between days due to uncertainty around the spatial variability of using ECMWF-ERA5 data.

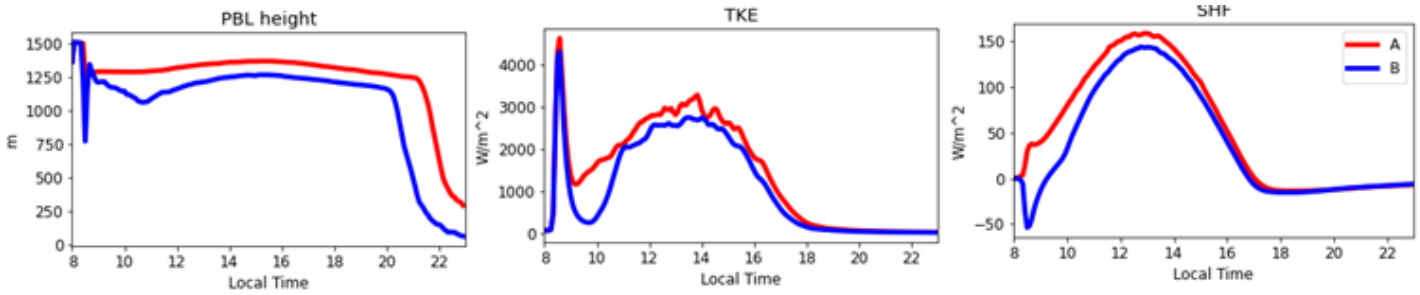

Figure 3.8: PBL Height, Turbulent Kinetic Energy (TKE) and Sensible Heat FLux (SHF) for simulations with surface temperature set at 3K lower than air temperature (blue lines) and at 2K lower than air temperature (red lines)

3.5 Model Limitations

3.5.1 Urban Surface Energy Balance

Urban and rural environments have significantly different characteristics. To set up the model for the urban environment of Beijing, sensitivity studies of several surface parameters were performed in an attempt to match observations. This included alterations to several urban surface parameters which are known to impact heat storage and heat fluxes including: water volume fraction, surface heat capacity, surface roughness and thermal conductivity of the surface. Furthermore, an estimated inclusion of an anthropogenic heat flux which peaked at ~ 70 W/m^2 was included. UCLALES showed high sensitivity to all parameters, which were tuned to best match observations as detailed in the previous section. However, UCLALES assumes surface homogeneity, whereby specified surface parameters which are equivalent across the entire

domain. However, urban surfaces are known to be heterogeneous, this heterogeneity impacts advection of heat and momentum as well as impacting pollutant dispersion. Consequently, this has an impact on the vertical structure of the urban boundary layer, which cannot be fully resolved with the simple surface scheme (Barlow, 2014). Attempts were made in this work to include some form of surface heterogeneity into the surface energy balance scheme, however their were several issues with this, including due to the periodic boundary conditions and the direction of flow through the boundaries. Therefore, the inclusion of surface heterogeneity in the existing version of UCLALES-SALSA would have taken too much time and resources which were not available at this stage of the PhD. This is consequently seen as a limitation of the modelling framework and may have an impact on the accuracy of boundary layer development in all simulations presented in this work. However, although inclusion of a specific urban surface energy balance scheme such as the Surface Urban Energy and Water Balance Scheme, would likely improve the accuracy of model simulations of the urban boundary layer, I believe this would have had limited effect on the conclusions presented in later chapters. This is because the main focus of the work is to examine the impact of aerosol feedback on boundary layer meteorology under different aerosol and meteorological conditions. As this limitation is present in all simulations, the effect of these different conditions can still be analysed. It is therefore acknowledged that the high sensitivity to surface parameters as well as the simplicity of the surface scheme used can be considered a limitation of the current setup of UCLALES-SALSA in investigations of urban environments. Consequently, adaptations of the surface scheme to make it more suitable to urban should be considered for future development.

3.5.2 Synoptic Conditions

UCLALES uses periodic boundary conditions, which means it is not influenced by and cannot simulate changing synoptic conditions. A significant cause of the onset and dissipation of Beijing haze episodes is considered to be the changing pressure systems bringing about stagnant atmospheric conditions, whereas the dissipation of pollution is caused by strong winds. Both of these processes are essential in the onset and longevity of pollution episodes. In particular, the shallow PBL conditions observed around the beginning of the haze episodes are brought about by changing conditions, without which the pollution episodes would be unlikely to occur. However, the aerosol-PBL feedback conditions are believed to occur under already stagnant conditions, which can be well simulated in the LES model. Although not responsible for the onset of haze episodes, aerosol-PBL feedback is thought to significantly enhance the episodes through promoting stagnation further and reducing PBL height, which allows for more aerosols accumulating and interacting with radiation. Consequently, the work presented in this thesis primarily focuses on the cumulative stage of the pollution episode.

3.5.3 Mass Loss

When performing simulations with varied vertical aerosol profiles, there was a noticeable loss in mass of aerosols over time, despite dry deposition being switched off. The reason for the decrease in total mass mixing ratio over time is due to UCLALES-SALSA's use of the anelastic approximation. Anelastic models filter out acoustic waves for computational efficiency and are accurate in isentropic systems, which although useful, has limitations when applied to realistic atmospheric processes when the isentropic base state doesn't hold true. The Ogura-Phillips anelastic approximation assumes that there are only small variations in pressure and density from static reference values over time, i.e they are non prognostic variables (Ogura and Phillips, 1962; Pressel et al., 2015) According to Byun (1999), "The anelastic assumption ignores the tendency term in the continuity equation and therefore provides a diagnostic relation among wind components and density". Perturbation of air density is not calculated directly but inferred from other meteorological fields such as temperature and pressure. In UCLALES-SALSA, heating throughout the day from surface fluxes increases temperature, while subsidence at the model top causes sinking of air which decreases air density. This temperature increase does not fully feed back on pressure changes due to the limitations of using the anelastic approximation, while the model volume stays constant due to static vertical boundary conditions. Consequently, when the mass tracers are pulled downward, the total mass of the air increases while the mass of SALSA tracers remains the same and therefore there is an apparent decrease in aerosol mass mixing ratio, as the model holds to constant volume of air rather than constant mass. The so called 'mass loss' is impacted by variations in density and so it will be altered for different case studies and for different vertical aerosol profiles. This can be considered a limitation in using meteorological models for air quality analysis. The author recognises that ~ 5 % decrease in mass mixing ratio of aerosol occurs over the time-span of the simulation, when using vertical aerosol profiles. As a consequence, overall conclusions must be mindful of this impact and the effect it may have on aerosol-PBL interactions. However, the relative reduction is the same for different meteorological and aerosol conditions and so comparisons examining the main effects of the aerosol-PBL feedback can still be performed (Durran, 1989; Byun and Schere, 2006; Pauluis, 2008; Smith and Bannon, 2008; Randall, 2013; Pressel et al., 2015).

3.5.4 Semi-Volatile Condensation

Condensation of semi-volatiles has been found to be important in Beijing pollution episodes, particularly when humidity increases during the later stages of the pollution episode. UCLALES-SALSA allows for the condensation of sulphuric acid vapour, semi-volatile organics and non-volatile organics on aerosol particles, however there is no current setup for the condensation of ammonia and nitric acid. The process of ammonium nitrate formation is considered to be one of the most important secondary aerosol formation pathways during Beijing haze, as shown by large increases in ammonium nitrate aerosol during pollution episodes (Xu et al., 2019). As not all these processes are fully considered in SALSA at the present moment and for simplicity, the results presented in this study does not consider semi-volatile condensation in any

form. Therefore, the effect that secondary aerosol formation may have in changing the composition, mixing state and size of the aerosols cannot be considered in this work.

References

Ackerman, A. S., VanZanten, M. C., Stevens, B., Savic-Jovcic, V., Bretherton, C. S., Chlond, A., Golaz, J.-C., Jiang, H., Khairoutdinov, M., Krueger, S. K., Lewellen, D. C., Lock, A., Moeng, C.-H., Nakamura, K., Petters, M. D., Snider, J. R., Weinbrecht, S., and Zulauf, M.: Large-Eddy Simulations of a Drizzling, Stratocumulus-Topped Marine Boundary Layer, Monthly Weather Review, 137, 1083–1110, https://doi.org/10.1175/2008MWR2582.1, 2009.

Ács, F., Mihailović, D. T., and Rajković, B.: A Coupled Soil Moisture and Surface Temperature Prediction Model, https://doi.org/10.1175/1520-0450(1991), 1991.

Allen, L., Lindberg, F., and Grimmond, C. S.: Global to city scale urban anthropogenic heat flux: Model and variability, International Journal of Climatology, 31, 1990–2005, https://doi.org/10.1002/joc.2210, 2011.

Barlow, J. F.: Progress in observing and modelling the urban boundary layer, Urban Climate, 10, 216–240, https://doi.org/10.1016/j.uclim.2014.03.011, 2014.

Boucher, O.: Atmospheric Aerosols. Properties and climate impacts, vol. 53, https://doi.org/10.1017/CBO9781107415324.004, 2013.

Boutle, I., Price, J., Kudzotsa, I., and Romakkaniemi, S.: Aerosol-fog interaction and the transition to well-mixed radiation fog, 2017.

Burman, J., Jonsson, L., and Rutgersson, A.: On possibilities to estimate local concentration variations with CFD-LES in real urban environments, vol. 19, Springer Netherlands, https://doi.org/10.1007/s10652-018-9650-4, 2019.

Byun, D. and Schere, K. L.: Review of the Governing Equations, Computational Algorithms, and Other Components of the Models-3 Community Multiscale Air Quality (CMAQ) Modeling System, Applied Mechanics Reviews, 59, 51, https://doi.org/10.1115/1.2128636, 2006.

Byun, D. W.: Dynamically consistent formulations in meteorological and air quality models for multiscale atmospheric studies. Part II: Mass conservation issues, Journal of the Atmospheric Sciences, 56, 3808–3820, https://doi.org/10.1175/1520-0469(1999)056<3808:DCFIMA>2.0.CO;2, 1999.

Cuchiara, G. C. and Rappenglück, B.: Performance analysis of WRF and LES in describing the evolution and structure of the planetary boundary layer, Environmental Fluid Mechanics, 18, 1257–1273, https://doi.org/10.1007/s10652-018-9597-5, 2018.

Durran, D. R.: Improving the anelastic approximation, https://doi.org/10.1175/1520-0469(1989)046<1453:ITAA>2.0.CO;2, 1989.

Fu, Q. and Liou, K. N.: Parameterization of the Radiative Properties of Cirrus Clouds, https://doi.org/10.1175/1520-0469(1993)050<2008:POTRPO>2.0.CO;2, 1993.

Herbert, R. J., Bellouin, N., Highwood, E. J., and Hill, A. A.: Diurnal cycle of the semi-direct effect from a persistent absorbing aerosol layer over marine stratocumulus in large-eddy simulations, Atmospheric Chemistry and Physics, 20, 1317–1340, https://doi.org/10.5194/acp-20-1317-2020, 2020.

Hoffmann, F., Raasch, S., and Noh, Y.: Entrainment of aerosols and their activation in a shallow cumulus cloud studied with a coupled LCM-LES approach, Atmospheric Research, 156, 43–57, https://doi.org/10.1016/j.atmosres.2014.12.008, 2015.

Hu, X. M., Nielsen-Gammon, J. W., and Zhang, F.: Evaluation of three planetary boundary layer schemes in the WRF model, Journal of Applied Meteorology and Climatology, 49, 1831–1844, https://doi.org/10.1175/2010JAMC2432.1, 2010.

Ikeda, R., Kusaka, H., Iizuka, S., and Boku, T.: Development of Urban Meteorological LES model for thermal environment at city scale, ICUC9 - 9th International Conference on Urban Climate jointly with

12th Symposium on the Urban Environment Development, 2012.

Jacobson, M.: Fundamentals of Atmospheric Modelling, 1997.

Jiang, H., Feingold, G., and Cotton, W. R.: Simulations of aerosol-cloud-dynamical feedbacks resulting from entrainment of aerosol into the marine boundary layer during the Atlantic Stratocumulus Transition Experiment, Journal of Geophysical Research Atmospheres, 107, 1–11, https://doi.org/10.1029/2001JD001502, 2002.

Jiang, Q. and Wang, S.: Aerosol Replenishment and Cloud Morphology: A VOCALS Example, Journal of the Atmospheric Sciences, 71, 300–311, https://doi.org/10.1175/JAS-D-13-0128.1, 2014.

Kokkola, H., Korhonen, H., Lehtinen, K. E. J., Makkonen, R., Asmi, A., Järvenoja, S., Anttila, T., Partanen, A.-I. I., Kulmala, M., Järvinen, H., Laaksonen, A., and Kerminen, V.-M. M.: SALSA - a sectional aerosol module for large scale applications, Atmospheric Chemistry and Physics, 8, 2469–2483, https://doi.org/10.5194/acp-8-2469-2008, 2008.

Kokkola, H., Kuhn, T., Laakso, A., Bergman, T., Lehtinen, K., Mielonen, T., Arola, A., Stadtler, S., Korhonen, H., Ferrachat, S., Lohmann, U., and Neubauer, D.: SALSA 2.0 : The sectional aerosol module of the aerosol – chemistry – climate model ECHAM6.3.0-HAM2 .3-MOZ1.0, Geoscientific Model Development, 11, 3833–3863, 2018.

Kurppa, M., Hellsten, A., Roldin, P., Kokkola, H., Tonttila, J., Auvinen, M., Kent, C., Kumar, P., Maronga, B., and Järvi, L.: Implementation of the sectional aerosol module SALSA2.0 into the PALM model system 6.0: Model development and first evaluation, Geoscientific Model Development, 12, 1403–1422, https://doi.org/10.5194/gmd-12-1403-2019, 2019.

Lu, Y., Wang, Q., Zhang, Y., Sun, P., and Qian, Y.: An estimate of anthropogenic heat emissions in China, International Journal of Climatology, 36, 1134–1142, https://doi.org/10.1002/joc.4407, 2016.

Maalick, Z.: Modelling studies on the effect of aerosols and cloud microphysics on cloud and fog properties, Ph.D. thesis, 2017.

Maalick, Z., Kuhn, T., Korhonen, H., Kokkola, H., Laaksonen, A., and Romakkaniemi, S.: Effect of aerosol concentration and absorbing aerosol on the radiation fog life cycle, Atmospheric Environment, 133, 26–33, https://doi.org/10.1016/j.atmosenv.2016.03.018, 2016.

Meyn, S. K. and Oke, T. R.: Heat fluxes through roofs and their relevance to estimates of urban heat storage, Energy and Buildings, 41, 745–752, https://doi.org/10.1016/j.enbuild.2009.02.005, 2009.

Nakayama, H., Takemi, T., and Nagai, H.: Large-eddy simulation of urban boundary-layer flows by generating turbulent inflows from mesoscale meteorological simulations, Atmospheric Science Letters, 13, 180–186, https://doi.org/10.1002/asl.377, 2012.

Ogura, Y. and Phillips, N. A.: Scale Analysis of Deep and Shallow Convection in the Atmosphere, https://doi.org/10.1175/1520-0469(1962)019<0173:saodas>2.0.co;2, 1962.

Ovchinnikov, M. and Easter, R. C.: Modeling aerosol growth by aqueous chemistry in a nonprecipitating stratiform cloud, Journal of Geophysical Research Atmospheres, 115, 1–14, https://doi.org/10.1029/2009JD012816, 2010.

Pauluis, O.: Thermodynamic consistency of the anelastic approximation for a moist atmosphere, Journal of the Atmospheric Sciences, 65, 2719–2729, https://doi.org/10.1175/2007JAS2475.1, 2008.

Pressel, K., Kaul, C., Schneider, T., Tan, Z., and Mishra, S.: Large eddy simulation in an anelastic framework with closed water and entropy balances, Journal of Advances in Modeling Earth Systems, 7, 1425–1456, https://doi.org/10.1002/2017MS001065, 2015.

Quah, A. K. L. and Roth, M.: Diurnal and weekly variation of anthropogenic heat emissions in a tropical city, Singapore, Atmospheric Environment, 46, 92–103, https://doi.org/10.1016/j.atmosenv.2011.10.015, 2012.

Randall, D.: The Anelastic and Boussinesq Approximations, Quick Studies in Atmospheric Science, pp. 1–14, 2013.

Roberts, S. M., Oke, T. R., Grimmond, C. S. B., Voogt, J. A., and Roberts, S. M.: Comparison of four methods to estimate urban heat storage, Journal of Applied Meteorology and Climatology, 45, 1766–1781, https://doi.org/10.1175/JAM2432.1, 2006.

Russell, E. S., Liu, H., Gao, Z., Finn, D., and Lamb, B.: Impacts of soil heat flux calculation methods on the surface energy balance closure, Agricultural and Forest Meteorology, 214-215, 189–200, https://doi.org/10.1016/j.agrformet.2015.08.255, 2015.

Siebesma, a. P., Bretherton, C. S., Brown, A., Chlond, A., Cuxart, J., Duynkerke, P. G., Jiang, H., Khairoutdinov, M., Lewellen, D., Moeng, C.-H., Sanchez, E., Stevens, B., and Stevens, D. E.: A Large Eddy Simulation Intercomparison Study of Shallow Cumulus Convection, Journal of the Atmospheric Sciences, 60, 1201–1219, https://doi.org/10.1175/1520-0469(2003)60<1201:ALESIS>2.0.CO;2, 2003.

Slater, J., Tonttila, J., Mcfiggans, G., Romakkaniemi, S., Kühn, T., and Coe, H.: Using a coupled LES-aerosol radiation model to investigate urban haze : Sensitivity to aerosol loading and meteorological conditions, Atmospheric Chemistry and Physics Discussions, 5, 1–23, 2020.

Smith, J. W. and Bannon, P. R.: A comparison of compressible and anelastic models of deep dry convection, Monthly Weather Review, 136, 4555–4571, https://doi.org/10.1175/2008MWR2343.1, 2008.

Stevens, B.: Introduction to UCLA-LES, pp. 1–20, 2010.

Stevens, B. and Feingold, G.: Untangling aerosol effects on clouds and precipitation in a buffered system., Nature, 461, 607–613, https://doi.org/10.1038/nature08281, 2009.

Stevens, B., Lenschow, D. H., Vali, G., Gerber, H., Bandy, A., Blomquist, B., Brenguier, J. L., Bretherton, C. S., Burnet, F., Campos, T., Chai, S., Faloona, I., Friesen, D., Haimov, S., Laursen, K., Lilly, D. K., Loehrer, S. M., Malinowski, S. P., Morley, B., Petters, M. D., Rogers, D. C., Russell, L., Savic-Jovcic, V., Snider, J. R., Straub, D., Szumowski, M. J., Takagi, H., Thornton, D. C., Tschudi, M., Twohy, C., Wetzel, M., and Van Zanten, M. C.: Dynamics and Chemistry of Marine Stratocumulus - DYCOMS-II, Bulletin of the American Meteorological Society, 84, 579–593, https://doi.org/10.1175/BAMS-84-5-579, 2003.

Stull, R.: Atmospheric Boundary Layer, in: Practical Meteorology: An Algebra-based Survey of Atmospheric Science, pp. 453–458, https://doi.org/10.1175/BAMS-89-4-453, 2015.

Takebayashi, H. and Moriyama, M.: Study on Surface Heat Budget of Various Pavements for Urban Heat Island Mitigation, Advances in Materials Science and Engineering, https://doi.org/10.1155/2012/523051, 2012.

Tonttila, J., Maalick, Z., Raatikainen, T., Kokkola, H., Kühn, T., and Romakkaniemi, S.: UCLALES-SALSA v1.0: a large-eddy model with interactive sectional microphysics for aerosols, clouds and drizzle, Geoscientific Model Development, 10, 169–188, https://doi.org/10.5194/gmd-10-169-2017, 2017.

Tonttila, J., Afzalifar, A., Kokkola, H., Raatikainen, T., Korhonen, H., and Romakkaniemi, S.: Precipitation enhancement in stratocumulus clouds through airbourne seeding: sensitivity analysis by UCLALES–SALSA, Atmospheric Chemistry and Physics, 21, 1035–1048, https://doi.org/10.5194/acp-21-1035-2021, 2021.

Wang, L., Liu, J., Gao, Z., Li, Y., Huang, M., Fan, S., Zhang, X., Yang, Y., Miao, S., Zou, H., Sun, Y., Chen, Y., and Yang, T.: Vertical observations of the atmospheric boundary layer structure over Beijing urban area during air pollution episodes, Atmospheric Chemistry and Physics, 19, 6949–6967, https://doi.org/10.5194/acp-19-6949-2019, 2019.

Xu, Q., Wang, S., Jiang, J., Bhattarai, N., Li, X., Chang, X., Qiu, X., Zheng, M., Hua, Y., and Hao, J.: Nitrate dominates the chemical composition of PM2.5 during haze event in Beijing, China, Science of the Total Environment, 689, 1293–1303, https://doi.org/10.1016/j.scitotenv.2019.06.294, 2019.

Zhang, Y., Easter, R. C., Ghan, S. J., and Abdul-Razzak, H.: Impact of aerosol size representation on modeling aerosol-cloud interactions, Journal of Geophysical Research Atmospheres, 107, AAC 4–1–AAC 4–17, https://doi.org/10.1029/2001JD001549, 2002.

Zou, J., Sun, J., Ding, A., Wang, M., Guo, W., and Fu, C.: Observation-based estimation of aerosol-induced reduction of planetary boundary layer height, Advances in Atmospheric Sciences, 34, 1057–1068, https://doi.org/10.1007/s00376-016-6259-8, 2017.

Chapter 4

Papers

4.1 Paper 1: Using a coupled LES-aerosol radiation model to investigate urban haze: Sensitivity to aerosol loading and meteorological conditions

Authors: Jessica Slater, Juha Tonttila, Gordon McFiggans, Paul Connolly, Sami Romakkaniemi, Thomas Kühn and Hugh Coe

Journal: Atmospheric Chemistry and Physics Discussions, 5, 1–23, 202, as part of the Special issue: In-depth study of air pollution sources and processes within Beijing and its surrounding region (APHH-Beijing)

Paper Overview

This paper lays out the set up of UCLALES-SALSA for an urban environment, which includes examining sensitivities in the urban surface energy balance scheme through comparing simulation outputs to meteorological observations. For this test case, we examined the 22nd November 2016, which was considered to be a classic example of a clean day with low measured levels of pollutant concentrations. This meant that we could focus on correctly simulating the urban boundary layer for our domain and compare with observations, which have not been influenced by aerosol interactions. This work shows that performing alterations to the surface energy balance in UCLALES-SALSA to account for the urban environment of Beijing, brought the modelled simulations closer to observations. Altering the surface parameters decreased nocturnal cooling and temperature throughout the profile and decreased both sensible and latent heat fluxes. Including an anthropogenic heat flux which peaked at 70 W/m^2 increased heat fluxes and temperatures in the profile, reducing nocturnal radiative cooling at the surface.

This work then examines three days over which observed pollutant concentrations increase (24th-26th November 2016), the first set of simulations in case 1 show that boundary layer development and dynamics over a day is dependent on the initial meteorological conditions, which vary over the three days. Case 2 shows that including aerosols causes a reduction in turbulent motion, heat fluxes and PBL height, due to the aerosol-radiation interactions. For all days simulated, the effect is larger for increased aerosol loading in the column, showing the direct impact of increasing aerosol concentrations on PBL meteorology. However, this work also shows that the magnitude of the impact is dependent on the initial meteorological conditions, with some periods being more susceptible to perturbations caused by aerosol-radiation interactions. This shows a decrease of 67 % in PBL height due to high aerosol concentrations on simulations of 26th Nov 2016 compared to a 16 % on 24th Nov 2016. In case 3, the impact of including an aerosol vertical profile is examined, which shows that simulations in case 2 with high aerosols aloft resulted in the formation of a turbulent layer to form close to model top, which decreases surface wind speeds.

Overall, this paper demonstrates the ability of a novel coupled LES-aerosol-radiation model for the first time. This work shows the models ability in simulating aerosol-radiative feedback on PBL dynamics in an urban environment. Furthermore, this work outlines sensitivities to be examined in the future work, including: aerosol loading, meteorological conditions and the aerosol vertical profiles.

In between submission and examination of this thesis, this paper was published. After the viva and subsequent discussion with the examiners some improvements to the paper were made for the revised thesis. Therefore, the paper presented here is different to the published paper, for which the reference is: Atmos. Chem. Phys., 20, 11893–11906, 2020 (https://doi.org/10.5194/acp-20-11893-2020). The main differences in the paper are to the results and discussion section including replotting of some of the key figures, this doesn't change the findings of the paper but clarifies some of the key points.

Author Contributions

The idea for this paper was conceived by Jessica Slater, Hugh Coe, Paul Connolly and Gordon McFiggans. The simulations were performed by Jessica Slater with assistance from Juha Tonttila and Sami Romakkianemi and model analysis was done by Jessica Slater, with help from Gordon Mcfiggans, Hugh Coe and Paul Connolly. The manuscript was written mainly by Jessica Slater, with input from all co-authors, including Thomas Kühn who contributed to the methods section aerosol-radiation interactions.

Using a coupled LES-aerosol radiation model to investigate urban haze: Sensitivity to aerosol loading and meteorological conditions

Jessica Slater[1], Juha Tonttila[2], Gordon McFiggans[1], Paul Connolly[1], Sami Romakkaniemi[2], Thomas Kühn[2,3], and Hugh Coe[1]

[1]Centre for Atmospheric Sciences, School of Earth and Environmental Sciences, University of Manchester, Manchester, UK
[2]Finnish Meteorological Institute, Atmospheric Research Centre of Eastern Finland, Kuopio, Finland
[3]Department of Applied Physics, University of Eastern Finland, Kuopio, Finland

Correspondence: Hugh Coe (hugh.coe@manchester.ac.uk)

Abstract. The aerosol-radiation-meteorological feedback loop is the process by which aerosols interact with solar radiation to influence boundary layer meteorology. Through this feedback, aerosols cause cooling of the surface, resulting in reduced buoyant turbulence, enhanced atmospheric stratification and suppressed boundary layer growth. These changes in meteorology result in the accumulation of aerosols in a shallow boundary layer, which can enhance the extent of aerosol-radiation interactions. The feedback effect is thought to be important during periods of high aerosol concentrations, for example during urban haze. However, direct quantification and isolation of the factors and processes affecting the feedback loop has thus far been limited to observations and low resolution modelling studies. The coupled LES-aerosol model, UCLALES-SALSA, allows for direct interpretation on the sensitivity of boundary layer dynamics to aerosol perturbations. In this work, UCLALES-SALSA has for the first time been explicitly set up to model the urban environment, including addition of an anthropogenic heat flux and treatment of heat storage terms, to examine the sensitivity of meteorology to the newly coupled aerosol-radiation scheme. We find that: a) Sensitivity of boundary layer dynamics in the model to initial meteorological conditions is extremely high, b) Simulations with high aerosol loading (220 μg/m^3) compared to low aerosol loading (55 μg/m^3) cause overall surface cooling and a reduction in sensible heat flux, turbulent kinetic energy and planetary boundary layer height for all three days examined and c) Initial meteorological conditions impact the vertical distribution of aerosols throughout the day.

1 Introduction

Severe air pollution events are a major health issue for megacities worldwide, particularly in nations with large populations and high levels of industrialisation such as India and China. Beijing, situated in the North China Plain is well known for its air quality issues, where concentrations of $PM_{2.5}$ (particulate matter with an aerodynamic diameter < 2.5 μm) frequently exceed the World Health Organisation's recommended 24 hour average hourly exposure limit of 25 μg/m^3. Heavy 'haze' periods envelop Beijing due to a complex combination of emission sources and unfavourable meteorology. Observations have identified the importance of changing synoptic conditions on the onset of haze episodes, while the longevity and intensity of the episodes are found to be affected by aerosol-radiation interactions (Wang et al., 2019). These interactions feedback on boundary

layer meteorology to cause unfavourable conditions such as temperature inversions, increased humidity and decreased wind speed (Dou et al., 2015; Zhang et al., 2015, 2017; Zhong et al., 2019b).

In addition to the unfavourable meteorological conditions; heavy emissions and regional transport of pollutants into Beijing cause high concentrations of urban aerosol particles to accumulate. These particles can either scatter or absorb solar radiation, depending on their composition. Observations predominantly show that aerosol particles cause net cooling at the surface and warming above the PBL. This consequently alters the thermal profile of the atmosphere, reducing turbulence due to buoyancy. Reduced turbulent mixing suppresses boundary layer development during the day, minimises the vertical mixing of pollutants and increases surface aerosol concentrations. Furthermore, reduction in planetary boundary layer (PBL) height due to the feedback effect also increases water vapour concentrations which can result in enhanced aqueous heterogeneous reactions, thus increasing the rate of secondary aerosol formation. If the aerosol particles are hygroscopic, increased water vapour concentrations will also cause particle growth, resulting in stronger aerosol-radiation interactions. This positive feedback loop between aerosols, radiation and meteorology can lead to sustained periods of stagnation and has been found to enhance pollution events (Figure 1) (Petäjä et al., 2016; Liu et al., 2018b; Luan et al., 2018).

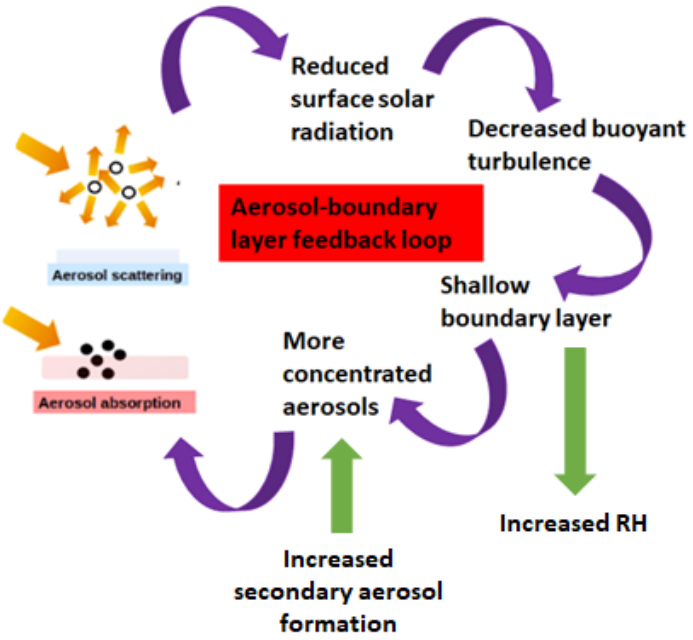

Figure 1. Schematic of the positive feedback loop between aerosols, radiation and meteorology thought to enhance pollution episodes in Beijing

Aerosol composition and size are the main factors impacting an aerosol particle's single scattering albedo thus impacting the extent by which it will interact with radiation. Most aerosol particles predominately scatter radiation and thus have an overall cooling effect, stabilising the boundary layer and allowing for further accumulation of aerosol particles. However, black carbon

(BC), an absorbing aerosol which can contribute up to 10 % of PM in Beijing (Liu et al., 2016) has the potential to have the opposite effect, through warming of the lower atmosphere, which promotes buoyancy and destabilises the boundary layer. However, depending on the vertical distribution of the BC layer, BC can also enhance stratification through causing warming in the upper PBL (Liu et al., 2018b; Zhong et al., 2018a; Ding et al., 2016).

Research examining the feedback effect on Beijing haze episodes has thus far relied upon observations or regional modelling studies. Gao et al. (2015), Liu et al. (2018b), Zhong et al. (2018b) and Wu et al. (2019) performed model simulations of pollution episodes using the Weather Research and Forecasting model with added chemistry (WRF-CHEM) to examine the feedback effect. Their results all confirm that aerosol-radiation interactions, aerosol hygroscopic growth and aqueous heterogeneous reactions all factor in the suppression of boundary layer development and result in increased surface $PM_{2.5}$ concentrations during polluted episodes in the North China Plain. Gao et al. (2015) suggests that aerosol-radiation interactions decrease temperature and shortwave (SW) radiation at the surface while increasing them aloft (925 hPa). Examining the feedback from a quantitative perspective, Wu et al. (2019) found that when $PM_{2.5}$ increased from 50 to 200 $\mu g/m^3$, maximum average boundary layer height decreased from 700 to 400 m. Furthermore, Zhong et al. (2019a) suggested that threshold $PM_{2.5}$ concentrations of 75 – 100 $\mu g/m^3$ exist in Beijing, above which the feedback effect is increasingly important and leads to aerosol accumulation and exacerbation of pollution episodes.

Observational studies also show a link between aerosol concentrations and boundary layer meteorology. Zou et al. (2017) studied the impact of high aerosol concentrations ($PM_{2.5}$ > 75 $\mu g/m^3$) on Beijing meteorology over a year long period. Their results demonstrate that the aerosol impact on meteorology was different depending on the season, with particularly large reductions in sensible heat flux (SHF), PBL height and surface SW radiation reported under high aerosol conditions in autumn and winter. Liu et al. (2019) used the same $PM_{2.5}$ threshold (> 75 $\mu g/m^3$) to estimate the impact of high aerosol concentrations on observed meteorological data over a one month period where haze episodes occurred every 4-7 days. Comparing high and low aerosol periods they found that on average surface SW radiation was 36 % lower and daily maximum PBL height was reduced from 1.3 km to 0.6 km for high compared to low aerosol periods.

Despite an increase in research in this area, quantification of aerosol perturbations on boundary layer meteorology is still uncertain. In WRF-CHEM, results are strongly dependent on the boundary layer scheme or parameterisation employed throughout the simulations, while observations of this effect, although useful, only show links between the phenomena without being able to quantify the processes or separate factors. High resolution sensitivity studies which allow for direct analysis of boundary layer meteorology are therefore needed to be able to assimilate the major contributions to haze events.

Large-eddy simulations (LES) can explicitly resolve large, high energy eddies while parameterising smaller eddies for computational efficiency. This allows for direct investigation of boundary layer meteorology, turbulent fluxes and statistics, while easily controlled conditions allow for insight into the sensitivity of aerosol interactions on PBL dynamics (Mazoyer et al., 2017; Liu et al., 2018b). Several studies have used LES models to examine the impact of aerosols on convective boundary layers, cumulus clouds and radiation fogs, primarily in rural or marine environments (Sullivan and Patton, 2011; Bellon and

Stevens, 2012; Andrejczuk et al., 2014; Mukherjee et al., 2016; Tonttila et al., 2017). In this work, a novel LES with a coupled sectional aerosol module (UCLALES-SALSA) has been developed to make it suitable for the urban environment of Beijing. The newly coupled aerosol-radiation scheme has been tested for the first time, in order to examine the feedback effect of aerosol loading on boundary layer dynamics. Model description and details of set up for an urban environment are outlined in section 2. Section 3 describes the experimental set up for all simulations. Section 4 shows results of the simulations for Case 1- No aerosols (4.1), Case 2- High and Low Aerosol Loading (4.2) and Case 3- Aerosol Vertical Profiles (4.3) and section 5 discusses the results, including sensitivity of UCLALES-SALSA to: 5.1 - Meteorological conditions, 5.2 – Aerosol loading and 5.3- Aerosol vertical profiles.

2 Model Description

The model used in this work is UCLALES-SALSA. A comprehensive description of the model and its previous uses can be found in the paper by Tonttila et al. (2017). The version used here can be downloaded at https://www.github.com/UCLALES-SALSA. A description of the model set up, validation and sensitivity to parameters are described below.

2.1 UCLALES

UCLALES is a large eddy simulation which has mainly been used in idealised cloud and fog studies. It is based on the Smagorinsky–Lilly subgrid model and solves the Ogura–Phillips anelastic equations with an Asselin filter. Boundary conditions are doubly periodic in the horizontal and fixed in the vertical. Momentum variables are advected with leapfrog time stepping and scalar variables through forward time stepping. In the standard model a two-moment warm rain microphysical scheme is used, the vertical is spanned by a stretchable grid and a sponge layer is applied at the domain top to prevent gravity waves being released into the boundary (Stevens et al., 2003, 2005; Tonttila et al., 2017). The surface scheme explicitly calculates sensible (SHF) and latent heat (LHF) fluxes at each time step and is based on a coupled soil moisture and surface temperature scheme by Ács et al. (1991) (Eq.1-2). This relates both SHF and LHF to surface temperature, SHF to changes in air temperature and LHF to changes in water vapour concentrations.

$$SHF = \rho C_p \left(\frac{(T_g - T_a)}{(r_a)}\right) \tag{1}$$

$$LHF = \frac{(\rho C_p)}{\gamma} \frac{(f_h e_s(T_g) - e_a)}{(r_{surf} + r_a)} \tag{2}$$

Here ρ is air density, C_p is specific heat capacity of dry air, T_g and T_a are surface and air temperature respectively, γ is the psychrometric constant, f_h is a dimensionless function related to water volume fraction and takes the value 0.267 in our case. $e_s(T_g)$ is saturation vapour pressure at surface temperature (T_g) and e_s is water vapour at 2 m height. r_{surf} is the surface resistance to bare soil and is related to surface friction velocity (u*). r_a is atmospheric resistance to water vapour and heat and is dependent on atmospheric stability (Ács et al., 1991).

$$\Delta Q_s = (\frac{\omega C_h \lambda}{2})^{\frac{1}{2}}(T_g - \bar{T}) \tag{3}$$

Surface parameters, which vary greatly in different environments, can be varied within the model input and largely affect the heat storage term (ΔQ_s) (Eq.3). Where C_h is volumetric heat capacity (J $m^{-3}K^{-1}$), λ is thermal conductivity (W m^{-1} K^{-1}), ω is angular frequency (s^{-1}) and $\bar{T}$ (K) is the average daily temperature in the 2 cm soil layer., ΔQ_s describes the rate of absorption and re-release of radiation by the surface. This in turn impacts surface fluxes through altering the surface energy balance (Eq.4). Further all parameters (SHF, LHF, ΔQ_s) interact and impact one another through the surface energy balance scheme detailed in (Eq. 4) where Q^* is net all wave radiation.

$$Q^* = SHF + LHF + \Delta Q_s \tag{4}$$

2.2 SALSA

The Sectional Aerosol Scheme for Large Scale Applications (SALSA), was developed by Kokkola et al. (2008) and has been coupled with large eddy simulation models (UCLALES) as well as a climate model (ECHAM) (Tonttila et al., 2017; Kokkola et al., 2018). SALSA bins aerosols according to size, allowing for a variety of aerosol sizes and compositions as well as for aerosols to be either internally or externally mixed (Figure 2) (Kokkola et al., 2008). When SALSA is used in these simulations, aerosol species included are black carbon, sulphate, organic carbon, nitrate and ammonium, with all aerosols assumed to be internally mixed. In terms of aerosol processes- coagulation and water vapour condensation are switched on, while nucleation, aerosol deposition, emissions and semi-volatile condensation are not considered here for simplicity but may be considered in future work.

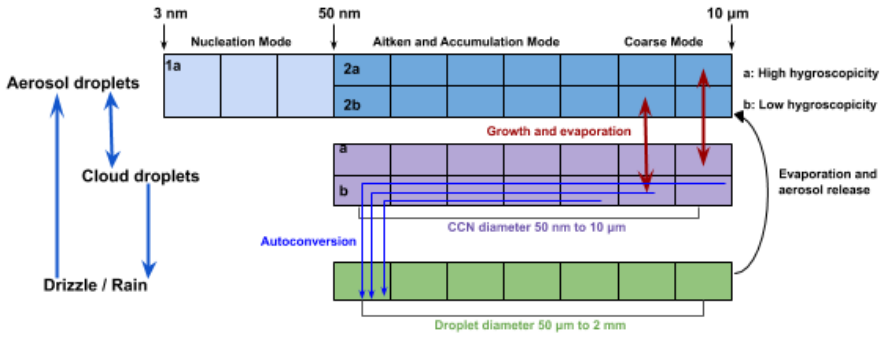

Figure 2. Schematic of the size bin layout for SALSA including the internal and external mixing size bins and the cloud and rain droplet bins (Tonttila et al., 2017)

2.3 UCLALES-SALSA

UCLALES-SALSA couples the UCLALES with SALSA and is primarily described in the paper by Tonttila et al. (2017). The version of UCLALES-SALSA here is a fully coupled radiation-dynamical model, whereby the aerosol-radiation interactions in SALSA are fully coupled with the four stream radiative solver in UCLALES which feeds back on boundary layer turbulence. This is the first time that aerosol-radiation interactions have been dynamically coupled to UCLALES and the work outlined here examines the sensitivity of aerosol loading on these interactions and feedback.

2.3.1 Aerosol-radiation interactions

The solution for radiative transfer in UCLALES is based on the 4-stream method integrating over 6 shortwave bands and 12 longwave bands according to Fu and Liou (1993). In this work, the scheme has been adapted to account for the sectional size distribution of the atmospheric aerosol. To this end we use pre-compiled look-up tables of the aerosol extinction cross-section, asymmetry parameter and single scattering albedo, which are given as a function of the size parameter (particle diameter divided by wavelength) and the real and imaginary parts of the refractive index. For a given aerosol constituent, the refractive indices are catalogued at specific wavelengths. Nearest-neighbour interpolation is used to find the values closest to the centres of the wavelength bands used by the radiation solver. Assuming a perfect internal mixture of all aerosol constituents within one aerosol size section, the refractive index in that size section is then calculated as a volume-weighted average of its constituents. This yields the optical thickness, single scattering albedo and phase function parameters weighted by the actual particle size distribution resolved by SALSA, which are then taken to the 4-stream integration.(Fu and Liou, 1993) The real and imaginary refractive indices for each aerosol component and their use in this simulation are based on (Bond and Bergstrom, 2006) and are detailed for the shortwave wavelengths in the table below.

λ (nm)	n (SO_4^-)	k (SO_4^-)	n (OC)	k (OC)	n (BC)	k(BC)	n (NO_3^-)	k (NO_3^-)	n (NH_4^+)	k (NH_4^+)
3460	1.361	1.4E-01	1.530	2.75E-02	1.984	8.98E-01	1.416	0.04	1.820	2.80E-01
2790	1.295	5.5E-02	1.510	7.33E-03	1.936	8.51E-01	1.177	0.124	1.440	9.51E-03
2330	1.364	2.1E-03	1.510	7.33E-03	1.917	8.12E-01	1.313	0	1.550	1.96E-03
2050	1.382	1.3E-03	1.420	4.58E-03	1.905	7.94E-01	1.333	0	1.560	1.91E-03
1780	1.393	5.1E-04	1.464	6.42E-03	1.894	7.77E-01	1.344	0	1.550	0
1460	1.406	9E-05	1.520	1.43E-02	1.869	7.40E-01	1.352	0	1.540	0
1270	1.413	7.9E-06	1.420	1.77E-02	1.1.861	7.27E-04	1.355	0	1.450	0
1010	1.422	1.3E-06	1.420	2.01E-02	1.861	7.11E-01	1.359	0	1.460	0
700	1.427	5.2E-08	1.530	1.50E-02	1.850	6.94E-01	1.361	0	1.450	0
530	1.432	1E-09	1.530	7.70E-03	1.850	7.21E-01	1.310	0	1.450	0
390	1.445	1E-09	1.530	9.75E-03	1.839	7.30E-01	1.300	0	1.470	0
300	1.450	1E-09	1.443	1.63E-02	1.839	7.59E-01	1.320	0	1.430	0
230	1.450	1E-09	1.530	5.27E-03	1.713	7.26E-01	1.350	0	1.420	0

Table 1. Real (n) and Imaginary (k) refractive indices across 13 shortwave wavelengths (λ for all aerosol components considered for aerosol-radiation interactions in this simulation

2.3.2 Set up in an urban environment

In the past few decades, rapid urbanisation has transformed the landscape in Beijing, creating a microclimate which can be represented by its own distinct physics. Part of this is the Urban Heat Island (UHI), which refers to the phenomenon where a city is significantly warmer than its surrounding areas. This is a result of: increased SW radiation absorption, decreased longwave (LW) radiation loss, decreased turbulent transport, increased heat storage and anthropogenic heat sources. Furthermore, urban environments often consist of mainly impervious surfaces, and therefore the urban heat island is also often characterised by low latent heat and comparatively higher sensible heat fluxes (Oke, 1982; Ikeda et al., 2012; Yang et al., 2016; Tong et al., 2017). To set up UCLALES for an urban environment, alterations to the surface energy balance equation (4) were performed.

Studies by Oke (1982) outline two terms which can be used to represent the presence of the urban heat island. The first is the alteration to ΔQ_s or the heat storage term which alters the rate of surface absorption and re-release of heat. In an urban environment, typically the surface has higher surface heat capacity (C_h), water fraction, soil hygroscopicity and lower thermal conductivity (λ) compared to rural environments. The second term is an additional anthropogenic heat flux (Q_f), which accounts for all activities which result in additional heat in a city. This can be split into heat from: buildings, industry, transport and human metabolism. Estimates of the anthropogenic heat flux are difficult to perform and have not been done in wintertime Beijing, although a recent study gives anthropogenic heat estimates for the summertime, which have a mean midday value of 67.2 W/m^2 (Dou et al., 2019). The anthropogenic heat flux has a distinct diurnal profile, attuned to anthropogenic activities within a given city. It is high in the daytime and decreases at night. The additional term is included in the surface energy balance

155 scheme for an urban environment as described in equation 5 (Grimmond and Oke, 1999; Schwarz et al., 2011; Hu et al., 2012; Xie et al., 2016; Yang et al., 2016).

$$Q^* + Q_f = SHF + LHF + \Delta Q_s \tag{5}$$

In order to set up UCLALES-SALSA for an urban environment, alterations to the heat storage term and a simplistic additional anthropogenic heat flux were included in the surface scheme and sensitivity studies were performed for a non polluted
160 day in Beijing (Figure 3). Simulation results were compared with observations taken during the Air Pollution and Human Health (APHH) Beijing field campaign as well as with ECMWF and radiosonde meteorological profiles. The 22nd November 2016 was chosen for the initial sensitivity simulations. As a non polluted day in Beijing, observations on 22nd November are not impacted by aerosol interactions. Potential temperature, moisture and wind profiles were taken from ECMWF ERA-5 reanalysis data and surface meteorological values taken from an automatic weather station based at the Institute for Atmo-
165 spheric Physics (IAP) in Beijing. In the simulation with no adaptation to the surface scheme there was a clear discrepancy between modelled and measured sensible and latent heat flux and potential temperature profiles. Particularly, there was a large difference in the lower potential temperature profiles in the evening, where the modelled simulations showed early radiative cooling when compared to observations. Delayed and reduced radiative cooling at the surface is frequently observed in urban environments including Beijing.

170 The model showed high variability to volumetric heat capacity (C_h). Increasing this term decreased maximum SHF, noticeably delayed nocturnal radiative cooling and slightly lowered the temperature through the profile (Figure 3). This is due to slower release of outgoing radiation, which is stored for longer in urban surfaces. Figure 3 shows the sensitivity to varying surface volumetric heat capacity (J $m^{-3}K^{-1}$) between the initial value (2x10^6) and chosen value (7x10^6). Higher volumetric heat capacity of the surface causes delayed nocturnal cooling, resulting in higher sensible and latent heat flux in the evening.
175 The surface urban energy balance is also affected by an anthropogenic heat flux which varies seasonally and spatially. A diurnal anthropogenic heat flux which peaks at 70 W/m^2 during the afternoon and remains around 20 W/m^2 in the evening was included in a further simulation. This diurnal profile (Fig 3c) was chosen as an estimate of Beijing wintertime based on Dou et al. (2019) estimation of Q_f in Beijing summertime. Inclusion of a diurnal Q_f profile increased overall temperatures as well as latent and sensible heat fluxes (Figure 3).

180 Figure 3 shows that modelled potential temperature profiles in the evening are lower than observations, while observed latent heat flux (Fig 3b) is higher than modelled values throughout the day and sensible heat flux for observations and model values are similar. A potential explanation for the difference in latent heat flux between observations and simulations may come from assumptions made in model setup about surface water. In our model simulations we assumed an initial constant water volume fraction at the surface and in each soil layer for each day. However, in reality, the environment will change and
185 measurements of latent heat flux will be affected by the variations of surface and soil water, which themselves are dependent

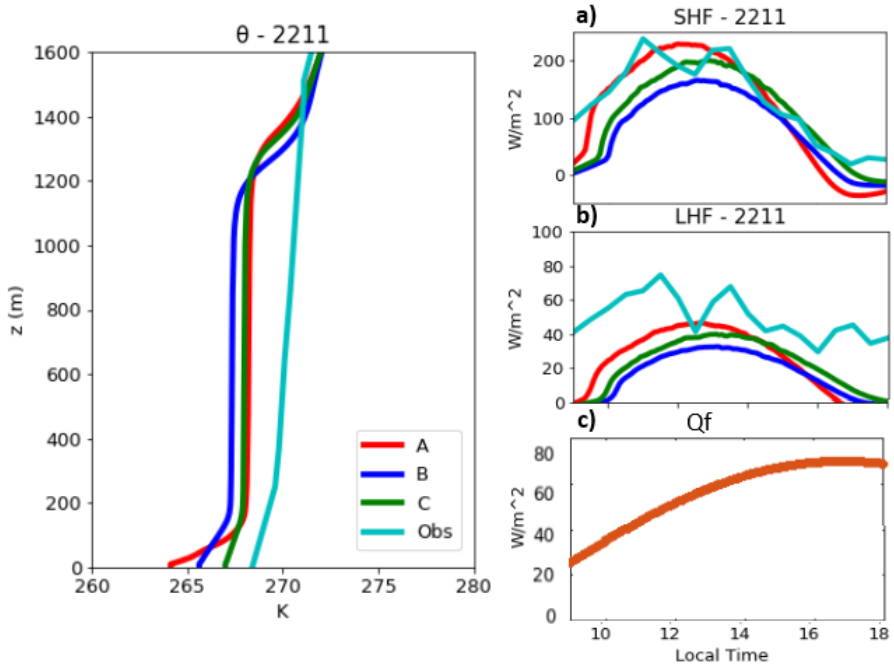

Figure 3. Plots of simulations and observations on 22/11 of (left) potential temperature (θ) profiles at 8 pm and (right) a) Sensible Heat Flux (SHF), b) Latent Heat Flux (LHF) and c) anthropogenic heat flux (Q_f) diurnal profiles. Simulations have different initial surface conditions: A) C_h = 2 x 10^6, Qf=0 (red lines), B) C_h = 7 x 10^6, Qf=0 (blue lines) and C) C_h = 7 x 10^6, Qf=diurnal as shown in panel c) (green lines). Observations (ECMWF-ERA5 reanalysis for potential temperature (θ)) are shown in turquoise and are ECMWF-ERA5 reanalysis for potential temperature (θ). and calculated flux values (SHF and LHF) from measurements taken during the APHH Beijing campaign. Errors for ECMWF-ERA5 reanalysis were around 0.1 K and there is natural variability in the SHF and LHF results which take into account the errors associated with the meteorological measurements of temperature, humidity and wind speed, used in the calculations

on surface properties as well as precipitation. The model also underestimates overall potential temperature profiles at 8pm (Figure 3 (left)) for all simulations, this might be a limitation of the homogeneous surface scheme, but could also be due to the changing synoptic conditions during the day which cannot be captured by the model.

This sensitivity work provides the setup for UCLALES-SALSA in an urban environment and this is utilised for the remainder of results presented below which all include a diurnal Q_f profile and heat capacity (C_h) set at 7x10^6 $Jm^{-3}K^{-1}$, which is a value typical of concrete (Takebayashi and Moriyama, 2012). The scope for variation of surface parameters within UCLALES is extremely high, therefore we recognise that within the model framework there is a strong dependence on parameters such as temperature, roughness, heat capacity, albedo and soil moisture. It is also likely that due to the simple homogeneous surface scheme used, some features of the urban environment that are observed cannot be replicated in the chosen model framework. Although the effect of these surface parameters is important to understand, the purpose of this paper is to examine the suitability of using an LES model in investigating urban haze. The parameters chosen here are based on identification of the urban

9

measurement site's characteristics, as well as from chosen literature values and are to the best of the authors' knowledge a fair representation of urban Beijing, as described in the next section.

3 Experimental Method

3.1 Observational Data

All measurements used in this study were taken at the Institute of Atmospheric Physics (IAP), Chinese Academy of Sciences, as part of the APHH Beijing campaign. Measurements taken include but are not limited to: NR-PM_1 (non refractory PM with a diameter < 1 μm) composition and aerosol and black carbon size and concentration measurements at the surface, as well as meteorological measurements at 15 levels on a 320 m tower. Sensible and latent heat flux measurements were calculated and a ceilometer was used to infer PBL height. For more information concerning the measurements taken as well as the APHH project and field campaign the reader is directed to the 'Introduction to the special issue "In-depth study of air pollution sources and processes within Beijing and its surrounding region (APHH-Beijing)' by Shi et al. (2019).

3.2 Experimental setup

The domain size for all model simulations spanned 5.4 km in the horizontal, with a resolution of 30 m and the model top was set to 1.8 km in the vertical with a resolution of 10 m. The model uses an adaptive timestep with a maximum timestep of 1 s. A haze period which took place within the APHH winter campaign period from 24th - 26th November 2016 was used to examine the sensitivity of boundary layer meteorology to varying aerosol concentrations. Meteorological data taken from ECMWF-ERA5 reanalysis and tower meteorological data was used to initialise vertical profiles at 8am (local time) on 24/11, 25/11 and 26/11 (Figure 4). Simulations were run from 8 am for 14 hours (10pm) including 1 hour spin up time. Simulations for all days were considered to be cloudless. Case studies for each day were simulated and compared to each other and are described as follows: Case 1 – No aerosols, Case 2-High and low aerosol loading, Case 3-Aerosol vertical profiles. For case 2 aerosol vertical profiles were constant in the column whereas case 3 examined the impact of including a varying aerosol vertical profile. Aerosol size distribution parameters and volume fraction of aerosol components were the same for all simulations, detailed in tables 1 and 2. The values for aerosol size distribution data used were measured by a scanning mobility particle sizer (SMPS) and aerosol composition measurements with an aerosol mass spectrometer (AMS). All in situ measurements were taken at IAP and values used were averaged between 07:30 and 08:30 on 24th November 2016. In all cases, BC can be considered to be the primary absorbing aerosol, with sulphate (SO_4^-), nitrate (NO_3^-) and ammonium (NH_4^+) strongly scattering and OC predominantly scattering with a small absorbing component (Table 1). Aerosol growth is considered through the processes of coagulation and water condensation, but semi-volatile condensation is not considered. Both wet and dry deposition are switched off in all simulations.

	Low	High
D_g (nm)	100	100
σ_g	1.55	1.55
N (#/mg)	10,000	40,000
PM (μg/m^3)	55	220

Table 2. Size distribution parameters used in the setup for simulations which included aerosols. D_g (geometric mean diameter), σ_g (geometric standard deviation), N (number concentration), as well as calculated surface PM concentration for low and high aerosol simulations

Composition	Fraction
OC	0.5
SO_4	0.1
NO_3	0.21
NH_4	0.09
BC	0.1

Table 3. Volume fraction of aerosols included in SALSA for all simulations in case 2 and case 3

4 Results

The results highlighted in this section aim to test the sensitivity of the newly coupled aerosol-radiation scheme in UCLALES-SALSA to aerosol loading, using meteorological conditions, urban characteristics and simplified aerosol conditions, associated with Beijing haze episodes. Case 1 shows boundary layer development for 24/11, 25/11 and 26/11 with no aerosols, case 2 examines the effect of high and low aerosol loading for each of the days and case 3 focuses on the impact of varying aerosol vertical profiles for 24/11 and 26/11. In all simulated results presented here, PBL height is taken as the height at which there is a maximum gradient in θ and SHF is surface SHF, all other variables unless stated are a direct model output. In this section we outline the influence of aerosols on the buoyant and shear terms of TKE generation, which are directly output from simulations. Equations 6 and 7 show how these are calculated and how the shear (S) term is related to wind speed and buoyancy (B) to temperature (Stull, 2015).

$$S = u*^2 + \frac{\Delta M}{\Delta z} \tag{6}$$

$$B = \frac{|g|}{T_v}.FH_{sfc} \tag{7}$$

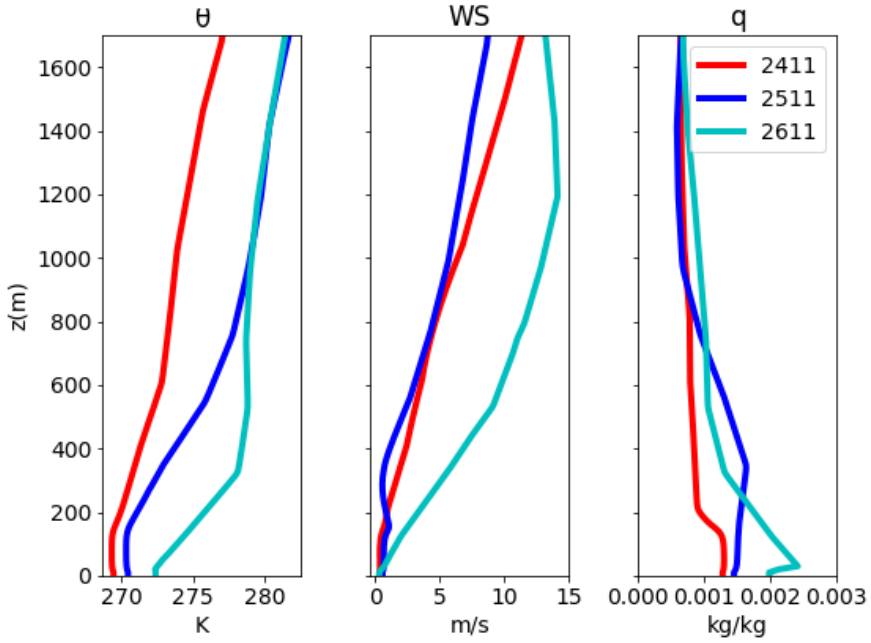

Figure 4. Initial vertical profiles of Potential Temperature (θ), Wind Speed (WS) and Total Water Mixing Ratio (q) for 24/11 (red), 25/11 (blue) and 26/11 (turquoise) for simulations with no aerosols (Case 1)

Where u^{*2} is surface frictional velocity and $\frac{\Delta M}{\Delta z}$ is wind shear, calculated as the change in wind speed (ΔM) over height (Δz). g is gravitational acceleration (9.8 m/s^2), T_v is the absolute virtual air temperature, and FH_{sfc} is the effective surface heat flux, which is normally positive during the daytime over land and negative at night.

4.1 Case 1- No Aerosols

Case 1 simulations built on the setup of the model to examine a haze episode which occurred from 24/11-26/11/2016. This case modelled the development of boundary layer dynamics on each day (24/11, 25/11 and 26/11) from 8am to 10pm without aerosol-radiation interactions. All 3 days were initialised with different meteorological vertical profiles taken from ECMWF-ERA5 reanalysis data, including potential temperature, wind speed and total water mixing ratio. On 25/11, a stronger temperature inversion existed at 8am compared to on 24/11, while on 26/11 there is a strong vertical wind shear, higher surface humidity and strong stability (large gradient in θ) in the lowest 300 m (Figure 4). Strong wind shear can cause mechanical turbulence while a large temperature inversion can prevent the growth of a turbulent boundary layer from buoyancy as the heating of the surface air throughout the day is not strong enough to create enough buoyant turbulence to move air parcels across the strong inversion, resulting in a shallow PBL.

Figure 5 shows the diurnal profiles of PBL height and SHF for each of the three days compared to observations. On 24/11, a well mixed PBL develops in the simulation, while ceilometer measurements show a constant PBL throughout the day (Fig.5a). On 25/11, the PBL is much shallower in both simulated and measured results (Fig. 5b) while on 26/11 the PBL is much slower to develop in both simulations and measurements, remaining low until around 13:00 hours where simulated values peak much higher than observations (Fig.5c). Simulated SHF is similar in magnitude for all 3 days, with a slight decrease in maximum values from 24/11 to 26/11, while observations show a large decrease in maximum and average daily SHF as the haze episode continues (Fig 5 d-f). From this we can see that the measurements of diurnal PBL and SHF profiles on each of the days in the pollution episode have differently shaped PBL and SHF diurnal profiles as well as different magnitudes and maximum values. On 26/11, measured PBL height and SHF are lower, suggesting less turbulence. The modelled simulations of each day without aerosols also show this variation, suggesting that although aerosol-PBL feedback may also influence the changing observed conditions, initial meteorological conditions have an impact on the maximum values of PBL and SHF as well as the shape of the diurnal profile.

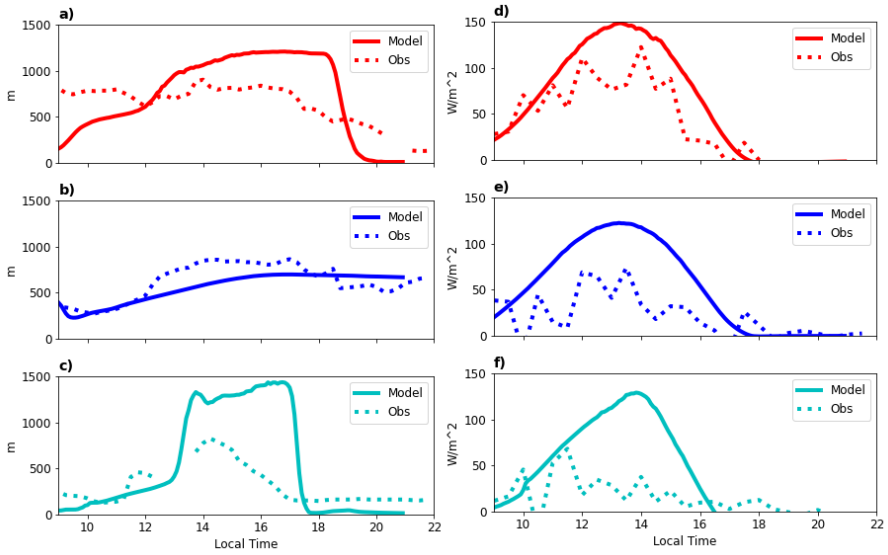

Figure 5. Simulated (solid line) and observed (dashed line) of PBL height (a-c) and SHF (d-f) for 24/11 (red), 25/11 (blue) and 26/11 (turquoise) where simulations have no aerosols included (Case 1)

The aim of this work is to showcase the development of turbulent dynamics on different days due to initial meteorological conditions without the influence of aerosol interactions. While observations are influenced both by meteorology and aerosol interactions. Therefore, simulations aren't trying to replicate observations but rather showcase the variation due to meteorological conditions in Beijing and compare this to observations. The changing conditions used here are typical for a Beijing haze episode and show that even without the consideration of aerosols, meteorological conditions can largely affect the diurnal development of boundary layer dynamics. The initial meteorological profiles for the simulations on 24/11 are taken prior to

the onset of the haze and are associated with clean conditions. This is likely the reason for the quick turbulent boundary layer development along with high SHF throughout the day. Observations show that aerosol concentrations begin to build up around midday on 24/11 and remain constant until the afternoon of 25/11 when concentrations build up rapidly, peaking overnight on 25/11 and remaining high until the afternoon of 26/11. Therefore, the initial conditions used in the simulation of 25/11 will have been slightly affected by aerosol-radiation interactions of the previous evening.

4.2 Case 2- High and Low Aerosol Loading

Section 4.1 shows that simulated boundary layer dynamics are impacted by initial meteorological conditions. In the simulations presented here, the sensitivity of boundary layer dynamics to aerosol loading is examined, where aerosol mixing ratios were constant throughout the profile. 'High' and 'low' aerosol loadings were chosen to be similar mass concentrations to what was observed at 8am on 26/11 and 24/11 respectively, and are detailed in Table 2. This was to approximately simulate aerosol conditions from the beginning and end of the haze period. However, aerosol size and composition were kept constant in all simulations, to minimise the variables examined (Table 3).

Table 4 shows the impact of including high and low aerosol loading on maximum SHF and maximum PBL height between 12:00 and 16:00 LST (Local Standard Time). Compared to 'low' aerosol loading simulations, high aerosol loading causes the largest % decrease in PBL height and SHF on 26/11 compared to simulations of 24/11 and 25/11. Ceiliometer measurements of PBL height on 26/11 show a delayed development of PBL but a maximum height of 826 m (Fig 5.c), which is between the maximum PBL height for 26/11 'high' (391 m) and 'low' (1169 m) aerosol loading simulations. On 24/11, the 'low' aerosol loading case simulation had a maximum PBL height of 1088 m while ceiliometer measurements show a maximum PBL height of 903 m. Therefore, the simulations overestimated the PBL height on 24/11 by a small amount (17 %) and underestimated in the case of 26/11 by a much larger amount (52 %) (Table 4). Potential reasons for this and a further discussion of these results is detailed in section 5.2.

In all cases inclusion of 'high' aerosol loading causes cooling in the lower planetary boundary layer, and warming above it (Figure 6). This is due to aerosol-radiation interactions absorbing and scattering incoming SW radiation to reduce the amount of solar radiation reaching the surface. However, on 24/11 and 26/11, we see a slight warming in the potential profiles for 'Low' aerosol loading compared to no aerosol simulations. Aerosols, specifically black carbon, in the atmosphere absorb radiation to causes warming. Including high aerosol concentrations (220 μg/m^3) compared to low aerosol concentrations (55 μg/m^3) maximised this effect. As in these cases aerosols are present at the same concentration through the column, in the 'high' aerosol case, the aerosols at higher altitudes will interact with incoming SW radiation first, reducing the degree of radiation available for aerosols-radiation interactions at lower levels. However, in the 'low' aerosol loading case, there are fewer aerosol-radiation interactions at higher altitudes which can result in absorption of BC at lower levels which might be the reason for the slight warming observed in figure 6.

Day	24/11	25/11	26/11
Max PBL height (None)	1240	695	1424
Max PBL height (Low)	1088	592	1169
Max PBL height (High)	915	475	391
Max PBL height (Obs)	903	857	826
% decrease in PBL height (High-Low)	16%	20%	67%
% decrease in PBL height (High-None)	26%	32%	73%
Max SHF (None)	148	123	129
Max SHF (Low)	126	97	100
Max SHF (High)	82	64	55
Max SHF (Obs)	111	74	68
% Decrease in SHF (High-Low)	35%	34%	45%
% Decrease in SHF (High-None)	45%	48%	57%

Table 4. Change in maximum PBL height (taken as the height between 12 and 4pm with a maximum gradient in potential temperature) and SHF for all 3 days with high and low aerosol loading. Observations (obs) are taken from ceiliometer data (PBL height) and calculated fluxes (SHF) as part of the APHH Beijing campaign

For the case of 25/11, the PBL is low and a temperature inversion of $\sim$ 4 K at 5pm exists for simulations without aerosols increasing to $\sim$ 6 K when aerosols are included (Figure 6). This is likely due to the strong temperature inversion in the initial meteorological conditions of $\sim$ 10 K at 8am (Figure 4) which means that SW heating of the surface is not strong enough to fully break the temperature inversion and allow the growth of a fully turbulent PBL. Furthermore, when aerosols interact with radiation there is even less SW heating of the surface to break the temperature inversion and PBL growth is suppressed further. The morning temperature inversion observed on 25/11 is likely due to a mix of synoptic conditions, and aerosols from the previous day causing cooling. These conditions are typical in haze episodes of Beijing and can lead to enhanced stagnation events.

For the 26/11 simulations, there is a very large (67 %) decrease in PBL height for 'high' aerosol loading compared to 'low' aerosol loading conditions. This is much greater than the decrease on both 24/11 (16 %) and 25/11 (20 %). A potential reason for this, might be the impact of aerosols on wind speeds which can reduce shear turbulence. This greater impact of aerosols on 26/11 PBL dynamics suggests that initial meteorological conditions have an impact on the magnitude of the aerosol-PBL feedback. However, in the simulations performed here, aerosol mass concentrations are high throughout the column to model top (1800 m). In reality, aerosols are more concentrated at the surface, particularly in the morning when the mixing layer is shallow. As the PBL develops they become vertically mixed within the layer with concentrations normally decreasing significantly above the PBL. Therefore, inclusion of high aerosols at higher altitudes in case 2 simulations are unrealistic and aerosol-radiation interactions near model top (above the PBL) on 26/11 may be the reason for such a large decrease in

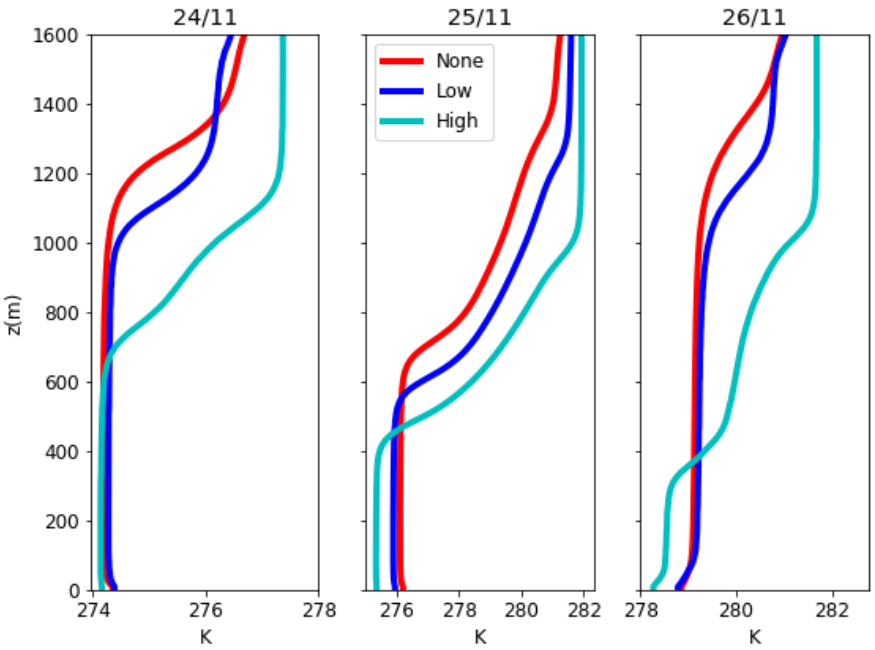

Figure 6. Potential temperature profiles at 5pm for 24/11, 25/11 and 26/11, with no aerosols (red), low aerosol loading (blue) and high aerosol loading(turquoise)

PBL height under high aerosol loading which is not represented in ceilometer observations. Therefore, in the next section we examined the impact of aerosol vertical profiles on aerosol-PBL interactions under 'high' and 'low' aerosol loading for 24/11 and 26/11.

4.3 Case 3- Aerosol Vertical Profiles

In these simulations, we investigate the impact of including aerosol vertical profiles for 'high' and 'low' aerosol loading cases on 24/11 and 26/11. These two days were chosen as a direct comparison study as in simulation results presented in section 4.1 they both had deep turbulent PBL's develop, while 25/11 was impacted by a strong morning temperature inversion (Figure 5). The main aim of this work is to examine what effect different aerosol loadings at high altitudes had on PBL development and therefore examination of the days where the PBL fully developed without aerosol inclusion was chosen to understand this effect of aerosols at high loading on PBL development.

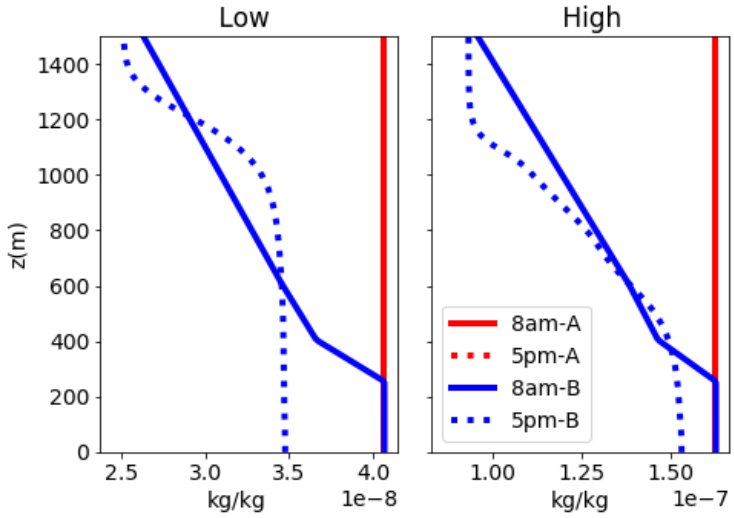

Figure 7. Aerosol mass mixing ratio vertical profiles for low and high aerosol loading simulations on 26/11, for constant aerosol profile (red (A)) and vertically varying aerosol profiles (blue (B)) at initial timestep (solid) and after 9 hours simulation (dashed). For the case of the constant vertical profiles (red lines), aerosol mass mixing ratio remains constant through time and so the dashed red lines are hidden behind the solid red

Figure 7 outlines both the varied (blue) and constant (red) vertical aerosol profiles initialised for 'low' and 'high' aerosol loading in case 3 (solid line). For the varied aerosol vertical profiles, as the simulated PBL develops, the aerosols become vertically mixed through the column. Initially aerosols at the surface are vertically mixed up to 300 m. In 'low' aerosol loading simulations on 26/11, by 5pm aerosols have mixed through the lowest 1000 m of the column while in high aerosol loading simulations they are only vertically mixed up to 600 m. When aerosols are well mixed vertically, they are less concentrated at the surface, which has implications for health, as well as reducing the intensity of aerosol-radiative feedback on PBL dynamics. The variation of the aerosol vertical profiles on the different days demonstrates the impact of boundary layer meteorology on surface aerosol concentrations, which is an essential component of the aerosol-PBL feedback (Figure 1). A shallow boundary layer will lead to more aerosols concentrated at the surface, stronger aerosol-radiation interactions and further suppression of PBL development.

Day	24/11	26/11
Max PBL height (Model)	1111	993
Max PBL height (Obs)	903	826
% difference	17.6	16.8

Table 5. Differences in maximum PBL height (taken as the height with the largest gradient in θ) between 12 and 4pm for 24/11 (low vertical profile) and 26/11 (high loading vertical profile) simulations and comparison with observations (taken from ceiliometer measurements)

Table 5 shows the differences in maximum PBL height for simulations with vertical profiles of 24/11 with 'low' aerosol loading and of 26/11 with 'high' aerosol loading, both with initial aerosol vertical profiles as show in figure 7 (blue lines). These simulations can be considered to have aerosol conditions closest to those observed. Therefore, we compare the maximum PBL height (m) with those taken using a ceiliometer at the IAP site during the APHH Beijing campaign. Results show that for maximum PBL height on each day the model overestimates PBL height by $\sim$ 17 %.

Figure 8 compares results from section 4.2 and 4.3, showing the variation in potential temperature (θ), wind speed (WS), and diurnal PBL height, SHF and variance in vertical velocity (σw^2) at 100 m, for simulations on 24/11 and 26/11 with 'high' and 'low' aerosol loading, and 'high' aerosol loading vertical profile simulations (Figure 7). We then compare the diurnal profiles to observations taken at the IAP site. Comparing 'high' aerosol loading (blue lines) with 'high (vprof)' (turquoise lines) simulations shows that the effect of varied vertical profiles on potential temperature profiles on 24/11 (Fig. 8a) and 26/11 (Fig. 8d) is a reduction in the strength of the temperature inversion, less cooling in the PBL and a higher PBL top for the 'high vertical profile' simulations compared to the 'high' aerosol loading simulations. On 26/11, this effect is significant, where maximum PBL height is 993 m for the 'high-vertical profile' aerosol simulations and 391 m for 'high' aerosol (Table 4 and 5). The maximum PBL height in the 'high-vertical profile' simulations are also closer to observed maximum value of 903 m for 24/11 and 826 m for 26/11 (Table 5) and simulations including the vertical profile are also closer to observed PBL and SHF diurnal variations, compared to 'high' aerosol loading simulations (Figure 8). For the case of 26/11, figure 8 (θ) shows that there are 3 distinct layers in the vertical profile for high aerosol loading at 5pm. A neutral layer up to around 300 m, followed by a stable layer up to 1000 m and a neutral layer to model top. For the low aerosol loading there is a neutral layer up to 1100 m followed by a slightly stable layer to model top. In these simulations, high aerosol loading leads to a reduction in θ and wind speed at the surface layer and increases it above the PBL compared to low aerosol loading. Figure 8 (k-i) shows the variance in vertical velocity (σw^2) at 100 m for all simulations compared to observations. σw^2 can be used to describe the level of turbulence within a layer, with higher values relating to a larger amount of turbulent motion (Wang et al., 2019). Model simulations generally show the diurnal variation of σw^2 well compared to observations, with 'high' and 'high-vprof' simulations having a much smaller maximum value compared to 'low' aerosol loading simulations.

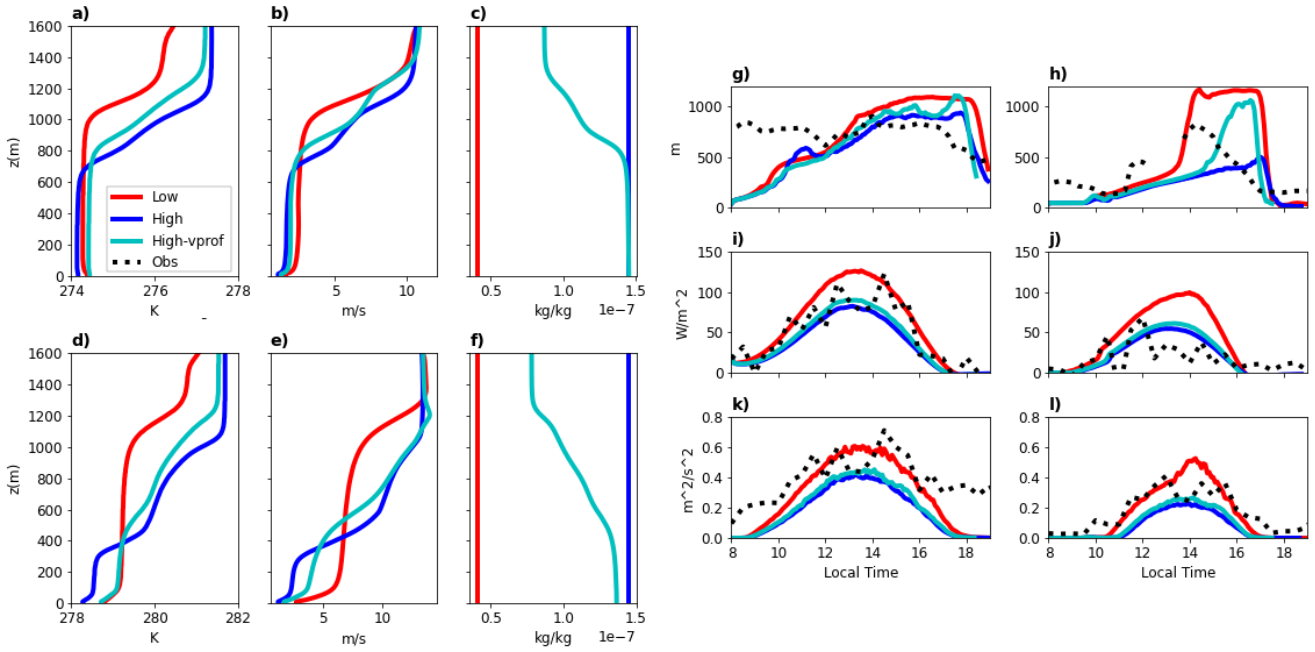

Figure 8. Potential Temperature (a and d), Wind Speed (b and e) and Aerosol Mass Mixing Ratios (c and f) profiles for 24/11 (a-c) and 26/11 (d-f) for low (red), high (blue) and high vertical profile (turquoise) simulations at 5pm (9 hours of simulation). Right panel - PBL height (g and h), SHF (i and j) and σw^2 (k and l) for simulations on 24/11 (g, i and k) and 26/11 (h, j and l) for low (red), high (blue) and high vertical profile (turquoise) and observations (black dots)

To investigate further the effect of aerosol vertical profiles and loading on PBL dynamics, we plotted variance in vertical velocity (σw^2) for case 2 and case 3 simulations as a function of height and time (Figure 10). Figure 10 shows horizontal domain averages of σw^2 for case 2 'low' (a and e) and 'high' (b and f) aerosol loadings and case 3 'high-vprof' (c and g) aerosol loading simulations. The results show that for case 2 'high' aerosol loading simulations (Fig. 9b and f) on both days there is strong turbulent layer ($\sigma w^2 > 0.2$ m$^2/s^2$) that develops at high altitudes (1200-1600 m). In previous studies, which use Doppler Lidar to extrapolate PBL height a $\sigma w^2 > 0.1$ m^2/s^2 can be used to describe a layer within the PBL (turbulent layer) (Wang et al., 2019). This highly turbulent layer can therefore be considered unusual as ordinarily through the day the PBL will be turbulent (unstable) but the area above the PBL will be extremely stable with low turbulence, like in the 'low' aerosol loading cases (Fig. 9a and 9e).

Plots of σw^2 for case 3 'high' simulations (Fig. 9c and g) show a much smaller layer of turbulence (high σw^2) between 1200-1600 m compared to case 2 'high' simulations. Figure 9 (d and h) shows the difference in σw^2 between the 'high-vprof' (c and g) and 'high' (b and f) simulations for both 24/11 (Fig. 9d) and 26/11 (Fig. 9h). This shows that including the vertical profile of aerosol simulations in the 'high' aerosol loading cases, reduces turbulence at model top for both days and increases

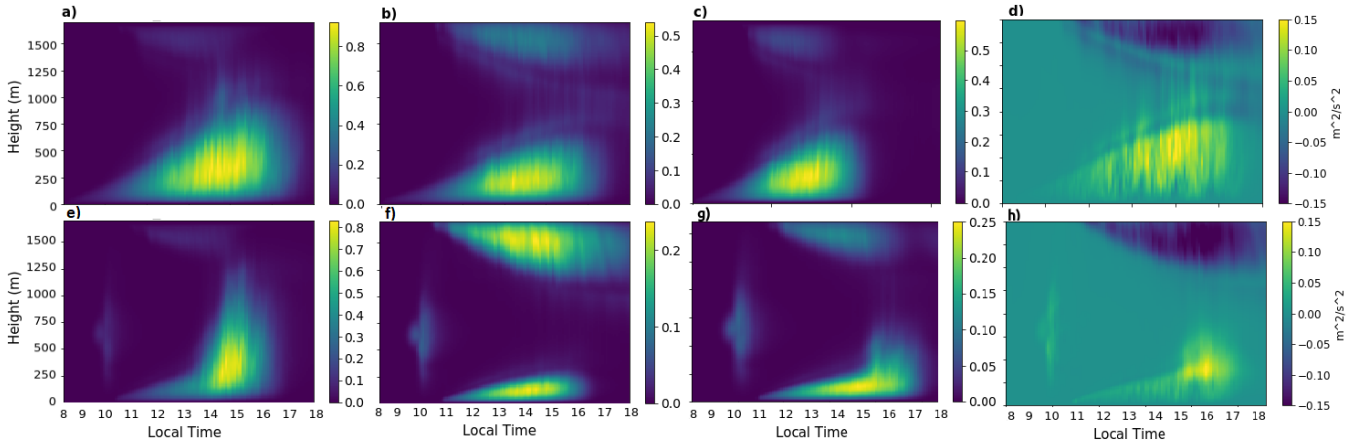

Figure 9. Variance in vertical velocity (σ_w^2) for simulations on 24/11 (a-d) and 26/11 (e-h) for case 2 'low' (a and e) and 'high' (b and f) aerosol loading simulations and for case 3 'high-vprof' (c and g) simulations. Panels d and f are difference plots showing 'high-vprof' - 'high' aerosol loading simulations

turbulence within the PBL (0-500 m). This indicates that the reason for the strong turbulence at model top seen in Fig. 9b and 9f is due to high aerosol loading and strong aerosol-radiation interactions within this layer in case 2 'high' simulations. This might alter the thermal profile of the atmosphere and reduce turbulence within the PBL, inhibiting growth. On 26/11 this effect is very strong, which may be the reason for the large reduction in PBL height for case 2 'high' simulations (Table 4). However, it is unusual for such high concentrations of aerosols to be present above PBL top and therefore the turbulent effect for case 2 'high' aerosol loading may be considered an artefact of the unrealistic constant aerosol profiles.

5 Discussion

The results highlighted above show the use of a novel coupled LES-aerosol radiation model to investigate haze in the urban environment of Beijing. Simulated sensitivity to urban surface parameters is high and these will be different for other urban locations. It is therefore necessary to evaluate and tune these parameters to observations in specific environments in order to use an LES model to fully explore boundary layer dynamic sensitivities. Aerosol-radiation interactions were tested for the first time in the model framework and showed that sensitivity of boundary layer meteorology and turbulence to aerosol loading was strong while also being dependent on initial meteorological conditions.

5.1 Sensitivity to meteorology

Section 4.1 identifies the importance of meteorological conditions on boundary layer dynamics throughout the day. Many observations in Beijing found that meteorological conditions are a main driver of both the onset and longevity of haze. Large

scale synoptic conditions such as southerly winds and low pressure often preempt pollution episodes which tend to occur every 4-7 days in Beijing wintertime (Liu et al., 2018a; Wang et al., 2019). These conditions are associated with the beginning of 'haze' as the switch in meteorological conditions from strong northwesterly to southerly winds advects pollution from surrounding provinces into Beijing. This change is also associated with the convergence of winds aloft which causes air to subside and warm, leading to a temperature inversion over urban Beijing (Gao et al., 2016).

Aerosol-radiation interactions reduce the amount of solar radiation reaching the surface which causes cooling, simultaneously black carbon aerosols will absorb radiation at PBL top. Although absorption by black carbon (BC) occurs throughout the column, several studies have shown that due to the higher incidence of solar radiation and lower density of air, BC causes warming at PBL top to a greater extent than at the surface (Ding et al., 2016). Overall, this causes a temperature inversion during periods where pollution is high and causes a shallow PBL to form during the day. This leads to stagnant conditions and can affect the meteorology of the next day, particularly when aerosols are suppressed in a shallow PBL. Additionally, during winter in Beijing, changes in pressure frequently cause warm polluted air to converge with cold clean air to create a layer of cold air under a layer of warm air, known as a temperature inversion. These conditions often preempt pollution episodes in Beijing and favour the accumulation of pollutants in a shallow boundary layer. These factors may cause the strong temperature inversion in the morning observed on both 25/11 compared to 24/11, which results in a shallow turbulent boundary layer forming in these simulations (Sun et al., 2016; Wang et al., 2017, 2018; Dang and Liao, 2019; Wang et al., 2019; Xiang et al., 2019).

On 26/11 (8 am), there is strong vertical wind shear, with slow wind speeds at the surface and strong winds above the PBL. In wintertime Beijing, strong winds from the North are often synonymous with the end of haze episodes, through causing the dissipation of pollutants and breaking the aerosol-PBL feedback loop. However, often the strong winds aloft will take a while to become entrained into the PBL, particularly when there is a strong temperature inversion and an extremely stable boundary layer. This can result in delayed development of the PBL as it takes a while for the strong winds to become entrained into the PBL. When this does occur, pollutants will quickly become dispersed and the PBL will grow strongly through both mechanical and buoyant turbulent motion (Wang et al., 2019). This is most likely the reason for the slow PBL development in both observations and case 1 simulations of 26/11 outlined in section 4.1.

Overall, the 3 days examined have different synoptic influences which result in different PBL dynamical conditions throughout the day. These changing conditions in turn influence the distribution and interactions of air pollutants, including aerosol-radiation interactions.

5.2 Sensitivity to aerosol loading

Aerosols alter the thermal profile of the atmosphere through absorbing and scattering solar radiation. The strength and type of the aerosol interactions is dependent on aerosol size, composition and loading. The influence this has on the thermal profile of the atmosphere is also affected by the vertical distribution of aerosols through the column as well as the total column aerosol

optical depth (AOD). In section 4.2, we outlined results examining the effect of aerosol loading on PBL dynamics for different days of a pollution episode. Other factors include changing aerosol size and composition which vary both during and between haze episodes. These factors may strongly impact aerosol-radiation interactions and a limitation of the work performed here is that these are not examined.

However, the results outlined in section 4.2 do show that high aerosol loading reduces turbulence and PBL height and increases temperature inversions at PBL top through causing cooling at the surface. In the case of 26/11, there is a much larger decrease in maximum PBL height (67 %) for high vs low aerosol loading simulations compared to both 24/11 (16 %) and 25/11 (20 %), even though the range in SHF % decrease between the days is not as large (45 % to 57 %). This indicates that although high aerosol loading on 26/11 has a large impact on the thermal profile of the atmosphere, reducing buoyant turbulence and the sensible heat flux by a larger amount compared to simulations on 24/11 and 25/11, other factors may be causing the large reduction in maximum PBL height.

Turbulence can be produced through the processes of wind shear and convection (movement of hot air). The wind shear term typically only becomes important at the surface when convection is minimal, such as when there is high stability in the PBL (Stull, 2015). On 26/11 there is strong wind shear and the lower PBL is stable. Therefore, it is likely that turbulence in simulations of 26/11 with no and 'low' aerosol loading is driven by both wind shear and convection. High aerosol loading will interact with solar radiation to reduce convection of air at the surface, reducing turbulence. However, high aerosol loading can also reduce surface wind speeds. High aerosol concentrations are known to stabilise the boundary layer through the reduction of vertical transport of momentum to the surface (Jacobson and Kaufman, 2006). This can reduce wind speeds at lower altitudes and thus decrease wind shear. High aerosol loading also causes a reduction in the variance of vertical velocity (σ_w^2), which can be considered a measure of turbulence (Stull, 2015).

In section 4.2 we show that high aerosol throughout the column causes warming in the upper layers and cooling in the lower layers, which causes strong stability throughout the profile. In reality, aerosols tend to be concentrated closer to the surface and within the boundary layer, although occasionally in Beijing regional transport can lead to higher aerosol concentrations aloft. Therefore, although the impact of aerosols at high altitudes may cause a strong reduction in turbulence on certain days as described in section 4.2, these types of conditions are unlikely to occur in Beijing and so should be treated with caution and as potential artefact of the model setup.

5.3 Vertical profiles

Results from section 4.2 showcase the variation in aerosol-PBL feedback due to different aerosol mass loadings as well as differences in initial meteorological conditions. As discussed in section 4.4, compared to ceiliometer measurements, simulated PBL height on 26/11 under 'high' aerosol loading condition is much lower.

Including vertical aerosol profiles allowed for examination of the effect of aerosol loading in the surface layer compared to aerosol loading aloft. When there is a reduction in high aerosol loading aloft, there is a smaller reduction in maximum PBL

height on both 24/11 and 26/11. However, this might be more of an impact of a lower total column aerosol loading during the case 3 simulations than the impact of aerosols aloft. The difference in vertical velocity, particularly in the 1200-1600 m layer in 26/11 'high' loading simulations is likely due to the aerosols aloft. This work outlines the relative importance of aerosol vertical profiles on understanding the magnitude of the aerosol-PBL feedback.

A recent study by Su et al. (2020) shows the importance of aerosol vertical profiles on the aerosol-PBL feedback. Their work examines three different vertical profiles of the aerosol extinction coefficient and examines the impact on PBL dynamics. Their results show that when aerosol extinction increases with height, there is a larger decrease in buoyancy and PBL height compared to when aerosols are more concentrated at the surface. Our work also finds that aerosol vertical profiles have an impact on bouyancy and the magnitude of the aerosol-PBL feedback effect. However, in the results presented here there is no variation of aerosol composition vertically in the column. The BC warming effect has been shown to be stronger at higher altitudes due to both the higher strength of solar radiation and lower density of air (Ding et al., 2016). Furthermore, aerosols aloft interact with solar radiation, which reduces the amount of solar radiation available for both heating of the surface and for interacting with aerosols in lower layers within the PBL. Consequently, in simulations with 'high' aerosol loading aloft, the large degree of cooling at the surface is likely due to the strong interactions of aerosols at higher altitudes. This identifies the importance of including accurate aerosol vertical profiles.

5.4 Model Limitations

Case 3 examined the impact of meteorological feedback on aerosol vertical mixing for high and low aerosol loading simulations by including aerosol vertical profiles on 24/11 and 26/11. It should be noted from the varied aerosol vertical profile simulations that total aerosol mass mixing ratio decreases by about 5 % over the course of the day. This is despite dry deposition not being included in these simulations. This is a result of UCLALES-SALSA using the Ogura-Philips anelastic approximation for filtering out acoustic waves. The approximation assumes that there are only small variations in pressure and density from static reference values over time. Throughout the day, surface fluxes increase air temperature, while subsidence of air at the model top decreases density (Ogura and Phillips, 1962; Byun, 1999; Pressel et al., 2015). The limitations of the anelastic approximation mean that these changes do not fully feed back to change pressure, and fixed boundary conditions mean that volume remains constant. As the model holds to constant volume rather then constant mass, when SALSA aerosol mass tracers are pulled downward, the total air mass increases while the mass of aerosols remain the same, this causes the apparent decrease in aerosol mass mixing ratio (Figure 7). We consider this to be a limitation of using a meteorological model for air quality analysis, however as the relative reduction is the same for different meteorological conditions, comparisons between different cases can still be performed.

6 Conclusions

UCLALES-SALSA was set up to model an urban environment for the first time, in order to investigate the impact of aerosol-radiation interactions on urban haze. During set up, sensitivity to urban surface parameters was shown to be high, and accounted

for the slower release of heat throughout the day as observed in urban Beijing. Inclusion of a diurnal anthropogenic heat flux in simulations resulted in a warmer environment typical of an urban heat island. Given the sensitivity to such parameters, accurate measurements of these properties can be considered paramount in order to improve modelling of the urban environment. Turbulent motion throughout the day in each simulation is further impacted by initial meteorological profiles. Conditions associated with clean periods in Beijing allow for the development of a highly turbulent boundary layer, while strong morning temperature inversions prevent the growth of a turbulent boundary layer throughout the day. High aerosol concentrations in all cases decreases surface SHF, σw^2 and PBL height, as well as causing cooling at the surface and reducing surface wind speeds. While in some cases, 'low' aerosol loading resulted in a slight warming in the PBL due to the effect of BC absorption. All simulations also show large sensitivity to aerosol loading, with more than a third reduction in SHF due to high aerosol loading in all simulations. Through comparing simulations with and without aerosol vertical profiles we observe that on 26/11 the simulated development of a turbulent boundary layer in the afternoon is impacted by high aerosol loading aloft (section 4.3).

The sensitivity work outlined above aims to isolate the aerosol and dynamical effects on pollution episodes through using a specific period with varying meteorological conditions and simplified aerosol conditions. LES models are limited in their ability to represent changing synoptic conditions without additionally forcing or nudging simulated profiles with mesoscale model results or through observations. However, these simulations do show the sensitivity to and importance of meteorological conditions on the development of boundary layer turbulence in Beijing. As well as assessing the importance of aerosol loading on the aerosol-meteorology feedback loop and the impact on PBL turbulent statistics. The aerosol feedback loop is thought to have the largest impact on haze episodes during the cumulative and dissipation stages of the pollution episode. Future work will focus particularly on these stages and the impact of aerosol-radiation-meteorology interactions. As aerosol optical properties play an important role in the feedback, future work will also take advantage of the SALSA framework to vary aerosol optical properties in a case study of Beijing haze.

Code availability. The code used in this manuscript can be downloaded at https://www.github.com/UCLALES-SALSA

Author contributions. The idea for the study was conceived by JS, GM and HC. All model simulations were performed by JS with the assistance of JT. JS wrote the paper with input from JT and TK. All co-authors discussed the results and commented on the manuscript. The authors declare that they have no conflicts of interest.

Competing interests. The authors declare that they have no conflict of interest.

Acknowledgements. Jessica Slater is fully funded by the National Centre for Atmospheric Science (NCAS). This work was carried out as part of AIRPRO (NE/N00695X/1) for which Jessica Slater, Hugh Coe and Gordon McFiggans also acknowledge funding. Sami Romakkaniemi and Juha Tonttila are supported by the Academy of Finland (projects 283031 and 309127) Model simulations were carried out on the ARCHER UK National Supercomputing Service (http://www.archer.ac.uk). We gratefully acknowledge Yele Sun's group and Pingqing Fu's group at IAP for aerosol composition data and tower meteorological data respectively, as well as Zifa Wang's group at Peking Univeristy for aerosol size data and Eiko Nemitz at CEH Edinburgh for heat flux data.

References

Ács, F., Mihailović, D. T., and Rajković, B.: A Coupled Soil Moisture and Surface Temperature Prediction Model, https://doi.org/10.1175/1520-0450(1991), 1991.

Andrejczuk, M., Gadian, A., and Blyth, A.: Numerical simulations of stratocumulus cloud response to aerosol perturbation, Atmospheric Research, 140-141, 76–84, https://doi.org/10.1016/j.atmosres.2014.01.006, 2014.

Bellon, G. and Stevens, B.: Using the sensitivity of large-eddy simulations to evaluate atmospheric boundary layer models, Journal of the Atmospheric Sciences, 69, 1582–1601, https://doi.org/10.1175/JAS-D-11-0160.1, 2012.

Bond, T. C. and Bergstrom, R. W.: Light absorption by carbonaceous particles: An investigative review, Aerosol Science and Technology, 40, 27–67, https://doi.org/10.1080/02786820500421521, 2006.

Byun, D. W.: Dynamically consistent formulations in meteorological and air quality models for multiscale atmospheric studies. Part II: Mass conservation issues, Journal of the Atmospheric Sciences, 56, 3808–3820, https://doi.org/10.1175/1520-0469(1999)056<3808:DCFIMA>2.0.CO;2, 1999.

Dang, R. and Liao, H.: Severe winter haze days in the Beijing-Tianjin-Hebei region from 1985ndash;2017 and the roles of anthropogenic emissions and meteorological parameters, Atmospheric Chemistry and Physics Discussions, 5, 1–31, https://doi.org/10.5194/acp-2019-306, 2019.

Ding, A. J., Huang, X., Nie, W., Sun, J. N., Kerminen, V. M., Petäjä, T., Su, H., Cheng, Y. F., Yang, X. Q., Wang, M. H., Chi, X. G., Wang, J. P., Virkkula, A., Guo, W. D., Yuan, J., Wang, S. Y., Zhang, R. J., Wu, Y. F., Song, Y., Zhu, T., Zilitinkevich, S., Kulmala, M., and Fu, C. B.: Enhanced haze pollution by black carbon in megacities in China, Geophysical Research Letters, 43, 2873–2879, https://doi.org/10.1002/2016GL067745, 2016.

Dou, J., Wang, Y., Bornstein, R., and Miao, S.: Observed spatial characteristics of Beijing urban climate impacts on summer thunderstorms, Journal of Applied Meteorology and Climatology, 54, 94–105, https://doi.org/10.1175/JAMC-D-13-0355.1, 2015.

Dou, J., Grimmond, S., Cheng, Z., Miao, S., Feng, D., and Liao, M.: Summertime surface energy balance fluxes at two Beijing sites, International Journal of Climatology, 39, 2793–2810, https://doi.org/10.1002/joc.5989, 2019.

Fu, Q. and Liou, K. N.: Parameterization of the Radiative Properties of Cirrus Clouds, https://doi.org/10.1175/1520-0469(1993)050<2008:POTRPO>2.0.CO;2, 1993.

Gao, M., Carmichael, G. R., Wang, Y., Saide, P. E., Yu, M., Xin, J., Liu, Z., and Wang, Z.: Modeling study of the 2010 regional haze event in the North China Plain, Atmospheric Chemistry and Physics, 16, 1673–1691, https://doi.org/10.5194/acp-16-1673-2016, 2016.

Gao, Y., Zhang, M., Liu, Z., Wang, L., Wang, P., Xia, X., Tao, M., and Zhu, L.: Modeling the feedback between aerosol and meteorological variables in the atmospheric boundary layer during a severe fog-haze event over the North China Plain, Atmospheric Chemistry and Physics, 15, 4279–4295, https://doi.org/10.5194/acp-15-4279-2015, 2015.

Grimmond, C. S. B. and Oke, T. R.: Heat Storage in Urban Areas: Local-Scale Observations and Evaluation of a Simple Model, Journal of Applied Meteorology, 38, 922–940, https://doi.org/10.1175/1520-0450(1999)038<0922:HSIUAL>2.0.CO;2, 1999.

Hu, D., Yang, L., Zhou, J., and Deng, L.: Estimation of urban energy heat flux and anthropogenic heat discharge using aster image and meteorological data: case study in Beijing metropolitan area, Journal of Applied Remote Sensing, 6, 063 559–1, https://doi.org/10.1117/1.JRS.6.063559, 2012.

Ikeda, R., Kusaka, H., Iizuka, S., and Boku, T.: Development of Urban Meteorological LES model for thermal environment at city scale, ICUC9 - 9th International Conference on Urban Climate jointly with 12th Symposium on the Urban Environment Development, 2012.

Jacobson, M. Z. and Kaufman, Y. J.: Wind reduction by aerosol particles, Geophysical Research Letters, 33, 1–6, https://doi.org/10.1029/2006GL027838, 2006.

Kokkola, H., Korhonen, H., Lehtinen, K. E. J., Makkonen, R., Asmi, A., Järvenoja, S., Anttila, T., Partanen, A.-I. I., Kulmala, M., Järvinen, H., Laaksonen, A., and Kerminen, V.-M. M.: SALSA - a sectional aerosol module for large scale applications, Atmospheric Chemistry and Physics, 8, 2469–2483, https://doi.org/10.5194/acp-8-2469-2008, 2008.

Kokkola, H., Kuhn, T., Laakso, A., Bergman, T., Lehtinen, K., Mielonen, T., Arola, A., Stadtler, S., Korhonen, H., Ferrachat, S., Lohmann, U., and Neubauer, D.: SALSA 2.0 : The sectional aerosol module of the aerosol – chemistry – climate model ECHAM6.3.0-HAM2 .3-MOZ1.0, Geoscientific Model Development, 11, 3833–3863, 2018.

Liu, B., Ma, Y., Gong, W., Zhang, M., and Shi, Y.: The relationship between black carbon and atmospheric boundary layer height, Atmospheric Pollution Research, 10, 65–72, https://doi.org/10.1016/j.apr.2018.06.007, https://doi.org/10.1016/j.apr.2018.06.007, 2019.

Liu, C., Huang, J., Fedorovich, E., Hu, X.-M., Wang, Y., and Lee, X.: The Effect of Aerosol Radiative Heating on Turbulence Statistics and Spectra in the Atmospheric Convective Boundary Layer: A Large-Eddy Simulation Study, Atmosphere, 9, 347, https://doi.org/10.3390/atmos9090347, 2018a.

Liu, Q., Ma, T., Olson, M. R., Liu, Y., Zhang, T., Wu, Y., and Schauer, J. J.: Temporal variations of black carbon during haze and non-haze days in Beijing, Scientific Reports, 6, https://doi.org/10.1038/srep33331, 2016.

Liu, Q., Jia, X., Quan, J., Li, J., Li, X., Wu, Y., Chen, D., Wang, Z., and Liu, Y.: New positive feedback mechanism between boundary layer meteorology and secondary aerosol formation during severe haze events, Scientific Reports, 8, 1–8, https://doi.org/10.1038/s41598-018-24366-3, 2018b.

Luan, T., Guo, X., Guo, L., and Zhang, T.: Quantifying the relationship between PM2.5 concentration, visibility and planetary boundary layer height for long-lasting haze and fog-haze mixed events in Beijing, Atmospheric Chemistry and Physics, 18, 203–225, https://doi.org/10.5194/acp-18-203-2018, 2018.

Mazoyer, M., Lac, C., Thouron, O., Bergot, T., Masson, V., and Musson-Genon, L.: Large eddy simulation of radiation fog: impact of dynamics on the fog life cycle, Atmos. Chem. Phys., 17, 13 017–13 035, https://doi.org/10.5194/acp-17-13017-2017, 2017.

Mukherjee, S., Schalkwijk, J., and Jonker, H. J. J.: Predictability of dry convective boundary layers: an LES study, Journal of the Atmospheric Sciences, 73, 2715–2725, https://doi.org/10.1175/JAS-D-15-0206.1, 2016.

Ogura, Y. and Phillips, N. A.: Scale Analysis of Deep and Shallow Convection in the Atmosphere, https://doi.org/10.1175/1520-0469(1962)019<0173:saodas>2.0.co;2, 1962.

Oke, T.: The energetic basis of the urban heat island, Quarterly Journal of the Royal Meteorological Society, 108, 1–24, 1982.

Petäjä, T., Järvi, L., Kerminen, V.-M., Ding, A. J., Sun, J. N., Nie, W., Kujansuu, J., Virkkula, A., Yang, X., Fu, C. B., Zilitinkevich, S., and Kulmala, M.: Enhanced air pollution via aerosol-boundary layer feedback in China., Scientific reports, 6, 18 998, https://doi.org/10.1038/srep18998, 2016.

Pressel, K., Kaul, C., Schneider, T., Tan, Z., and Mishra, S.: Large eddy simulation in an anelastic framework with closed water and entropy balances, Journal of Advances in Modeling Earth Systems, 7, 1425–1456, https://doi.org/10.1002/2017MS001065, 2015.

Schwarz, N., Lautenbach, S., and Seppelt, R.: Exploring indicators for quantifying surface urban heat islands of European cities with MODIS land surface temperatures, Remote Sensing of Environment, 115, 3175–3186, https://doi.org/10.1016/j.rse.2011.07.003, 2011.

Shi, Z., Vu, T., Kotthaus, S., Harrison, R. M., Grimmond, S., Yue, S., Zhu, T., Lee, J., Han, Y., Demuzere, M., Dunmore, R. E., Ren, L., Liu, D., Wang, Y., Wild, O., Allan, J., Joe Acton, W., Barlow, J., Barratt, B., Beddows, D., Bloss, W. J., Calzolai, G., Carruthers, D., Carslaw, D. C., Chan, Q., Chatzidiakou, L., Chen, Y., Crilley, L., Coe, H., Dai, T., Doherty, R., Duan, F., Fu, P., Ge, B., Ge, M., Guan, D.,

Hamilton, J. F., He, K., Heal, M., Heard, D., Nicholas Hewitt, C., Hollaway, M., Hu, M., Ji, D., Jiang, X., Jones, R., Kalberer, M., Kelly, F. J., Kramer, L., Langford, B., Lin, C., Lewis, A. C., Li, J., Li, W., Liu, H., Liu, J., Loh, M., Lu, K., Lucarelli, F., Mann, G., McFiggans, G., Miller, M. R., Mills, G., Monk, P., Nemitz, E., O'Connor, F., Ouyang, B., Palmer, P. I., Percival, C., Popoola, O., Reeves, C., Rickard, A. R., Shao, L., Shi, G., Spracklen, D., Stevenson, D., Sun, Y., Sun, Z., Tao, S., Tong, S., Wang, Q., Wang, W., Wang, X., Wang, X., Wang, Z., Wei, L., Whalley, L., Wu, X., Wu, Z., Xie, P., Yang, F., Zhang, Q., Zhang, Y., Zhang, Y., and Zheng, M.: Introduction to the special issue "in-depth study of air pollution sources and processes within Beijing and its surrounding region (APHH-Beijing)", Atmospheric Chemistry and Physics, 19, 7519–7546, https://doi.org/10.5194/acp-19-7519-2019, 2019.

Stevens, B., Lenschow, D. H., Vali, G., Gerber, H., Bandy, A., Blomquist, B., Brenguier, J. L., Bretherton, C. S., Burnet, F., Campos, T., Chai, S., Faloona, I., Friesen, D., Haimov, S., Laursen, K., Lilly, D. K., Loehrer, S. M., Malinowski, S. P., Morley, B., Petters, M. D., Rogers, D. C., Russell, L., Savic-Jovcic, V., Snider, J. R., Straub, D., Szumowski, M. J., Takagi, H., Thornton, D. C., Tschudi, M., Twohy, C., Wetzel, M., and Van Zanten, M. C.: Dynamics and Chemistry of Marine Stratocumulus - DYCOMS-II, Bulletin of the American Meteorological Society, 84, 579–593, https://doi.org/10.1175/BAMS-84-5-579, 2003.

Stevens, B., Moeng, C.-H., Ackerman, A. S., Bretherton, C. S., Chlond, A., de Roode, S., Edwards, J., Golaz, J.-C., Jiang, H., Khairoutdinov, M., Kirkpatrick, M. P., Lewellen, D. C., Lock, A., Müller, F., Stevens, D. E., Whelan, E., and Zhu, P.: Evaluation of Large-Eddy Simulations via Observations of Nocturnal Marine Stratocumulus, Monthly Weather Review, 133, 1443–1462, https://doi.org/10.1175/MWR2930.1, 2005.

Stull, R.: Atmospheric Boundary Layer, in: Practical Meteorology: An Algebra-based Survey of Atmospheric Science, pp. 453–458, https://doi.org/10.1175/BAMS-89-4-453, 2015.

Su, T., Li, Z., Li, C., Li, J., Han, W., Shen, C., Tan, W., Wei, J., and Guo, J.: The significant impact of aerosol vertical structure on lower atmosphere stability and its critical role in aerosol8211;planetary boundary layer (PBL) interactions, Atmospheric Chemistry and Physics, 20, 3713–3724, https://doi.org/10.5194/acp-20-3713-2020, 2020.

Sullivan, P. P. and Patton, E. G.: The Effect of Mesh Resolution on Convective Boundary Layer Statistics and Structures Generated by Large-Eddy Simulation, Journal of the Atmospheric Sciences, 68, 2395–2415, https://doi.org/10.1175/JAS-D-10-05010.1, 2011.

Sun, Y., Wang, Z., Wild, O., Xu, W., Chen, C., Fu, P., Du, W., Zhou, L., Zhang, Q., Han, T., Wang, Q., Pan, X., Zheng, H., Li, J., Guo, X., Liu, J., and Worsnop, D. R.: "APEC Blue": Secondary Aerosol Reductions from Emission Controls in Beijing., Scientific reports, 6, 20 668, https://doi.org/10.1038/srep20668, http://www.nature.com/srep/2016/160218/srep20668/full/srep20668.html, 2016.

Takebayashi, H. and Moriyama, M.: Study on Surface Heat Budget of Various Pavements for Urban Heat Island Mitigation, Advances in Materials Science and Engineering, https://doi.org/10.1155/2012/523051, 2012.

Tong, S., Wong, N. H., Tan, C. L., Jusuf, S. K., Ignatius, M., and Tan, E.: Impact of urban morphology on microclimate and thermal comfort in northern China, Solar Energy, 155, 212–223, https://doi.org/10.1016/j.solener.2017.06.027, 2017.

Tonttila, J., Maalick, Z., Raatikainen, T., Kokkola, H., Kühn, T., and Romakkaniemi, S.: UCLALES-SALSA v1.0: a large-eddy model with interactive sectional microphysics for aerosols, clouds and drizzle, Geoscientific Model Development, 10, 169–188, https://doi.org/10.5194/gmd-10-169-2017, 2017.

Wang, L., Liu, J., Gao, Z., Li, Y., Huang, M., Fan, S., Zhang, X., Yang, Y., Miao, S., Zou, H., Sun, Y., Chen, Y., and Yang, T.: Vertical observations of the atmospheric boundary layer structure over Beijing urban area during air pollution episodes, Atmospheric Chemistry and Physics, 19, 6949–6967, https://doi.org/10.5194/acp-19-6949-2019, 2019.

Wang, Y., Cheng, K., Wu, W., Tian, H., Yi, P., Zhi, G., Fan, J., and Liu, S.: Atmospheric emissions of typical toxic heavy metals from open burning of municipal solid waste in China, Atmospheric Environment, 152, 6–15, https://doi.org/10.1016/j.atmosenv.2016.12.017, http://linkinghub.elsevier.com/retrieve/pii/S1352231016309761, 2017.

Wang, Z., Huang, X., and Ding, A.: Dome effect of black carbon and its key influencing factors: A one-dimensional modelling study, Atmospheric Chemistry and Physics, 18, 2821–2834, https://doi.org/10.5194/acp-18-2821-2018, 2018.

Wu, J., Bei, N., Hu, B., Liu, S., Zhou, M., Wang, Q., Li, X., Liu, L., Feng, T., Liu, Z., Wang, Y., Cao, J., Tie, X., Wang, J., Molina, L. T., Li, G., Chemistry, A., Physics, A., Engineering, B., City, I., and Jolla, L.: Aerosol-radiation feedback deteriorates the wintertime haze in North China Plain, Atmospheric Chemistry and Physics Discussions, pp. 1–50, 2019.

Xiang, Y., Zhang, T., Liu, J., Lv, L., Dong, Y., and Chen, Z.: Atmosphere boundary layer height and its effect on air pollutants in Beijing during winter heavy pollution, Atmospheric Research, 215, 305–316, https://doi.org/10.1016/j.atmosres.2018.09.014, https://doi.org/10.1016/j.atmosres.2018.09.014, 2019.

Xie, M., Liao, J., Wang, T., Zhu, K., Zhuang, B., Han, Y., Li, M., and Li, S.: Modeling of the anthropogenic heat flux and its effect on regional meteorology and air quality over the Yangtze River Delta region, China, Atmospheric Chemistry and Physics, 16, 6071–6089, https://doi.org/10.5194/acp-16-6071-2016, 2016.

Yang, L., Qian, F., Song, D. X., and Zheng, K. J.: Research on Urban Heat-Island Effect, Procedia Engineering, 169, 11–18, https://doi.org/10.1016/j.proeng.2016.10.002, 2016.

Zhang, X. Y., Wang, J. Z., Wang, Y. Q., Liu, H. L., Sun, J. Y., and Zhang, Y. M.: Changes in chemical components of aerosol particles in different haze regions in China from 2006 to 2013 and contribution of meteorological factors, Atmospheric Chemistry and Physics, 15, 12 935–12 952, https://doi.org/10.5194/acp-15-12935-2015, 2015.

Zhang, Z., Zhang, X., Zhang, Y., Wang, Y., Zhou, H., Shen, X., Che, H., Sun, J., and Zhang, L.: Characteristics of chemical composition and role of meteorological factors during heavy aerosol pollution episodes in northern Beijing area in autumn and winter of 2015, Tellus B: Chemical and Physical Meteorology, 69, 1347 484, https://doi.org/10.1080/16000889.2017.1347484, 2017.

Zhong, J., Zhang, X., Wang, Y., Liu, C., and Dong, Y.: Heavy aerosol pollution episodes in winter Beijing enhanced by radiative cooling effects of aerosols, Atmospheric Research, 209, 59–64, https://doi.org/10.1016/j.atmosres.2018.03.011, https://doi.org/10.1016/j.atmosres.2018.03.011, 2018a.

Zhong, J., Zhang, X., Wang, Y., Liu, C., and Dong, Y.: Heavy aerosol pollution episodes in winter Beijing enhanced by radiative cooling effects of aerosols, Atmospheric Research, 209, 59–64, https://doi.org/10.1016/j.atmosres.2018.03.011, 2018b.

Zhong, J., Zhang, X., and Wang, Y.: Relatively weak meteorological feedback effect on PM 2.5 mass change in Winter 2017/18 in the Beijing area: Observational evidence and machine-learning estimations, Science of the Total Environment, 664, 140–147, https://doi.org/10.1016/j.scitotenv.2019.01.420, 2019a.

Zhong, J., Zhang, X., Wang, Y., Wang, J., Shen, X., Zhang, H., Wang, T., Xie, Z., Liu, C., Zhang, H., Zhao, T., Sun, J., Fan, S., Gao, Z., Li, Y., and Wang, L.: The two-way feedback mechanism between unfavorable meteorological conditions and cumulative aerosol pollution in various haze regions of China, Atmospheric Chemistry and Physics, 19, 3287–3306, https://doi.org/10.5194/acp-19-3287-2019, 2019b.

Zou, J., Sun, J., Ding, A., Wang, M., Guo, W., and Fu, C.: Observation-based estimation of aerosol-induced reduction of planetary boundary layer height, Advances in Atmospheric Sciences, 34, 1057–1068, https://doi.org/10.1007/s00376-016-6259-8, 2017.

4.2 Paper 2: Using a coupled LES aerosol-radiation model to investigate the importance of aerosol-boundary layer feedback on a Beijing haze episode

Authors: Jessica Slater, Hugh Coe, Gordon McFiggans, Juha Tonttila, Sami Romakkaniemi, Yele Sun, Pingqing Fu and Zifa Wang **Journal:** Faraday Discussions (currently with co-authors)

Paper Overview

This paper examines a specific haze episode, which occurred in Beijing from 01-04 Dec 2016, the evolution of which is well characterised by Wang et. al (2019). In their work, they show that changing synoptic conditions were the main cause of a reduction in PBL height of 44 % between 01 Dec and 02 Dec 2016, while the aerosol-PBL feedback was important in the reduction of PBL height by 20 % between 02 Dec and 03 Dec. Our work builds on this, to show directly that the difference in simulated PBL height is largely due to the difference in initial meteorological conditions rather than aerosol-PBL feedback. Directly, this paper identifies meteorological conditions as being responsible for a difference in maximum PBL height of 71.4 %, while aerosol inclusion on 03 Dec causes a decrease in PBL height of 17.4 %.

The observational study by Wang et. al (2019) clearly highlights the main stages of this haze episode and suggests the key mechanisms at force during each stage. The work presented here supports the hypothesis in that study that the impact of synoptic meteorological changes has a larger impact than the aerosol-PBL feedback on suppressing turbulence and PBL growth. Due to the isolation of specific factors allowed for in the high resolution modelling study presented here, in contrast to the work by Wang et. al (2019), we can explicitly show the impact of aerosol-radiation interactions and changes in initial conditions on the PBL height difference between two stages of this pollution episode. Further, this work examines the hypothesis presented in other studies that the aerosol-PBL feedback is stronger under higher aerosol loadings. Finally, this work also identifies that under some meteorological conditions, the aerosol-PBL feedback effect is stronger.

Through a more thorough understanding of the large scale conditions effecting the period, this work identifies the ability of UCLALES-SALSA to well characterise periods of the pollution episode which are not impacted by large scale atmospheric changes (03 Dec 2016). This paper presents the impact of increasing aerosol loading on the change in PBL height, to examine the idea of a threshold value above which the process increases in importance. The results presented here show that for the aerosol compositions examined here, the decrease in PBL height to due to increased aerosol loading is linear and so a threshold PM value for the aerosol-PBL feedback does not exist. However, through performing model simulations on the end of the haze episode, the paper presents the idea that the aerosol-PBL feedback effect on PBL height

has more impact under conditions which favour a shallow initial PBL height. For example, there is a 13.6 % decrease in PBL height for the shallow PBL conditions compared to a 9.7 % decrease in PBL height for the 'normal' PBL conditions due to including surface aerosol concentrations of 107 μg/m^3. Therefore, the paper concludes that as the haze episode evolved and aerosol concentrations increase, the PBL becomes shallower due to aerosol-PBL feedback and under these conditions the aerosol-PBL feedback increases in importance.

In between submission and examination of this thesis, this paper was published. After the viva and subsequent discussion with the examiners some improvements to the paper were made for the revised thesis. Therefore, the paper presented here is different to the published paper, for which the reference is: Faraday Discuss., 2021, Advance Article (https://doi.org/10.1039/D0FD00085J)

Compared to paper 1, only small adaptations were made to this paper, including replotting of some figures and clarifying key points in the results and discussion sections.

Author Contributions

The idea for this study was conceived by Jessica Slater, with the assistance of Hugh Coe and Gordon McFiggans. Model simulations were performed by Jessica Slater with assistance in the setup from Juha Tonttila. Model analysis was performed by Jessica Slater. The manuscript was written by Jessica Slater with contribution from Hugh Coe and Gordon McFiggans. Data used for model initialisation of this case study was provided by Yele Sun, Pingqing Fu and Zifa Wang's group. This manuscript is currently with co-authors and has been accepted for presentation at the Faraday Discussions-Air Quality in Megacities, which will take place in November 2020.

Journal Name

ARTICLE TYPE

Cite this: DOI: 00.0000/xxxxxxxxxx

'Using a coupled LES aerosol-radiation model to investigate the importance of aerosol-boundary layer feedback on a Beijing haze episode†

Jessica Slater,*[a] Juha Tonttila[b], Gordon McFiggans[a], Hugh Coe[a], Sami Romakkaniemi [b], Yele Sun [c], Weiqi Xu [c], Pingqing Fu [d] and Zifa Wang,[e]

Received Date
Accepted Date

DOI: 00.0000/xxxxxxxxxx

Haze episodes, characterised by extremely high aerosol concentrations and a reduction in visibility to less than 10 km are a frequent occurrence in wintertime Beijing, despite policy interventions leading to an overall improvement in average annual air quality. The main drivers in the onset of haze episodes in wintertime Beijing are changing synoptic conditions however, aerosol radiation interactions and their feedback on boundary layer meteorology are thought to play an essential role in the intensity and longevity of haze episodes. In this study we use a coupled LES-aerosol radiation model (UCLALES-SALSA), which we have recently configured for the urban environment of Beijing. The model's high resolution and control over meteorological and aerosol conditions as well as atmospheric processes means we can directly elucidate and quantify the importance of specific aspects of the aerosol-radiation-meteorological feedback on the cumulative stage of Beijing haze. The main results presented here show a) synoptic scale meteorology has a larger impact on boundary layer suppression than high aerosol concentrations and b) unlike previous results using regional models or observationally driven analyses, there is no threshold value at which the aerosol-radiation-meteorology feedback has a significant effect on PBL height. Rather our work shows that for the aerosol composition in this case study, the role of the feedback effect in reducing PBL height increases under shallow boundary layer conditions and with increasing pollution loading in an almost linear fashion. This lack of a threshold found for our case study, has important policy implications since interventions based on such a value will not result in large reductions associated with turning off the feedback process. Furthermore, this work directly shows that although the right synoptic changes are a prerequisite for pollution episodes in Beijing, local and regional emissions drive increases in aerosol load that are sufficient to initiate the aerosol feedback loop. This further drives suppression of the boundary layer top and promotes stagnation of air and increased stability, which can be self-sustaining. This results in higher surface aerosol concentrations for extended periods of time, with severe consequences for human health.

Introduction

Beijing, a megacity in the North China Plain, is well known for its poor air quality which has severe consequences for human health. In Beijing, concentrations of $PM_{2.5}$ (particulate matter with a diameter $< 2.5\mu$m) frequently exceed the World Health Organization's guidelines of a 24 hour average of 25 $\mu g/m^3$, particularly during heavy pollution episodes known as haze[1,2]. Despite policy interventions leading to an average annual decrease in pollutant concentrations in Beijing, these haze episodes are still a frequent occurrence and major concern[3]. Beijing haze episodes, which most commonly occur in autumn and winter can be defined by a decrease in visibility < 10 km with relative humidity < 90 %. The decrease in visibility is primarily caused by the accumulation of $PM_{2.5}$, with concentrations commonly reaching > 75 $\mu g/m^3$ [4–7]. Due to their frequency and severe impact on both human health and the Chinese economy, Beijing haze episodes have been subject to extended research and characterisation[4,8–11]. Most research agrees that the onset of haze episodes in Beijing is preempted by changing synoptic conditions, which bring about atmospheric stagnation[12–14]. These conditions, which typically occur every 4-7 days in wintertime Beijing, are synonymous with peaks

[a] *Centre for Atmospheric Science, University of Manchester, Manchester, United Kingdom*
[b] *Finnish Meteorological Institute, Kuopio, Finland*
[c] *Institute of Atmospheric Physics, Chinese Academy of Sciences, Beijing, China*
[d] *Institute of Surface-Earth System Science, Tianjin University, Tianjin, China*
[d] *College of Environmental Science and Engineering, Peking University, Beijing, China*

in $PM_{2.5}$ concentrations. Studies characterising the episodes classify them into 3 stages each with distinct meteorology. The clean stage occurs prior to the onset of pollution and is identified by strong northerly winds, low humidity and high surface pressure. A change in wind direction to south-westerly and a decrease in surface pressure due to changing synoptic conditions usually marks the beginning of the transport stage (TS) which causes pollutants to be transported from surrounding provinces into the city. During the cumulative stage (CS), pollutant concentrations increase rapidly (often doubling within several hours), humidity increases, and a strong temperature inversion exists. Following this, a change in synoptic conditions, normally clean air from the North, results in dissipation of pollution, with concentrations of PM decreasing rapidly with increasing wind speed [10,14,15].

Although synoptic conditions are a major cause of the onset of haze episodes, several factors are thought to influence the pollution episodes intensity and longevity. One such process, which may enhance air pollution in Beijing is the aerosol-PBL feedback. This occurs when aerosols interact with radiation and impact the thermal structure of the atmosphere, which can feed back on turbulent buoyancy and cause suppression of the planetary boundary layer (PBL). This effect is believed to strongly influence the cumulative stage of the haze episode, prevent vertical mixing of aerosols and delay dissipation of pollutants [11,14,16]. Investigations of the aerosol-PBL feedback on Beijing haze episodes have thus far focused on observational analyses and regional modelling studies [11,16–18]. Observational analyses, specifically those which have been performed over multi-year periods provide large amounts of evidence for the importance of the aerosol-PBL feedback on Beijing haze episodes. Here, strong anti-correlations between PM concentrations, PBL height, sensible heat flux (SHF) and surface shortwave radiation (SWR) were found. [19–21]. However, these studies are limited as they cannot isolate or quantify the specific factors which influence the feedback effect.

Modelling studies can provide more information on the aerosol-PBL feedback through switching off certain atmospheric processes or changing and controlling certain variables in order to quantify specific contributions to the feedback effect. WRF-CHEM (Weather Research and Forecasting model with Chemistry) is a regional model which is frequently used to investigate the pollution episodes in Beijing and the North China Plain. Several studies have used WRF-CHEM to attempt to elucidate the aerosol-PBL feedback and the impact on urban haze [18,22–24]. However, temperature, moisture and wind as well as turbulent and momentum fluxes in WRF-CHEM are strongly dependent on the chosen PBL parameterisation scheme. Particularly, the ability to correctly simulate turbulent diffusion, which is essential in both characterising the PBL as well as the distribution and interaction of pollutants, varies significantly depending on the chosen scheme [25–27]. In a comprehensive review on the effect of PBL parameterisation schemes on aerosol pollution simulations, Zhang et. al (2020) [26] found that most PBL schemes used in WRF overestimate surface wind speeds and have difficulty correctly simulating turbulent structures in the lower PBL, particularly during stable conditions. Therefore, higher resolution models which can directly calculate turbulent motions can be extremely useful, particularly when looking at the feedback of aerosol-radiation interactions on boundary layer meteorology. This work utilises a high resolution large eddy simulation (LES) model to characterise and further understanding of a specific haze episode which occurred in Beijing from 01 to 04 December (01/12-04/12) 2016.

The pollution episode which occurred between 01/12-04/12 2016, has been well characterised by Wang et. al (2019) [14]. The analysis provided here utilises this work and presents observations taken at the Institute of Atmospheric Physics as part of the Air Pollution and Human Health (APHH) Beijing field campaign, which are subsequently used in the case study presented. During the period PM_1 concentrations increased steadily, with a rapid increase from around 100 $\mu g/m^3$ at 12:00 LST on 03/12 to > 300 $\mu g/m^3$ by 19:00 LST (Figure 1), with a peak > 450 $\mu g/m^3$ in the late evening of 03/12. Concentrations remain high until early morning on 04/12, when a sudden drop in surface aerosol concentrations occurs at 12:00 LST on 04/12 which coincides with an increase in wind speed, reduction in humidity and the formation of a turbulent boundary layer. Over the haze period, from 01/12-03/12/2016, midday (12:00-14:00 LST) measured maximum surface SW radiation reduces by 25 % and sensible heat flux reduces by 44 %. Surface layer relative humidity increases to become supersaturated on the evening of 03/12, which coincides with the rapid increases in PM_1 (Figure 1). Increased water vapour concentrations favour secondary aerosol formation, due to hygroscopic aerosols taking on water to increasing particle surface size, which enhances surface reactions. Furthermore, uptake of water vapour by hygroscopic aerosols increases their particle diameter and enhances the aerosol radiation interactions which can reduce the amount of solar radiation reaching the surface. This alters the thermal profile of the atmosphere, resulting in reduced buoyant turbulence. This allows for the accumulation of pollutants in a shallow daytime boundary layer [14,28].

Temperature inversions form overnight throughout the haze episode. This is due to reduced surface warming caused by the aerosol layer throughout the daytime which leads to enhanced nocturnal inversions. These inversions decrease nocturnal mixing and lead to extremely stagnant air, delaying boundary layer development on the following day. This further worsens and sustains air pollution episodes. In contrast to the mornings of 02/12 and 03/12, where the temperature inversion is broken by solar heating, a temperature inversion exists on 04/12 until 12:00 LST, this suggests an extremely strong inversion formed overnight, causing strong stability which could not be broken by solar heating and no clean air was being entrained from the free troposphere [29]. For a comprehensive detailing of the meteorological conditions of this haze episode, including large scale synoptic conditions, the reader is directed to the paper by Wang et. al (2019) [14].

Aerosol composition, size and concentration all change throughout the haze episode. There is an increase in the relative contribution of secondary aerosols (ammonium nitrate and sulphate) to PM as the pollution episode evolves (Figure 1). This suggests the importance of gas-particle partitioning and secondary aerosol formation in the intensity and sustenance of the

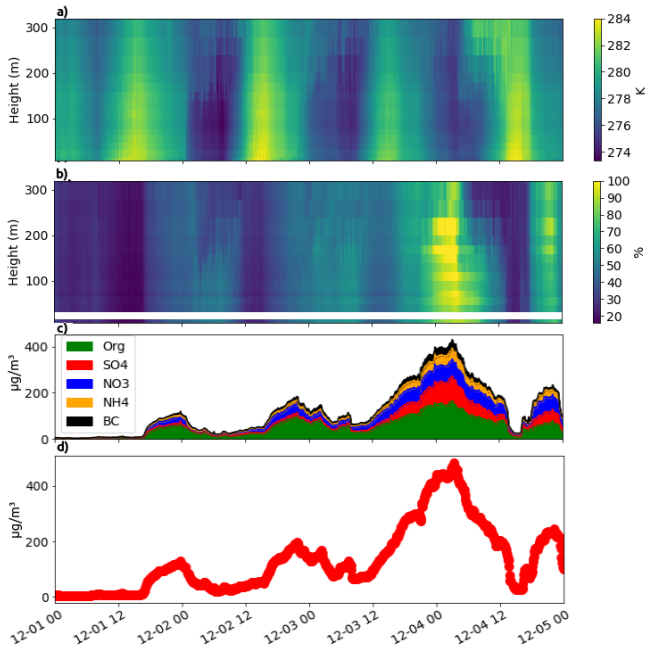

Fig. 1 (a)Temperature, (b) Relative Humidity, (c) NR-PM_1 concentration by composition and (d) Total PM_1 concentration for a haze episode occurring on 01/12-04/12/2016

haze period. The average size of the aerosols also increases throughout the period due to semi-volatile partitioning, hygroscopic growth and aerosol coagulation. Furthermore, the relative contribution of black carbon, a primary aerosol, reduces over the period (due to such large increases in other secondary components). This indicates the potential importance of secondary aerosols over primary emissions during this period [30,31].

Observational analysis of the pollution episode has identified the aerosol-PBL feedback as being important during the cumulative stage of the episode. In this stage, the aerosol-PBL feedback is thought to contribute to enhanced atmospheric stability allowing for the rapid accumulation of pollutants in a shallow PBL [14]. Overall, several factors are believed to contribute to the aerosol-PBL feedback and the impact it will exert on pollution episodes [16]. Identification and quantification of such factors allow for a better understanding of the processes impacting pollution episode, with direct benefit for both policy and regional model parameterisations. High resolution modelling studies such as large eddy simulation (LES) models can directly quantify aerosol perturbations on PBL dynamics, without the need for parameterisation. A coupled dynamical large eddy scale model (UCLALES-SALSA) has previously been set up and tested for the urban environment of Beijing to examine sensitivity of aerosol-radiation interactions and the feedback on boundary layer meteorology [32]. This study builds on the previous work and uses measurements taken during the APHH Beijing winter field campaign to quantify the importance of aerosol and meteorological conditions on the cumulative stage of a specific haze episode which occurred in Beijing on 01/12-04/12/2016. The paper is set out as follows: Section 2 describes experimental set up, section 3 details the results of a) Synoptic conditions vs aerosol-radiation interactions b) Aerosol loading and c) Shallow boundary layer conditions and section 4 briefly discusses the implications and limitations of the results.

Methodology

Model Description

The model used in this study is UCLALES-SALSA [33], which has previously been used to examine aerosol effects on marine stratocumulus clouds, radiation fog and cloud seeding [33,34]. In a recent study, UCLALES-SALSA was set up for the urban environment of Beijing and sensitivities to the aerosol-PBL feedback examined [32]. The model comprises of the LES model, UCLALES fully coupled to the sectional aerosol module, SALSA, this allows for direct calculation of aerosol-radiation interactions and their perturbation on boundary layer meteorology. UCLALES is a large eddy simulation model which is based on the Smagorinsky–Lilly subgrid model. Advection of momentum variables uses time stepping based on the leapfrog method, while scalar variables are advected based on fourth-order differential equations and follow a simple forward time stepping method. Boundary conditions are doubly periodic in the horizontal and fixed in the vertical. The surface scheme explicitly calculates surface temperature, sensible (SHF) and latent (LHF) heat fluxes at each time step and is based on a coupled soil moisture and surface temperature scheme by Ács et al. (1991) [35].

SALSA is a sectional aerosol model which bins aerosol particles according to size and calculates the appropriate atmospheric processes. Particle composition includes sulphate, nitrate, ammonium, organic carbon and black carbon. It is possible for the particles to be externally mixed through initialising with two parallel sets of size bins, but in this work all aerosols are considered to be internally mixed and so the size distribution for each component is the same. The model has the ability to simulate a variety of atmospheric processes, however, for simplicity, the main processes considered here are aerosol coagulation and water condensation on particles, while semi-volatile condensation and aerosol dry deposition are switched off. Further details of the model can be found in Tonttila et. al (2017) [33] and the model code is available at www.github.com/UCLALES-SALSA. Alterations to the model for the set up of the Beijing urban environment, including the coupling of aerosol-radiation interactions can be found in Slater et. al (2020) [32].

Experimental Setup

The work presented here is in three parts, with simulations performed for all 4 days (01/12-04/12) of the haze episode initially, to examine the models representation. Initial meteorological vertical profiles for all days are from radiosonde meausrements. Aerosol concentrations and size parameters were taken from ground based measurements taken during the APHH winter field campaign (Shi et. al 2019). Aerosol vertical profiles were estimated based on the gradient of boundary layer profiles. The model was set up at 08:00 LST and run for 12 hours including 1 hour spin up time. The horizontal domain size was 5.4 x 5.4 km with a resolution of 30 m and the model top was 1800 m

with a vertical resolution of 10 m. For the low PBL simulations in part c) of the results, meteorological conditions used were from radiosonde data on the morning of 04/12.

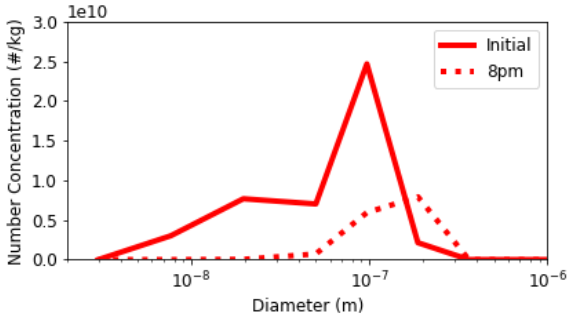

Fig. 2 : Aerosol size distribution for the simulations with aerosols on 03/12 at the initial timestep (solid) and after 12 hours of simulation (dashed)

For simulations examining aerosol loading, aerosol composition and size distribution were kept constant and concentrations were increased gradually. Table 1 shows the aerosol size parameters and table 2 aerosol composition fraction by volume for all simulations. Aerosol size parameters, including geometric mean diameter (D_g) for each mode and geometric standard deviation (σ_g) were calculated from measurements taken at 8 am on 03/12 during the APHH Beijing winter field campaign and used as inputs into the model as detailed in table 1, to represent the aerosol size distribution as shown in figure 2. Figure 2 shows how the aerosol size distribution varies over time, as aerosols coagulate and take up water they grow and increase in size, while relative aerosol composition will stay constant over time.

Parameter	Mode 1	Mode 2
D_g (nm)	22	121
σ_g	1.28	1.32

Table 1 Size distribution input data - geometric mean diameter (D_g) and geometric standard deviation (σ_g)

Component	Volumetric Fraction
SO_4	0.1
OC	0.45
NO_3	0.25
NH_4	0.1
BC	0.1

Table 2 Volumetric aerosol fractional composition for all simulations including aerosols

Model Validation

The haze period of 01/12-04/12/2016 is characterised by different meteorological and aerosol conditions. To assess the ability of the model to capture the diurnal profiles of each stage of the episode, we ran simulations from 8am until 8pm on all days of the episode (01/12-04/12/2016). Potential temperature profiles for each day at 8pm are compared to radiosonde and tower measurements in figure 3. The model represents the conditions of 02/12 and 03/12 better than those on 01/12 and 04/12. As the beginning and end of the haze episode (01/12 and 04/12) are known to be driven by changes in synoptic conditions, particularly pressure and wind changes, the model's ability to capture the processes impacting the diurnal variation on these days is limited, due to the unsuitability of using LES models to examine large scale weather conditions. For example, during the daytime of 04/12 the conditions change, and a strong low level jet helps to dissipate the pollution. However, due to the strong inversion and stagnation of air at the surface, the clean air aloft takes a long time to become entrained into the shallow PBL. Meaning the period of clean up takes longer and pollution persists into the afternoon. LES models are not capable of simulating the changes in large scale conditions, and the model doesn't represent these periods as well as at representing the stagnant conditions of 02/12 and 03/12 (Figure 3).

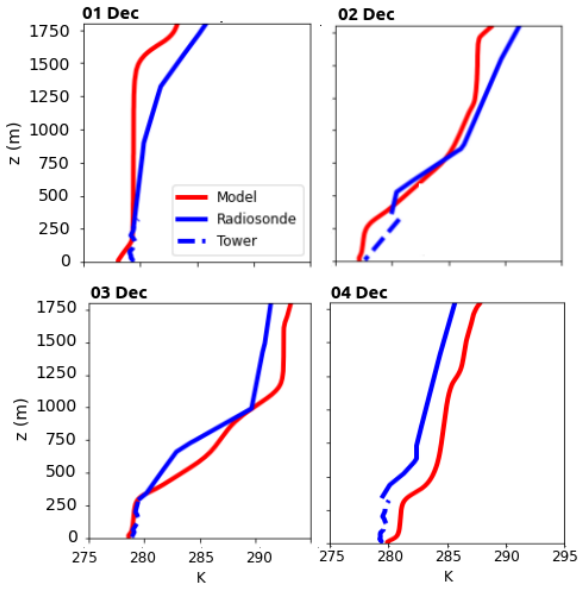

Fig. 3 : Vertical profiles of potential temperature (θ) for simulations of each day without aerosols(red) compared to observational potential temperature profiles taken from radiosonde data (solid blue) and tower data (dashed blue) at 8pm

The aerosol-PBL feedback is thought to be most important during the cumulative stage of the haze episode, which is characterised by stable atmospheric conditions. We therefore assess the model's ability to simulate observed meteorological conditions on 03/12, using measured aerosols from the morning, to simulate the aerosol-PBL feedback. The idealised model simulations of 03/12 which include measured aerosols generally characterise the observed meteorological conditions well, slightly underestimating both surface wind speed and specific humidity, while overestimating potential temperature compared to radiosonde observations at 8pm (Figure 4). Particularly, we can see that the model

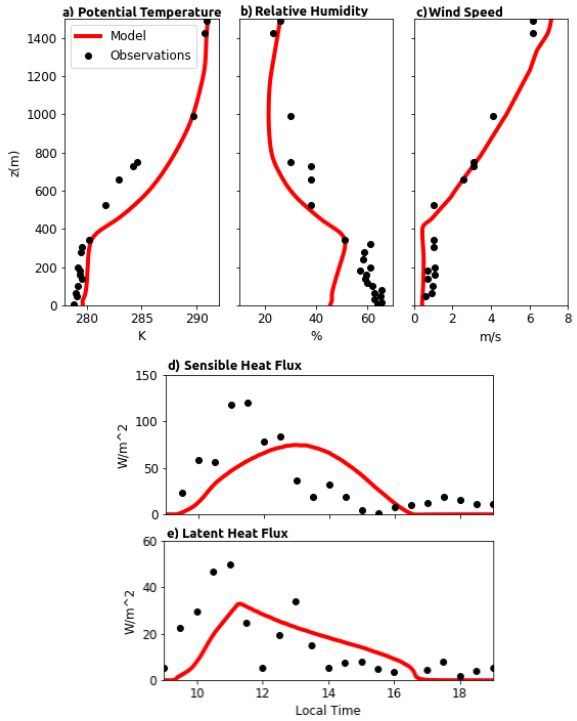

Fig. 4 : a) Potential temperature b) Relative Humidity c) Wind Speed profiles at 8pm on 03/12 for simulations with measured aerosols (red), compared with radiosonde and tower data (black dots). Diurnal profiles of d) Sensible heat flux (SHF) and e) latent heat flux (LHF) for simulations with measured aerosols (red) compared with observations on 03/12 (black dots)

well simulates the diurnal variation in both sensible and latent heat flux, however the maximum values in the simulations are lower than the maximum observed values. This variation could be due to several factors including the simple homogeneous surface scheme used in the model, or the use of radiosonde data for vertical profiles of meteorological variables (above 300 m). The homogeneous surface scheme does not account for variability in surface roughness due to urban layout, nor does it represent phenomena such as urban canopy layers, both of which may impact the heat flux measurements, while location of the radiosonde measurements was Beijing airport which is almost 10 km away from the tower and consequently outside of the model domain, this might lead to discrepancies in the model outputs[32]. Sensitivities of the simulated meteorological variables to aerosol loading is examined in the next section.

Results

Aerosols vs Meteorology

In these simulations we compare the impact of aerosol-radiation interactions and initial meteorological conditions on maximum PBL height and SHF. Observations show that over the haze episode, maximum PBL height and SHF decreased, while there were distinct changes in vertical profiles of potential temperautre, wind speed and humidity. To separate the influence of cited changes in synoptic scale meteorology over the period and the influence of aerosol-PBL feedback, we performed simulations to identify the influence of initial meteorological conditions and aerosol-PBL feedback separately. These simulations aimed to identify which effect contributed the most to the observed decrease in maximum PBL height (between 12-16 LST) from (1136 m to 519 m). To identify the comparable influence of initial meteorological conditions (and changing synoptic conditions) compared to the influence of aerosol-radiation interactions. We firstly performed simulations on 01/12 and 03/12 without aerosols. The differences in the output dynamics were identified as being due to the initial meteorological conditions used in the model setup which is a proxy for the change in large scale meteorology over this period. The difference in these simulations of modelled maximum PBL height (taken as the height where there is the largest gradient in theta), was large. Maximum simulated PBL height on 01 Dec was 1779 m and on 03 Dec it was 510 m, without the influence of aerosol-radiation interactions, which is a decrease of 71 % (Table 3).

To examine the influence of aerosols on the 03 Dec case study, we performed simulations with measured aerosols and compared to the simulation without aerosols, this was in order to understand the influence of aerosols on the cumulative stage, which is believed to occur between 12:00 and 19:00 LST on 03/12. As the period is pretty stagnant and is not thought to be influenced heavily by synoptic changes, it is the ideal period for examining the influence of these interactions (Figure 4). We then compared the results with a simulation of 01/12, where the initial conditions were characteristic of the clean stage of the pollution episode. This section of the work aims to quantify the reduction in turbulent motion due to aerosol-radiation interactions and compare with the reduction caused by synoptic changes.

To quantify the magnitude of the aerosol-radiation effect compared to changing synoptic meteorology, we analysed key parameters from simulations of the clean stage (01/12) without aerosols and the cumulative stage (03/12) with and without aerosols. Here, we state that the effect due to synoptic meteorology is the difference between 01/12 and 03/12 without aerosol inclusion. While the effect due to aerosols is the difference in 03/12 simulations with and without aerosol. The combined effect of aerosols and synoptic meteorology is the difference between the simulated clean stage (01/12) without aerosols and cumulative stage (03/12) with aerosols. These results can then be compared to observations on 01/12 and 03/12 taken during the APHH Beijing winter field campaign (Table 3).

Without inclusion of aerosols, simulations of 03/12 and 01/12 show a maximum PBL height of 535 m and 1779 m and a maximum sensible heat flux of 112.3 W/m2 and 180.6 W/m2 respectively. Including an aerosol profile in the 03/12 simulations decreased the SHF and PBL height, decreasing TKE, surface wind speeds and causing cooling in the lower boundary layer and warming above it, enhancing the temperature inversion and stagnation. This shows the effect that aerosol-radiation interactions can have on boundary layer meteorology. However, table 3 shows that the relative impact of the initial conditions, caused by synoptic changes, has much larger an effect. The large decrease in

measured PBL height between 01/12 and 03/12 can therefore be attributed primarily to the difference in conditions, rather than the aerosol-PBL feedback. These conditions lead to a shallow PBL and a temperature inversion overnight on 02/12 and a highly stable temperature profile in the morning of 03/12, which prevents the growth of a turbulent boundary layer in the simulations even without aerosols [14].

Values	PBL height (m)	SHF (W/m^2)
01/12 (Simulation)	1779	180.6
01/12 (Observation)	1136	167.8
03/12 (Simulation)	510	112.2
03/12 (Simulation with aerosols)	421	71.7
03/12 (Observation)	519	83.5
% decrease		
Meteorology	71.4 %	37.8 %
Aerosols	17.4 %	36.1 %
Aerosols + Meteorology	76.3 %	58.6 %
Observed	54.3 %	50.2 %

Table 3 Maximum values (between 12:00 and 16:00 LST) of PBL height (m) and SHF (W/m^2) for observations and simulations performed on 01/12 and 03/12. % decrease due to aerosols (03/12 with aerosols - 03/12 without aerosols) and synoptic scale meteorology (01/12 - 03/12) in maximum PBL height and maximum SHF between 12:00-16:00 LST

Table 3 shows the measured % decrease in PBL height and SHF observed between 01/12 and 03/12 is much larger than accounted for by the modelled decrease by aerosol particles alone, but also in the case of sensible heat flux, too small to be accounted for solely by changing initial conditions (Table 3). Indicating that the aerosol-radiation interactions also play a role in the atmospheric stagnation. Several studies have outlined changing synoptic conditions as the driver behind haze episodes. Results presented in this work agree with this showing that aerosols contribute a 17 % decrease in PBL height, whereas the synoptic scale changes contribute 70 % of PBL suppression. Wang et. al (2019) observed a decrease in PBL height from 900 to 500 m between 01/12 and 02/12 due to synoptic scale changes, compared to a decrease from 500 to 400 m between 02/12 and 03/12 thought to be due to the aerosol-PBL feedback [14].

Threshold PM Values

Although synoptic conditions prime the period for a pollution episode to occur, the modelled effect of aerosol-radiation interactions still causes a reduction of around 100 m on PBL height (Table 3). Several studies have noted the importance of the aerosol-radiation feedback on surface temperature, RH, wind speeds and PBL height during haze days in Beijing, but few directly quantify or elucidate the impact of specific aerosol or meteorological conditions on this feedback effect [16,36,37]. Of particular interest is quantifying the relationship between PM concentrations and PBL height. A study by Wu et al. (2019) [24], shows little observed change in PBL height when PM > 200 $\mu g/m^3$ suggesting that there appears to be a limit above which the feedback effect becomes less important. Their work also shows that below 250 $\mu g/m^3$, PBL height decreases quite linearly with increasing PM concentrations, particularly between (75-250 $\mu g/m^3$) when PBL height decreases by 20% [24].

To identify whether a threshold value exists and the potential value of such a decrease, simulations of 03/12 with varied surface aerosol concentrations were performed. The effect on the PBL, SHF and surface downwelling SWR is outlined below. Here, we've taken a range of values from low to very high loading to represent different stages of the pollution episode as concentrations build up in the cumulative stage. We then compared against simulations with 'no' aerosol loading or the clean stage. Figure 5 shows low, medium and high aerosol simulations and the relevant maximum PBL height associated with these changes.

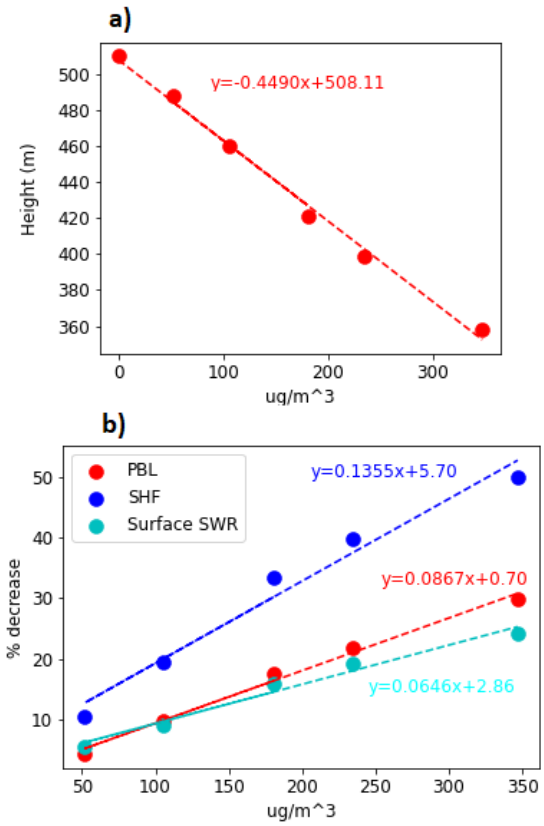

Fig. 5 a) PM concentrations vs PBL height for simulations of 03/12 on different aerosol loading b) % decrease in PBL height (red), Sensible Heat Flux (blue) and surface shortwave radiation (cyan) due to increasing PM concentrations on simulations of 03/12

In these simulations, the decrease due to changing aerosol loading in this case study is approximately linear. This suggests that the idea of a threshold value may not be correct, but that when the conditions allow it, combined with high emissions and secondary aerosol formation at higher concentrations of aerosols the aerosol-radiation interactions continues to cause suppression on PBL height. These types of concentration are typical for the beginning of cumulative stage periods and are synonymous with stagnant conditions as described in the previous section. Aerosol-

radiation interactions during the cumulative stage of the haze episode can therefore be considered to be a prominent cause of stagnant air flow and decreasing turbulence.

Figure 5 shows the impact of aerosol concentration on sensible heat flux, surface SWR and PBL height. It shows that the % decrease in maximum daytime SHF due to increased aerosol loading is much greater than the % decrease in maximum surface SWR and PBL height. This could potentially be due to the impact of black carbon, which reduces SWR reaching the surface and thus minimises surface fluxes, but provides heating within the aerosol layer to slightly increase PBL development and turbulence. This work shows the impact of aerosol loading on the feedback effect for specific conditions. To examine the effect of different conditions, specifically the later stages of the haze episode where the PBL is very shallow, we simulated the impact of low, medium and high aerosol loading for a low PBL condition.

Effect of PBL height

To assess the impact of initial meteorological conditions on the predisposition for the aerosol-radiation feedback, we performed further analysis of the aerosol loading effect on meteorological conditions which had a lower 'initial' PBL height. From this, we found that a lower initial PBL height (z0) had a larger impact on the aerosol-radiation meteorological feedback, compared to a higher initial PBL height. Results show a 17 % decrease in PBL height due to 182 $\mu g/m^3$ of aerosols for higher initial PBL conditions compared to a 23.5 % decrease in PBL height for the low PBL conditions (Table 4). Although the case study outlined above shows the effect of aerosol loading on boundary layer meteorology for a case study period, these results show that the aerosol-PBL feedback is enhanced under shallow PBL conditions. These conditions are more likely to occur during a pollution episode, where aerosol concentrations are already high. In this study we can see that these 'high aerosols' combined with 'shallow PBL' increases the magnitude of the aerosol-radiation feedback effect on changes in PBL height (Figure 6).

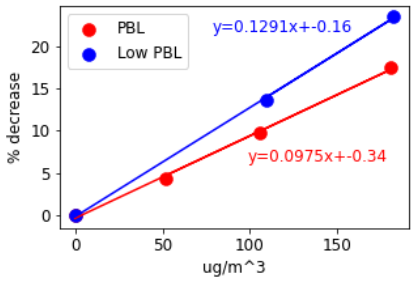

Fig. 6 : Aerosol concentration vs PBL % decrease for low initial PBL simulations and original PBL simulations, due to different aerosol loadings

This work shows that aerosol-radiation interactions feedback on boundary layer meteorology to different extents depending on the initial conditions, with larger impacts when the PBL is already shallow. Although the differences are reasonably small (4-6 %) this shows susceptibility to different conditions are important when quantifying the aerosol-radiation meteorological feedback. Furthermore, as the feedback effect is enhanced when aerosol concentrations are higher, this will lead to a shallower PBL which will in turn lead to enhanced aerosol-radiation feedback and increase surface concentrations further. Therefore, towards the end of pollution episodes when concentrations are high and the PBL is shallow, the feedbacks between aerosol-radiation interactions and meteorology are stronger. This significantly reduces vertical mixing of aerosols through reducing buoyancy due to turbulence and enhancing the stagnation of air.

PBL Conditions	Normal	Low
PBL Height (m) (0 $\mu g/m^3$)	510.1	409.2
PBL Height (m) (107 $\mu g/m^3$)	460.1	353.5
PBL Height (m) (182 $\mu g/m^3$)	421.0	312.8
% decrease in maximum PBL height (107 $\mu g/m^3$)	9.7 %	13.6 %
% decrease in maximum PBL height (182 $\mu g/m^3$)	17.4 %	23.6 %

Table 4 Values of and % decrease in maximum PBL height (12:00-16:00 LST) for simulations initialised with normal and low PBL conditions due to aerosol concentrations of 107 $\mu g/m^3$ and 182 $\mu g/m^3$

Discussion

This work investigates a haze episode which occurred over 4 days from 01/12-04/12/2016, which had been well characterised in a study by Wang et. al (2019)[14]. In their research they identify that changing synoptic conditions contributes to a reduction in PBL height from 900 to 500 m between 01/12-02/12, which is a larger contribution than the decrease from 500 to 400 m from 02/12-03/12 estimated to be due the impact of aerosol-PBL feedback. In this work, we show a decrease from 1779 m to 510 m due to synoptic meteorology, and a decrease from 510 m to 421 m due to aerosols. Results show that simulations on 01/12 significantly overestimate PBL height compared to ceiliometer measurements taken during the APHH Beijing campaign. Some of this will be due to the changing synoptic conditions over the day which due to the model's boundary conditions (periodic with no large scale forcing) cannot be represented in these results. However, the simulated PBL height is much higher than would be expected for wintertime Beijing, even during clean periods. This could be a limitation of the model setup, specifically the homogeneous surface scheme as described in Slater et. al (2020)[32]. Furthermore, it could be a limitation of using the height where there is a maximum gradient in potential temperature as a proxy for PBL height when the PBL is strongly turbulent or neutral. When there is a strong temperature inversion, the variation in θ at PBL top is large but under conditions observed on 01/12 the gradient is small, meaning this metric is less pronounced and can be less relied upon. However, the decrease in PBL height due to aerosol-PBL feedback presented in this case for 03 Dec is similar to that presented in the work by Wang et. al (2019)[14]. Although, the research presented by Wang et. al (2019) well characterises the haze episode examined in this paper, in this piece of work we directly elucidate factors (aerosol loading, meteorological conditions) which have an impact on the pollution episode and suggest reasons for this. This outlines the importance of combining

observations with high resolution modelling studies to provide a broader understanding of the complex interactions taking place in Beijing haze episodes and the factors affecting them.

Results in this paper highlight three areas of importance when considering aerosol-PBL feedback: a) changes in meteorology have a larger impact on suppressing turbulent motion than increasing aerosol concentrations, b) PBL height decreases linearly with increasing aerosol concentrations at constant composition and c) aerosol-PBL feedback has an enhanced effect under shallow PBL conditions. Shallow PBL conditions are primarily brought about by changing synoptic conditions, which allow for aerosols to accumulate. Increased aerosol concentrations will lead to a further decrease in PBL height due to the aerosol-PBL feedback and this further will enhance the impact of the aerosol-PBL feedback, which has a greater impact under shallow PBL conditions. Consequently, the feedback combined with local emissions and regional transport of pollutants will likely slowly increase in intensity throughout the pollution episode. In Beijing, haze episodes can be classified into different circulation types which outline the changing synoptic conditions which preempt each episode[38]. This leads to pollution episodes with different characteristics, influencing aerosol concentrations and composition as well as meteorological conditions such as wind speed, humidity and temperature. Therefore, the haze episode which occurred on 01/12-04/12/2016 cannot be considered fully representative of all wintertime Beijing haze episodes. However, in most cases, temperature inversions and stagnant conditions do preempt these episodes to some degree, causing a reduction in PBL height prior to the accumulation of aerosols. As this work explicitly examines the interactions which occur after these changes, we consider the influence of the aerosol-PBL feedback outlined in this work well represents a process which could impact haze episodes in Beijing. However, studies of more pollution episodes would be beneficial to further understand the processes presented here.

This study finds no threshold value above which the aerosol-feedback effect increases with importance but rather finds a linear decrease in PBL height of 45 m per 100 $\mu g/m^3$ increase in $PM_{2.5}$, even at lower aerosol concentrations. This is in contrast to other studies where a threshold value between 75-100 $\mu g/m^3$ has been suggested below which the aerosol-PBL feedback does not occur. Through analysis of 28 heavy pollution episodes which occurred in winter Beijing from 2013 to 2017, Zhong et. al (2019)[29] suggests that under low wind conditions, the feedback between aerosols and radiation is triggered when $PM_{2.5}$ surface concentrations reach 100 $\mu g/m^3$, suggesting that keeping values below this level in Beijing would successfully limit the intensity of heavy pollution episodes. However the range of values where the feedback was triggered was extremely large, ranging from 50 to 250 $\mu g/m^3$, with higher thresholds during heavy pollution episodes. Zhang et. al (2019)[39] examined the contribution of aerosol-PBL feedback in Lanzhou and Urumqi, two North Eastern Chinese cities. They suggest that in Lanzhou, the strength of inversion increases significantly above 75 $\mu g/m^3$ and below this level the aerosol-radiation feedback had little effect. In Urumqi, the study finds that no inversion occurred until concentrations reached 100 $\mu g/m^3$ and the strength of the inversion was most obvious when concentrations were between 100-250 $\mu g/m^3$. Here, we suggest that these observational studies do not separate the link between meteorology and aerosol concentrations but rather observe that temperature inversions in Beijing are often synonymous with $PM_{2.5}$ concentrations > 100 $mu g/m^3$. In this work we show that the likely cause of the strong initial temperature inversions is synoptic scale meteorological changes which has more of an impact on suppressing PBL development than aerosol-PBL feedback. We also show that under lower PBL conditions there is a larger impact of aerosol-PBL feedback. Our study shows a simulated 12.9 % decrease in PBL height per 100 $\mu g/m^3$ under our 'low' PBL height simulations compared to a 9.8 % decrease per 100 $\mu g/m^3$ for the original PBL simulations. Figure 7 outlines our proposed mechanism for the influence of aerosol-PBL feedback on Beijing haze episodes and how this develops over time.

Comparing observations of measured sensible heat flux and boundary layer height on 01/12 and 02/12, there is a clear reduction in turbulence between the two days. Model simulations of the period show this change without inclusion of aerosol-radiation interactions (Figure 3). Therefore, the slight increase in aerosol concentrations on 02/12 (Figure 1) is unlikely to be the driver in the reduction of boundary layer height and turbulence during this period. Synoptic conditions cause a shallow boundary layer to form on 02/12[14]. These initial conditions mean that any primary aerosols emitted or secondary aerosols formed are accumulated in a shallow polluted boundary layer throughout the day which extends into the night. The existence of aerosol particles reduces the amount of surface solar heating, to suppress buoyant turbulence. This can lead to a temperature inversion, enhancing atmospheric stratification the next day. In the morning of 03/12, aerosols are accumulated in a shallow boundary layer and emissions throughout the day lead to increased concentrations of pollutants in Beijing. Specifically, on 03/12 rapidly increasing aerosol concentrations in the afternoon were observed in the afternoon of 03/12, suggesting the rate of emissions or secondary aerosol formation must be higher than the entrainment of clean air from the free troposphere, with a shallow boundary layer existing throughout the day.

In this study, aerosol composition was kept constant. BC, a strong absorber of solar radiation, and the most radiatively efficient aerosol species, is thought to suppress PBL development in Beijing through warming the upper boundary layer which alters the thermal profile and enhances atmospheric stratification. In our simulations, we see that increasing aerosol concentrations causes cooling in the lower boundary layer and warming above it, resulting in a shallow PBL. From observational analyses of polluted periods in Beijing, Ding et. al (2016) show that the reduced surface fluxes associated with BC have a stronger impact on pollution episodes compared to the impact caused by $PM_{2.5}$ alone. As a whole they found that the impact of BC on the aerosol-PBL feedback will saturate at a certain concentration of PM, due to weaker solar radiation associated with heavy pollution episodes. Consequently, the impact of BC on the results presented here should be

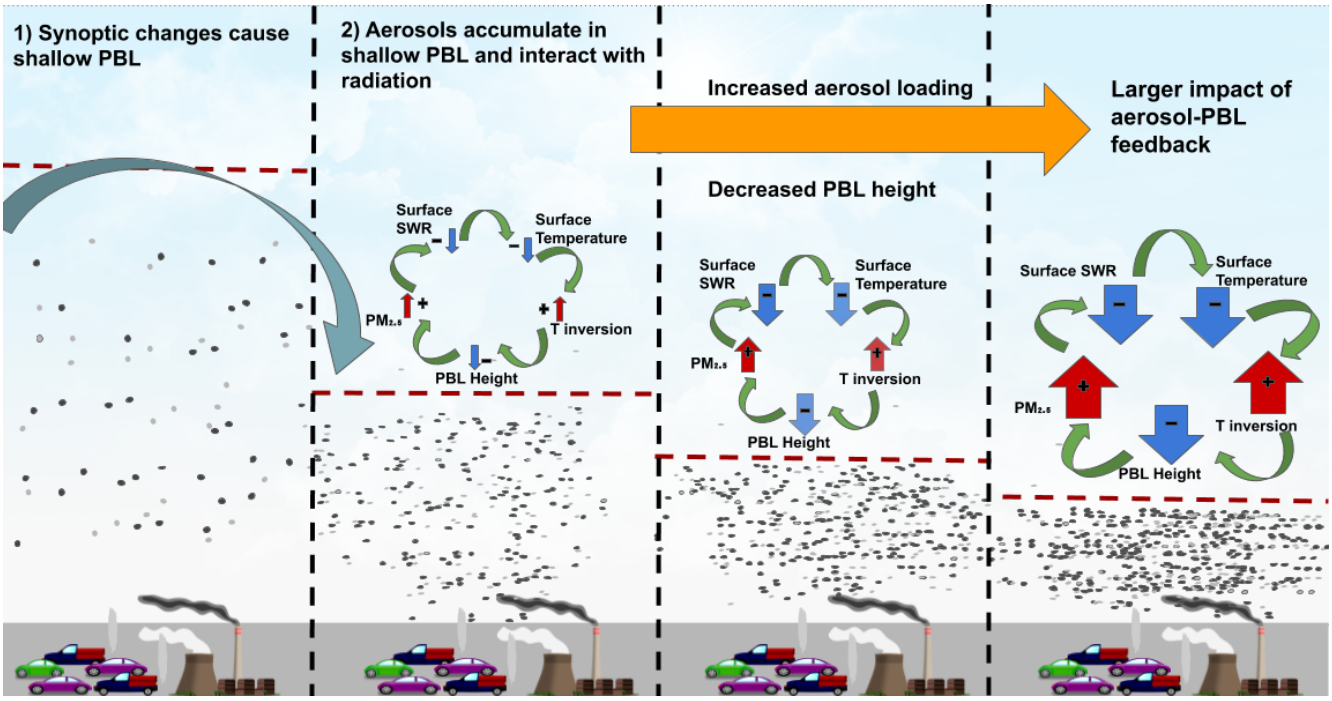

Fig. 7 : The development of a haze episode and the importance of aerosol-PBL feedback on enhancing atmospheric stabilisation and increased aerosol concentrations

considered.

Furthermore, this study does not directly examine the impact of emissions or several atmospheric processes thought to impact pollution episodes, such as semi-volatile condensation or secondary aerosol formation. However, under such conditions outlined above, these processes will likely be enhanced and will further impact the intensity of aerosol-radiation interactions and their feedback on meteorology due to increasing aerosol concentrations. Semi-volatile condensation to form secondary aerosols is known to be enhanced under high humidity conditions[28]. Increases in humidity are common in the cumulative stages of haze episodes due to aerosol-radiation interactions suppressing boundary layer development, which leads to increased water vapour concentrations. This will allow for enhanced aqueous heterogeneous reactions, which will further increase aerosol concentrations. Furthermore, high humidity will cause hygroscopic aerosol particles to swell in size, potentially increasing the extent of their interaction with radiation, but also impacting their atmospheric lifetime.

A study by Li et. al (2020) suggests that in the growth stage of moderate haze, the feedback induced by physical processes (horizontal and vertical advection and diffusion and dry deposition) had slightly more of an impact on $PM_{2.5}$ increase than chemical processes (secondary aerosol formation and heterogeneous reactions), but in extreme haze episodes chemical processes have much larger an impact compared to physical processes[40]. Therefore, in order to fully quantify the impact of aerosol-radiation interactions on boundary layer meteorology for the Beijing haze episode of 01-04/12 processes such as this need to be further elucidated and included in modelling studies.

Conclusions

This work aimed to identify the importance of aerosol-PBL feedback on pollution episodes through examining three potential factors. We examined a specific haze episode in Beijing which occurred on 01-04/12 2016 and examined the impact of aerosol loading and meteorological conditions on the cumulative stage of the episode. Overall, we showed that the difference in meteorological conditions between 01/12 and 03/12 was important in decreasing PBL height to $\sim$ 500 m, whereas the decrease caused by inclusion of aerosols decreased the PBL further to 400 m. Therefore, as has been presented in other work, we can assert that changing synoptic initial conditions are found to be more essential in the initial suppression of boundary layer development than increased aerosol concentrations. These synoptic conditions are typically associated with the beginning of haze episodes and occur every 4-7 days within Beijing. When combined with high emissions locally and regional transport, these conditions will allow for strong accumulation of aerosols in the Beijing area. Therefore, future policy should aim to reduce emissions particularly when these conditions are predicted to occur, in order to reduce the effect of aerosol-radiation interactions enhancing the pollution episode further.

Several studies have highlighted a threshold value, whereby above this value the aerosol-PBL feedback increases in importance. However, here we suggest that rather than a threshold value, the reduction of planetary boundary layer height scales approximately linearly with increased aerosol load across the whole range of loads we studied. Therefore, rather than limiting aerosol

concentrations below a threshold value, concentrations should be kept to as low as possible in order to reduce the impacts of the aerosol-radiation interactions on PBL height. Furthermore, the impact of the initial PBL height on the aerosol-PBL feedback was also found to be important, with lower PBL conditions found to enhance the impact of aerosol-PBL feedback by 4-6%.

Conflicts of interest

The authors declare that there are no conflicts of interest.

Acknowledgements

Jessica Slater is fully funded by the National Centre for Atmospheric Science (NCAS). This work was carried out as part of AIRPRO (NE/N00695X/1). Sami Romakkaniemi and Juha Tonttila are supported by the Academy of Finland (projects 283031 and 309127) Model simulations were carried out on the ARCHER UK National Supercomputing Service (http://www.archer.ac.uk).

Notes and references

1 B. Lv, B. Zhang and Y. Bai, *Atmospheric Environment*, 2016, **124**, 98–108.

2 WHO, *Pollution Atmospherique*, 2006, 169.

3 Q. Zhang, Y. Zheng, D. Tong, M. Shao, S. Wang, Y. Zhang, X. Xu, J. Wang, H. He, W. Liu, Y. Ding, Y. Lei, J. Li, Z. Wang, X. Zhang, Y. Wang, J. Cheng, Y. Liu, Q. Shi, L. Yan, G. Geng, C. Hong, M. Li, F. Liu, B. Zheng, J. Cao, A. Ding, J. Gao, Q. Fu, J. Huo, B. Liu, Z. Liu, F. Yang, K. He and J. Hao, *Proceedings of the National Academy of Sciences of the United States of America*, 2019, **116**, 24463–24469.

4 Y. Sun, G. Zhuang, A. Tang, Y. Wang and Z. An, *Environmental Science Technology*, 2006, **40**, 3148–3155.

5 L. Pei, Z. Yan, Z. Sun, S. Miao and Y. Yao, *Atmospheric Chemistry and Physics*, 2018, **18**, 3173–3183.

6 L. Zhang, T. Wang, M. Lv and Q. Zhang, *Atmospheric Environment*, 2015, **104**, 11–21.

7 H. Fu and J. Chen, *Science of The Total Environment*, 2016, **578**, 121–138.

8 Y. Zhang, J. He, S. Zhu and B. Gantt, *Journal of Geophysical Research: Atmospheres*, 2016, 6014–6048.

9 J. Wang, S. Wang, J. Jiang, A. Ding, M. Zheng, B. Zhao, D. C. Wong, W. Zhou, G. Zheng, L. Wang, J. E. Pleim and J. Hao, *Environmental Research Letters*, 2014, **9**, 94002.

10 J. Zhong, X. Zhang, Y. Dong, Y. Wang, C. Liu, J. Wang, Y. Zhang and H. Che, *Atmospheric Chemistry and Physics*, 2018, **18**, 247–258.

11 Y. Miao, J. Li, S. Miao, H. Che, Y. Wang, X. Zhang, R. Zhu and S. Liu, *Current Pollution Reports*, 2019, 261–271.

12 S. Guo, M. Hu, M. L. Zamora, J. Peng, D. Shang, J. Zheng, Z. Du, Z. Wu, M. Shao, L. Zeng, M. J. Molina and R. Zhang, *Proceedings of the National Academy of Sciences of the United States of America*, 2014, **111**, 17373–8.

13 G. J. Zheng, F. K. Duan, H. Su, Y. L. Ma, Y. Cheng, B. Zheng, Q. Zhang, T. Huang, T. Kimoto, D. Chang, U. Pöschl, Y. F. Cheng and K. B. He, *Atmospheric Chemistry and Physics*, 2015, **15**, 2969–2983.

14 L. Wang, J. Liu, Z. Gao, Y. Li, M. Huang, S. Fan, X. Zhang, Y. Yang, S. Miao, H. Zou, Y. Sun, Y. Chen and T. Yang, *Atmospheric Chemistry and Physics*, 2019, **19**, 6949–6967.

15 J. Zhong, X. Zhang, Y. Wang, J. Wang, X. Shen, H. Zhang, T. Wang, Z. Xie, C. Liu, H. Zhang, T. Zhao, J. Sun, S. Fan, Z. Gao, Y. Li and L. Wang, *Atmospheric Chemistry and Physics*, 2019, **19**, 3287–3306.

16 T. Petäjä, L. Järvi, V.-M. Kerminen, A. J. Ding, J. N. Sun, W. Nie, J. Kujansuu, A. Virkkula, X. Yang, C. B. Fu, S. Zilitinkevich and M. Kulmala, *Scientific reports*, 2016, **6**, 18998.

17 Q. Liu, X. Jia, J. Quan, J. Li, X. Li, Y. Wu, D. Chen, Z. Wang and Y. Liu, *Scientific Reports*, 2018, **8**, 1–8.

18 M. Gao, S. K. Guttikunda, G. R. Carmichael, Y. Wang, Z. Liu, C. O. Stanier, P. E. Saide and M. Yu, *Science of the Total Environment*, 2015, **511**, 553–561.

19 X. Huang, Z. Wang and A. Ding, *Geophysical Research Letters*, 2018, **45**, 8596–8603.

20 H. Wang, Z. Li, Y. Lv, H. Xu, K. Li, D. Li, W. Hou, F. Zheng, Y. Wei and B. Ge, *Environmental Pollution*, 2019, **252**, 897–906.

21 Y. Miao and S. Liu, *Science of the Total Environment*, 2019, **650**, 288–296.

22 X. Zhang, Q. Zhang, C. Hong, Y. Zheng, G. Geng, D. Tong, Y. Zhang and X. Zhang, *Journal of Geophysical Research: Atmospheres*, 2018, **123**, 1179–1194.

23 Y. Qiu, H. Liao, R. Zhang and J. Hu, *Journal of Geophysical Research*, 2017, **122**, 5955–5975.

24 J. Wu, N. Bei, B. Hu, S. Liu, M. Zhou, Q. Wang, X. Li, L. Liu, T. Feng, Z. Liu, Y. Wang, J. Cao, X. Tie, J. Wang, L. T. Molina and G. Li, *Atmospheric Chemistry and Physics*, 2019, **19**, 8703–8719.

25 T. Li, H. Wang, T. Zhao, M. Xue, Y. Wang, H. Che and C. Jiang, *Advances in Meteorology*, 2016, **2016**, year.

26 X. Zhang, M. Mao and H. Chen, *Journal of Atmospheric and Solar-Terrestrial Physics*, 2020, **198**, 105180.

27 W. Jia and X. Zhang, *Atmospheric Research*, 2020, **239**, 104890.

28 X. Tie, R. J. Huang, J. Cao, Q. Zhang, Y. Cheng, H. Su, D. Chang, U. Pöschl, T. Hoffmann, U. Dusek, G. Li, D. R. Worsnop and C. D. O'Dowd, *Scientific Reports*, 2017, **7**, 1–8.

29 J. Zhong, X. Zhang and Y. Wang, *Tellus, Series B: Chemical and Physical Meteorology*, 2019, **71**, 1–7.

30 Y. Liu, J. Wu, D. Yu and Q. Ma, *Environmental Science and Pollution Research*, 2018, **25**, 15554–15567.

31 Y. Sun, Q. Jiang, Z. Wang, P. Fu, J. Li, T. Yang and Y. Yin, *Journal of Geophysical Research: Atmospheres*, 2014, **119**, 4380–4398.

32 J. Slater, J. Tonttila, G. Mcfiggans, S. Romakkaniemi, T. Kühn and H. Coe, *Atmospheric Chemistry and Physics Discussions*, 2020, **5**, 1–23.

33 J. Tonttila, Z. Maalick, T. Raatikainen, H. Kokkola, T. Kühn and S. Romakkaniemi, *Geoscientific Model Development*, 2017, **10**, 169–188.

34 J. Tonttila, A. Afzalifar, H. Kokkola, T. Raatikainen, H. Ko-

rhonen and S. Romakkaniemi, *Atmospheric Chemistry and Physics*, 2021, **21**, 1035–1048.

35 F. Ács, D. T. Mihailović and B. Rajković, *A Coupled Soil Moisture and Surface Temperature Prediction Model*, 1991.

36 M. Gao, G. R. Carmichael, Y. Wang, P. E. Saide, M. Yu, J. Xin, Z. Liu and Z. Wang, *Atmospheric Chemistry and Physics*, 2016, **16**, 1673–1691.

37 A. J. Ding, X. Huang, W. Nie, J. N. Sun, V. M. Kerminen, T. Petäjä, H. Su, Y. F. Cheng, X. Q. Yang, M. H. Wang, X. G. Chi, J. P. Wang, A. Virkkula, W. D. Guo, J. Yuan, S. Y. Wang, R. J. Zhang, Y. F. Wu, Y. Song, T. Zhu, S. Zilitinkevich, M. Kulmala and C. B. Fu, *Geophysical Research Letters*, 2016, **43**, 2873–2879.

38 Z. Shi, T. Vu, S. Kotthaus, S. Grimmond, R. M. Harrison, S. Yue, T. Zhu, J. Lee, Y. Han, M. Hu, D. Ji, X. Jiang, R. Jones, M. Kalberer, F. J. Kelly, B. Langford, C. Lin, A. C. Lewis, J. Li, W. Li, H. Liu, K. Lu, G. Mann, G. Mcfiggans, M. Miller, G. Mills, E. Nemitz, B. Ouyang, P. I. Palmer, C. Percival, O. Popoola, C. Reeves, A. R. Rickard, L. Shao, G. Shi, D. Spracklen, D. Stevenson, Y. Sun, Z. Sun, S. Tao, S. Tong, Q. Wang, W. Wang, X. Wang, Z. Wang, L. Whalley, X. Wu, Z. Wu, P. Xie, F. Yang, Q. Zhang, Y. Zhang, Y. Zhang, E. Polytechnique, W. Atmospheric, C. Laboratories, E. S. Division, L. E. Centre, C. Environmental and R. Energy, *Atmospheric Chemistry and Physics Discussions*, 2018.

39 W. Zhang, X. Zhang, J. Zhong, Y. Wang, J. Wang, Y. Zhao and S. Bu, *Science of the Total Environment*, 2019, **688**, 642–652.

40 J. Li, Z. Han, Y. Wu, Z. Xiong, X. Xia, J. Li, L. Liang and R. Zhang, *Atmospheric Chemistry and Physics*, 2020, **20**, 8659–8690.

4.3 Paper 3: The effect of black carbon on aerosol boundary layer feedback: Potential implications for Beijing haze episodes

Authors: Jessica Slater, Hugh Coe and Gordon McFiggans

Journal: to be submitted to Atmospheric Chemistry and Physics

This paper shows the specific impact of black carbon (BC) on the aerosol-planetary boundary layer (PBL) feedback effect. Specifically, it investigates the dome effect of black carbon, which is first presented in the paper by Ding et. al (2016). The idea of the dome effect is that in heavily polluted regions, black carbon absorbs radiation efficiently in the upper atmosphere to reduce shortwave radiation reaching the surface and warm the upper atmospheric layer. This decreases buoyant turbulence and suppresses PBL development. This paper shows directly the influence of black carbon on causing surface cooling is higher than the effect of scattering aerosols alone. We also show that the heating rate of black carbon is about 0.2 K/h for concentrations used in this study, which works out around 0.01 - 0.016 $\mathrm{Kh}^{-1}/\mu\mathrm{gm}^{-3}$ of BC.

Paper Overview

This work builds on the research conducted by Ding et. al (2016) and provides results for further examination of BC in multiple layers through the column. This work also shows the influence of initial conditions is high as shown in Papers 1 and 2 of this thesis, which is not considered in the work by Ding et. al (2016) or Wang et. al (2018). This is important as these conditions are shown to change over the pollution episode (as identified in paper 2). Specifically, through altering the altitude of the absorbing black carbon layer, this paper shows that the heating of black carbon at the surface causes warming but that on our case study of 03 Dec 2016, the initial temperature inversion is too high for the surface heating to break the inversion and sufficiently enhance the development of the PBL. However, under slightly lower temperature inversion conditions of 02 Dec 2016, the surface heating increases maximum PBL height by 5 % compared to 0.26 % on 03 Dec. However, the overall heating caused by black carbon (1-2 K) is still too low to fully break such a strong temperature inversion (4 K on 02 Dec and 7 K on 03 Dec 2016). This work shows that BC above the PBL effectively decreases maximum PBL height, and the effect is maximised the closer BC is to the PBL top. In the discussions section of the paper a mechanism by which locally emitted black carbon could have significant impact on pollution episodes in Beijing is suggested.

Author Contributions

The idea for this study was conceived by Jessica Slater, with the assistance of Hugh Coe and Gordon McFiggans. Model simulations were performed by Jessica Slater. Model analysis was performed by Jessica

Slater with assistance from Hugh Coe. The manuscript was written by Jessica Slater with contributions from Hugh Coe and Gordon McFiggans.

The effect of black carbon on aerosol-boundary layer feedback: Potential implications for Beijing haze episodes

Jessica Slater[1,2], Hugh Coe[1], Gordon McFiggans[1], Juha Tonttila[3], and Sami Romakkaniemi[3]

[1]Stockholm Environment Institute, Department of Environment and Geography, University of York, York, UK
[2]Centre for Atmospheric Science, School of Earth and Environmental Sciences, University of Manchester, Manchester, UK
[3]Finnish Meteorological Institute, Atmospheric Research Centre of Eastern Finland, Kuopio, Finland

Correspondence: Hugh Coe (hugh.coe@manchester.ac.uk)

Abstract. Beijing suffers from poor air quality particularly during wintertime haze episodes when concentrations of $PM_{2.5}$ can peak at > 400 ug/m^3. Black carbon, an aerosol which strongly absorbs solar radiation can make up to 10 % of $PM_{2.5}$ in Beijing. Black carbon is of interest due to its climatic and health impacts. Black carbon has also been found to impact planetary boundary layer (PBL) meteorology, through altering the thermal profile of the lower atmosphere. The so-called dome effect of BC outlines how when BC exists above the PBL, it will act to warm the layer above the PBL while cooling below it, through reducing the amount of shortwave radiation reaching the surface. This alters the thermal profile of the PBL and suppresses buoyant turbulence, thus enhancing atmospheric stagnation. Consequently, aerosols accumulate in a shallow PBL, leading to higher surface PM concentrations and worsened haze episodes. Further, this lowers surface wind speeds, reducing the horizontal dissipation of the pollutants. Thus far, the dome effect has been investigated through the use of regional models which are limited both by resolution and the chosen boundary layer schemes. In this work, we apply a coupled large eddy simulation-aerosol-radiation model (UCLALES-SALSA) to examine the impact of black carbon on the aerosol-PBL interactions using conditions from a specific haze episode which occurred from 1st-4th Dec 2016. Specifically in this work we show the impact of BC altitude and initial meteorological conditions on the magnitude of aerosol-PBL feedback and the implications for Beijing air pollution. Furthermore, we hypothesise a potential mechanism for how the distribution of BC may change throughout the pollution episode and the effect this may have on enhancing the intensity of the pollution episode but also through assisting with its dissipation.

1 Introduction

Beijing, a megacity situated in the North China Plain, experiences extremely poor air quality. Typically in Beijing wintertime, heavy pollution episodes termed 'haze' envelop the city and concentrations of $PM_{2.5}$ (particulate mass with a diameter < 2.5 μm) frequently exceed the recommended World Health Organization exposure limits (WHO, 2006). Poor air quality has been linked to various respiratory and cardiovascular diseases as well as neurodegenerative diseases such as Parkinson's and

dementia (Yang et al., 2013; Lelieveld et al., 2015; Chen et al., 2017). Improving air quality is therefore a public health priority for the Chinese government. However, despite policy interventions which have improved annual average air quality in Beijing over the past decade, heavy pollution episodes are still a major issue (Chan and Yao, 2008). Black carbon (BC), primarily emitted through incomplete combustion, is a strongly absorbing aerosol present in high concentrations in Chinese megacities (Fu and Chen, 2016). In Beijing, BC can contribute up to 10 % total particulate matter (PM) during polluted periods (Liu et al., 2016). Major sources of BC in Beijing are: traffic, biomass burning and coal combustion for both residential and industrial use (Streets et al., 2001).

BC is of interest globally due to its climatic and health impacts. As a short lived climate pollutant which strongly absorbs radiation across the shortwave (SW) spectrum, BC can directly cause atmospheric warming and is considered to be the largest anthropogenic contributor to global warming after carbon dioxide (Bond et al., 2013). Furthermore, due to its relatively short lifetime in the atmosphere (days) compared to carbon dioxide (years), reducing concentrations of BC in the atmosphere could have a rapid impact on global temperatures, with the added benefit of improving air quality for human health. The global direct radiative forcing of BC at top of atmosphere (TOA) is estimated to be between 0.2-1.2 W/m^2 (Ramanathan and Carmichael, 2008; Bond et al., 2013). Calculating the global direct radiative forcing effect (DRE) of BC is complicated by its spatial heterogeneity, with a higher effect (up to 10 W/m^2) in heavy polluted urban areas where BC concentrations are significantly higher (Ferrero et al., 2014; Li and Han, 2016). Furthermore, the DRE of BC is significantly affected by its source, vertical distribution, atmospheric conditions and its mixing with other components of PM within the atmosphere to change its optical properties (Zhao et al., 2020).

Through absorbing radiation and altering the thermal profile of the atmosphere, BC may play an important role in the enhancement of Beijing pollution episodes via the aerosol-PBL feedback mechanism. The mechanism can be described as follows: scattering and absorbing aerosol particles interact with solar radiation to reduce the amount of shortwave radiation (SWR) reaching the surface, causing surface cooling. Furthermore, absorbing aerosol particles can lead to warming of the air above the surface. This alters the thermal profile of the atmosphere and reduces buoyant turbulence, suppressing PBL development and allowing aerosols to accumulate in a shallow PBL. This can also increase water vapour concentrations which can cause some aerosols to grow in size, while also enhancing the rate of secondary aerosol formation. These factors increase aerosol-radiation interactions further, leading to a positive feedback between aerosol concentrations and PBL height (Gao et al., 2015; Ding et al., 2016; Petäjä et al., 2016; Zou et al., 2017).

The effect of BC on PBL development and the aerosol-PBL mechanism is highly dependent on the properties of BC as well as the altitude of the BC layer. In theory, concentrations of BC at the surface will warm the lower layer, promoting buoyant turbulence and decreasing atmospheric stability, while a layer of BC aloft is thought to further enhance the temperature inversions, increasing temperatures aloft and decreasing them at the surface leading to atmospheric stabilisation (Figure 1). Upper level BC (BC above the PBL) is also believed to have a higher heating efficiency due to a combination of the lower density of air and higher incident radiation flux at higher altitudes, allowing for BC particles to absorb more radiation and heat

air at a higher rate. This suggests that even low concentrations of BC at high altitudes may lead to atmospheric stabilisation. This is considered to be the so-called 'dome effect' of BC (Ding et al., 2016; Wang et al., 2018).

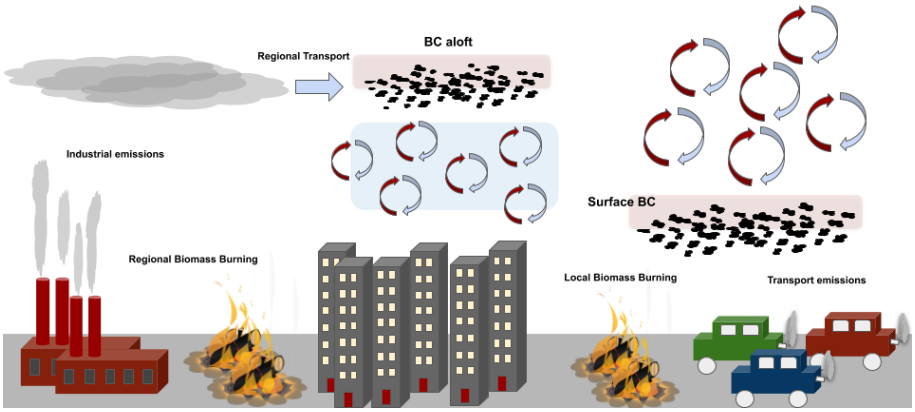

Figure 1. Schematic showing some of the sources of BC, how different altitude layers of BC might exist and the effect of BC layer height on PBL interactions in Beijing

The impact of BC on the aerosol-PBL feedback is dependent on several factors, including: the altitude of the BC layer, its concentration and mixing state. Ding et al. (2016) found that BC enhanced haze episodes through warming the air above the PBL and enhancing stratification of the boundary layer. Wang et al. (2018) found that surface BC promoted PBL development through warming but that this effect was negated by the stronger interactions of BC aloft which suppressed PBL growth. Ding et al. (2016) first showed the importance of the BC dome effect through conducting simulations of three megacities in Eastern China and changing the level of aerosol feedback. Through this, they directly characterised the feedback effect of BC compared to that of other aerosols. Their results showed that a maximum change in SWR due to BC occurred at the top of the PBL (arund 400 m in this case) and that BC at this altitude was primarily responsible for the large suppression in PBL height, despite only making up 30 % of the column BC concentration. Furthermore, BC reduces downwelling surface SW radiation, leading to surface cooling and contributing up to 50 % of the total aerosol reduction in surface fluxes. In a 1D modelling study, Wang et. al (2018) found that BC aloft was essential in the suppression of PBL height, with surface BC increasing both turbulence and PBL height. Furthermore, they found that a BC layer close to the PBL top and internal mixing of BC with scattering aerosols (sulphate, nitrate, ammonium) significantly enhanced the dome effect of BC, leading to a potential reduction in PBL height of 15 %. BC can exist above the PBL in Beijing, due to aerosols being transported from surrounding regions through synoptic scale winds and through aerosols remaining in the residual layer overnight after being mixed through the PBL in the previous day (Wang et al., 2016; Zhao et al., 2020).

Thus far methods of examining the impact of BC on the aerosol-PBL feedback in Beijing have been with observational or regional modelling studies, with specific radiative transfer models used to calculate direct radiative effects (Ding et al., 2016, 2017; Wang et al., 2018; Zhao et al., 2020). Large eddy simulation (LES) models directly simulate turbulent motion and PBL

development without the parameterisation of boundary layer processes which is necessary in regional models such as WRF-CHEM. This gives them a significant advantage in understanding and quantifying perturbations to the PBL. LES models have been used to examine the effect of absorbing aerosol layers on the development of stratocumulus and cumulus clouds. Herbert et al. (2020) examined the effect of an absorbing layer on stratocumulus clouds and thus the PBL development and rates of entrainment, finding a significant reduction in the entrainment rate the closer the absorbing layer was to cloud top. Related to dissipation of radiation fog, Maalick et al. (2016) found that in a polluted conditions BC has a warming effect close to the fog top, and BC enhances fog dissipation due to absorption of solar radiation. However, if the increase in BC concentration is accompanied with an increase in CCN and thus fog droplet concentration, the CCN effect increasing fog lifetime is much stronger than BC effect that shortens fog lifetime.

In this work, we use the coupled LES-aerosol-radiation model (UCLALES-SALSA), which has previously been set up and tested in Beijing, to examine the impact of BC on aerosol-PBL interactions and the implication on Beijing haze episodes (Slater et al., 2020, 2021). The high resolution of LES models and their ability to calculate turbulent fluxes and perturbations thereof, allows for isolation and quantification of the different factors impacting the 'dome effect' of BC. We use meteorological conditions from 2 days in the middle of a haze episode (2nd and 3rd Dec 2016), where a strong temperature inversion and shallow PBL already exist due to the convergence of cold northerly air masses with southerly warm air masses (Wang et al., 2019). Specifically, this work investigates the 'dome effect' of BC, through isolating the impact of BC both above and within the PBL and the impact on PBL dynamics. This paper is set out as follows. Section 2 describes model set up, including experimental setup for the different sensitivities examined, while section 3 details the results for the corresponding sensitivity studies. Section 4 briefly discusses the overall results and their implications in more detail.

2 Methods

2.1 Model Description

The model used in this study is UCLALES-SALSA, which is a large eddy simulation model (UCLALES) fully coupled to the sectional aerosol model (SALSA). UCLALES-SALSA has been used to examine the impact of aerosols on stratocumulus clouds, radiation fog, cloud seeding and to examine the aerosol-PBL feedback in Beijing (Tonttila et al., 2017; Slater et al., 2020; Tonttila et al., 2021; Slater et al., 2021). UCLALES is based on the Smagorinsky-Lilly subgrid model, with leapfrog time stepping used for advection of momentum variables and forward time stepping for advection of scalar variables, based on fourth order differential equations. Boundary conditions are doubly periodic in the horizontal and fixed in the vertical. The surface scheme is based on a coupled soil moisture and surface temperature scheme by Ács et al. (1991), which explicitly calculates surface temperature and, sensible and latent heat fluxes. The surface scheme used in this case has been adapted and tested for the urban environment of Beijing and the set up is as detailed in Slater et al. (2020).

SALSA is a sectional aerosol model which has been fully coupled to both UCLALES and the climate model ECHAM Kokkola et al. (2008, 2018). SALSA bins aerosol particles according to size and has two sets of parallel size bins which allow

for aerosols to be both internally and externally mixed. In the results set out here, we assume all particles to be internally mixed. Processes including deposition of aerosols, semi-volatile condensation, nucleation and emissions are switched off but aerosol coagulation and water condensation on aerosol particles are turned on. For these simulations, organic carbon, sulphate, nitrate, black carbon and ammonium are included. We use the same size distribution for all simulations (Table 1) and composition is varied slightly to examine the impact of fractional composition changes of BC (Table 2).

To calculate aerosol-radiation interactions, SALSA uses a four stream radiative transfer scheme based on the work by Fu and Liou (1993). This scheme is fully coupled to UCLALES to allow feed back on turbulent dynamics and is a four stream method integrating over 6 SW bands and 12 LW bands. To account for the impact of size on aerosol-radiation interactions we use set refractive indices, and use look up tables for the aerosol-extinction cross section, asymmetry parameter and single-scattering albedo, which are calculated as a function of the size parameter ($\alpha = \frac{D_p}{\lambda}$). In this work we set all imaginary parts of the refractive indices in the SW to zero apart from BC which is set to values according to Bond and Bergstrom (2006). This allows us to consider BC as the only absorbing aerosol. SALSA treats internal mixing for optical properties simply, through volume averaging of the complex refractive index of each component in each particle. Optical properties of the entire particle are calculated from the average refractive index of the particle according to volume as detailed in Jacobson (2005). Therefore, the potential of scattering aerosols to enhance absorption of BC through the 'lensing effect' is not considered here.

2.2 Experimental Setup

The work presented here is divided into three sections and specific set up for each sensitivity is detailed in the appropriate section. We perform simulations for 2nd and 3rd Dec 2016 in Beijing, varying the altitude of the aerosol layers and fractional composition. Initial meteorological conditions were taken from radiosonde profiles. Aerosol composition and size parameters were calculated based on ground based measurements taken at 8am on 3rd Dec 2016 during the APHH winter field campaign (Shi et. al 2019). The initial aerosol vertical profiles were estimated based on the gradient of boundary layer profiles. The model was set up at 08:00 LST and run for 12 hours including 1 hour spin up time. The horizontal domain size was 5.4 x 5.4 km with a resolution of 30 m and the model top was 1800 m with a vertical resolution of 10 m. For all simulations, the initial size distribution is outlined in Table 2. For all results, PBL top or maximum PBL height is taken as the height at which there is a maximum gradient in potential temperature (θ).

Parameter	Mode 1	Mode 2
D_g (nm)	22	121
σ_g	1.28	1.32

Table 1. Size distribution input data - geometric mean diameter (D_g) and geometric standard deviation (σ_g)

Individual case set up for the changing conditions examined in this paper are detailed in sections 2.3-2.5. Section 2.3 outlines the setup of simulations for case 1 where a comparison of 6 simulations are performed on 03 Dec, these are varied so that there

are 3 different altitudes for an aerosol layer and each layer either has a composition of 10 % BC or no BC. In these cases, the aerosols are only present within the specified layer, with no aerosols present initially above or below the layer. Section 2.4 outlines the setup for case 2 simulations where we include a surface aerosol layer only for simulations of 02 Dec and 03 Dec. This case compares the impact of BC heating within the PBL on boundary layer meteorology for the different initial meteorological conditions. Section 2.3 describes the setup for case 3 simulations which vary the fraction of BC in vertical layers within a full column aerosol profile.

2.3 Case 1 - Vertically varied aerosol loading

To isolate the impact of BC and the altitude of the BC layer on the aerosol-PBL feedback, we performed sensitivity studies with meteorological conditions taken from measurements on the morning of 3rd Dec 2016. In the simulations presented in this section, we varied the altitude of the aerosol layer as well as the fractional composition of the aerosols, to either have BC or no BC within the layer (Table 2). We included aerosol layers with identical mass mixing ratios within the PBL (0-350 m), at and above PBL top (500-950 m) and high aloft (700-1150 m) as shown in figure 2 (red, blue and cyan lines respectively). Maximum PBL height (top) was considered to be 510 m based on simulations performed on this day without aerosols. For all simulations in this section, total aerosol loading was kept constant, while the composition was varied as detailed in Table 2 and concentrations and altitudes of each of the aerosol layers as shown in figure 2.

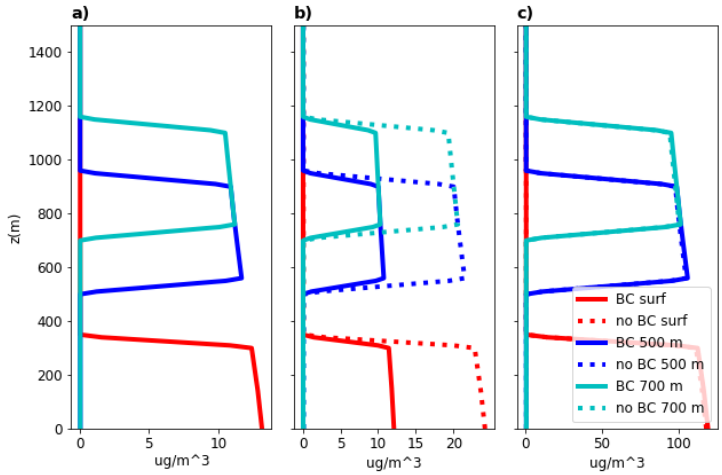

Figure 2. Initial mass concentrations of a) Black Carbon, b) Sulphate and c) Total aerosol concentrations for simulations in case 1. Different heights were chosen for the initial aerosol layers, which were 0-350 m (red lines), 500-950 m (blue lines) and 700-1150 m (cyan lines). Simulations which included black carbon are depicted by solid lines and those without are dashed lines

Figure 2 shows the vertical aerosol profiles for each of the simulations. Figure 2 (a) shows the variation in BC concentrations for the 3 simulations which include BC (solid lines), while the simulations without BC (dashed lines) have no BC through

the whole layer. Figure 3 (b) shows the variation in $SO_4{}^{2-}$ aerosol concentrations. As shown in table 2 and figure 2 (c), for simulations without BC, the initial aerosol concentrations are the same as the simulations with BC but the fractional composition is varied so that there is double the concentration of $SO_4{}^{2-}$. Figure 2 (c) shows the overall vertical variation in aerosol layers for the different simulations, where the BC and no BC simulations for each of the 3 different layers have the same aerosol vertical profiles.

	SO_4	**BC**	**OC**	**NO_3**	**NH_4**
BC case	0.1	0.1	0.45	0.25	0.1
No BC case	0.2	0.0	0.45	0.25	0.1

Table 2. Volume fractional composition for BC and no BC simulations in all simulations

2.4 Case 2- Varying initial conditions

To examine how sensitive BC heating at the surface is to the initial meteorological conditions, particularly the strength of temperature inversions both in the morning and throughout the day, we included an aerosol layer with BC at the surface for simulations on 2nd Dec and compared the results to simulations performed on 3rd Dec. We then compared each simulation to a base case, which was simulations not including aerosol-radiation interactions. The difference in initial meteorological conditions are outlined in figure 3. We can see that on the 2nd Dec, relative humidity is lower, while surface wind speeds are higher and the total temperature inversion throughout the profile is weaker than on 3rd Dec. Furthermore, initial conditions show that at 9am there is a shallow layer with a sharp inversion at the surface in the 2nd Dec initial profile. However, the free tropospheric lapse rates for 3rd Dec is more stable, which may also impact PBL growth throughout the day. The aim of this case study was to examine the influence of these initial conditions on BC heating within the PBL and the associated impact on PBL dynamics.

For these simulations, the aerosol profiles for each day were kept the same so the only variable was the different initial meteorological profiles and surface values (surface temperature). The included aerosol profiles are the same as BC surface in section 2.3 (solid red lines in figure 2).

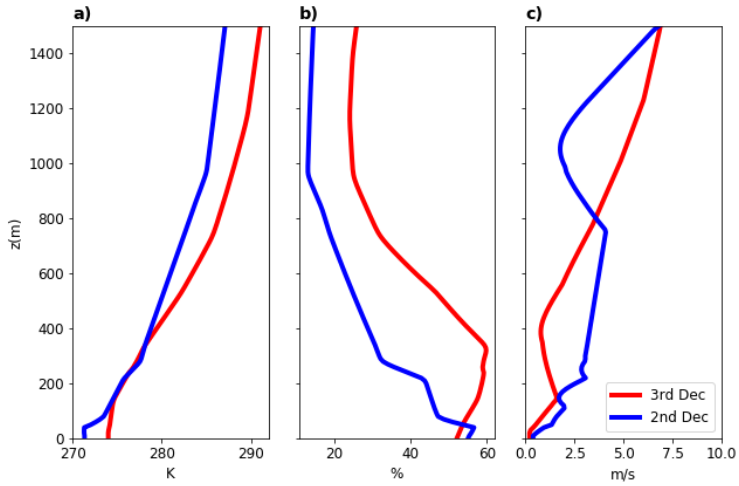

Figure 3. a) Potential temperature, b) Relative Humidity and c) Wind Speed profiles at 9am for 3rd Dec (blue) and 2nd Dec (red)

2.5 Case 3 - Vertically varied BC loading

Simulations in this setup examined the impact of changing the fractional composition of BC in different aerosol layers, so keeping aerosol loading in the column the same but changing composition in different layers, unlike the setup in section 2.3 which compared different aerosol loading layers. This setup was done as a proxy to examine the idea of reducing BC at the surface without tackling regional emissions of BC which may get transported from surrounding areas leading to high concentrations above the PBL.

The set up here uses meteorological conditions from 3rd Dec 2016 as outlined in section 2.3 and 2.4 but includes aerosols throughout the column, rather than just in specific layers. Details of the variation in BC concentrations are outlined in figure 4, and include BC throughout the column (red lines), BC above 500 m (blue lines), BC above 1000 m (cyan lines) and no BC (green lines). As in the set up described in section 3.1, the aerosol loading throughout the column is the same with changes in composition for the 'BC' and 'No BC' cases as detailed in table 1. Figure 5 (a) shows the variation in BC loading, figure 4 (b) shows the variation in SO_4^{2-} loading and figure 4 (c) shows total aerosol vertical profiles for all simulations.

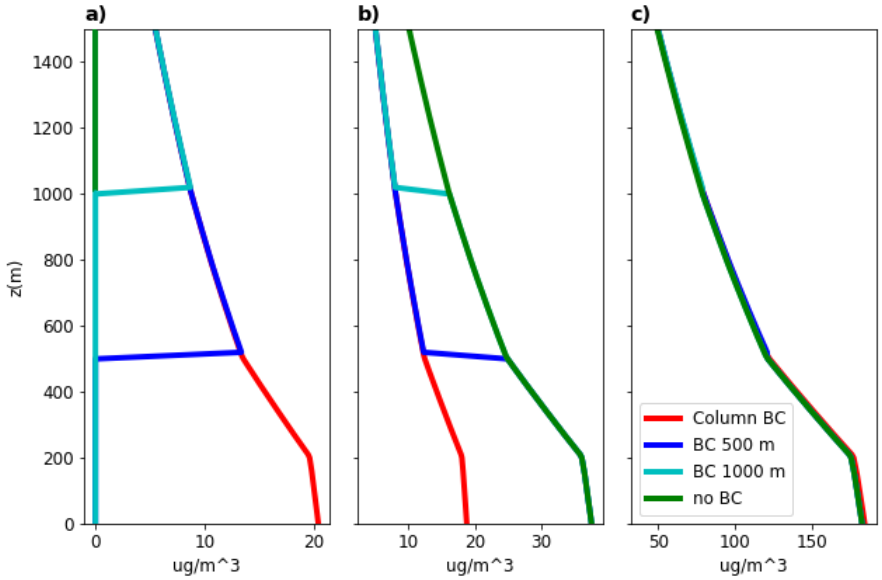

Figure 4. Initial mass concentrations of a) Black Carbon, b) Sulphate and c) Total aerosol for each of the experiments outlined. For simulations with the same aerosol concentration but varying composition across the column to have: BC through the column (red), BC above 500m (blue), BC above 100m (cyan) and no BC throughout the column (green)

3 Results

The results here are separated into 3 sections based on the experimental setup outlined in section 2.3-2.5. Section 3.1 outlines results from case 1 simulations performed as outlined in section 2.3 for vertically varied aerosol layers, section 3.2 shows results from simulations of case 2 looking at the effect of initial meteorological conditions as described in the set up in section 2.4. Finally, section 3.3 showcases results from case 3, which examines the effect of varying BC loading in different vertical layers as described in the setup in section 2.5.

3.1 Case 1 - Vertically varied aerosol layers

Results from varying the height of aerosol layers in the column, with and without BC aerosols show that at all altitudes, BC in the aerosol layer has more impact on PBL dynamics than the effect of scattering aerosols alone (No BC simulations) (Table 3). Specifically, simulations without BC have a small effect on surface temperature, sensible heat flux and PBL height. At the surface, BC decreases downwelling surface SWR by 4 % compared to including only scattering aerosols (No BC simulations), due to the increased absorption caused by increasing the BC fraction. This decreases maximum surface sensible heat flux (SHF) and surface temperature. However, BC absorption of SWR causes warming of the layer, leading to an increase in air temperature at 10 m and slight increase in PBL height compared to no BC surface simulations (Table 3).

For further analysis, we calculates SW heating rate by BC as the change in SW radiative flux (↓SW - ↑SW) divided by specific heat capacity of air (C_p) multiplied by density of air (ρ) as in equation 1.

$$SWHeatingRate_{(t)} = \frac{(\downarrow SW - \uparrow SW)_{(t+1)} - (\downarrow SW - \uparrow SW)_{(t)}}{C_p * \rho} \quad (1)$$

We calculate that the heating rate of BC varied between 0.1-0.2 K/h which will lead to a maximum heating of the PBL throughout the day in wintertime Beijing of 1.6 - 2 K. If the temperature inversion, during the day was small (1-3 K), this additional heating by BC within the PBL and at PBL top of 1.6 - 2 K could break the inversion at PBL top and increase PBL height. However, under a strong temperature inversion as on 03 Dec, this heating within the PBL was not strong enough to reduce the temperature inversion fully and so there was a very small increase in PBL height. Consequently, BC heating within the PBL in this case only resulted in a very small increase in PBL height (Table 3). Furthermore, the low albedo (0.2) and high heat capacity of the underlying surface, typical of an urban environment, mean that BC at the surface will have a lower impact than studies which have examined the effect of polluted environments over high albedo surfaces, for example, clouds or rural environments (Wang et al., 2018).

	SHF (W/m^2)	**PBL Height (m)**	**Surface T (K)**	**↓ SWR surface (W/m^2)**	**↑ SWR top (W/m^2)**	**T at 10 m (K)**
BC surface	98.19	511.43	285.04	490.18	102.35	279.55
No BC surface	111.7	509.43	285.11	511.02	108.41	279.31
BC 700 m	105.18	494.99	284.69	491.72	101.91	279.02
No BC 700 m	111.85	510.19	285.11	515.56	109.44	279.30
BC 500 m	105.0	474.28	284.69	494.00	102.39	279.04
No BC 500 m	111.84	508.57	285.11	515.52	109.44	279.30
No aerosol	112.29	510.10	285.12	516.14	109.28	279.31

Table 3. Maximum sensible heat flux (SHF), planetary boundary layer (PBL) height (taken as the height with the largest gradient in θ), surface temperature (T), downwelling shortwave radiation (↓SWR) at the surface, upwelling shortwave radiation (↑SWR) at model top (1800 m) and air temperature (T) at 10 m. Values are the maximum between 12:00 and 16:00 local standard time (LST)

Figure 5 outlines the changes in SW downwelling and upwelling radiation as well as the SW heating rate due to the presence of BC in the aerosol layers for all three simulations throughout the day. In the case of BC aloft, there is a reduction in downwelling SW radiation both within and under the aerosol layer (Fig. 5 d) and a reduction in SW upwelling radiation (Fig. 5 g) through the layer due to absorption. The reduction in downwelling radiation beneath the aerosol layer leads to a cooling effect due to less available radiation heating the air. Meanwhile the absorption of SW radiation in the aerosol layer causes heating. This results in a change in the thermal profile of the atmosphere and enhances the temperature inversion, decreases maximum PBL height and atmospheric temperature (Table 3). There is slight subsidence of the aerosol layers aloft over time, while aerosols at the surface become vertically mixed throughout the day as the PBL develops (Figure 5).

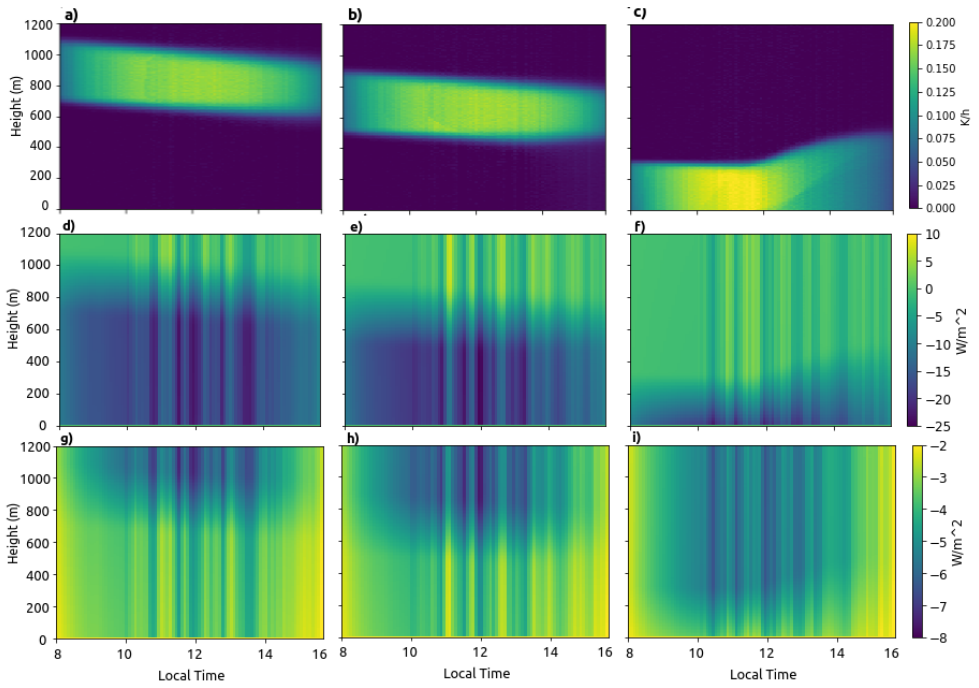

Figure 5. SW heating rate (a-c), loss in downwelling (d-f) and upwelling (g-i) SW radiation due to BC inclusion in the aerosol layer. All plots are normalised against no BC simulations (BC in the aerosol layer - no BC in the aerosol layer) for the aerosol layers at 700 m (a,d and g), 500 m (b, e and h) and the surface (c, f and i)

Aerosol layers with identical mass mixing ratios are initialised between 500-950 m and 700-1150 m to examine the impact of the altitude of the layer. When there are aerosols at 500m, aerosols can become entrained into the upper PBL, as the PBL develops and the aerosol layer subsides. This results in a strong heating at the top of and above the PBL, causing a decrease in 6.7 % in PBL height compared to no aerosols. This is a decrease of 4.2 % in PBL height for the high aerosol layer (700-1150 m) compared to the low aerosol layer (500-950 m). Figure 6 shows the potential temperature lapse rate throughout the day for each of the aerosol layers. This shows the inversion for including the aerosol layer at 500 m is much stronger than for the 700 m aerosol layer. This causes the larger suppression of PBL development observed under these conditions.

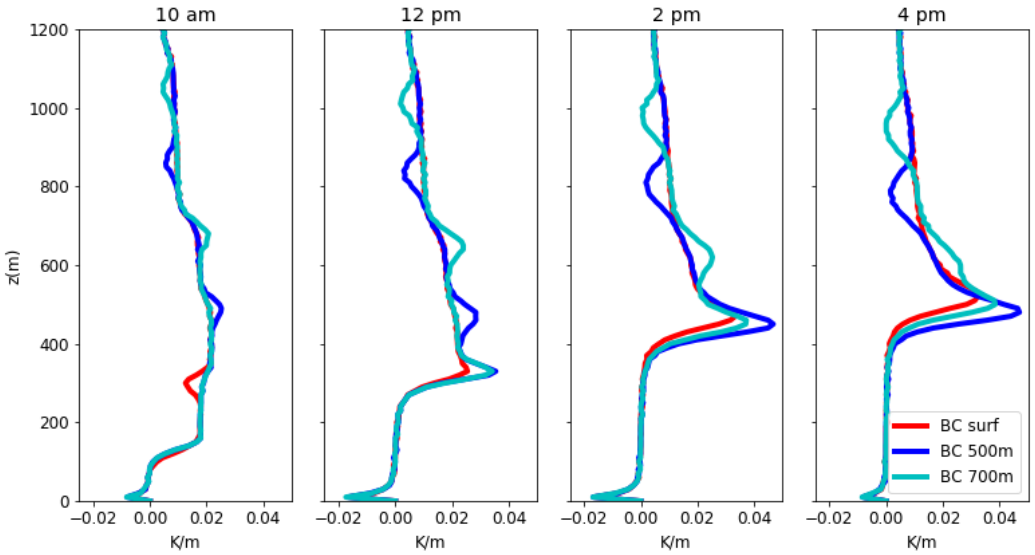

Figure 6. Potential temperature lapse rate for simulations on 3rd Dec at 10am, 12pm, 2pm and 4pm for surface BC (red), BC above 500m (blue) and BC above 700m (cyan)

3.2 Case 2-Varied Initial Conditions

In these simulations we examined the sensitivity of BC surface heating on turbulent dynamics to different meteorological conditions. Specifically, we assessed whether BC at the surface can cause heating to a large enough extent to overcome the temperature inversion and enhance PBL development, under different initial conditions. On the 2nd Dec, simulations with no aerosols show a temperature inversion for the 400 m above PBL top of $\sim$ 4 K at 14:00 LST, compared to $\sim$ 7 K on 3rd Dec (Figure 7). Consequently, including BC at the surface shows a larger enhancement in turbulence for 2nd Dec, when the initial temperature inversion is lower. In this case, BC at the surface causes a 5% increase in PBL height, increasing TKE and minimising the decrease in sensible heat flux. This is despite the change in SW downwelling and upwelling radiation being similar for both days (Figure 8).

Due to the variation in initial meteorological conditions such as humidity, temperature and wind (Figure 3), it is difficult to ascertain whether the difference in PBL development caused by BC surface heating is a direct impact of the strength of the temperature inversion. However, it is clear that at least for the case of BC within the PBL, meteorological conditions affect the magnitude of surface heating on PBL development. These results highlight the susceptibility of the aerosol-PBL feedback to initial conditions as has been outlined in previous work by Slater et al. (2020) and Slater et al. (2021). In both cases, the BC concentrations cause a heating rate of 0.2 K/h at the surface, which leads to increases in the surface air temperature. Although there is increased turbulence caused by BC heating on 2nd Dec, the level of heating within and at the top of the PBL is not enough to overcome the strong temperature inversion and the stagnation caused by aerosol-PBL feedback. Consequently,

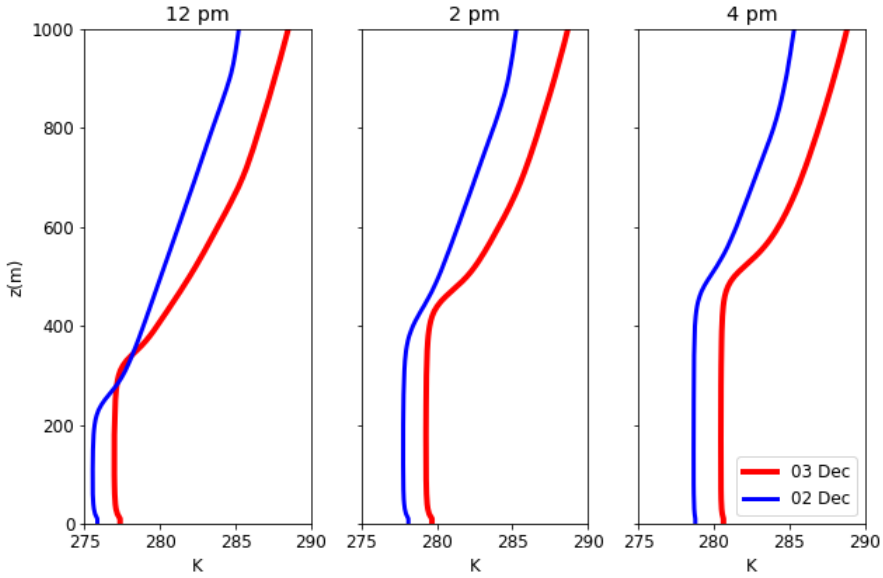

Figure 7. Potential temperature profiles for simulations with no aerosols for 03 Dec(red lines) and 02 Dec (blue lines) at 12pm, 2pm and 4pm

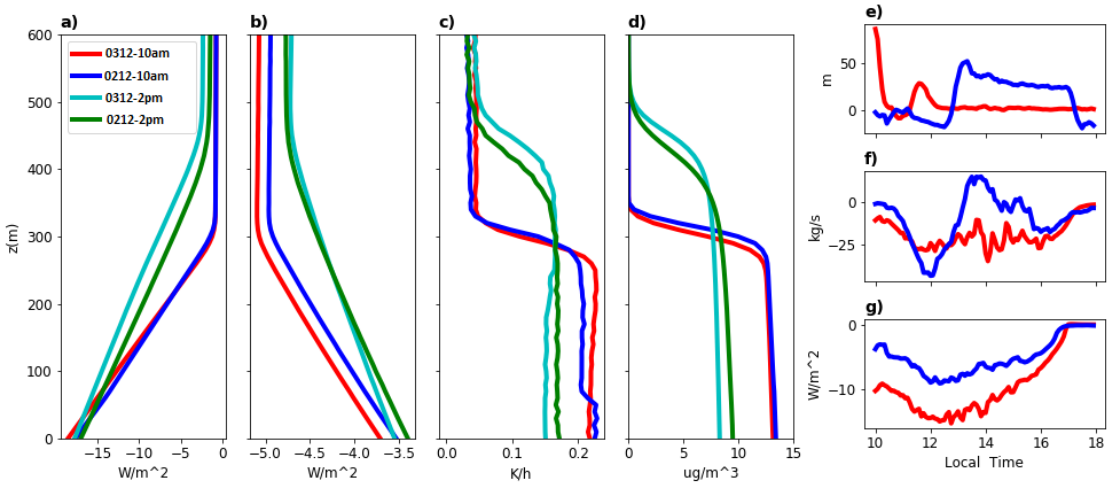

Figure 8. Change (surface aerosol - no aerosols) in a) downwelling and b) upwelling SW radiation, c) SW heating rate, and d) BC concentrations for simulations on 3rd Dec (red and cyan) and 2nd Dec (blue and green) at 10am (red and blue) and 2pm (cyan and green). (e-g) Change (surface aerosol - no aerosols) in e) PBL height, f) Vertical integral of Turbulent Kinetic Energy (TKE) and g) Sensible Heat Flux for 3rd Dec (red) and 2nd Dec (blue)

BC heating within the PBL under these conditions will be unlikely to promote haze dissipation due to the strength of the temperature inversion.

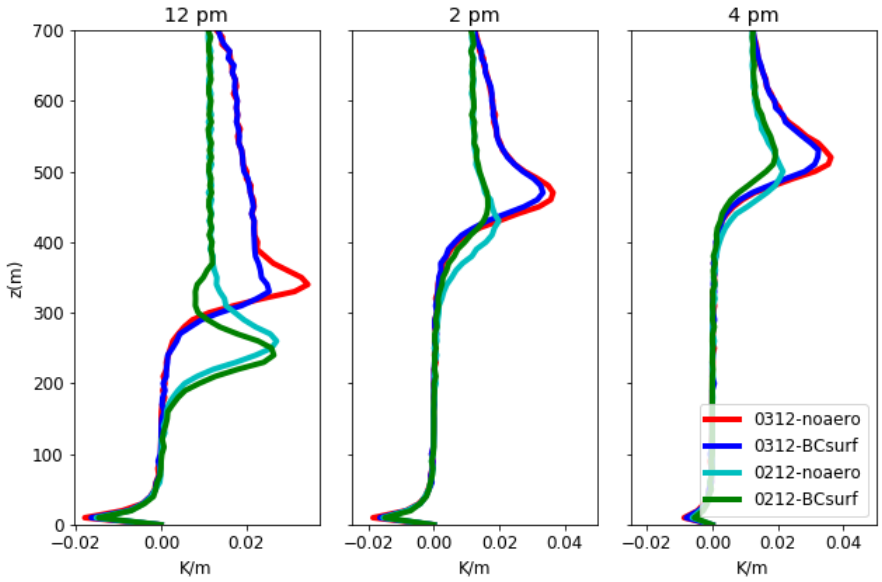

Figure 9. Potential Temperature Lapse Rate at 12pm, 2pm and 4pm for simulations with surface aerosols (blue and green) and no aerosols (red and cyan) on 2nd Dec (cyan and green) and 3rd Dec (red and blue)

Figure 9 shows the potential temperature lapse rate at 12pm, 2pm and 4pm for simulations with no aerosols and with BC at the surface for 2nd Dec and 3rd Dec. This shows BC at the surface reduces the inversion at PBL top in both cases. Furthermore, at 2pm the PBL top is higher on 2nd Dec for simulations including BC at the surface. Here, compared to 3rd Dec, the heating within the PBL and at PBL top appears to be almost strong enough to break the temperature inversion at PBL top and enhance PBL development. As can be seen in figure 8 (d), the aerosol layer becomes vertically mixed throughout the day as the PBL develops. These results show that under conditions with a weaker temperature inversion, BC heating at the surface enhances turbulent mixing to increase PBL development. If the heating caused by BC at the surface is strong enough or under conditions where the temperature inversion is weaker, this may allow for BC to become vertically mixed to high levels. When the PBL collapses overnight, this leads to BC being present above the PBL which may enhance atmospheric stagnation and enhance the intensity of pollution events.

3.3 Case 3- Vertically varied BC

Section 3.1 shows the aerosol radiative forcing and perturbations due to BC are higher than the scattering effect of other aerosols. However, this case only identifies the effect of either aerosol concentrations within or above the PBL, where they can exist both within and above the PBL for several reasons. Here, we examine the idea of fully reducing BC at the surface as a

proxy to decreasing BC emissions locally, where other species are still present. So for example targeting sources of BC, such as biomass burning without tackling other sources of inorganic aerosols or volatile gases. BC aloft is considered to be brought into Beijing through regional transport or entrainment from a polluted residual layer. A study by Ferrero et al. (2014) suggested that the impact of local BC emissions will heat the PBL and lead to pollutant dissipation through promoting atmospheric buoyant turbulence. Results from section 3.1 show the reasonably low impact of BC at the surface in enhancing PBL development, compared to the suppression caused by the BC layer at PBL top. Furthermore, if BC from the surface gets mixed into the residual layer it will negatively impact turbulent mixing the next day. This section looks at including BC and other aerosols both within and above the PBL and changing the relative BC concentration in the column.

In this section, we include aerosols throughout the column and varied the fractional aerosol composition to have BC and no BC throughout the profile and BC above 500m and 1000 m (Figure 9). This was done as a proxy to examine the impact of tackling local emissions of BC but allowing regional emissions of BC. Our results show that including BC both within and above the PBL causes a large reduction in PBL height (17 %) compared to no BC (Table 4). In section 3.1 and 3.2 simulations with BC have a slightly higher PBL height compared to those without (Table 3). Therefore, the decrease in PBL height for these simulations (BC within and above the PBL) indicates that the potential enhancement in turbulence by BC within the PBL (as seen in sections 3.1 and 3.2) is eclipsed by the effect of BC above the PBL which acts strongly to prevent PBL development through the day. This is likely due to the low level of SWR available for BC heating at the surface in the full column BC simulations, due to absorption by BC at higher altitudes.

	SHF (W/m^2)	**PBL Height (m)**	**Surface T (K)**	**↓ SWR surface (W/m^2)**	**↑ SWR top (W/m^2)**	**T at 10 m (K)**
BC 1000 m	98.40	482.84	284.43	479.90	98.42	278.85
BC 500 m	98.42	423.51	283.78	455.60	91.22	278.85
Full column BC	84.78	419.52	283.85	432.00	84.77	279.06
No BC	111.03	507.39	285.10	503.79	107.90	279.29

Table 4. Maximum sensible heat flux (SHF), planetary boundary layer (PBL) height (taken as the height with the largest gradient in θ), surface temperature (T), downwelling shortwave radiation (↓SWR) at the surface, upwelling shortwave radiation (↑SWR) at model top (1800 m) and air temperature (T) at 10 m. For including aerosols throughout the column but changing the composition for BC only above 1000m, BC only above 500m, BC throughout the column, and no BC in the column. Values are the maximum between 12:00 and 16:00 local standard time (LST)

Table 4 shows that including BC has a significant impact on reducing SW downwelling and upwelling radiation, which consequently feeds back and reduces surface temperature and sensible heat flux. Simulations including BC across the entire column, show the largest decrease in downwelling and upwelling SW radiation, due to the overall larger columnar concentration of BC. Including BC at the surface (Full column BC) leads to higher air temperature at 10 m compared to simulations with BC aloft (BC 500 m and BC 1000 m) only, but lower air temperature at 10 m than not including BC at the surface (No BC).

This is likely due to BC throughout the column absorbing radiation, which leads to heating but also reduces the amount of SW radiation reaching the air at the surface, consequently reducing surfac air temperature. This work shows that any increase in PBL height due to BC at the surface is outweighed compared to the stronger impact of BC above and at PBL top (BC 500 m), which results in the largest decrease in PBL height for simulation with BC across the column.

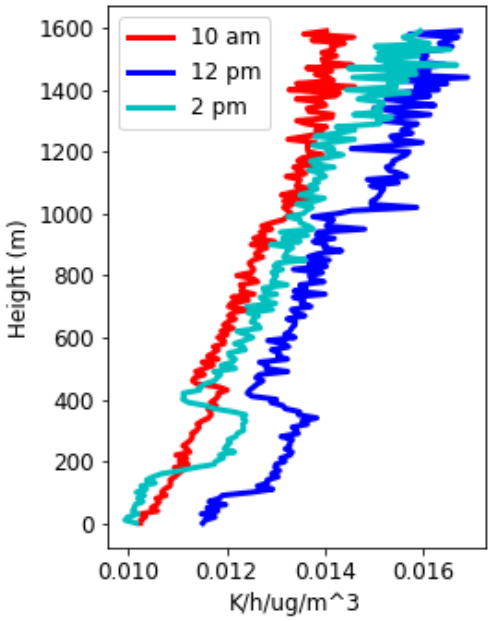

Figure 10. SW heating rate per unit mass of BC at 10am, 12pm and 2pm on 3rd Dec for simulations with BC throughout the column

Figure 10 shows the BC heating rate per unit mass of BC, taken as the heating rate for column aerosol with BC - without BC. This shows the heating rate per unit mass of BC increases with height as suggested by Wang et al. (2018). Firstly, we see a strong heating effect increasing up to the bottom of the PBL with a decrease in heating rate across the PBL, and a further constant increase above the PBL. The larger heating rate of BC at higher altitudes is thought to be due to the higher incident radiation available for BC absorption. Consequently, the heating caused by BC in the atmosphere and the effect on PBL development will be dependent on the altitude of the BC layer as well as the total BC within the aerosol column. This may be important when examining the impact of BC within the PBL as if BC also exists aloft, as there will be less SW radiation reaching the surface due to BC at higher altitudes and consequently as shown here, BC heating in the lower layers will be smaller.

4 Discussion

The results here show that BC causes heating in the atmosphere, and that absorption of solar radiation by BC has the largest impact on the temperature profile of the PBL compared to the effect of scattering aerosols. Specifically, BC can cause surface cooling through reducing SW radiation reaching the surface. In this study, BC causes heating in the aerosol layer at a rate of around 0.01-0.016 K $h^{-1}/\mu gm^{-3}$ of BC (Figure 10) , which is similar to that proposed by Ding et. al (2016) and Wang et. al (2018). For the concentrations used in this study, this works out at an overall heating of around 0.2 K/h or 1-1.6 K/day, showing the potential impacts of BC on climate through warming the atmosphere. Furthermore, this work directly investigates the impact of BC altitude on the layer, where BC is considered to be the only absorbing aerosol.

From examining the potential temperature lapse rate, we can see that BC at 500 m has the largest impact through increasing the temperature inversion at PBL top compared to simulations with BC at 700 m. This suggests that the absorbing layer has the most impact when it exists at PBL top. Furthermore, throughout the day the aerosol layer becomes entrained into the PBL as it develops, this can further increase surface concentrations if the aerosols at PBL top mix down to the surface. When aerosols are included throughout the column, we observe an enhanced effect on PBL suppression, with a decrease of 16 % compared to not including BC and only slightly less effect than having BC throughout the entire column (Section 3.3). When there are aerosols throughout the column, BC at the surface will receive less SW downwelling radiation compared to BC aloft due to the interactions of the aerosols above it preventing SW downwelling reaching lower levels. Consequently, there will be more SW radiation available for the BC aloft to absorb and heat the atmosphere. Figure 10 shows that the heating rate per unit mass of BC is higher aloft than at the surface, meaning that the impact of PBL suppression by BC aloft will often negate the impact of surface BC promoting PBL development.

At the surface, including BC increases air temperature, but decreases sensible heat flux through reducing the amount of SW radiation reaching the surface. We examine the impact of BC at the surface for a case study including the 2nd and 3rd Dec 2016 and find that the magnitude of the impact is different on each day, suggesting the importance of meteorology and initial conditions on the impact BC might have on the aerosol-PBL feedback. In section 3.1 and 3.2, we identify that the strong temperature inversion at PBL top throughout the day on the 3rd Dec prevents BC heating from enhancing PBL development. The impact of BC within the PBL on PBL height in our simulation is small (0.26 % increase), compared to a 4-6 % increase suggested by Wang et al. (2018), despite the heating rates due to BC being similar. We believe this is due to the strength of the temperature inversion caused by the initial conditions on 3rd Dec (Figure 3a). A temperature inversion, often known as the capping inversion is the sharp increase in temperature at PBL top and can be enhanced or diminished by aerosol-radiation interactions (Stull, 2015). Warming of the air at PBL top by BC can reduce the difference in temperature between the PBL and free atmosphere, reducing the temperature inversion and making it easier for air parcels to move upwards. In some cases, this will increase PBL height. In the work by Wang et al. (2018), the inversion at PBL top to 400m above PBL top at 14:00 LST without aerosol inclusion is $\sim$ 3 K, in our case it is $\sim$ 7 K.

Temperature inversions and stable conditions are frequently brought about by synoptic condition changes in wintertime Beijing, are strengthened over the pollution episode as aerosols cool the surface. The specific haze episode examined here is

from 01 -04 Dec 2016 and the meteorological and synoptic condtions are detailed in the paper by Wang et al. (2019). In their work, they suggest the strong temperature inversion on the 3rd Dec is due to both the impact of synoptic conditions and the aerosol-PBL feedback from the previous day causing surface cooling. Overall, we find that surface BC causes warming and enhances turbulence. This increases PBL height by 0.26 % on 3rd Dec due to the strong initial temperature inversion (7.0 K in the lowest 500m at 10am) but increases PBL height by 5 % on 2nd Dec due to the weaker temperature inversion (4.2 K in the lowest 500 m at 10am). However in these conditions, the heating rate is still not enough to fully weaken the strong temperature inversion (Figure 9).

This work shows that BC heating may significantly increase the PBL height, specifically under conditions with weaker temperature inversions. However, surface BC has a small effect on enhancing PBL development under strongly stagnant meteorological conditions. It is therefore unlikely that under polluted conditions in wintertime Beijing, that the BC heating at the surface will strongly impact the aerosol-PBL feedback loop to lessen the severity of pollution episodes in Beijing. It may be however, that under certain conditions when the temperature inversion is low that the heating of BC impacts PBL development and may enhance the recovery phase of a pollution event though we have not focused on this aspect in this paper. We calculate a heating rate of around 0.2 K/h, and assuming a daytime heating in Beijing winter of 8 hours, the heating at PBL top could reach around 1.6 K which is too small to change temperature inversions which are common during haze episodes and are typically 4-7 K. However, in cases with weaker temperature inversions (1-2 K), the heating caused by surface BC may be strong enough to cause modifications to the PBL development. This allows for increased vertical mixing of aerosols and may allow for BC to be mixed higher into the PBL, when the PBL collapses overnight leaving a polluted aerosol layer aloft. The next day this polluted absorbing layer will heat the layer above the PBL, thus changing the temperature profile of the PBL to reduce buoyancy. This reduces PBL height and enhances the aerosol-PBL feedback to increase surface $PM_{2.5}$ and intensify pollution episodes (Figure 11). Our results show that BC above the PBL has more impact than BC below and consequently if BC is present throughout the column, the effect of suppressing turbulent motion by BC is greater than the enhancement effect.

In performing simulations including BC throughout the column (at multiple layers) this work can directly show that the impact of BC heating within the PBL is negated by the stronger impact of BC aloft, which absorbs a significant proportion of SW solar radiation, meaning less absorption of SW radiation by BC within the PBL or at lower altitudes. This work therefore adds on to the studies by Ding et al. (2016), which only shows the effect of BC at and above PBL top, and Wang et al. (2018) which examines the impact of BC layers at different altitudes separately rather than the effect of multiple BC layers. Our work also shows the importance of initial conditions on the BC surface heating effect as outlined for aerosols in general by Slater et al. (2020) and Slater et al. (2021). This is important as these conditions change over the course of the haze episode, with PBL height found to decrease by as much as 50 % due to synoptic influences alone (Wang et al., 2019; Slater et al., 2021). In the work by Wang et al. (2018) only one set of meteorological conditions are examined, which limits the applicability of the results to periods with similar conditions. While our work shows that conditions on 02 Dec lead to a PBL enhancement of 5 %, compared to 0.4 % on 03 Dec. Combining all the results presented in this paper as well as other research by Wang et al. (2018) and Ding et al. (2016), here we detail a potential mechanism for the influence of BC on air pollution episodes in

Beijing (Figure 11). Although this mechanism has not been fully tested in this work due to computational cost, we hypothesise that locally emitted BC which heats the PBL could promote PBL development (section 3.2), resulting in the BC becoming well mixed through the PBL. When the PBL collapses overnight, the BC will remain in the residual layer overnight and exist above the PBL the next day. This would then suppress PBL development as shown in section 3.1 and 3.3 of this work and in the work by Ding et al. (2016). However, if synoptic conditions on the next day changed to weaken the temperature inversion and the PBL developed, as observed during this haze episode by Wang et al. (2019), the BC aloft could become entrained into the PBL to heat the surface layer and help promote buoyant turbulence and the dissipation of pollutants (Figure 11). This mechanism could have strong influences for policy and we would therefore recommend that further research be performed to directly investigate the mechanism and its potential to influence the severity and longevity of haze episodes.

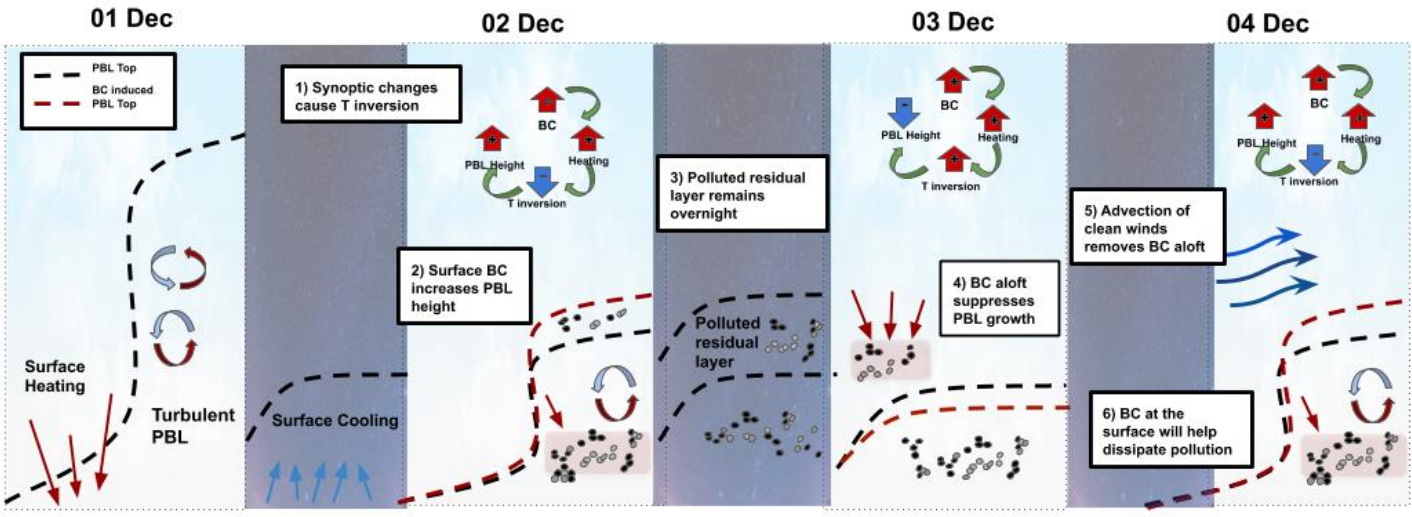

Figure 11. Schematic to show the potential impact of BC on a Beijing haze episode which occurred between 1st and 4th Dec 2016, where both the onset and dissipation of the pollution episode is brought about by changing synoptic patterns. The black dashed lines indicate PBL top with the red dashed lines indicating the change caused by BC interactions and the type of impact is dependent on the altitude of the BC layer.

5 Conclusions

From this work, we suggest: a) The impact of BC aloft on PBL suppression is dependent on the altitude of the aerosol layer in relation to PBL height, b) BC surface heating impact on PBL development is dependent on the strength of the initial

temperature inversion and c) When BC is present throughout the column the strong interactions aloft eclipse the impact of BC surface heating. Overall, we show that BC causes heating at a rate of 0.15-0.2 K/h during the daytime which suggests that BC direct radiative forcing has implications for climate, through warming the atmosphere. In terms of the local effect of BC on the aerosol-PBL feedback, BC high above the PBL has little impact on PBL development, while BC just above the PBL suppresses PBL growth. Furthermore, controlling regional emissions of BC will significantly reduce the amount of BC aloft which may reduce the severity of pollution episodes associated with atmospheric stagnation in Beijing. Here, as shown in figure 11, we propose a novel mechanism on how BC may impact pollution episodes in Beijing:

1. At the beginning of the haze episode, synoptic conditions lead to a saddle type pressure field over the region which leads to a temperature inversion and light winds at the surface, allowing for pollution accumulation in a shallow PBL.
2. BC emitted locally and regionally will be trapped in the surface layer and our results show that this will heat the air at the surface
3. If the inversion is weak (1-3 K) then this will cause sufficient heating at the aerosol loads often found in Beijing to break the temperature inversion at PBL top and enhance vertical mixing to move BC higher in the layer.
4. As the PBL collapses overnight, BC concentrations will exist in residual layers above the nocturnal inversion close to the surface.
5. The following day, these BC layers will heat the air above the PBL and due to the higher SW downwelling radiation aloft, will outweigh the effect of surface BC heating to enhance stability in the column and cause the suppression of the PBL. This exacerbates the pollution event on subsequent days.
6. When changes in synoptic conditions cause the pressure system to move away and upper level winds advect in cleaner air the suppression of the PBL by BC heating diminishes. High BC concentrations in the PBL remain but as we have shown these act to heat the surface and will aid the recovery of the PBL and lessen impact of pollution by promoting mixing at PBL top as the inversion strength weakens (Figure 11).

References

Ács, F., Mihailović, D. T., and Rajković, B.: A Coupled Soil Moisture and Surface Temperature Prediction Model, https://doi.org/10.1175/1520-0450(1991), 1991.

Bond, T. C. and Bergstrom, R. W.: Light absorption by carbonaceous particles: An investigative review, Aerosol Science and Technology, 40, 27–67, https://doi.org/10.1080/02786820500421521, 2006.

Bond, T. C., Doherty, S. J., Fahey, D. W., Forster, P. M., Berntsen, T., Deangelo, B. J., Flanner, M. G., Ghan, S., Kärcher, B., Koch, D., Kinne, S., Kondo, Y., Quinn, P. K., Sarofim, M. C., Schultz, M. G., Schulz, M., Venkataraman, C., Zhang, H., Zhang, S., Bellouin, N., Guttikunda, S. K., Hopke, P. K., Jacobson, M. Z., Kaiser, J. W., Klimont, Z., Lohmann, U., Schwarz, J. P., Shindell, D., Storelvmo, T., Warren, S. G., and Zender, C. S.: Bounding the role of black carbon in the climate system: A scientific assessment, Journal of Geophysical Research Atmospheres, 118, 5380–5552, https://doi.org/10.1002/jgrd.50171, 2013.

Chan, C. K. and Yao, X.: Air pollution in mega cities in China, Atmospheric Environment, 42, 1–42, https://doi.org/10.1016/j.atmosenv.2007.09.003, 2008.

Chen, H., Rey, J., Kwong, C., Copes, R., Tu, K., Villeneuve, P. J., Van Donkelaar, A., Hystad, P., Martin, R. V., Murray, B. J., Jessiman, B., Wilton, A. S., Kopp, A., and Burnett, R. T.: Living near major roads and the incidence of dementia, Parkinson's disease, and multiple sclerosis: a population-based cohort study, 6736, 1–9, https://doi.org/10.1016/S0140-6736(16)32399-6, 2017.

Ding, A. J., Huang, X., Nie, W., Sun, J. N., Kerminen, V. M., Petäjä, T., Su, H., Cheng, Y. F., Yang, X. Q., Wang, M. H., Chi, X. G., Wang, J. P., Virkkula, A., Guo, W. D., Yuan, J., Wang, S. Y., Zhang, R. J., Wu, Y. F., Song, Y., Zhu, T., Zilitinkevich, S., Kulmala, M., and Fu, C. B.: Enhanced haze pollution by black carbon in megacities in China, Geophysical Research Letters, 43, 2873–2879, https://doi.org/10.1002/2016GL067745, 2016.

Ding, Y., Wu, P., Liu, Y., and Song, Y.: Environmental and Dynamic Conditions for the Occurrence of Persistent Haze Events in North China, Engineering, 3, 266–271, https://doi.org/10.1016/J.ENG.2017.01.009, http://dx.doi.org/10.1016/J.ENG.2017.01.009, 2017.

Ferrero, L., Castelli, M., Ferrini, B. S., Moscatelli, M., Perrone, M. G., Sangiorgi, G., D'Angelo, L., Rovelli, G., Moroni, B., Scardazza, F., Mocnik, G., Bolzacchini, E., Petitta, M., and Cappelletti, D.: Impact of black carbon aerosol over Italian basin valleys: High-resolution measurements along vertical profiles, radiative forcing and heating rate, Atmospheric Chemistry and Physics, 14, 9641–9664, https://doi.org/10.5194/acp-14-9641-2014, 2014.

Fu, H. and Chen, J.: Formation, features and controlling strategies of severe haze-fog pollutions in China, Science of The Total Environment, 578, 121–138, https://doi.org/http://dx.doi.org/10.1016/j.scitotenv.2016.10.201, http://www.sciencedirect.com/science/article/pii/S0048969716323920, 2016.

Fu, Q. and Liou, K. N.: Parameterization of the Radiative Properties of Cirrus Clouds, https://doi.org/10.1175/1520-0469(1993)050<2008:POTRPO>2.0.CO;2, 1993.

Gao, M., Guttikunda, S. K., Carmichael, G. R., Wang, Y., Liu, Z., Stanier, C. O., Saide, P. E., and Yu, M.: Health impacts and economic losses assessment of the 2013 severe haze event in Beijing area, Science of the Total Environment, 511, 553–561, https://doi.org/10.1016/j.scitotenv.2015.01.005, 2015.

Herbert, R. J., Bellouin, N., Highwood, E. J., and Hill, A. A.: Diurnal cycle of the semi-direct effect from a persistent absorbing aerosol layer over marine stratocumulus in large-eddy simulations, Atmospheric Chemistry and Physics, 20, 1317–1340, https://doi.org/10.5194/acp-20-1317-2020, 2020.

Jacobson, M. Z.: Fundamentals of Atmospheric Modelling, 2005.

Kokkola, H., Korhonen, H., Lehtinen, K. E. J., Makkonen, R., Asmi, A., Järvenoja, S., Anttila, T., Partanen, A.-I. I., Kulmala, M., Järvinen, H., Laaksonen, A., and Kerminen, V.-M. M.: SALSA - a sectional aerosol module for large scale applications, Atmospheric Chemistry and Physics, 8, 2469–2483, https://doi.org/10.5194/acp-8-2469-2008, 2008.

Kokkola, H., Kuhn, T., Laakso, A., Bergman, T., Lehtinen, K., Mielonen, T., Arola, A., Stadtler, S., Korhonen, H., Ferrachat, S., Lohmann, U., and Neubauer, D.: SALSA 2.0 : The sectional aerosol module of the aerosol – chemistry – climate model ECHAM6.3.0-HAM2 .3-MOZ1.0, Geoscientific Model Development, 11, 3833–3863, 2018.

Lelieveld, J., Evans, J. S., Fnais, M., Giannadaki, D., and Pozzer, A.: The contribution of outdoor air pollution sources to premature mortality on a global scale., Nature, 525, 367–71, https://doi.org/10.1038/nature15371, http://www.ncbi.nlm.nih.gov/pubmed/26381985, 2015.

Li, J. and Han, Z.: A modeling study of severe winter haze events in Beijing and its neighboring regions, Atmospheric Research, 170, 87–97, https://doi.org/10.1016/j.atmosres.2015.11.009, http://dx.doi.org/10.1016/j.atmosres.2015.11.009, 2016.

Liu, Q., Ma, T., Olson, M. R., Liu, Y., Zhang, T., Wu, Y., and Schauer, J. J.: Temporal variations of black carbon during haze and non-haze days in Beijing, Scientific Reports, 6, https://doi.org/10.1038/srep33331, 2016.

Maalick, Z., Kuhn, T., Korhonen, H., Kokkola, H., Laaksonen, A., and Romakkaniemi, S.: Effect of aerosol concentration and absorbing aerosol on the radiation fog life cycle, Atmospheric Environment, 133, 26–33, https://doi.org/10.1016/j.atmosenv.2016.03.018, http://dx.doi.org/10.1016/j.atmosenv.2016.03.018, 2016.

Petäjä, T., Järvi, L., Kerminen, V.-M., Ding, A. J., Sun, J. N., Nie, W., Kujansuu, J., Virkkula, A., Yang, X., Fu, C. B., Zilitinkevich, S., and Kulmala, M.: Enhanced air pollution via aerosol-boundary layer feedback in China., Scientific reports, 6, 18 998, https://doi.org/10.1038/srep18998, 2016.

Ramanathan, V. and Carmichael, G.: Global and regional climate changes due to black carbon, Nature Geoscience, 1, 221–227, https://doi.org/10.1038/ngeo156, 2008.

Slater, J., Tonttila, J., Mcfiggans, G., Romakkaniemi, S., Kühn, T., and Coe, H.: Using a coupled LES-aerosol radiation model to investigate urban haze : Sensitivity to aerosol loading and meteorological conditions, Atmospheric Chemistry and Physics Discussions, 5, 1–23, 2020.

Slater, J., Tonttila, J., McFiggans, G., Coe, H., Romakkaniemi, S., Sun, Y., Xu, W., Fu, P., and Wang, Z.: Using a coupled LES aerosol–radiation model to investigate the importance of aerosol–boundary layer feedback in a Beijing haze episode, Faraday Discussions, https://doi.org/10.1039/d0fd00085j, 2021.

Streets, D. G., Gupta, S., Waldhoff, S. T., Wang, M. Q., Bond, T. C., and Yiyun, B.: Black carbon emissions in China, Atmospheric Environment, 35, 4281–4296, https://doi.org/10.1016/S1352-2310(01)00179-0, 2001.

Stull, R.: Atmospheric Boundary Layer, in: Practical Meteorology: An Algebra-based Survey of Atmospheric Science, pp. 453–458, https://doi.org/10.1175/BAMS-89-4-453, 2015.

Tonttila, J., Maalick, Z., Raatikainen, T., Kokkola, H., Kühn, T., and Romakkaniemi, S.: UCLALES-SALSA v1.0: a large-eddy model with interactive sectional microphysics for aerosols, clouds and drizzle, Geoscientific Model Development, 10, 169–188, https://doi.org/10.5194/gmd-10-169-2017, 2017.

Tonttila, J., Afzalifar, A., Kokkola, H., Raatikainen, T., Korhonen, H., and Romakkaniemi, S.: Precipitation enhancement in stratocumulus clouds through airbourne seeding: sensitivity analysis by UCLALES–SALSA, Atmospheric Chemistry and Physics, 21, 1035–1048, https://doi.org/10.5194/acp-21-1035-2021, 2021.

Wang, L., Liu, J., Gao, Z., Li, Y., Huang, M., Fan, S., Zhang, X., Yang, Y., Miao, S., Zou, H., Sun, Y., Chen, Y., and Yang, T.: Vertical observations of the atmospheric boundary layer structure over Beijing urban area during air pollution episodes, Atmospheric Chemistry and Physics, 19, 6949–6967, https://doi.org/10.5194/acp-19-6949-2019, 2019.

Wang, Q., Huang, R. J., Cao, J., Tie, X., Shen, Z., Zhao, S., Han, Y., Li, G., Li, Z., Ni, H., Zhou, Y., Wang, M., Chen, Y., and Su, X.: Contribution of regional transport to the black carbon aerosol during winter haze period in Beijing, Atmospheric Environment, 132, 11–18, https://doi.org/10.1016/j.atmosenv.2016.02.031, http://dx.doi.org/10.1016/j.atmosenv.2016.02.031, 2016.

Wang, Z., Huang, X., and Ding, A.: Dome effect of black carbon and its key influencing factors: A one-dimensional modelling study, Atmospheric Chemistry and Physics, 18, 2821–2834, https://doi.org/10.5194/acp-18-2821-2018, 2018.

WHO: Health risks of particulate matter from long-range transboundary air pollution, Pollution Atmospherique, p. 169, https://doi.org/ISBN 978 92 890 42895, 2006.

Yang, G., Wang, Y., Zeng, Y., Gao, G. F., Liang, X., Zhou, M., Wan, X., Yu, S., Jiang, Y., Naghavi, M., Vos, T., Wang, H., Lopez, A. D., and Murray, C. J. L.: Rapid health transition in China, 1990-2010: Findings from the Global Burden of disease study 2010, The Lancet, 381, 1987–2015, https://doi.org/10.1016/S0140-6736(13)61097-1, http://dx.doi.org/10.1016/S0140-6736(13)61097-1, 2013.

Zhao, D., Liu, D., Yu, C., Tian, P., Hu, D., Zhou, W., Ding, S., Hu, K., Sun, Z., Huang, M., Huang, Y., Yang, Y., Wang, F., Sheng, J., Liu, Q., Kong, S., Li, X., He, H., and Ding, D.: Vertical evolution of black carbon characteristics and heating rate during a haze event in Beijing winter, Science of the Total Environment, 709, 136 251, https://doi.org/10.1016/j.scitotenv.2019.136251, https://doi.org/10.1016/j.scitotenv.2019.136251, 2020.

Zou, J., Sun, J., Ding, A., Wang, M., Guo, W., and Fu, C.: Observation-based estimation of aerosol-induced reduction of planetary boundary layer height, Advances in Atmospheric Sciences, 34, 1057–1068, https://doi.org/10.1007/s00376-016-6259-8, 2017.

Chapter 5

Conclusions

In this thesis, measurements taken during an intensive field campaign have been used to initialise and assess model simulations of interactions affecting Beijing haze. Specifically, this work examines the aerosol-PBL feedback and its importance for air quality in Beijing. This work has been centred around the three papers outlined above, consisting of the novel set up and testing of UCLALES-SALSA for an urban environment (Paper 1), the investigation of the impact of synoptic conditions and aerosol loading on the aerosol-PBL feedback (Paper 2) and the effect of aerosol composition and the altitude of aerosol layers (Paper 3). The idea behind this work was to further the understanding of the importance and contribution of aerosol-PBL dynamical feedback to Beijing haze episodes. This work presents for the first time, an LES model which allows for direct calculation of boundary layer fluxes, fully coupled to an interactive aerosol-radiation scheme. Furthermore, SALSA allows for specific changes in the composition, size distribution and number concentration of aerosols. In this work, measured aerosol and meteorological values taken during the APHH Beijing field campaign were used to initialise model simulations and sensitivities to aerosol composition and aerosol loading were performed. The use of UCLALES-SALSA in the work presented here, has allowed for direct interpretation and understanding of the process of aerosol-PBL feedback.

Beijing is well known for its poor air quality, particularly during wintertime, where heavy pollution episodes with high concentrations of $PM_{2.5}$ ($> 100\ \mu g/m^3$) persist for several days. This is an issue for both public health and the economy, and therefore a paramount issue for the Chinese government. Observational studies have found that high concentrations of pollutants in wintertime Beijing are associated with a shallow boundary layer. This is primarily due to the changing large scale conditions which occur prior to the onset of haze episodes in Beijing. Specifically, surrounding high pressure systems exist to the north and south of Beijing, which will either advect cold clean air or warm polluted air into the city. When these systems (winds) converge, the air will subside to cause a temperature inversion which favours the accumulation of pollutants. This effect may be considered characteristic of the unique meteorology, topography and pollutant sources in Beijing. However, the interactions between aerosol and radiation to enhance atmospheric stability are known to worsen pollution episodes in Beijing, and may also be relevant in other urban areas with high aerosol concentrations. Thus far, the relative importance and the processes affecting the aerosol-PBL feedback and its contribution to severe pollution is poorly understood. Through the development of the LES model, UCLALES-SALSA, this work directly elucidates and provides more

understanding of the processes which impact the aerosol-PBL feedback process. Furthermore, the research presented in this thesis showcases the impact of these processes on Beijing air quality, including implications for future policy.

5.1 Summary of Key Findings

This work outlines the considerations necessary in using a large eddy simulation model to analyse the interactions of aerosols, radiation and PBL dynamics in a polluted urban environment. This is the first time that such a model has been used in an urban environment and the set up and development required significant work. Firstly, the model showed high sensitivity to urban surface parameters such as: surface heat capacity, surface temperature and water volume fraction of the surface. All of these parameters contribute to the rate of heat storage, impacting sensible and latent heat fluxes which affect boundary layer development during the day and boundary layer collapse in the evening. These parameters are dependent on the properties of the surface which vary both between cities and within a city itself. Consequently, appropriate understanding of the properties of urban environments both for observational and modelling studies are important, even if they are accepted as a potential variable which can impact results. It is also likely that the spatial heterogeneity of the surface causes variations in turbulence and pollutant dispersion, and this again will vary within a city. Overall, these results show that adapting the surface scheme for an urban environment, increases PBL height and reduces radiative cooling in the evening. Furthermore, including a diurnal anthropogenic heat flux increases temperatures throughout the profiles.

The work in paper 1 shows that there is high sensitivity to initial meteorological conditions, which will primarily govern the development of the boundary layer dynamics throughout the day. In Beijing wintertime, these conditions are primarily affected by synoptic pressure system changes, but also under high aerosol concentrations, the aerosol-PBL feedback was found to decrease surface temperature, sensible heat flux and PBL height, through reducing buoyant turbulence. These effects were found to be magnified under high aerosol loadings, which also caused a decrease in surface wind speeds. The results presented also show that high concentrations of aerosols aloft can have significant impacts on atmospheric stability through absorbing radiation and creating a turbulent layer aloft, which acts to reduce turbulent motion at the surface.

The work in paper 2 focuses on a specific haze episode which occurred from 01 - 04 Dec 2016, which is well characterised in the work by Wang et al. (2019) and follows on from the work and set up of paper 1. This work explicitly shows the contribution of aerosol-PBL feedback alone is much smaller than the contribution by synoptic conditions and suggests that the feedback effect alone would not be enough to suppress the PBL to levels observed in Beijing during the haze episode examined. Therefore, it can be concluded that the initial meteorological conditions, brought about by synoptic influences are paramount for the formation of haze episodes in Beijing. However, this work also showed the importance of aerosol-

PBL feedback on atmospheric stability and the vertical mixing of pollutants. Furthermore, in contrast to other work, the results presented here show that, at least for the aerosol size and compositions used in this study, there is no threshold value above which the aerosol-PBL feedback increases in importance. Rather this work shows an almost linear relationship between aerosol loading and decrease in PBL height, with larger decreases at higher aerosol loadings. The susceptibility to the feedback on initial conditions was also examined through looking at the impact on conditions under which a shallower PBL would form without aerosol-radiation interactions, finding higher susceptibility under these conditions. This shows that under preempted atmospherically stagnant conditions, the aerosol-PBL feedback will decrease PBL height, allowing for accumulation of aerosols in an increasingly suppressed PBL, which will be increasingly more susceptible to the aerosol-PBL feedback as the haze episode progresses.

Paper 3 isolates the effects of black carbon, which for this study is considered to be the only absorbing aerosol, negating the potential impacts of brown carbon. Results here show that, under low humidity conditions, and assuming no large size impacts, the effect of absorbing aerosol is much higher than scattering aerosol in terms of its radiative feedback on boundary layer meteorology. This work shows that when the BC layer is restricted solely within the PBL, this can enhance PBL development. However, the degree of the development will depend on the temperature inversion at PBL top, as well as the concentrations of BC. Results from paper 3 show an estimated BC heating could contribute a warming of 1-1.6 K in the PBL, which is too low to break the temperature inversion of 4-7 K on the two days tested in this work. The results presented in paper 3, also show that the effect of BC aloft is highly dependent on the altitude of the absorbing aerosol layer, with an enhanced impact for the 500-950 m layer compared to the 700-1150 m layer. Furthermore, in agreement with other work by Wang et al. (2018), this study shows that BC heating aloft is more efficient per unit mass of BC than at the surface and that when BC exists both below and above the PBL, the effect of BC aloft in suppressing PBL development outweighs the impact of BC warming at the surface. This can be considered to be both due to the aerosols aloft interacting with SW radiation to reduce the amount available for absorption at the surface and the stronger impact on PBL dynamics caused by BC aloft enhancing the temperature inversion. This work hypothesises a mechanism by which locally emitted BC could have a significant effect on PBL suppression during Beijing haze, with potential impacts for air quality policy in Beijing. When BC is emitted locally from residential coal combustion or traffic, it will initially exist in the PBL. The work here shows that this will promote vertical mixing, and, under certain conditions will break the temperature inversion to increase the vertical dissipation of the pollution. Overnight, when the PBL collapses the BC will remain in the residual layer and the next day will exist above the PBL. The effect of warming of the BC layer aloft is higher than the effect of BC warming in the PBL. Therefore, this will causes boundary layer suppression through enhancing the temperature inversion at PBL top. This shows how BC can enhance the aerosol-PBL feedback. However, during the clean up process, when wind from the North, advects cold clean air into Beijing, the BC above the PBL will get removed quickly, while BC at the surface may stay longer due to the high atmospheric stability within the PBL. In this case, BC at the surface will act to enhance PBL development, promote vertical mixing and aid in the dissipation of pollution.

5.2 Implications and Future Recommendations

The results highlighted in this thesis outline and investigate some of the key processes impacting pollution episodes in wintertime Beijing. Haze episodes in Beijing typically occur every 4-7 days and are preempted by changes in large scale pressure gradients which lead to the transport of polluted, humid air and the occurrence of temperature inversions and stagnant atmospheric conditions over Beijing. Regionally transported and locally emitted pollutants will then be trapped in a shallow PBL. The extent of the aerosol-PBL feedback on the haze episode will likely then govern the intensity of the pollution episode. This work outlines the processes which impact this. Primarily, this work directly shows that the concentrations of aerosols present, their composition, vertical profile through the atmosphere, and the initial temperature inversion, which may be governed by synoptic conditions, as key factors influencing the impact. This will directly influence surface PM concentrations, with implications for the severity of the haze episodes and human health.

Throughout this thesis, the simulation results shows high sensitivities to a variety of processes and parameters, which govern the development of the urban boundary layer. In order to characterise the interactions and perturbations of aerosols on boundary layer dynamics it is consequently essential to fully understand and simulate these processes. Furthermore, the results and sensitivities of the processes presented in this thesis could, with further research allow for better parameterisation in regional and air quality models, particularly with regard to the development of the PBL. As shown in this thesis, PBL development is dependent on several factors including surface and aerosol properties, and meteorology. Frequently, larger scale models use PBL schemes which parameterise a lot of the processes governing PBL development explicitly modelled by LES models. These parameterisations are often developed based on numerical modelling results from for example LES models. Consequently, results showing the sensitivites of PBL development to several factors in polluted urban environments could be used to improve these parameterisations.

As discussed in this thesis, the onset of Beijing haze is dependent on synoptic or regional forcing. LES models can't capture these large scale changes, and therefore, regional models are needed in order to properly capture and understand the overall processes impacting the development and dissipation of haze episodes in Beijing. However, regional modelling studies will not be able to fully capture small process changes and neither will they be able to decouple some of the processes shown in this work. Recently some studies have started to incorporate LES models into WRF as part of a nested domain setup (Udina et al., 2020). This gives the advantage of being able to simulate large scale conditions along with the more detailed boundary layer processes and effects presented in this work. The work presented here has allowed for understanding of the fundamental interactions and sensitivities of the aerosol-PBL feedback, which can be used in conjunction with regional models to improve understanding of Beijing haze episodes.

5.2.1 Modelling the Urban Boundary Layer

This work simulates the development of the urban boundary layer on several days, showing good agreement with measurements during conditions which aren't impacted by large scale changes. The results presented in all 3 papers show strong sensitivity to various perturbations including aerosol properties, surface parameters and initial meteorological conditions. Modelling studies examining the aerosol-PBL feedback in Beijing have mainly used WRF-CHEM. Boundary layer development in WRF-CHEM is reliant on chosen boundary layer schemes and parameterisations. Results here show that the aerosol-PBL feedback is highly dependent on the initial conditions, consequently, relying on boundary layer schemes which don't take these processes into account may incorrectly over or under emphasise the importance of the aerosol-PBL feedback on pollution episodes. Therefore, it is recommended that to better understand the processes affecting aerosol-PBL feedback more high resolution studies which can directly simulate perturbations to boundary layer processes are needed. If this feedback process can be accurately elucidated, it may then be possible to include a better representation for use in regional models.

Further, this work shows the importance of the urban heat island on boundary layer development and in accurately simulating boundary layer processes. These properties are typically dependent on both the surface properties and layout, as such they are often not well measured. This work also shows the dependence of boundary layer dynamics on the aerosol vertical distribution and feedback on PBL. Consequently, in order to further understanding of urban pollution, it is necessary to have accurate measurements or parameters for different urban areas, including the anthropogenic heat flux and urban heat storage. If this is not possible, it is important to at least recognise the impact these factors might have on modelling the urban boundary layer.

5.2.2 Threshold PM Values

Typically investigations of the aerosol-PBL feedback have utilised either observational data or regional modellling studies. Petäjä et al. (2016) performed theoretical analysis on observations in Nanjing to suggest a critical PM concentration of ~ 250 μg/m^3 which may cause the PBL to become statically stable across megacities in China. However, in paper 2, this work shows that under the conditions tested, such a value doesn't exist but rather the reduction in PBL due to increasing PM is approximately linear, even when surface concentrations reach > 300 μg/m^3. Furthermore, these results clearly show that the major association with PBL stability is the initial meteorological conditions, where aerosol loading works to enhance stability and can cause significant decreases in PBL height but that extremely shallow PBL conditions (< 500 m) cannot solely be caused by aerosol-PBl feedback (Paper 2). These results instead suggest that the aerosol-PBL feedback is important for enhancing stability in already stable conditions, and will in these circumstances act to enhance air pollution episodes in Beijing. This work provides potential impacts for policy, which should focus on reducing emissions rapidly when unfavourable meteorological conditions are predicted to occur, and not focus on keeping concentrations below a certain threshold limit.

One limitation of this work and an idea that needs to be examined for the future is that of semi-volatile condensation. This is believed to play an important role in the cumulative stage of haze episodes, through increasing secondary aerosol formation and the size of the aerosols and altering their optical properties. In the studies presented here, the only process which could lead to changing aerosol size was condensation of water and aerosol coagulation. Furthermore, humidity levels were not high enough for rapid uptake of water. However observations show that on 04 Dec 2016, surface humidity reaches > 90 % and the pollution becomes a polluted fog. This increase in humidity under highly polluted conditions is common in wintertime Beijing (Figure 2.2), and will enhance aerosol processing and heterogeneous reactions further. Of particular interest and potential importance is nitrate formation, which is believed to occur rapidly under humid conditions in Beijing haze episodes (Wang et al., 2020; Xu et al., 2019). This will contribute substantially to PM concentrations and may be important in the explosive growth of PM observed in many pollution episodes.

Including semi-volatile condensation would likely show an enhanced impact of aerosol-PBL interactions through increasing average aerosol size. The impact of the aerosol size distribution was also not examined in this work but may have a significant effect on increasing the magnitude of aerosol-radiation interactions. Increased aerosol size will lead to stronger aerosol-radiation interactions and may cause an enhancement of the aerosol-PBL feedback. Aerosol size is known to increase over the haze episode due to enhanced coagulation and the condensation of water vapour and semi-volatiles. Therefore, it may be that as the haze episode increases, the mass concentrations of aerosols are dominated by larger particles. Paper 2 examines the effect of aerosol loading by increasing aerosol number concentration but assumed the same initial size distribution. It may be in fact that as the haze episode advances, aerosol size increases which increases the aerosol mass loading in a shallow PBL. The impact of increased size leads to enhanced aerosol-radiation interaction which results in the non-linear aerosol-PBL effect (where PBL decreases more rapidly under higher aerosol loadings) observed in some studies. Furthermore, it may be that these processes play a different role depending on the properties and concentration of the aerosol particles and semi-volatile gases, and the atmospheric conditions. Consequently, the linear aerosol-PBL feedback effect simulated in our study may be a result of keeping aerosol size and composition constant through the day. Therefore, in order to fully elucidate the aerosol-PBL feedback, the understanding of these conditions and sensitivities to these process are essential.

5.2.3 Absorbing Aerosols

This work (paper 3) shows directly the impact of BC and the altitude of the absorbing aerosol layer on suppressing or enhancing PBL development. Specifically, considering an internally mixed aerosol distribution, the impact of absorption contributes the most to altering the thermal profile of the planetary boundary layer. Furthermore, this work shows that in theory, surface BC can contribute a heating rate equivalent to that of BC aloft. However, if absorbing aerosols exist both at the surface and aloft, the layer aloft will absorb significant amounts of downwelling SW radiation, this will lead to less radiation being

available for interaction with aerosols at the surface. Consequently in these cases, the impact of absorbing aerosol suppressing the PBL has a larger impact than the effect of PBL enhancement. Further, as suggested in the work by Wang et al. (2018), the results here also show the important impact of the altitude of the BC layer aloft. While the coupled interactions used in this study, show that due to subsidence of the aerosol layer and PBL development through the day, the aerosols aloft will sink and could become entrained into the PBL.

This work also suggests a mechanism by which, as well as BC being regionally transported into Beijing, BC emitted locally can cause vertical mixing to contribute to the observed BC above the PBL. Through this, a new mechanism is presented which outlines the important contribution of locally emitted BC to the aerosol-PBL feedback in Beijing. This mechanism is likely to be more important under conditions with low temperature inversions, when BC surface heating of ~ 0.2 K/h could break the inversion to fully promote vertical mixing of aerosols. In the past decade, policy in Beijing has acted to improve its air quality through banning local biomass burning and relocated industry out of the city. This has resulted in a reduction in the overall concentrations of BC within the city. However, as this policy is only city wide and due to the relocation of industry typically to the south of Beijing, this can lead to large concentrations of BC existing across the region generally. Consequently, the process of BC aloft suppressing PBL development is likely to remain important due to the regional emissions of BC. Meanwhile, the mechanism described in paper 3, where locally emitted BC enhances vertical mixing to cause high concentrations of BC, will be important in urban areas where sources of BC pollution such as biomass burning and traffic remain high (Kumar et al., 2015; Tyagi et al., 2019).

Showcasing the impact of BC on potentially enhancing air pollution episodes is crucial as the control of BC emissions is often overlooked. Furthermore, BC is known to contribute to global warming through absorbing solar radiation and warming the atmosphere. The processes that impact BC absorption enhancement have not been investigated in this work but are believed to have a significant impact on its radiative properties. Mainly, the internal mixing with other aerosols by BC is thought to create a lensing effect which will contribute to the radiative forcing by BC. This may have an impact on the heating rate of BC, which will contribute to its impact on aerosol-PBL feedback, both through enhancing its ability to warm the surface and promote PBL development and aloft to suppress PBL turbulence. Although, Wang et al. (2018) showed enhancement of BC warming in simulations which included scattering aerosols, the potential for investigating the details of this effect in a high resolution coupled dynamical model such as UCLALES-SALSA, would allow for direct interpretation of some of the factors influencing the absorption enhancement and the magnitude of its impact on aerosol-PBL interactions.

There is potential within UCLALES-SALSA to examine the potentially important impact of brown carbon (BrC). The contribution of BrC, is believed to be important but measuring concentrations and understanding of BrC's radiative impact on Beijing haze episodes is still poorly understood. This work has highlighted the important contribution that absorbing aerosols have on enhancing pollution episodes,

which may have more impact than scattering aerosols on cooling the surface and enhancing the aerosol-PBL feedback. BrC is likely to be present in high concentrations in Beijing and other megacities in India and China. Despite its lower absorption capacity compared to black carbon, the high concentrations of BrC may mean that its impact on aerosol radiative forcing and aerosol-PBL interactions is of equivalent importance. Therefore, further understanding of the optical properties, concentrations and vertical profiles of BrC in polluted megacities, will allow for better constraint and accuracy when understanding of the aerosol-PBL interactions.

5.3 Overall implications

This work has been separated into three research papers which build upon each other. After setting up the model for an urban environment as detailed in chapter 3, the first paper showcases some of the key changes and the sensitivities to parameters and conditions in the modelling framework. This paper examines a haze episode which occurred from 24/11-26/11/2016 and uses measured vertical meteorological profiles as well as reanalysis data to initialise the model in the morning of each day. This work first showcases that i) initial meteorological conditions vary greatly over this 3 day period and that ii) the conditions affect the PBL dynamics throughout the day. As the aerosol-PBL feedback loop investigated in this thesis examines the interaction between PBL dynamics and aerosol-radiation interactions, these initial conditions were found to greatly influence the magnitude of the aerosol-PBL feedback. Primarily, this paper identified that aerosol-radiation interactions caused a cooling in the lower layers and suppressed PBL development for all days. This effect was magnified under higher aerosol loading. Through examining recent literature, I identified that the changing meteorological conditions over the three days of the haze episode on 24/11-26/11 were likely due to not only aerosol-PBL feedback enhancing stagnation but also that changing synoptic conditions were a primary factor and potentially a leading cause of the pollution episode beginning. However, this haze episode was not well characterised in literature and so it was hard to discern the exact type and time of changes in synoptic conditions which influenced the episode. The next piece of work therefore identified a new haze episode within the APHH Beijing winter campaign which was well characterised in literature.

In paper 2, I examined my previous hypothesis on the influence of aerosol-PBL feedback vs synoptic scale meteorological influences on Beijing haze through the use of a case study haze episode which occurred from 01 Dec 2016 to 04 Dec 2016, where the meteorology and dynamics had been well characterized by Wang et al. (2019). In this work, I compared the decrease in observed PBL height on 01 Dec, when aerosol loading was low and there was a deep turbulent PBL and 03 Dec, when aerosol loading was high and a shallow weakly turbulent PBL existed throughout the day. Firstly, simulations were run for both days without aerosols and resulting dynamical outputs were compared. This was chosen as a proxy to examine only the impacts of meteorology without aerosol influence and how this affected PBL height. Maximum PBL height (taken as the height with the highest gradient in θ) for 01 Dec was 1779

m compared to 535 m for 03 Dec. This showed the strong influence the initial meteorological conditions had on PBL dynamics. Wang et al. (2019) identifies a change in synoptic conditions on 02 Dec, which causes a temperature inversion and enhances atmospheric stagnation, which exists until strong winds break the inversion on 04 Dec. To examine the influence of aerosols compared to that of meteorology, aerosol measurements taken at IAP were used to initialise aerosol profiles on the morning of 03 Dec. Including aerosols had the influence of reducing PBL height by 17 % to 443 m. Comparing the reduction in PBL height from changing meteorological conditions (difference in simulated PBL height from 01 to 03 Dec) and aerosols (difference from including aerosols in 03 Dec), it was concluded that the changing meteorological conditions had much more of a pronounced effect on maximum PBL height than aerosol-PBL feedback.

Despite the strong influence of synoptic changes on PBL height in Beijing, aerosol-radiation interactions have an impact on enhancing the atmospheric stability in the PBL through the aerosol-PBL feedback effect. In the first part of paper 2, this was identified as a 17 % decrease. The aerosol loading in that case was reasonably low compared to the high loading sometimes measured during Beijing haze episodes. Therefore, the next step taken was to look at the impact of aerosol loading on changes in maximum PBL height, surface shortwave radiation and sensible heat flux. These results showed that PBL height decreased linearly with increasing aerosol mass loading. To examine whether this would be the case under other conditions - for example later on in the haze episode, where there is an enhanced temperature inversion and extremely stagnant shallow PBL, we used conditions from the morning of 04 Dec and called this 'low PBL' conditions. Equally, this could have been called strong T inversion or strongly stable conditions. This effect showed an enhanced impact compared to the original case test which used initial conditions for 03 Dec. In this work, for the cases examined, PBL height decreases linearly with increasing loading (constant aerosol profiles, composition and size), while initial conditions impact the magnitude of this decrease, with sharp temperature inversions and stable conditions enhancing the effect. This is similar to the results we found in paper 1, where PBL height decreased by a larger % on 26/11 compared to both 25/11 and 24/11.

In papers 1 and 2, the aerosol-PBL feedback was shown to suppress PBL development in all cases. However, BC has been found to warm the PBL to enhance buoyancy and increase PBL depth. Building on this work, and to examine the impact of aerosol composition, paper 3 focused on including BC layers at different altitudes. The first part of this work examined the impact of aerosol layers at specific altitudes, both with BC and without BC. The same haze episode as paper 2 was chosen to do this, in order to examine the impact of BC on the results presented in that paper. The results show that BC within the PBL will enhance PBL height through increasing surface air temperature compared to no aerosol simulations. This was even when fractional composition of BC in the aerosol was only 10 %. However, this effect was small compared to the impact of BC above the PBL suppressing PBL development. As in paper 2, results from paper 3 could also be due to the particular conditions of the specific haze episode on 01-04 Dec 2016 and therefore not representative. For example, the impact of BC within the PBL in other studies had a stronger impact on PBL development, despite similar heating rates of BC found in the results presented in paper 3.

A potential reason for this is the strong temperature inversion on 03 Dec. Including BC within the PBL on 02 Dec, promotes PBL development to a larger degree than on 03 Dec. However, the effect is still quite small. It may be that under higher aerosol loadings, as shown in paper 2, if BC fraction is higher, or if conditions are suitable, then BC heating may have a significant impact on PBL development.

Paper 3 identifies that the more aerosols above the PBL, the weaker the BC heating at the surface will be due to aerosol-radiation interactions reducing the amount of SWR reaching the surface. Therefore, relating these results back to papers 1 and 2, where there were significant amounts of aerosol above the PBL, it is likely that this caused a reduction in the potential impact of BC heating on PBL dynamics in these cases. To look at this in more detail in paper 3 including BC (and other aerosols) throughout the column, as in paper 2, reduces the PBL by the largest amount. Even more than including aerosols only above 500 m (around maximum PBL height). Therefore the impact of BC heating at the concentrations tested is important only when concentrations of aerosols aloft are significantly low. The work in paper 3 can feedback into what was outlined in paper 1, on the importance of aerosol vertical profiles on the aerosol-PBL feedback. This is due to the effect of aerosol-radiation interactions which impact the thermal profile of the atmosphere, either through warming as shown in paper 3, or through reducing the SWR reaching the surface and causing cooling.

In paper 2, results showed that increasing aerosol loading had a linear impact on the decreasing PBL height. Combining this work with the results in paper 3, there are several potential outcomes. Primarily, this would depend on the relative concentration of BC, where it appeared in the aerosol layer, as well as the aerosol layer itself. If fractional BC within the PBL was high and there were few aerosols aloft, increasing aerosol loading would likely increase PBL height by small amounts. However, under the same conditions but with higher aerosols aloft, increasing aerosol loading would likely decrease PBL height at a similar rate as in paper 2 as paper 3 shows limited effect of surface BC heating when there are aerosols aloft which interact with radiation. If BC concentrations were high above the PBL (so fractional composition of BC was higher than in paper 2), there would be an enhanced rate of decrease in PBL height due to the strong effect of BC warming above the PBL and the resulting cooling below the PBL as shown in paper 3. Furthermore, paper 2 shows that the aerosol-PBL feedback is stronger under low PBL conditions (which normally occur towards the end of the haze episode). While paper 3 shows that under strong temperature inversions (often associated with low PBL height), BC heating is less effective at promoting PBL development. Therefore, these conditions combined show that towards the middle and end of haze episodes, when there is frequently strong temperature inversions, the aerosol-PBL feedback is stronger and the impact of BC heating on breaking this cycle is minimal.

Combining all the results presented in the three papers showcases a story which provides some explanation of the processes governing haze episodes in Beijing. Firstly, the synoptic changes in pressure cause temperature inversion and stagnant atmospheric conditions to form over Beijing. Aerosols are trapped in a shallower layer which leads to strong aerosol-radiation interactions and cooling of the surface to prevent

buoyant turbulence. If BC is in high concentrations at this time and the temperature inversion isn't too strong, then this may lead to a slight enhancement rather than suppression of the PBL. However, if BC or other aerosols exist aloft this effect will be minimal and there will be an overall suppression of the PBL and an enhancement of the temperature inversion. If this is the case, this will reinforce the temperature inversion and stagnant conditions on the next day. The reduction in PBL height and the scale of reinforcement will depend on both the initial conditions and the aerosol loading, which will linearly decrease PBL height with increasing aerosol loading when all other conditions remain the same. However, if the BC promotes atmospheric turbulence, this may have a positive impact on the haze episode allowing the PBL growth and stopping the cycle of increasing stagnation which leads to increasingly concentrated aerosols. The work in paper 3 also suggests that if the BC becomes vertically mixed it may stay in a polluted residual layer until the next day. This would mean that it has a negative impact on PBL height and atmospheric mixing through warming the layer above the PBL and reducing SWR to the surface. This would enhance the effect of the aerosol-PBL feedback. As the haze episode continues aerosol concentrations will increase, due to shallow and poor vertical atmospheric mixing. On the third and following days of the haze episode, increasing concentrations of aerosols will have a magnified effect as the conditions are pre-susceptible for this. This allows for strong inversions and conditions which are so stagnant they will not break until there are again strong changes in synoptic conditions.

5.4 Closing Remarks

Air pollution in Beijing and in megacities worldwide is an ongoing concern for human health and the economy. Furthermore, black carbon, which causes atmospheric warming, is present in significant concentrations in megacities across India and China, which has implications for climate change. Studies examining air pollution in Beijing are numerous, but the unique processes which govern wintertime pollution episodes are still being understood. Results presented here examine the aerosol-PBL feedback and its importance as a process affecting Beijing haze episodes. The aerosol-PBL feedback process has been investigated in Beijing wintertime in several studies over the past decade, as a mechanism which significantly enhances pollution. Early studies, believed that this process was the main mechanism causing the shallow PBL during pollution episodes, through showing observed correlations between increasing PM concentrations and reduced PBL height. More recently it has been outlined that the major factor affecting the initial formation of a shallow PBL in Beijing are the changes in synoptic conditions which force air to subside and lead to a temperature inversion to occur. Following this, the aerosol-PBL feedback becomes increasingly important in enhancing the stable conditions, resulting in more intense and long-lasting pollution episodes.

Results presented here agree with the previous literature and suggest that large scale atmospheric conditions are likely primarily responsible for the initial decrease in PBL observed during Beijing haze episodes. While the aerosol-PBL feedback becomes more important once a shallow stable PBL already

exists over Beijing. Further, this work shows that the initial meteorological conditions impact the magnitude of the aerosol-PBL feedback. These conditions are likely to be specific to Beijing due to its unique location and topography. Therefore, although the mechanism of the aerosol-PBL feedback is understood, several factors have been shown to influence its intensity and relative contribution to air pollution episodes. Consequently, when considering the impact of the aerosol-PBL feedback in other polluted urban environments, the overall atmospheric conditions, properties and vertical distribution of the aerosol layer need to be well characterised. This combined with high resolution process modelling like the work detailed here, will allow for more understanding of the magnitude of the aerosol-PBL interactions in governing air pollution episodes in megacities.

References

Kumar, P., Khare, M., Harrison, R. M., Bloss, W. J., Lewis, A. C., Coe, H., and Morawska, L.: New directions: Air pollution challenges for developing megacities like Delhi, Atmospheric Environment, 122, 657–661, https://doi.org/10.1016/j.atmosenv.2015.10.032, 2015.

Petäjä, T., Järvi, L., Kerminen, V.-M., Ding, A. J., Sun, J. N., Nie, W., Kujansuu, J., Virkkula, A., Yang, X., Fu, C. B., Zilitinkevich, S., and Kulmala, M.: Enhanced air pollution via aerosol-boundary layer feedback in China., Scientific reports, 6, 18 998, https://doi.org/10.1038/srep18998, 2016.

Tyagi, C., Gupta, N. C., Soni, V. K., and Sarma, K.: Seasonal Variation of Black Carbon Emissions in Urban Delhi, India, Environmental Claims Journal, 32, 1–11, https://doi.org/10.1080/10406026.2019.1699723, 2019.

Udina, M., Montornès, À., Casso, P., Kosović, B., and Bech, J.: Wrf-les simulation of the boundary layer turbulent processes during the bllast campaign, Atmosphere, 11, https://doi.org/10.3390/atmos11111149, 2020.

Wang, L., Liu, J., Gao, Z., Li, Y., Huang, M., Fan, S., Zhang, X., Yang, Y., Miao, S., Zou, H., Sun, Y., Chen, Y., and Yang, T.: Vertical observations of the atmospheric boundary layer structure over Beijing urban area during air pollution episodes, Atmospheric Chemistry and Physics, 19, 6949–6967, https://doi.org/10.5194/acp-19-6949-2019, 2019.

Wang, Y., Chen, Y., Wu, Z., Shang, D., Bian, Y., Du, Z., H. Schmitt, S., Su, R., I. Gkatzelis, G., Schlag, P., Hohaus, T., Voliotis, A., Lu, K., Zeng, L., Zhao, C., Rami Alfarra, M., McFiggans, G., Wiedensohler, A., Kiendler-Scharr, A., Zhang, Y., and Hu, M.: Mutual promotion between aerosol particle liquid water and particulate nitrate enhancement leads to severe nitrate-dominated particulate matter pollution and low visibility, Atmospheric Chemistry and Physics, 20, 2161–2175, https://doi.org/10.5194/acp-20-2161-2020, 2020.

Wang, Z., Huang, X., and Ding, A.: Dome effect of black carbon and its key influencing factors: A one-dimensional modelling study, Atmospheric Chemistry and Physics, 18, 2821–2834, https://doi.org/10.5194/acp-18-2821-2018, 2018.

Xu, W., Ovadnevaite, J., Fossum, K. N., Lin, C., Huang, R.-j., Dowd, C. O., and Ceburnis, D.: Aerosol hygroscopicity and its link to chemical composition in coastal atmosphere of Mace Head : marine and continental air masses, 2019.